Biodegradation of slowly biodegradable organic matter in wastewater treatment plant (WWTP) : In depth analysis of physical and biological factors affecting hydrolysis of large particles

Mourad Benneouala

THÈSE

En vue de l'obtention du

DOCTORAT DE L'UNIVERSITE DE TOULOUSE

Délivré par :
Institut National des Sciences Appliquées de Toulouse (INSA de Toulouse)

Présentée et soutenue par :
Mourad BENNEOUALA

Le **Jeudi 4 mai 2017**

Titre :

Biodegradation of slowly biodegradable organic matter in wastewater treatment plant (WWTP): in depth analysis of physical and biological factors affecting hydrolysis of large particles

---

Ecole doctorale et discipline ou spécialité :
ED MEGEP : Génie des procédés de l'Environnement

Unité de recherche :
Laboratoire d'Ingénierie des Systèmes biologiques et des procédés (LISBP)

Directeur/trice(s) de Thèse :
Dr. Yolaine Bessiere
Pr. Etienne Paul

Jury :

Elisabeth Girbal-Neuhauser	Professeur, LBAE, Auch	Présidente du jury
Mathieu Spérandio	Professeur, INSA de Toulouse	Examinateur
Yoan Pechaud	Maître de conférence, Université Paris-Est	Examinateur
Sylvie Gillot	Directrice de recherche, Irstea, Lyon	Rapporteur
Nicolas Bernet	Directeur de recherche, INRA, Montpellier	Rapporteur

To

Lycia & Liam

and my whole family

ACKNOWLEDGEMENTS

First, I would like to thank Pr. M. Sperandio for this heartily welcome in his team and to have allowed me to discover the world of high-level scientific research.

Then, I would like to express my sincere gratitude to my supervisor, Yolaine, for her guidance, encouragements and moral support throughout this thesis despite the several obstacles that I had encountered.

I am also grateful and respectful to my co-supervisor, Pr. E. Paul, for his knowledge, enthusiasm and his constructive criticisms.

I would like to that particularly Pr. E. Girbal-Neuhauser for her guidance, sympathy and the kindness she showed to me.

I obviously would like to thank M. Y. Pechaud, S. Gillot and N. Bernet for serving in my oral examination of thesis.

Finally, thanks are owed to all the people that I gathered in the LISBP and particularly to those of the EAD9, among other: Lucas, Emeline, Younes, Naila, Noureddine, Zheng Jun, Ana, Anil, Amaury, Pieter, Lang, Mathieu PL, Mathieu P, Laetitia, Sophie, Mansour, Evrard, Simon, Delphine, Sébastien, Xavier, Hélène, Guillermina, Alexis, Michel, Julie, Aurore, Nathalie, Cédric, Clarisse, Kathy, …

SCIENTIFIC PRODUCTIONS

1. Research articles

M. Benneouala, Y. Bareha, E. Paul, E. Girbal-Neuhauser, M. Spérandio, E. Mengelle, D. Delagnes, M. Bounouba, Y. Bessiere. *"Introduction of the colonisation phase in a new conceptual framework to describe hydrolysis under aerobic conditions"*.

(to be submitted).

M. Benneouala, Y. Bareha, E. Paul, E. Girbal-Neuhauser, M. Spérandio, E. Mengelle, D. Delagnes, M. Bounouba, Y. Bessiere. *"Hydrolysis of particulate settleable solids (PSS) in activated sludge is determined by the bacteria initially adsorbed in the sewage"*.

(submitted to Water Research).

2. Conference

M. Benneouala, E. Paul, E. Girbal-Neuhauser, M. Spérandio, Y. Bessiere. *"From experimental observations to modelling of particulate settleable solids hydrolysis: applications to the optimization of the COD use in a wastewater treatment plant (WWTP)."*

10th European Congress of Chemical Engineering, from September 27th to October 1st, 2015 - Acropolis, Nice, France.

ABSTRACT

In this work, the fate and biodegradation of slowly biodegradable organic matter contained in wastewaters were investigated. The hydrolysis process was particularly targeted as many sources proved that it controls the fate of the considered substrate. First, a synopsis of the literature results related to this topic as well as internal results were investigated especially in terms of respirometric aspects (OUR measurement) in order to identify differences and/or similarities between the experiments and, thus, address gaps in knowledge of the mechanisms that are involved in the hydrolysis of this matter. Then, in the second part of this thesis, experimental data from batch respirometric tests (performed in our laboratory), involving typical slowly biodegradable matter that are found in wastewaters (e.g. Particulate settleable solids, toilet paper…), were confronted to conventional (IAWQ models) and non-conventional models to evaluate the efficiencies of those models to describe the hydrolysis step. In the third part of this thesis, based on hypotheses, a novel conceptual framework was developed in order to enhance the description of the hydrolysis process. The physical properties (density, size, shape) of the components (bacteria and substrate) were taken into account in this model. Finally, in the fourth and last chapter of this thesis, the specific role of each bacterial population involved in the biodegradation of slowly biodegradable organic matter was assessed. It was here clearly evidenced that the hydrolysis of PSS in activated sludge processes appears more influenced by the initially adsorbed bacteria onto the sewage than by the added AS-inoculum concentration.

RESUME EN FRANÇAIS

Dans cette thèse, la biodégradation et le devenir des matières organiques lentement biodégradables contenues dans les eaux usées ont été étudiés. La thèse s'est particulièrement penchée sur l'étude du processus d'hydrolyse dans la mesure où plusieurs auteurs considèrent qu'il s'agit du processus limitant durant la dégradation des matières considérées. L'analyse des résultats de la littérature en complétés de ceux que nous avons obtenu en laboratoire a permis d'identifier et ainsi souligner les manques par rapport aux mécanismes qui régissent la dégradation des matières organiques lentement biodégradables. Ensuite, nous avons confronté ces résultats expérimentaux (expériences réalisées en batch sur des substrats type « particules décantables ») aux modèles conventionnels du traitement des eaux mais aussi à d'autres modèles moins usuels afin d'évaluer les performances de ces derniers à décrire l'hydrolyse des différents substrats. La difficulté de ces modèles à décrire la diversité des situations rencontrées nous a amené à développer un nouveau modèle qui tient compte des propriétés physiques et géométriques du substrat et qui permettrait d'améliorer la caractérisation du processus d'hydrolyse. Enfin, nous nous sommes intéressés à la distinction d'une biomasse hydrolytique dans la masse cellulaire totale et de déterminer son origine. Il a été clairement démontré que l'hydrolyse des PSS dans les procédés à boues activées était plus impactée par les bactéries indigènes, initialement adsorbées dans le réseau, que par les bactéries exogènes, en provenance d'un inoculum de boues activées.

RESUME EN FRANÇAIS (VERSION LONGUE)

Dans ce travail, nous nous sommes intéressés à la biodégradation et au devenir des matières décantables issues des eaux résiduaires urbaines. Elles constituent une grande partie de la pollution contenue dans cette dernière (jusqu'à 75% en DCO). La majorité de ces matières sont retenues par le décanteur primaire dans les stations d'épuration (STEP) qui en disposent.

Durant des décennies, la dégradation de ces matières n'a pas été considérée car leur élimination n'est pas problématique dans la mesure où elles sont retenues par le décanteur secondaire de la STEP. Néanmoins, une partie de ces matières atteignent le bassin biologique et leur nature "lentement biodegradable", couplée à de faibles âges de boue, entraine leur accumulation dans les boues biologiques, ce qui, d'une part, altère la qualité des boues secondaires produites et, d'autre part, génère des quantités de boues excédentaires supplémentaires à traiter, ce qui, en conséquence, augmente considérablement les frais de fonctionnement de la STEP. Pourtant, ces matières décantables sont une source de carbone intéressante pour réaliser le traitement de l'azote (dénitrification) et du phosphore, d'une part, et la production de biogaz, d'autre part. Ainsi, une meilleure caractérisation de ces matières (évaluation de leur degré d'oxydation) permettrait de les valoriser et maitriser la qualité des boues secondaires.

La dégradation de ces matières nécessite une étape préalable d'hydrolyse enzymatique. Plusieurs auteurs ont montré qu'il s'agit du processus limitant lors de leur élimination. Actuellement, l'outil incontournable et indispensable pour caractériser le processus d'hydrolyse dans le traitement des eaux est la modélisation. Elle permet à la fois de prédire le comportement de ces matières mais aussi et surtout de mieux comprendre les mécanismes qui les régissent. De nombreux modèles ont été développés à cet effet, notamment les modèles ASM (Henze et al., 1987 ; Gujer et al., 1995 ; Gujer et al., 1999). Néanmoins, ces ils ne sont pas toujours efficaces car la définition même de l'hydrolyse est encore très floue. En réalité, ce mécanisme est assez complexe car il intègre plusieurs processus de type physique (transport and adsorption des microorganismes à la surface du substrat), biologique (sécrétion des enzymes hydrolytiques) et aussi de type chimique (composition chimique).

La partie bibliographique de cette thèse a montré qu'il y avait très peu d'auteurs qui se sont intéressé par le passé à ces matières, notamment aux interactions entre celles-ci et les microorganismes. D'ailleurs, dans les modèles ces interactions sont traduites par un rapport de concentration. Or, la surface de substrat biodisponible dépend de ces propriétés physiques, notamment la taille des particules, qui diminue au cours du temps (dégradation). Cette partie a aussi mis en évidence le peu d'informations concernant le mode d'action et la provenance des

bactéries avec un potentiel hydrolytique. Dans les modèles conventionnels, la concentration en biomasse est souvent considérée comme étant la concentration en bactéries hydrolytiques. Or, dans le cas d'une boue activée par exemple, la quantité de biomasse hydrolytique dépend fortement de sa nature et de l'âge de boue.

Pour apporter notre contribution à l'étude et la compréhension des mécanismes d'hydrolyse des matières décantables, nous avons réalisé une palette d'expériences en utilisant des respiromètres de type « batch », dans lesquels nous avons suivi la biodégradation de matières décantables issues d'effluents réels de différentes origines (prélevées en amont et en aval du réseau d'assainissement), de différentes formes (fibres de papier toilette des particules de blanc d'œuf de forme sphérique) et de différentes tailles (petites et grosses particules de blanc d'œuf). Nous avons ensuite confronté les résultats expérimentaux obtenus aux modèles. En parallèle du suivi respirométrique de ces expériences, nous avons réalisé un suivi analytique (DCO particulaire et ammonium) afin de contraindre ces modèles et donc de tester leurs limites.

Dans le premier chapitre de résultats, nous nous sommes intéressés à examiner les réponses respirométriques obtenues pour les différents substrats mais aussi quelques résultats de la littérature. Les temps caractéristiques de ces expériences varient de quelques heures (environ 6 heures) à plusieurs jours (>10 jours). Ce qui a amené à nous questionner sur l'aspect "bioaccessibilité" du substrat par les microorganismes, qui est étroitement liée à la structure (taille, forme…) et les propriétés biochimiques (composition) du substrat. Les profiles respirométriques obtenues peuvent être globalement subdivisés en deux catégories : les matière décantables issues d'une eau usée prélevé au niveau de la STEP (en aval du réseau) étaient caractérisées par un profile respirométrique qui présentait un pic initial et une diminution monotone de l'activité biologique alors que celles issues d'une eau usée prélevé en amont du réseau ainsi que les substrats modèles (papier toilette, cellulose, xylan) présentaient deux phases, soit, une augmentation progressive de l'activité biologique jusqu'à un pic (un maximum), ensuite, l'activité diminuait jusqu'à atteindre une valeur proche de la respiration endogène. De plus, une phase de latence initiale a été systématiquement observée. Ces résultats couplés aux évolutions de la DCO particulaire et à l'ammonium nous permet conclure que le degré de colonisation (contamination) du substrat par les bactéries à l'état initial était certainement un facteur clé pour expliquer ces différences.

Dans le second chapitre, afin de mieux comprendre le processus d'hydrolyse, nous avons confronté les résultats expérimentaux obtenus à la modélisation. Ainsi, nous nous sommes intéressé à évaluer les modèles conventionnellement utilisés dans le traitement des

eaux en condition aérobie (les modèle UCT et de Contois), mais aussi un modèle plus communément utilisé pour les processus en condition anaérobie et qui considère l'évolution dynamique de particules de forme sphérique (SBK). La première conclusion était que la plupart des expériences nécessitaient la prise en compte de deux substrats différents avec des propriétés biocinétiques différentes. Ensuite, nous avons montré que seulement une partie de la biomasse était des bactéries hydrolytiques. Le reste étant sans doute de la matière inerte et des bactéries sans potentiel hydrolytique. Néanmoins, à ce stade nous n'avons pas pu définir, ni la concentration précise de ces bactéries, ni leur origine. De plus, les modèles utilisés n'ont pas toujours été efficaces et souvent ils n'arrivent à décrire que des cas bien spécifiques.

Ainsi, dans le troisième chapitre de résultats, nous avons proposé une nouvelle approche de modélisation qui intègre les aspects physiques du processus d'hydrolyse au sens propre (il a été appelé : M_SBK), en prenant en compte les propriétés physiques (densité) et géométriques (forme, taille) des substrats et les bactéries. Ce modèle est basé sur le modèle ASM-1 et prend en compte l'étape de colonisation du substrat par les bactéries hydrolytiques. Le modèle M_SBK a réussi à décrire avec précision les substrats complexes, se présentant avec une distribution de tailles de particules (matières décantables, papier toilette) alors qu'il n'a pas réussi à décrire correctement les petites et grosses particules de blanc d'œuf simultanément. Néanmoins, le modèle reste plus réaliste que les modèles conventionnels car, d'un point de vue qualitatif, il représente bien l'effet de la modification de la taille des particules (surface spécifique). L'évaluation théorique du modèle (indépendamment de résultats expérimentaux) a montré des aspects intéressants, notamment l'effet de la taille et de la forme des particules mais aussi l'impact de la distribution de taille des particules sur les réponses respirométriques. Ce qui confère à ce modèle un rôle d'outil de compréhension des mécanismes qui régissent les matières décantables. D'ailleurs, il a aussi montré une importante influence du degré de contamination initial du substrat par les bactéries sur les comportement biocinétiques simulés.

Dès lors, l'objectif du dernier chapitre de résultats était de définir les rôles et les origines des populations bactériennes qui interviennent durant la biodégradation des matières décantables : toutes les populations bactéries ont-elles un potentiel hydrolytique ? Sont-elles issues de la source de bactérie externe (dans notre cas, une boue activée) ou proviennent-elles du substrat lui-même (initialement adhérées) ? Pour répondre à ces questions mais aussi pour quantifier avec précision la quantité de bactéries hydrolytiques nous avons utilisé une approche de modélisation originale, basée sur ASM-1, qui comprend un second type de bactéries qui ne sont capables, ni d'hydrolyser le substrat, ni de consommer les produits issus de l'hydrolyse. Les conclusions étaient que la boue activée contenait finalement très peu de bactéries

hydrolytiques et que leur quantité diminuait quand le degré de contamination (colonisation) augmentait. D'ailleurs, elles ne participent pas à la dégradation des matières décantables prélevées en aval du réseau d'assainissement qui ont été hypothétiquement considérées au départ comme étant hautement contaminées. Dans ce dernier cas, le modèle indique que ce sont les bactéries initialement adhérées au substrat qui étaient responsables de leur hydrolyse. Ces bactéries, dîtes « indigènes », se sont certainement développées à l'intérieur du réseau d'assainissement, c'est-à-dire, en amont de la STEP.

NOMENCLATURE

A	Substrate available surface area [m^2]
A_{XCB_cyl}	Available substrate surface area of a cylindrical particle [m^2]
A_{XCB_sph}	Available substrate surface area of a spherical particle [m^2]
$A_{XOHO,\ ads}$	Adsorbed heterotrophic bacteria surface area [m^2]
$AlCl_3$	Aluminium chloride
AS	Activated sludge
ASM	Activated sludge model
ATP	Adenosine triphosphate
ATU	N-Allylthiourea
BOD	Biological oxygen demand [$mgO_2.L^{-1}$]
BOD_5	5-days biological oxygen demand [$mgO_2.L^{-1}$]
BSA	Bovine serum albumin
b_{OHO}	Endogenous respiration rate for active biomass [d^{-1}]
Cellulose_COD	Cellulose concentration [$mgCOD.L^{-1}$]
COD	Chemical oxygen demand [$mgCOD.L^{-1}$]
COD_P	Particulate COD [$mgCOD.L^{-1}$]
COD_S	Soluble COD [$mgCOD.L^{-1}$]
COD_T	Total COD [$mgCOD.L^{-1}$]
C_{av}	Constant in the PBM [$m^2.\ gCOD^{-1}$]
DHM	Dual hydrolysis model
DNA	Deoxyribonucleic acid
DWW	Domestic wastewater
d_{XOHO}	Diameter of a single heterotrophic microorganism [µm]
d_{XCB_cyl}	Diameter of a cylindrical particle of substrate [µm]
$d_{XCB\_cyl,\ ini}$	Initial diameter of a cylindrical particle of substrate [µm]
d_{XCB_sph}	Diameter of a spherical particle of substrate [µm]
$d_{XCB\_sph,\ ini}$	Initial diameter of a spherical particle of substrate [µm]
EP	Egg white particles
EDTA	Ethylenediaminetetraacetic acid
EPS	Extracellular polymeric substances
ER	Endogenous respiration
$FeCl_3$	Iron chloride
FOHM	First-order hydrolysis model
FODHM	First-order dual hydrolysis model
f_{av}	Surface to volume ratio variable [m^{-1}]
f_{ma}	Maximum adsorbable fraction [$mgCOD.mgCOD^{-1}$]
$f_{XU\_Bio,\ lys}$	Inert fraction of the biomass [$mgCOD.mgCOD^{-1}$]
IAWQ	International Association on Water Quality
Inoc_COD	Inoculum concentration [$mgCOD.L^{-1}$]
i_{N_XBIO}	Ammonia content of heterotrophic biomass [$mgN.mgCOD^{-1}$]
i_{N_XU}	Ammonia content of particulate unbiodegradable organics [$mgN.mgCOD^{-1}$]
k_{ADS}	Adsorption constant [$kg.m^{-5}.\ d^{-1}$]

k_{SBK}	Surface-based hydrolysis rate constant for XC_B [kg. m^{-5}. d^{-1}]
k_{SBK_1}	Surface-based hydrolysis rate constant for XC_{B1} [kg. m^{-5}. d^{-1}]
k_{SBK_2}	Surface-based hydrolysis rate constant for XC_{B2} [kg. m^{-5}. d^{-1}]
k'_{SBK}	Modified surface-based hydrolysis rate constant for XC_B [$kg^{1/3}$. m^{-1}. d^{-1}]
K_La	Oxygen transfer coefficient [h^{-1}]
$K_{SB,\ OHO}$	Half-saturation coefficient for growth [mgCOD.L^{-1}]
$K_{SH,\ hyd}$	Half-saturation coefficient for hydrolysis of S_H [mgCOD.$mgCOD^{-1}$]
$K_{XCB\_PSS\_SB,\ hyd}$	Half-saturation coefficient for hydrolysis of XC_{B_PSS} [mgCOD.$mgCOD^{-1}$]
$K_{XCB\_SB,\ hyd}$	Half-saturation coefficient for hydrolysis of XC_B [mgCOD.$mgCOD^{-1}$]
$K''_{XCB\_SB,\ hyd}$	Modified half-saturation coefficient for hydrolysis of XC_B [m^2.m^{-2}]
$K_{XCB1\_SB,\ hyd}$	Half-saturation coefficient for hydrolysis of XC_{B1} [mgCOD.$mgCOD^{-1}$]
$K_{XCB2\_SB,\ hyd}$	Half-saturation coefficient for hydrolysis of XC_{B2} [mgCOD.$mgCOD^{-1}$]
$K_{XCB\_PSS\_SB,\ hyd}$	Half-saturation coefficient for hydrolysis of XC_{B_PSS} [mgCOD.$mgCOD^{-1}$]
L_{XCB_cyl}	length of a cylindrical particle of substrate [µm]
$L_{XCB\_cyl,\ ini}$	initial length of a cylindrical particle of substrate [µm]
m_S	Specific rate of substrate utilization for maintenance [gCOD/gCOD]
M_SBK	Modified surface-based kinetic model
N_{DP}	Denitrification potential [gN. L^{-1}. h^{-1}]
n_{XOHO}	number of heterotrophic bacteria [-]
n_{XCB_cyl}	number of cylindrical substrate particles [-]
n_{XCB_sph}	number of spherical substrate particles [-]
OUR	Oxygen uptake rate [mgO_2. L^{-1}. h^{-1}]
PBM	Particle breakup model
PBS	Polybutylene succinate
PCL	Polycaprolactone
PHA	Polyhydroxyalkanoate
PHB	Polyhydroxybutanoate
POM	Particulate organic matter
PSS	Particulate settleable solids
PSS_COD	Particulate settleable solids concentration [mgCOD. L^{-1}]
$q_{SH\_SB,\ hyd}$	Hydrolysis rate constant for hydrolysis of S_H [d^{-1}]
$q_{XCB\_PSS\_SB,\ HYD}$	Hydrolysis rate constant for XC_{B_PSS} [d^{-1}]
$q_{XCB\_SB,\ HYD}$	Hydrolysis rate constant for hydrolysis of XC_B [d^{-1}]
$q_{XCB1\_SB,\ HYD}$	Hydrolysis rate constant for hydrolysis of XC_{B1} [d^{-1}]
$q'_{XCB\_SB,\ HYD}$	Modified hydrolysis rate constant for hydrolysis of XC_B [mgCOD. $mgCOD^{-1}$. d^{-1}]
$q''_{XCB\_SB,\ HYD}$	Modified hydrolysis rate constant for hydrolysis of XC_B in M_SBK [mgCOD.L^{-1}.d^{-1}.m^{-2}]
$q_{XCB2\_SB,\ HYD}$	Hydrolysis rate constant for hydrolysis of XC_{B2} [d^{-1}]
$q'_{XCB1\_SB,\ HYD}$	Modified hydrolysis rate constant for hydrolysis of XC_{B1} [d^{-1}]
$q'_{XCB2\_SB,\ HYD}$	Modified hydrolysis rate constant for hydrolysis of XC_{B2} [d^{-1}]
$q_{XCB\_PSS\_SB,\ HYD}$	Hydrolysis rate constant for XC_{B_PSS} [d^{-1}]
RBCOD	Readily hydrolysable COD [mgCOD.L^{-1}]

SBCOD	Slowly hydrolysable COD [mgCOD.L^{-1}]
RMS	Root mean square
rO_2	Dissolved oxygen concentration decrease [mgO_2. L^{-1}. h^{-1}]
SBK	Surface-based kinetic model
SBK	Dual hydrolysis surface-based kinetic model
SS	Suspended solids [g.L^{-1}]
SRT	Sludge retention time [d]
$S_{B,\,hyd}$	Soluble biodegradable COD [mgCOD.L^{-1}]
S_{O2}	Dissolved oxygen [mgO_2.L^{-1}]
S_{NH4}	Dissolved ammonia [mgN.L^{-1}]
$S_{U,\,INF}$	Influent unbiodegradable soluble organics [mgCOD.L^{-1}]
T	Temperature [°C]
TOC	Total organic carbon
TDS	Total dissolved solids
TP	Toilet paper
TS	Total solids
TSS	Total suspended solids
VSS	Volatile suspended solids
WW	Wastewater
WWTP	Wastewater treatment plant
X_T	Total cellular biomass
X_{OHO}	Heterotrophic biomass concentration [mgCOD.L^{-1}]
$X_{OHO,\,ads}$	Adsorbed heterotrophic biomass [mgCOD.L^{-1}]
$X_{OHO,\,bulk}$	Heterotrophic biomass present in the bulk phase [mgCOD.L^{-1}]
X_{OHO_ER}	Heterotrophic biomass of the inoculum [mgCOD.L^{-1}]
$X_{OHO\_ER\_inoc,\,ini}$	Initial concentration of inoculum heterotrophs that perform only endogenous respiration (passive bacteria) [mgCOD.L^{-1}]
$X_{OHO\_ER\_PSS,\,ini}$	Initial concentration of PSS adsorbed heterotrophs that perform only endogenous respiration (passive bacteria) [mgCOD.L^{-1}]
X_{OHO_hyd}	Hydrolytic heterotrophs concentration [mgCOD.L^{-1}]
$X_{OHO\_hyd\_inoc,\,ini}$	Initial concentration of hydrolytic heterotrophs from inoculum [mgCOD.L^{-1}]
$X_{OHO\_hyd\_PSS,\,ini}$	Initial concentration of hydrolytic heterotrophs that are adsorbed to PSS [mgCOD.L^{-1}]
X_{OHO_inoc}	Heterotrophic biomass of the inoculum [mgCOD.L^{-1}]
XC_B	Slowly biodegradable substrate [mgCOD.L^{-1}]
$XC_{B,\,ini}$	Initial concentration of slowly biodegradable substrate [mgCOD.L^{-1}]
$XC_{B\_inoc,\,ini}$	Initial slowly biodegradable matter of the inoculum [mgCOD.L^{-1}]
$XC_{B,\,NA}$	Unadsorbed slowly biodegradable substrate [mgCOD.L^{-1}]
XC_{B_PSS}	Particulate settleable solids concentration [mgCOD.L^{-1}]
$XC_{B\_PSS,\,ini}$	Initial particulate settleable solids concentration [mgCOD.L^{-1}]
$X_{U\_Bio,\,lys}$	Endogenous residue [mgCOD.L^{-1}]
$X_{U\_\,inoc,\,ini}$	Initial particulate unbiodegradable matter of the inoculum [mgCOD.L^{-1}]
$X_{U,\,Inf}$	Influent unbiodegradable solid organics [mgCOD.L^{-1}]

Y	Growth yield coefficient [mgCOD.mgCOD^{-1}]
Y_{OBS}	Observed growth yield coefficient [mgCOD.mgCOD^{-1}]
Y_{OHO}	Growth yield coefficient for heterotrophs [mgCOD.mgCOD^{-1}]
η_{OHO}	Reduction factor [-]
ρ_{XCB_cyl}	density of a cylindrical particle of substrate [kg. L^{-1}]
ρ_{XCB_sph}	density of a spherical particle of substrate [kg. L^{-1}]
ρ_{XOHO}	density of a single heterotrophic microorganism [kg. L^{-1}]
$\mu_{OHO,\,MAX}$	Maximum heterotrophic growth rate [d^{-1}]
θ	Temperature correction coefficient [-]

TABLE OF CONTENT

Literature review

Experimental and modeling material and methods

PREFACE

Domestic wastewater treatment is since decades achieved with the means of wastewater treatment plants (WWTPs). The great majority of these WWTPs use biological processes (e.g.: activated sludge) to degrade the soluble biodegradable fraction of wastewaters while physical (e.g.: sedimentation, settling) and chemical processes (e.g.: coagulation and flocculation) are employed for the elimination of the insoluble fraction. Even if the absolute majority of insoluble matter is trapped in the primary settling tank, a not inconsiderable fraction could reach the aerated tank (secondary treatment). As this matter is of a "slowly biodegradable" nature, it accumulates in the sludge faster than it is degraded (the amount of secondary sludge which is generated strongly depend on the sludge retention time).

The presence of slowly biodegradable matter in the secondary sludge however increases the amount of sludge production in WWTPs (excess sludge). Their treatment involves additional costs that represent a great part of the total WWTP operating costs (up to 60%). But, in another hand, the organic part of the sludge could be an interesting unexpansive carbon source for biogas production (methane) in anaerobic fermenters and could be utilized as an alternative carbon source (e.g.: to methanol) to eliminate nitrogen during the denitrification process and phosphorus elimination, which both require a supply of organic matter.

Nevertheless, the biodegradation of slowly biodegradable matter remains problematical as the parameters and mechanisms that control the kinetics that are involved are not well understood. It was demonstrated that the dynamic models, which were developed mainly by researchers of the International Association on Water Quality (IAWQ) group, are powerful tools for the understanding and optimization of WWTP processes. Nevertheless, they have the ability to characterize only specific cases and often present a lack of precision. A better understanding of the fate of slowly biodegradable matter is necessary in order to predict the overall WWTP performances and reduce sludge production by the same token. Moreover, a breakthrough on this issue would certainly decide about carbon orientation in WWTP units.

Thus, the objective of this thesis is to provide our contribution in the analysis and the comprehension of the mechanisms that are involved and that control the biodegradation of slowly biodegradable matter which are present in domestic wastewaters.

LITERATURE REVIEW

1. INTRODUCTION

The analysis of particulate organic matter (POM) is a generic topic in wastewater treatment plant (WWTP) processes and even in organic waste treatment. Even if the fate of high-sized (particulate) organic matter in WWTP processes was not considered as a priority, nowadays this matter is not considered anymore as a waste but as a valuable carbon source that can be utilized for the purpose of nutrient removal (nitrogen, phosphorus) after some conditioning operations (dehydration, thickening, etc.) and/or for valorisation. In the aerated tank, particulate matter is rapidly adsorbed to flocs of microorganisms and thus removed with the excess sludge. In one hand, a better handling or control of this matter would improve the overall performance of WWTPs and, in a second hand, it would contribute in the reduction of excess sludge production.

In this literature review, we will first describe the wastewater characteristics, its fractionation to underline the possible fate of particulate settleable solids, specifically in regard with nitrogen compounds removal (§2).

The second part (§3) will be dedicated to the investigation of the main mechanism which is responsible of the treatment of POM (hydrolysis) and the factors that influence the efficiency of this crucial step (bioavailability, process operating conditions, …).

In the third part (§4), we will describe the biological processes that are involved in the removal of POM (growth, endogenous respiration, cryptic growth…).

The fourth part (§5) of this chapter was devoted to the mathematical expressions that describe sludge production and the several ones that were developed by authors to represent the hydrolysis process.

In the fifth part of this chapter (§6) we will make an inventory of the studies that were achieved and the corresponding tools which were used for the purpose of POM hydrolysis comprehension.

Finally, in the conclusion (§7), we will among other things underline the limits of the modeling approaches and the main questions to be addressed in the following chapters of this thesis.

2.PRIMARY SETTLEMENT STEP: A TRAP FOR PARTICULATE SETTLEABLE SOLIDS

2.1. DOMESTIC WASTEWATERS CARBONACEOUS COMPOSITION AND FRACTIONATION

Domestic wastewaters (DWW) are heterogeneous mixtures of all kind of pollutants. The composition differs from a wastewater to another depending on wastewater origin (only domestic influent, domestic/industrial influent), location (city, country) and the size of the WWTP.

2.1.1.Chemical composition: domestic wastewaters, a complex environment

DWW are composed by simple elements, mainly carbon, nitrogen and phosphorus. Besides, there are more complex molecules (macromolecules) which are constituted by those simple elements such as amino acids, proteins and polysaccharides. Creatinine, urea, micro-pollutants, cationic and anionic detergents are also encountered but in weak quantities.

Table 1 shows the major pollutants as well as the undefined COD fraction in several case studies. A huge variability in the percentage of each major component could be observed: proteins vary between 12 and 30% of total COD, polysaccharides are comprised between 6 and 16% of total COD. It has to be mentioned that a large part of the COD remained undefined in the major studies (between 20 and 59% of the total COD).

According to Huang et *al.* (2010), fibers however represent the major part of domestic wastewaters, followed by proteins and polysaccharides with respectively 20.64, 12.38 and 10.65 % of the TOC. The fibers are of cellulosic nature and the main source of cellulose in wastewaters is toilet paper (Elefsiniotis, 1993).

Table 1: Chemical composition of domestic wastewaters at various WWTP processes stages.

Sample	Location	COD (mg/L)	Cellulose (%)	Carbohydrate (%)	Protein (%)	Lipid (%)	Other (%)	Unidentified (%)	Source
Raw wastewater	Nagoya City, Japan	446	5	15	38	N.D.	N.D.	42	Jenkins, (2013)
Raw wastewater	Shanghai, China	304[a]	N.D.	11	12	N.D.	21[b]	56	Huang et *al.* (2010)
Primary effluent[c]	Tokyo, Japan	259	N.D.	6	12	19	14	49	Tanaka et *al.* (1991)
Primary effluent	Urbana, USA	309	N.D.	6	12	82	N.D.	0	Sophonsiri and Morgenroth (2004)
Primary effluent	Compiègne, France	967	N.D.	16	18	7	N.D.	59	Dignac et *al.* (2000)
Primary sludge	N.D.	N.D.	8 - 15	N.D.	20 - 30	13 - 35	N.D.	20 - 59	Kole et *al.* (2012)

[a] Expressed in TOC (Total Organic Carbon)
[b] This value represents the percentage of fibers (which are composed by cellulose, hemicellulose and lignin)
[c] Primary effluent is wastewater after primary sedimentation (primary clarifier)

2.1.2. Wastewater fractionation approaches

Three types of wastewater fractionation were reported in this work: particle size, physical separation and COD fractionation. The last type of fractionation is currently used as a basis for the modeling of the WWTPs processes (see §5).

2.1.2.1. Particle size fractionation

Wastewaters (WW) is often classified in function of pollutant particle size. Four major fractions are classically used to define it: soluble, colloidal, supra-colloidal and settleable organic matter. In some cases, settleable is replaced by particulate to define all the pollutants in the form of particles without distinguishing suspended solids and settleable ones. Table 2 reports the different particulate cut-off sizes that were defined in some studies.

For example, Balmat (1957) defined soluble organic matter as <0.08 µm while Klopp and Koppe (1990) defined this same fraction as <0.007 µm and Guellil et *al.* (2001) as <0.22 µm.

Concerning the settleable fraction, Sophonsiri and Morgenroth (2004) defined it as the group of particles larger than 63 µm while they were defined as larger than 12 µm in Levine et *al.* (1985) and as the particle which were larger than 100 µm by Balmat (1957).

It could be noticed that there is no a consensus between the authors around the definition of these fractions. Each author defined specific cut-off sizes according to separation processes (e.g.: settling with or without the addition of coagulants/flocculants, membrane filtration, ultrafiltration, etc.).

Table 2: Summary of the cut-off sizes range for wastewater fractions (unit: µm)

Wastewater fractions				Reference
Soluble	Colloidal	Supracolloidal	Settleable	
<0.1	0.1 - 1.2	1.2 - 63	>63	Sophonsiri and Morgenroth (2004)
<0.01	0.01 - 1	>1	N.D.	Hu et *al.* (2002)
<0.1	0.1 - 1	1 - 12	>12	Levine et *al.* (1985)
<0.007	0.007 - 2	>2	>2	Klopp and Koppe (1990)
<0.08	0.08 - 1	1 - 100	>100	Balmat (1957)

2.1.2.2. Physical separation

In Guellil et *al.* (2001), settleable solids were defined not as a cut-off size range but according to a separation process (2 hours sedimentation). It is also possible to classify organic matter according to other physical separation processes such as coagulation, filterability, etc.

Figure 1 illustrates wastewater fractionation with respect to particle size versus physical separation methods.

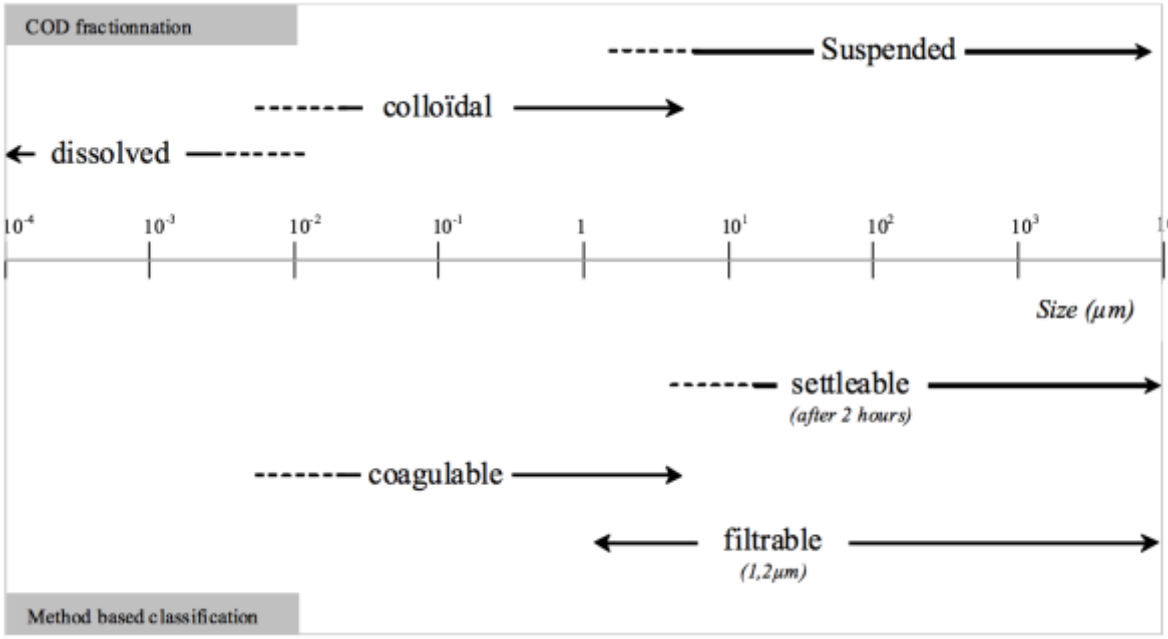

Figure 1: Wastewater fractionation with respect to particle size versus physical separation (Paul et al., 2012)

Table 3 regroups information about the percentage of organic matter in each size class. It could be noticed that the organic content of each fraction is different from an author to another. The reasons are that the wastewaters have different origins (City/country) and that they were collected at different steps of the treatment process (e.g.: raw wastewater or after primary sedimentation).

Except in Munch et *al.* (1980), the soluble fraction represented the highest organic content fraction (about 74% in Rickert and Hunter (1971)). This last one was followed by the supracolloidal fractions which could reach 50% of the total COD (Klopp and Koppe, 1990). The colloidal fraction was of the weakest percentage. Concerning the settleable fraction, it could attain till 45% of the total COD in raw wastewaters according to Guellil et *al.* (2001). In primary effluent, their amount was weaker (between 7 and 28% of total COD) as a part of the settleable solids was retained by the primary clarifier.

Table 3: Size distribution of wastewater organic matter (adapted from Sophonsiri and Morgenroth (2004))

Sample	Origin (city/country)	% of organic matter in COD				Reference
		Soluble	Colloidal	Supracolloidal	Settleable	
Raw effluent wastewater*	New Jersey, USA	41	16	28	15	Balmat (1957)[a]
Raw effluent wastewater*	N.D.	64	7	12	17	H. Heukelekian (1959)
Raw effluent wastewater*	Bernardsville, N.J., USA	40	10	21	29	Rickert and Hunter (1971)
Raw effluent wastewater*	N.D.	12	15	30	43	Munch et *al.* (1980)
Raw effluent wastewater	Connecticut, USA	47	15	38	N.D.	Hu et *al.* (2002)
Raw effluent wastewater	Maxéville, France	24		31	45	Guellil et *al.* (2001)
Settled wastewater	N.D.	9	48	15	28	Munch et *al.* (1980)
Settled wastewater	N.D.	51	8	34	7	Levine et *al.* (1985)
Settled wastewater *	Germany	38	12	50	N.D.	Klopp and Koppe (1990)
Settled wastewater	Urbana, USA	46	9	19	26	Sophonsiri and Morgenroth (2004)

* Domestic wastewater was fractionated according to Balmat's (1957) cut-off sizes
[a] In Balmat (1957), the percentage of organic matter was measured in ppm

2.1.2.3. COD fractionation

Wastewater COD fractionation is a key factor in design and operation of WWTP processes. Electron acceptor utilization would be certainly optimized if COD fractions are well defined. Since the development of the first mathematical models, the number of COD compartments increased progressively with the increase of the complexity of the wastewaters composition and properties, the development of wastewater treatment new approaches and technologies and the variations of the operating conditions during the processes. The COD fractions are defined according to chemical, physical and biological properties of the considered matter. In a chemical point of view, pollutants could be organic or mineral and could be biologically biodegradable (B) or unbiodegradable (U). In the case of physical fractionation, the conventional models of the IWA group (Gujer et al., 1999, 1995; Henze, 2008) dissociated matter into soluble, colloidal and particulate fractions as they were not degraded at the same rates (see §6). Today, the colloidal fraction and the particulate one are considered amalgamated and are noted XC according to Corominas et *al.* (2010). This way of fractionation evolved lately by the recognition of additional COD fractions which were defined not according to particle size or nature but depending on separation methods (sedimentation, filtration, etc.). For example, Orhon et *al.* (2002) found out that the whole particulate matter had different characteristics compared to the settleable fraction. Thus, he integrated in current models an additional particulate fraction that characterizes settleable matter (X_{SS}) besides the rest of particulate (hydrolysable) matter (X_{NSS}). Figure 1 illustrates the COD fractionation of a conventional domestic wastewater.

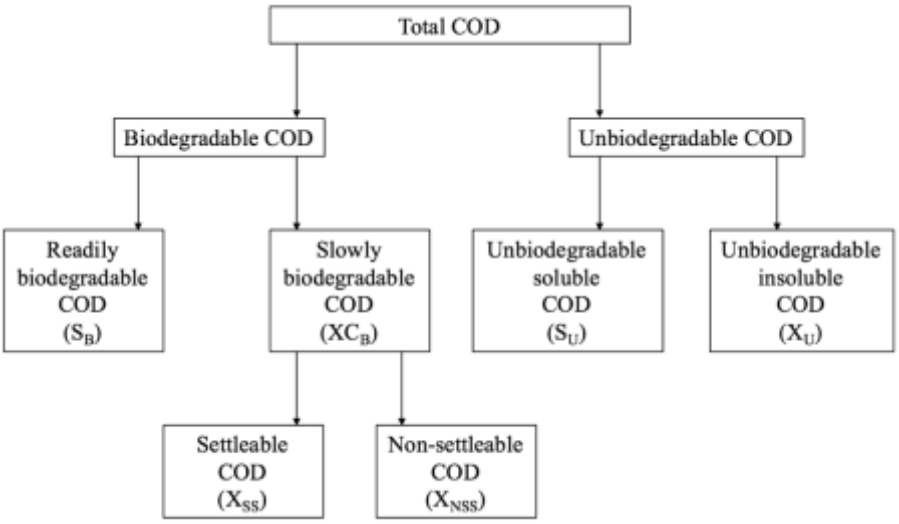

Figure 2: COD fractionation of a conventional DWW (adapted from Paul et al., 2012)

2.2. NITROGEN REMOVAL FROM WASTEWATERS

Beside phosphorus, nitrogen is one of the most watched pollutant of domestic wastewaters (DWW). It could be found in four different forms in DWW: organic nitrogen (C-N), ammonia (ionized and free ammonia), nitrite (NO_2^-) and nitrates (NO_3^-). Ammonia is however found to represent the majority of total nitrogen with about 75% (Henze, 2008).

The elimination of nitrogen is achieved with the means of a two-step process: nitrification followed by heterotrophic denitrification. The first one converts ammonia into nitrates (NO_3^-) under anoxic condition while the second one converts the resulting NO_3^- (electron acceptor) into nitrogen gas (N_2) with the presence of organic carbon (electron donor). Simplified reaction of nitrification and denitrification (with methanol) are illustrated with equations (1) and (2).

Nitrification:

$$NH_4^+ + 1.86O_2 + 1.98HCO_3 \rightarrow 0.98NO_3^- + 0.021C_5H_7NO_2 + 1.041H_2O + 1.88H_2CO_3 \quad (1)$$

Denitrification:

$$6NO^- + 5CHOH \rightarrow 3N + 5CO + 7HO + 6OH^- \quad (2)$$

The total oxidization of this matter requires satisfying a COD/N ratio of 2.86 gCOD/gN-NO_3^-. This ratio is however affected by bacterial synthesis and thus conducted by the bacterial growth yield (equation (3)). Accordingly, the values of this ratio are found to be higher in practice as reported in Table 4. Hence the organic matter entering in the oxidization basin must be tuned to optimize the process: at least ensuring nitrogen removal to meet regulatory constraints and when possible valorising the excess organic carbon instead of converting it directly into CO_2.

$$\frac{\Delta COD_s}{\Delta N - NO_3^-} = \frac{2.86}{1 - Y_{OHO}} \quad (3)$$

Table 4: COD/N ratios for different substrates

Origin of substrate	Type of substrate	COD/N (gCOD/gN-NO_3^-)	Reference
Real influent (internal C source)	Raw wastewater	3.5 – 5	Henze et *al.* (1994)
	Primary sludge hydrolysate	4.5	Æsøy and Ødegaard (1994)
External C source	Acetate	3.5 – 4.5	Isaacs and Henze (1995)
	Acetate	5.3	Tam et *al.* (1992)
	Acetate	5.9	Carley and Mavinic (1991)
	Methanol	6.2	Carley and Mavinic (1991)
	Meat extract	8.5	Carley and Mavinic (1991)
	Glucose	9	Carley and Mavinic (1991)

1.1.1. Denitrification potential and organic carbon sources for denitrification

The denitrification potential (N_{DP}) is the measurement of the electron acceptor (nitrates) demand of the available organic carbon under anoxic conditions. The organic carbon is usually provided by wastewaters (WWs) to perform the denitrification process. However, the available carbon content of WW is often not enough (when a primary settler is used). Thus, the addition of external organic carbon is achieved in order to improve the denitrification process.

1.1.1.1. Traditional external carbon sources

External carbon sources are since a long time employed for the denitrification process in systems with not sufficient available organic carbon. The most utilised organic carbon sources are methanol, ethanol and acetate (Fonseca et al., 2000; Aravinthan et al., 2001; Christensson et al., 1994; Hallin et al., 1996; Hallin and Pell, 1998; Isaacs et al., 1994). Methanol is the most efficient chemical but also the most toxic (Liu et al., 2012). All these chemicals are found to have a great denitrification potential but they also often generate troubles in the WWTP systems as nitrites accumulation and carbon breakthrough (Her and Huang, 1995). Moreover, they generate important costs. As for example, the use of methanol for the purpose of nitrogen removal represents about 70% of the total maintenance and operating costs of a the Rosedale WWTP located in Auckland, in New-Zealand (Elefsiniotis and Li, 2006).

1.1.1.2. External alternative carbon sources

Alternative substances to traditional carbon sources for denitrification are multiple: glucose syrup, sucrose, cellulose-rich materials and biodegradable polymers.

1.1.1.2.1 Carbohydrates by-products

Glucose syrup and sucrose were investigated for their denitrification potential. Glucose syrup was found to be more efficient than methanol, ethanol and acetic acid while sucrose was the least efficient for nitrates removal. This last one led to filter clog near nitrates accumulation in the supernatant contrarily to glucose syrup (Gómez et al., 2000).

1.1.1.2.2 Cellulose-rich materials

Renewable cellulose-rich materials consist in cotton (Soares et al., 2000; Volokita et al., 1996a), newspaper (Volokita et al., 1996b), wheat straw (Aslan and Türkman, 2003; Soares and Abeliovich, 1998), sawdust (Gibert et al., 2008; Israel et al., 2009; Robertson, 2010; Robertson et al., 2000; Robertson and Cherry, 1995; Schipper and Vojvodić-Vuković, 2000), straw (Shao

et al., 2009), rice husk (Xu and Shi, 2001) and corncob (Cameron and Schipper, 2010; Greenan et al., 2006; Xu et al., 2009). The inexpensiveness and effectiveness of the last material and softwood were highlighted by Gibert et *al.* (2008) and Shao et *al.* (2013). Greenan et *al.* (2006) showed that maize stalks removed a higher amount of nitrates than woodchips. A review about cellulose-rich materials underlined the inexpensiveness, availability and nontoxicity ot those materials but also several disadvantages such as higher leaching concentrations of ammonia and soluble carbon, extra biomass production and high chroma content in the effluent (Liu et al., 2012).

1.1.1.2.3 Biodegradable polymers

The utilisation of biodegardable polymers as a carbon source for nitrogen removal is not currently spread enough in worldwide research. It is still at laboratory-stage (Liu et al., 2012). Only a little number of those polymers were investigated for their denitrification potential such as PHA[1] (Boley et al., 2000), PHB[2] (an intracellular polymeric substance), intermixtures of starch and polyesters (Zhou et al., 2006; G. Z. Zhou et al., 2008). The two last biopolymers are less expansive compared to PHAs and PHB.

A summary of the denitification potential of conventional and alternative external carbon sources are reported in Table 5.

Table 5: Nitrates removal rates of the conventional and some alternative external carbon sources for denitrification

Type of substrate	Substrate	Nitrogen removal rate (mgN/L/h)	Reference
Alcohols/acids	Methanol	42 – 1,125	Park and Yoo (2009)
	Ethanol	17 – 50	Park and Yoo (2009)
Cellulose-rich materials	Cotton	2.0 – 3.4	Volokita et *al.* (1996a)
	Wheat straw	1.6 – 2.2	Soares and Abeliovich (1998)
	Rice husk	2.7 – 5.9	Xu and Shi (2001)
Biodegradable polymers	PCL[3]	21 – 166	Boley et *al.* (2000)
	PHB	7 – 41	Boley et *al.* (2000)
	PHA	11.2 – 15.8	Su et *al.* (2006)
	PBS[4]	22.9	Zhou et *al.* (2006)

1.1.2. Primary sludge as an alternative to external carbon sources for nitrogen removal

[1] Polyhydroxyalkanoates
[2] Polyhydroxybutanoate
[3] Polycaprolactone
[4] Polybutylene succinate

Primary settling is a solid-liquid separation process which consists in the removal of particulate settleable solids (PSS) which are contained in domestic WW influents. This operation is found to remove between 50 and 70% of the suspended solids (SS) and between 25 and 40% of the 5-days biological oxygen demand (DBO_5) (Tchobanoglous et al., 2003).

1.1.2.1. Primary sludge hydrolysate as a denitrifier

Primary sludge was widely investigated for its ability to provide organic carbon for nitrogen removal. It has the advantage to reduce treatment costs of about 0.2 – 0.3 \$/kgN-NO_3^- removed compared to the addition of traditional carbon sources (methanol, ethanol, etc.) (Galí et al., 2006). They are usually used in the form of hydrolysate: it is often the volatile fatty acids (VFA) of the soluble COD that result from the anaerobic fermentation of primary sludge that provides the readily biodegradable COD for denitrification (Æsøy and Ødegaard, 1994; Canziani et al., 1995; Bolzonella et al., 2001). Galí et *al.* (2006) showed that primary sludge was a good organic carbon source for nitrogen removal with a denitrification capacity up to 95%. Æsøy and Ødegaard (1994) showed that the stoichiometric ratio between organic carbon provided by the primary hydrolysate and nitrogen was 4.5 $gCOD_{VFA}$/gN-NO_3^- and was of the same range than acetate (Table 4). The maximum nitrogen removal rate of the primary sludge hydrolysate was of 37.5 mgN-NO_3^-/L/h. This is comparable to ethanol which denitrification rate was comprised between 17 and 50 mgN-NO_3^-/L/h according to Park and Yoo (2009) (Table 4). Therefore, with characteristics close to conventional external carbon sources (ethanol, methanol), primary sludge hydrolysate is found to be a great alternative to these costly components.

Among raw wastewaters and primary sludge, other possibilities of internal organic carbon sources exist. Galí et *al.* (2006) studied other carbon sources that were collected at specific points of a domestic WWTP (reject water at the exit of the treatment plant, secondary influent at the exit of the aerated tank and hydrolyzed secondary sludge) but concluded that they were not interesting as they contained weak amount of available COD and thus they led to very low denitrification capacity (5 – 6% only).

1.1.2.2. Direct feeding of the aerobic tank with primary sludge

As reported in the previously enunciated studies, primary sludge could be considered as an interesting carbon source and a good substitute for the conventional utilized chemicals (methanol, acetate, ethanol…) for nitrogen removal, with the advantage to be unexpansive compared to those chemicals. However, the utilization of primary sludge for the purpose of denitrification involves a preliminary hydrolysis of the particulate COD (PSS). For this, several

methods exist to achieve this operation such as thermal hydrolysis (Barlindhaug and Ødegaard, 1996), biological coupled with chemicals hydrolysis (Æsøy and Ødegaard, 1994; Canziani et al., 1995) and chemical hydrolysis with the means of acid and alkali (Aravinthan et al., 2001). The common point between these methods is that they are expensive and thus involve additional costs.

An original alternative would be the direct feeding of the aerobic tank with primary sludge. In this case, besides readily biodegradable COD initially present in WW, PSS would be the only carbon source available for denitrification.

To our knowledge, only the study of Tas et *al.* (2009) investigated the denitrification potential of PSS. They showed that the contribution of PSS to the total N_{DP} generated in the system can reach 40% for the domestic wastewater that was studied. It has to be mentioned that the PSS were isolated from WW in the laboratory, thus they were devoid of chemicals such as coagulants and flocculants which are usually contained in the primary sludge. Thus, distinction must be made between PSS and primary sludge.

The utilisation of PSS and more generally POM is, however, found to be limited by their bioavailability (Barret et al., 2010) and conducted by the hydrolysis process (Eliosov and Argaman, 1995; Morgenroth et al., 2002). This way, in the next section, we will describe the main mechanism (hydrolysis) which is implied in the degradation of PSS and globally POM.

3. HYDROLYSIS OF ORGANIC MATTER

Hydrolysis is an enzymatic mechanism that transforms polymers or macromolecules with important sizes into smaller units (<0.08 µm), which are able to cross the bacterial cell membrane and thus could be assimilated by bacterial cells (Levine et al., 1985). Figure 3 illustrates the hydrolysis mechanism principle (adapted from Sperandio (1998)). Higher microorganisms such as protozoa could however consume a part of the hydrolysed matter but little information is known about their mechanism of action in WWTP processes. They have the ability to release some captured hydrolysed matter to the supernatant which is then consumed by bacteria (Morgenroth et al., 2002).

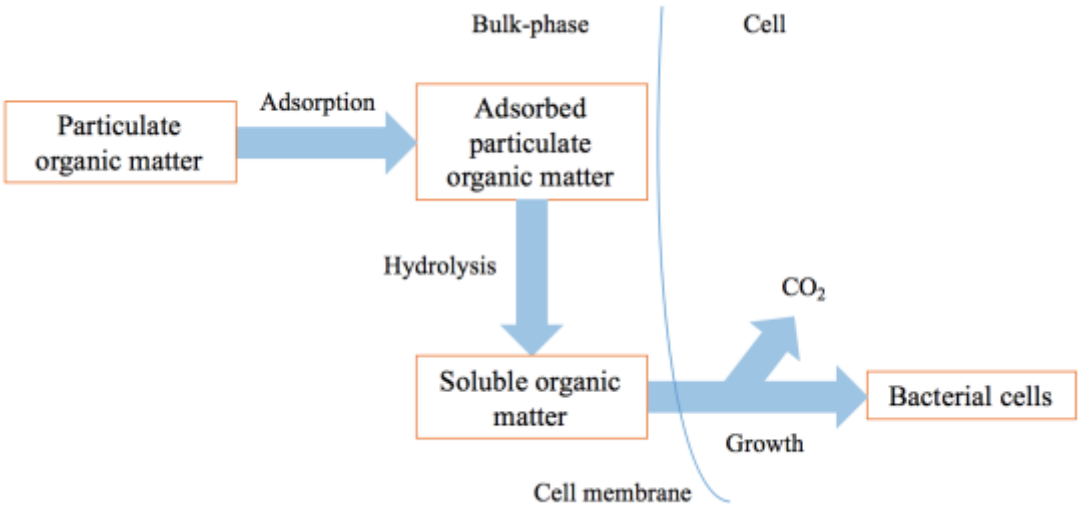

Figure 3: Hydrolysis principle scheme (adapted from Sperandio (1998))

3.1. CHARACTERISTICS OF HYDROLYSIS ENZYMES

The hydrolysis of PSS and more generally of any solid organic matter involves the presence of enzymes. Depending on their nature, each type of substrate needs a specific enzyme or group of enzymes as, for example, lipids could be hydrolyzed by lipases, proteins by proteases and carbohydrates by glucosidases (Boczar et al., 1992; Frolund et al., 1995; Nybroe et al., 1992a).

3.1.1.Origins

The origins of those enzymes are several: they can originate from the raw wastewater influent (human bodies, kitchen wastes…), activated sludge (cell autolysis) or generated during bacterial cells growth (Frolund et al., 1995; Nybroe et al., 1992a).

3.1.2.Types and location of hydrolytic exoenzymes

Most of the exoenzymes are found to be "hydrolases": Schomburg (1997) identified 197 extracellular enzymes in which 145 were hydrolases and only 11 were lyases.

Exoenzymes are found to be either attached to bacteria cell surface (ectoenzymes) or present in a free form inside the bulk phase (supernatant) or adsorbed into the exopolymeric network (Cadoret et al., 2002; Frolund et al., 1995; Vavilin et al., 1996). In the case of activated sludge. Boczar et *al.* (1992), Frolund et *al.* (1995) and Goel et *al.* (1998) reported that enzymes were attached to the surface cells in activated sludge and were negligible in the liquid phase.

The types of enzymes that are available for organic substrate depend on the characteristics of the considered sludge and/or influent: for example, Boczar et *al.* (1992) found out that both phosphatase and aminopeptidase activities were predominant in activated sludge. The phosphatase activity was also associated to the particulate fraction of primary sludge in Guellil et *al.* (2001) in addition of the protease activity. The same study underlined that glycolytic activity dominated in the colloidal fraction of wastewater.

Nevertheless, the precise location of the enzymes, whether they were cell-associated or enmeshed in the exopolymeric network is not known currently.

3.1.3.Enzymes mode of operation

Little is known about the mode of operation of exoenzymes in domestic wastewater, particularly the mechanisms that deal with proteins and lipids, which involve proteases and lipases, respectively. Nevertheless, Márquez and Vázquez (1999) revealed a large number of peptides bonds (proteins) that involve several proteases in particulate settleable solids (PSS).

There is however more information about the modes of operation of glycosidases which are involved in the hydrolysis of cellulose, for example: two distinct types of enzymes are involved in the depolymerisation mechanisms: exo- and endo-glucanase. The first one acts on the non-reducing ends while the second one acts randomly on bounds located inside the polymer chains (excluding the monomers at the extremities). Figure 4 illustrates enzymes attacks on a cellulosic chain.

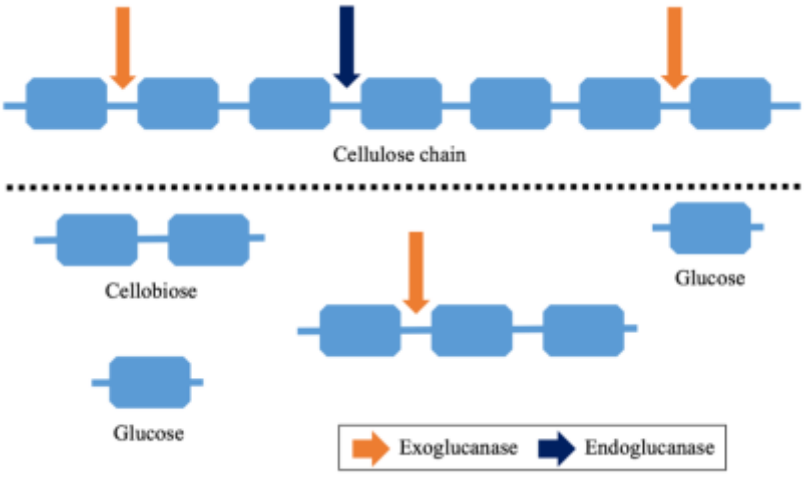

Figure 4: Schematic representation of enzymatic attacks on a cellulose chain

3.2. FACTORS THAT INFLUENCE ENZYME ACTIVITY

Exoenzymes activities could be affected by various factors mainly wastewater composition, the types and amounts of metabolic intermediates, process operating conditions such as temperature and pH (Burgess and Pletschke, 2008) and the bioavailability of the substrate.

3.2.1.Metabolic products

The presence of some metabolic intermediates and microbial products may affect negatively (inhibition) or positively (enhancement) the enzymatic activity. Watson et *al.* (2004) and Whiteley et *al.* (2002, 2003) reported that beta-glucosidases and proteases activities were reduced by the presence of specific sulphur metabolites (sulphides) and were completely inhibited with high levels of sulphate under anaerobic condition. In addition, Whiteley et *al.* (2002, 2003) reported that lipase activities increased with the presence of sulphide and sulphite but were inhibited by sulphates under anaerobic conditions.

3.2.2.pH and temperature

In order to satisfy optimal enzymatic activities, pH must be comprised in a specific range, usually 6.5 and 8.5, depending off course on the wastewater and the considered treatment process (carbon removal, nitrification, denitrification…). An ideal pH however does not exist as each process involves different microbial species (and thus different enzymes), with growth rates that are tightly linked to the pH values. In addition, each bacterial population may secrete different types of enzymes, which have also their own pH optima. In general, the defined value of pH is not optimal but a compromise between the involved enzymes and metabolic processes (Burgess and Pletschke, 2008).

The pH in treatment process is not stable and changes according to the process which is in progress: the production of CO_2 during aerobic growth and decay (endogenous respiration, maintenance, …), CO_2 removal by stripping mainly in aeration processes, ammonia conversion into nitrates for the purpose of growth of nitrifiers under anoxic conditions (nitrification), acidic acids (acetate) uptake during aerobic growth, etc. Overall, the majority of the microbial metabolic processes are affected by the pH changes (storage products generation and degradation, substrate uptake and growth of microorganisms) (Burgess and Pletschke, 2008). Thus, pH control is necessary and primordial in water treatment processes in order to handle these variations.

Concerning the temperature, it is found to influence most of the microbial reactions. Each enzyme has its own optima range of temperature. The temperature effect is usually modelled using the Arrhenius equation (4).

$$r(T) = r(20°C)\ \theta^{(T-20)} \quad (4)$$

Where θ is the temperature correction coefficient.

3.2.3.Bioavailability of substrate

Called also "bio-accessibility", bioavailability of substrate could be defined as the ability of bacterial cells to reach, hydrolyse and consume a substrate. Moreover, it could be defined as the reason why high-sized organic matter hydrolysis rate declines with time during degradation (Bansal et al., 2012). This aspect is, for example, studied in the case of lignocellulosic materials as they are recalcitrant and difficult to hydrolyse because of the presence of lignin which is found to be resistant (or refractory) to bacterial enzymatic attacks.

Many factors may influence the bioavailability of a substrate such as the chemical composition, the structure of substrate and even the involved chemical bounds (Van Der Walls, ionic, hydrogen, osidic, etc.).

3.2.3.1. Extracellular polymeric substances (EPS)

Extracellular polymeric substances (EPS) are viscous components with high molecular weights. They are mainly composed by proteins, polysaccharides beside other components such as humic acids, DNA and lipids, but in weaker amounts (Caudan et al., 2012; Nielsen et al., 1996; Pellicer-Nacher et al., 2013; Ras et al., 2008; Subramanian et al., 2010). They could be generated either during growth and decay of bacteria (see §4) or transported by wastewater influents (Ras et al., 2008; Sheng et al., 2010; Wang et al., 2007).

EPS are found to play a role in sludge settleability, dewatering and the adhesion of bacterial cells to particulate substrate (Costerton et al., 1987; Laspidou and Rittmann, 2002; Raszka et al., 2006). However, several studies underlined their weak bioavailability (Zhang et al., 2007, 2008) which prevents the access of hydrolytic enzymes to the biodegradable substrate.

3.2.3.2. Chemical bounds

Low and high energy chemical bounds are found to affect substrate bioavailability: for example, cationic bounds (e.g. Mg-Al) have the ability to enhance floc stabilisation and thus to reduce considerably their bioavailability in activated sludge process (Park et al., 2006; Park and Novak, 2007). Some chemical bounds however could be broken in order to enhance

dynamically the bioavailability of the substrate towards the bacteria. Several methods could be utilized: mechanical tools such as ultrasounds (Clark and Nujjoo, 2000; Ding et al., 2006; Schläfer et al., 2000; Tiehm et al., 2001; Yu et al., 2008; Zhang et al., 2013), chemicals such as EDTA (Ras et al., 2008; Sheng et al., 2005), heat pre-treatments (Perez et al., 2009) and enzymatic attacks with proteases and glucosidases (Caudan et al., 2012). Some of these methods could break specific bounds. For example, EDTA is able to break cationic bounds while ultrasounds (at a certain intensity) could break all the weak chemical bounds (Van der Walls, ionic, hydrogen, hydrophilic, etc.). These methods were often utilised in order to enhance anaerobic sludge fermentation by increasing the amount of soluble COD and gas production (Perez et al., 2009; Schläfer et al., 2000; Tiehm et al., 2001, 1997). Moreover, Yu et *al.* (2008) showed the benefit of ultrasounds to enhance aerobic sludge digestion.

3.3. KINETICS OF HYDROLYSIS

Enzymatic hydrolysis was found to follow the Michaelis-Menten expression by some authors while other ones identified a first-order kinetic behavior which could be explained by a weak affinity for substrate and a high rate of depolymerisation (Tauber and Stern, 1949). In practice, however, enzymatic kinetics are not necessarily utilized in order to predict wastewater treatment processes as additional processes occur during organic matter uptake by bacteria (adsorption, growth, endogenous respiration, …). More adapted models (ASM) that take into account these features were developed by the International Association on Water Quality.

3.3.1. Rate-limiting substrate uptake

During substrate elimination, the soluble biodegradable fraction or the readily biodegradable COD (RBCOD) content of WW is directly assimilated by bacteria and thus does not require a hydrolysis step. RBCOD degradation rate is then mainly conducted by the growth rate and the bacterial cells affinity to the substrate. In contrary, in the case of hydrolysable matter (e.g. SBCOD), it is the hydrolysis rate which conducts the reaction as it is often slower than the growth rate of bacterial cells. Thus, it is now commonly accepted that hydrolysis was the rate-limiting step during substrate uptake by bacteria since the earlier conventional IAWQ models that were developed by the IWA research group (Gujer et al., 1999, 1995; Henze et al., 1987). Subsequently, this was supported by several studies and authors (Morgenroth et al., 2002; San Pedro et al., 1994; Tiehm et al., 2001; Yu et al., 2008).

3.4. BACTERIAL CELLS AND PSS ADHESION

The attachment between bacterial cells and a solid substrate is called adhesion (Garrett et al., 2008). As reported in section 3.1.2., some enzymes are stuck to the bacterial cells that secreted them and thus require contact with the substrate to be hydrolysed.

Fletcher (1980) described this phenomenon as a sequence of three successive steps: (i) adsorption or accumulation of particles of substrate onto bacterial cell surface, (ii) attachment, what means the consolidation between the accumulated particles of substrate and the cell surface. This step often involves polymer bounds between bacterial cells and the substrate. Finally, (iii) colonisation, what involves growth of the bacterial cells on the substrate surface.

In WWTP processes, adhesion is known to be characteristic of microbial cultures in biofilms processes. Thusly, it was less investigated in the case of freely suspended bacterial cells processes. Spérandio (1998) has however showed that bacterial cells could proliferate at the surface of particles of PSS (fibers which could be of cellulosic nature) in a continuously stirred batch reactor (suspended bacteria). With the means of a microscopic monitoring, a layer of bacterial cells was observed. The volume of this later increased with time.

The concept of adhesion was introduced the first time in the conventional IAWQ models in the study of Dold et *al.* (1980), in which hydrolysis was described as a surface mechanism that requires a preliminary adsorption of substrate to bacterial cells surface. But, their objective was to describe the whole adhesion mechanism, including adsorption, attachment and colonisation, which are complementary mechanisms but different.

4. SLUDGE PRODUCTION IN AS SYSTEMS

In wastewater treatment systems, pollutants degraders are usually bacterial cells (besides champignons, algae, protozoa, etc.). Those bacteria have many origins and are mainly generated by human beings and their activities (raw WW) or by the treatment processes themselves. Their natures depend on the characteristics of the influent and the operating conditions of the considered process (organic load, sludge age, temperature, etc.).

Depending on the targeted pollutant and process, several species of bacteria could be involved in WWTPs: the elimination of ammonia (into nitrates) is achieved by the means of nitrifying bacteria (ammonia- and nitrite-oxidizing bacteria, AOB and NOB, respectively) under aerobic condition, nitrates are, in their turn, degraded by heterotrophic (denitrifying) bacteria under anoxic conditions. Other types of bacteria could be, however, encountered as anaerobic bacteria

that are involved in the fermentation pathways (methane production) and sulfate-reducing bacteria which proliferate generally in the sewerage system.

In the next section, we focussed on the processes that generate bacteria that are responsible of organic carbon removal under aerobic conditions.

4.1. GROWTH OF HETEROTROPHIC BACTERIA AND GROWTH YIELD

Readily biodegradable matter or RBCOD is directly consumed by heterotrophic bacteria as their size allows them to cross the bacterial cell membrane without a preliminar extracellular hydrolysis step. A part of the organic matter is oxidized in carbon dioxide and the rest is transformed into new bacteria (Metcalf and Eddy, 2003). With these information, the growth yield (noted *Y*) is calculated regarding to the electron donor (5). Typical growth yields (*Y*) are presented in the Table 6.

$$Y = \frac{\text{grams of produced bacteria}}{\text{grams of consumed substrate}} \quad (5)$$

It is also possible to estimate an observed growth yield (Y_{OBS}) which is lower than the *Y* as it takes into account the degradation of bacterial cells.

Authors used several tools to quantify bacterial cells amounts. They could be expressed in grams of VSS (or TSS) (Eliosov and Argaman, 1995; Mino et al., 1995; San Pedro et al., 1994), protein content, DNA or ATP or estimated with the means of modeling (Dimock and Morgenroth, 2006; Orhon et al., 2002). In some studies, the amounts of active bacteria were first measured in VSS according to Standard Methods (1989) then they were estimated with mathematical models.

Table 6: Typical growth yields of heterotrophs on RBCOD from WW under aerobic condition

Author	Growth yield (gCOD/gCOD)
Henze et *al.* (1987)	0.67
Ekama et *al.* (1986)	0.66
Sollfrank and Gujer (1991)	0.64
Gujer et *al.* (1995)	0.63
Torrijos et *al.* (1994)	0.61

4.2. DEGRADATION OF BACTERIAL CELLS

The decay of bacterial cells and the hydrolysis mechanism are often amalgamated and difficult to dissociate as the order of magnitude of decay rates of bacterial cells are found to be of the same magnitude as hydrolysis rates.

The concept of bacterial cells degradation or decay was (and is still) under questioning during decades as some authors measures it as a loss of bacterial activity while other ones interpreted it as a decrease of the number of active bacteria. The study of Kaprelyants and Kell (1996) indicates that bacteria could be in a dormant state and do not die. The degradation of biomass occurs during several biological processes: maintenance, cryptic growth, predation and endogenous respiration. They are presented in details in the sections below.

4.2.1.Mechanism of maintenance

The mechanism of maintenance was introduced in the activated sludge processes by Pirt (1965). It implies the utilization of additional energy supplies by active bacterial cells for the purpose of efficiency preservation. This mechanism regroups mechanical and chemical operations that are performed by bacteria. The mechanical processes consist in intracellular motility, osmotic control and molecules transport while the chemical ones are mainly membrane cell wall and flagella restructuring (Grady et al., 1999; Van Loosdrecht and Henze, 1999).

4.2.2.Endogenous respiration metabolism and cryptic growth (death-regeneration concept)

It was concluded by Porges et *al.* (1953) that endogenous respiration is when bacteria consume oxygen even in the absence of external substrate. Dawes and Ribbons (1964) found out that endogenous respiration was the result of internal reserve material (PHA, glycogen) conversion into energy for maintenance. Besides, another concept of decay raised, death-regeneration or cryptic growth, which supposes that live bacteria consume decayed microorganisms, in other terms, they degrade their own tissue (Kountz and Forney, 1959).

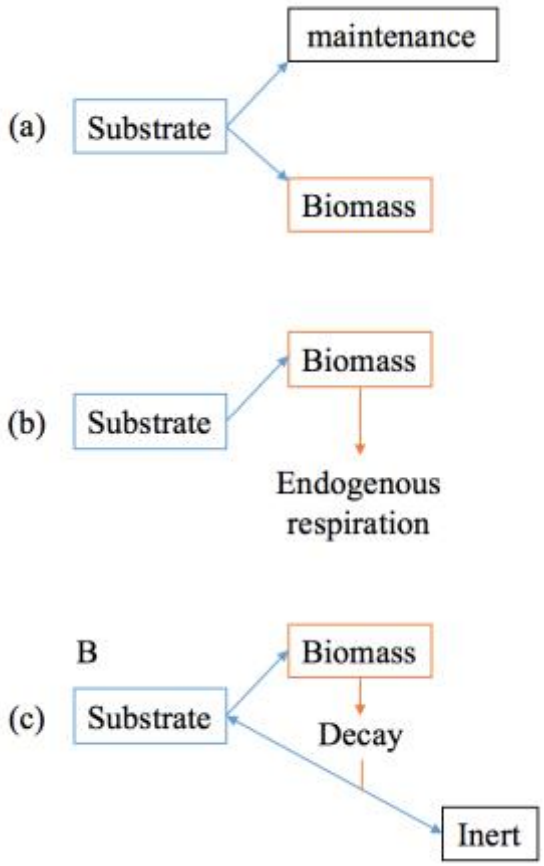

Figure 5: Schematic representation of bacteria degradation processes: (a) maintenance, (b) endogenous respiration and (c) cryptic growth (Van Loosdrecht and Henze (1999)).

4.2.3.Predation

Various kinds of microorganisms are present and encountered in activated sludge processes near conventional bacterial (heterotrophs and autotrophs) cells such as protozoa and metazoa (higher organisms). The predation of bacteria by those single celled organisms is a form of degradation or decay resulting in the deconstruction of the membrane cell wall and the release of bacteria content (proteins, DNA, etc.).

5. MATHEMATICAL DESCRIPTION OF HYDROLYSIS AND THE MAIN SLUDGE PRODUCTION PROCESSES

This section is dedicated to the mathematical description of the main mechanisms that are involved in particulate matter biodegradation (growth and decay of bacteria, adsorption, hydrolysis).

5.1. BACTERIAL GROWTH

Heterotrophs growth is represented by a Monod kinetic expression with a first-order reaction with respect to the heterotrophs concentration (X_{OHO}) (Dold et al., 1980). The mathematical expression (6)) includes a limitation term for the available biodegradable substrate ($S_{B,\,HYD}$).

$$\frac{dX_{OHO}}{dt} = -\frac{dS_{B,hyd}}{dt} = \mu_{OHO,max}\frac{S_{B,hyd}}{K_{SB,hyd}+S_{B,hyd}}X_{OHO} \quad (6)$$

Where:

X_{OHO} is heterotrophic bacteria concentration [mgCOD.L^{-1}],

$S_{B,\,hyd}$ is the rapidly biodegradable substrate concentration [mgCOD.L^{-1}],

$\mu_{OHO,\,max}$ is the maximum growth rate [d^{-1}],

$K_{SB,\,hyd}$ is the half-saturation constant for growth [mgCOD.L^{-1}].

5.2. MAINTENANCE

The following expression (equation ((7)) represents the mathematical expression of maintenance which was introduced by Pirt (1965).

$$\frac{1}{Y_{OBS}} = \frac{1}{Y_{OHO}} + \frac{m_S}{\mu_{OHO}} \quad (7)$$

Where:

Y_{OBS} is the observed growth yield [gCOD/gCOD],

Y_{OHO} is the growth yield [gCOD/gCOD],

m_S is the specific rate of substrate utilization for the purpose of maintenance [gCOD/gCOD],

μ_{OHO} is the specific growth rate [d^{-1}],

and:

$$\frac{dS_{B,hyd}}{dt} = m_S X_{OHO} \quad (8)$$

5.3. BIOMASS DEGRADATION

Two different models were proposed to describe the degradation of heterotrophic biomass: the endogenous respiration and the death-regeneration models.

The first one was introduced by Dold et *al.* (1980) and was utilized in the *IAWQ* model n°2, n°2D and n°3 (Gujer et al., 1999, 1995; Henze et al., 1999). It consists in the decrease of the concentration of bacteria with an endogenous respiration rate constant (b_{OHO}). This constant could be estimated by the monitoring of oxygen consumption under extended aeration according to Marais and Ekama (1976). Several values were identified by authors and are found to be comprised between 0.1 and 0.4 d^{-1} (Ekama and Marais, 1979; Kappeler and Gujer, 1992; Sollfrank and Gujer, 1991).

The second model (death-regeneration model) is equivalent to the first one but considers that lysis bacterial cells products are utilized by active bacteria for the purpose of aerobic growth. These two models however lead to the same result. This model was applied in the *IAWQ* model n°1 (Henze et al., 1987) to describe biomass degradation. The decay rate constants that were identified are however higher than the ones identified for the purpose of the endogenous respiration model. They are comprised between 0.4 and 0.62 d^{-1}.

In both models, a part of the lysed heterotrophic bacteria is oxidized ($1-f_{XU,\ Bio\_Lys}$) to generate energy for maintenance while the other part ($f_{XU,\ Bio\_Lys}$), which is in the particulate form, accumulates as unbiodegradable matter or endogenous residue ($X_{U\_Bio,\ Lys}$). The set of equations for each model is summarized in Table 7.

Table 7: Summary of equations for biomass degradation. With b_{OHO} the endogenous respiration rate constant, b'_{OHO} is the decay rate constant [mgCOD. mgCOD $^{-1}$. d^{-1}]; $f_{XU\_Bio,\ Lys}$ and $f'_{XU\_Bio,\ Lys}$ is the inert fraction of heterotrophs [mgCOD. mgCOD $^{-1}$]; $X_{U\_Bio,\ Lys}$ is the endogenous respiration residue and XC_B is the slowly biodegradable matter [mgCOD. L^{-1}].

Mechanism	Endogenous respiration (Dold et *al.* (1980))	Death-regeneration (Henze et al., 1987)
Schematic representation	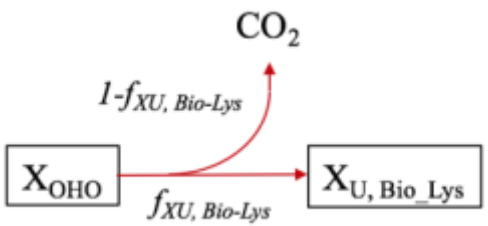	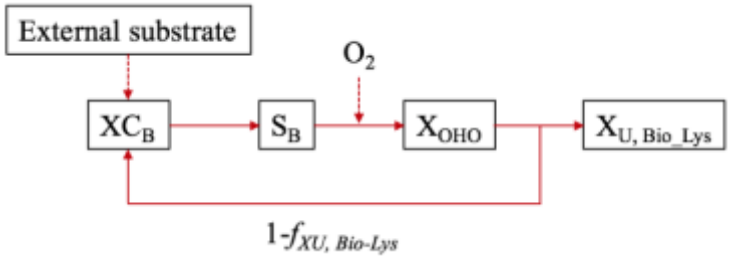
$\frac{dX_{OHO}}{dt}$	$-b_{OHO}X_{OHO}$	$-b'_{OHO}X_{OHO}$
$\frac{dX_{U_{Bio,lys}}}{dt}$	$-f_{XU_{Bio,lys}}\frac{dX_{OHO}}{dt}=f_{XU_{Bio,lys}}b_{OHO}X_{OHO}$	$-f'_{XU_{Bio,lys}}\frac{dX_{OHO}}{dt}=f'_{XU_{Bio,lys}}b'_{OHO}X_{OHO}$
$\frac{dXC_B}{dt}$		$(1-f'_{XU_{Bio,lys}})b'_{OHO}X_{OHO}$

The recent study of Ramdani et *al.* (2012) has however proved that the endogenous residue of activated sludge could be degraded but at a very low rate compared to the earlier identified values (0.005 d^{-1} and 0.012 d^{-1} in an anaerobic unit and an alternating aerated/non-aerated unit, respectively). The mechanisms of biomass degradation are however still not well understood. In current studies, the endogenous respiration model is more frequently utilized compared to the death-regeneration model and the endogenous respiration rate constant is often fixed to one of the standard values which were identified in the past. A summary of the decay rate constants (b_{OHO}) and the bacteria inert fraction ($f_{XU,\ Bio\_Lys}$) that are reported in the literature at 20°C are presented in Table 8.

Table 8: Summary of the decay rate constants (b_{OHO}) and the bacteria inert fraction ($f_{XU,\ Bio\_Lys}$) that are reported in the literature (at 20°C) for endogenous respiration and death-regeneration models.

Model	b_{OHO}	$f_{XU,\ Bio\_Lys}$	Reference
Endogenous respiration	0.24	0.2	(Marais and Ekama, 1976)
	0.24	N.D.	(Sollfrank and Gujer, 1991)
	0.1 – 0.4	0.2	(Kappeler and Gujer, 1992)
	0.12	0.15	(Metcalf and Eddy, 2003)
	0.18	0.23	(Henze et al., 1999)
Death-regeneration	0.62	0.08	(Henze et al., 1987)
	0.4	0.1	(Gujer et al., 1995)

5.4. HYDROLYSIS

5.4.1.Stoichiometry of models

Several approaches were proposed these last decades to describe hydrolysis of slowly biodegradable COD in WWTP processes. The first modeling approach was based on the growth of a unique bacterial population on both readily and slowly biodegradable COD (Stenstrom, 1976). The distinguishing of hydrolysis appeared in Ekama and Maris (1979). They suggested that two distinct bacterial populations are involved: a hydrolytic biomass that grows-up on the hydrolysis products and another bacterial population that consumes RBCOD that is initially present in the influent. They also introduced the mechanism of adsorption, assuming that substrate adsorbs, first, to biomass to perform hydrolysis. Later, Henze et *al.* (1987) introduced the one-step hydrolysis process in the IAWQ model n°1 which consists in the hydrolysis of SBCOD into RBCOD, which is consumed by the same bacterial population. This hypothesis was then utilized as a basis for the following activated sludge models (Gujer et al., 1999, 1995; Henze et al., 1999). Sollfrank and Gujer (1991) proposed a model that considers one bacterial population that grows-up on multiple SBCOD fractions. This last model inspired Orhon et *al.*

(1998) who splitted hydrolysable matter into two distinct fractions in the dual hydrolysis model (DHM). A schematic representation of each model is presented in Figure 6. Stoichiometry of the enunciated models are presented in Table 9.

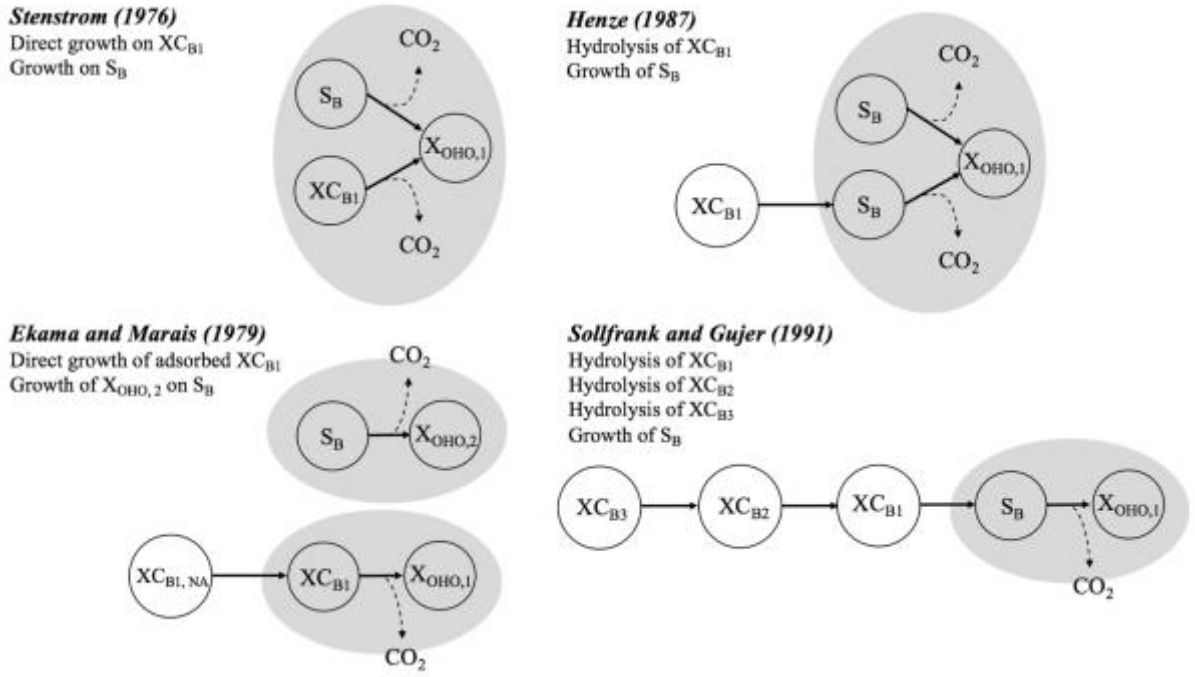

Figure 6: Schematic representation of the developed hydrolysis models

Table 9: Models stoichiometry (adapted from Morgenroth et *al.* (2002))

Process	XC_{B1}	XC_{B2}	XC_{B3}	$XC_{B1,\,NA}$[1]	S_B	S_{O2}	$X_{OHO,\,1}$	$X_{OHO,\,2}$
Stenstrom (1976)								
Growth on XC_{B1}	$-1/Y_{OHO}$					$-(1-Y_{OHO})/\,Y_{OHO}$	1	
Growth on S_B					$-1/Y_{OHO}$	$-(1-Y_{OHO})/\,Y_{OHO}$	1	
Ekama and Maris (1979)								
Adsorption of hydrolysable COD	-1			1				
Direct growth on adsorbed COD				$-1/Y_{OHO}$		$-(1-Y_{OHO})/\,Y_{OHO}$	1	
Growth on soluble COD					$-1/Y_{OHO}$	$-(1-Y_{OHO})/\,Y_{OHO}$		1
Henze et al., (1987)								
Hydrolysis of XC_{B1} into S_B	-1				1			
Growth on S_B					$-1/Y_{OHO}$	$-(1-Y_{OHO})/\,Y_{OHO}$	1	
Sollfrank and Gujer (1991)								
Hydrolysis of slowly hydrolysable COD (XC_{B1})	-1	1						
Hydrolysis of intermediate hydrolysable COD (XC_{B2})		-1	1					
Hydrolysis of rapidly hydrolysable COD (XC_{B3})			-1		1			
Growth on S_B					$-1/Y_{OHO}$	$-(1-Y_{OHO})/\,Y_{OHO}$	1	

[1] $X_{CB1,\,NA}$ is the non-adsorbed slowly biodegradable matter

5.4.2.Mathematical expressions

Hydrolysis is described in literature with several mathematic expressions that were developed according to more or less strong hypothesis and experiments. An adsorption step is however found to be required before the hydrolysis step occurs. The following section was dedicated to describe, first, the preliminary adsorption step prior hydrolysis, then, the conventional and less conventional hydrolysis models.

5.4.2.1. Adsorption, a preliminary step to hydrolysis

As reported in section 6.5, Dold et *al.* (1980) considers that bacteria, first, adsorb to SBCOD, then, extracellular enzymes perform hydrolysis. The mechanism of adsorption was introduced in a biological model by Ekama and Marais (1979) then Dold et *al.* (1980). The mathematical expression (Equation (9)) was based on Blackwell (1971)).

$$\frac{dXC_{B,NA}}{dt} = -\frac{dXC_B}{dt} = -K_{ADS} XC_{B,NA} X_{OHO} (f_{ma} - \frac{XC_B}{X_{OHO}}) \quad (9)$$

Where XC_B is the slowly biodegradable COD concentration [mgCOD.L^{-1}], $XC_{B,NA}$ is the non-adsorbed slowly biodegradable COD concentration [mgCOD.L^{-1}], X_{OHO} is the heterotrophs concentration [mgCOD.L^{-1}], K_{ADS} is the adsorption constant [kg.m^{-5}. d^{-1}], f_{ma} is the maximum adsorbable fraction [mgCOD. mgCOD^{-1}]. In this model, adsorbed particulate substrate is limited by the amount of active bacteria and the maximum adsorbable substrate fraction, f_{ma}. The value of this constant was estimated by Dold et *al.* (1980) (f_{ma}=1), Spérandio and Paul (2000) (f_{ma}=1.06) and Lagarde et *al.* (2005) (f_{ma}=4), assuming two SBCOD fractions.

5.4.2.2. Surface-based hydrolysis expression

Based on the same studies (Dold et *al.* (1980)), Henze et al. (1987) considered hydrolysis as a surface-limiting process in the IAWQ model n°1. The corresponding mathematical expression includes a hydrolysis rate constant ($q_{XCB\_SB,HYD}$) and depends on the biomass concentration (X_{OHO}). The surface phenomenon aspect is described with a limitation term which includes the ratio between substrate and biomass which are both expressed in mass concentration (equation (10)).

$$\frac{dXC_B}{dt} = -q_{XCB_{SB},hyd} \frac{XC_B / X_{OHO}}{K_{XCB,hyd} + XC_B / X_{OHO}} X_{OHO} \quad (10)$$

Where $q_{XCB\_SB,hyd}$ is the hydrolysis rate constant [d^{-1}] and $K_{XCB,hyd}$ is the half-saturation constant for hydrolysis [mgCOD. mgCOD^{-1}].

5.4.2.3. Effect of the electron acceptor

A reduction factor (noted η_{OHO}) was introduced in equation (10) because it was found that electron acceptor affects the hydrolysis rates. In the IAWQ model n°1 (Henze et al., 1987), η_{OHO} was equal to 0.4 and in the IAWQ model n°2 (Gujer et al., 1995) η_{OHO} was equal to 0.1 or 0.6 for anaerobic and anoxic conditions respectively (for θ=20°C). In this case, the hydrolysis rate could be expressed by equation (11).

$$\frac{dXC_B}{dt} = -\eta_{OHO} q_{XCB_{SB},hyd} \left(\frac{XC_B / X_{OHO}}{K_{XCB,hyd} + XC_B / X_{OHO}} X_{OHO} \right) \quad (11)$$

San Pedro et *al.* (1994) showed that there is no a significant effect of electron acceptor during the hydrolysis of particles of starch and finally this reduction factor was however abandoned in the IAWQ model n°3 (Gujer et al., 1999).

5.4.2.4. First-order models

Depending on the substrate to biomass ratio (high or low X_{CB}/X_{OHO}), equation (10) could be simplified to a first-order hydrolysis model with respect to substrate when $XC_B << X_{OHO}$ ($K_{XCB,\,HYD} >> XC_B/X_{OHO}$) (equation(12)) (Henze and Mladenovski, 1991; Janning et al., 1998; Kappeler and Gujer, 1992; San Pedro et al., 1994; Sollfrank and Gujer, 1991; Spérandio and Paul, 2000) or into a first-order hydrolysis model with respect to biomass when $XC_B >> X_{OHO}$ ($K_{XCB,\,HYD} << XC_B/X_{OHO}$) (equation (13)) (Goel et al., 1997), where $q'_{XCB\_SB,\,hyd} = q_{XCB\_SB,\,hyd}/K_{XCB,\,hyd}$, or a zero-order hydrolysis with respect to substrate (equation (14)), with $q''_{XCB\_SB,\,hyd} = q'_{XCB\_SB,\,hyd} X_{OHO}$.

$$\frac{dXC_B}{dt} = -q'_{XCB_{SB},hyd} XC_B \quad (12)$$

$$\frac{dXC_B}{dt} = -q'_{XCB_{SB},hyd} X_{OHO} \quad (13)$$

$$\frac{dXC_B}{dt} = -q''_{XCB_{SB},hyd} \quad (14)$$

Where $q'_{XCB\_SB,\,hyd}$ is the modified hydrolysis rate constant [mgCOD. mgCOD $^{-1}$. d^{-1}].

5.4.2.5. Influence of substrate particle size on the hydrolysis rate

The study of Balmat (1957) highlighted the importance of separating particles of substrate in function of their size and characterized them separately. He concluded that the hydrolysis rate increases while particle size decreases. Moreover, Aldin et *al.* (2011) found out that when particle size decreases from 500 to 50 µm, the hydrolysis rate coefficient (with a first-

order model) increased from 0.034 to 0.298 d^{-1} (more than 8 times) for particles of casein under anaerobic conditions.

Based on Hobson (1987), Sanders et *al.* (2000) introduced a model (Surface-Based Kinetic Model, noted SBK) that correlates hydrolysis rate with particle size when they investigated spherical fresh potatoes particles biodegradation under anaerobic conditions (Model 5). The model assumes that active bacteria secrete exo-enzymes that cover all the substrate surface area. The consumption of the substrate leads to the decrease of the particle diameter and thusly to the increase of the specific surface area of the substrate which is accompanied by the increase of the hydrolysis rate. The kinetic expression of the hydrolysis could be written as below (Equation (15)).

$$\frac{dXC_B}{dt} = - k_{sbk} A \tag{15}$$

In the previous expression, k_{sbk} is a surface-based hydrolysis constant [$kg.m^{-5}.d^{-1}$] and *A* is the available substrate (XC_B) surface area [m^2]. In this model, it is assumed that hydrolysis continuously reduces substrate particle diameter. The surface area of similar shaped particles could be replaced by $(XC_B)^{2/3}$ and equation 4 could be simplified by equation (16).

$$\frac{dXC_B}{dt} = - k'_{sbk} (XC_B)^{2/3} \tag{16}$$

Where k'_{sbk} is a modified surface-based hydrolysis constant [$kg^{1/3}.m^{-1}.d^{-1}$].

Dimock and Morgenroth (2006) studied the hydrolysis of particles of hard-boiled egg whites (proteins) under aerobic conditions. They developed a model (Particle breakup Model, noted PBM) which assumes that particles of substrate are broken down into smaller units during hydrolysis. This results in the increase of the specific surface area of substrate which is colonized by bacteria. The corresponding mathematical expression that describes this model is presented in equation (17).

$$\frac{dXC_B}{dt} = - q'_{XCB_{SB},hyd} f_{av} XC_B \tag{17}$$

Where f_{av} is a surface to volume ratio variable [m^{-1}]. This last one is defined as a state variable that increases during particle breakup and is directly related to the hydrolysis rate as reported in equation (18).

$$\frac{df_{av}}{dt} = C_{av} \frac{dXC_B}{dt} \tag{18}$$

Where C_{av} is a constant that correlates f_{av} to the hydrolysis rate [m^2. $gCOD^{-1}$].

5.4.2.6. Summary of the hydrolysis rate expressions

The previously enunciated hydrolysis rate expressions are reported in Table 10. In addition, other less conventional models that describe hydrolysis are reported in the same table: a zero-order hydrolysis expression (Model 7) was used in Andrews and Tien (1977), Cliff (1980), Dennis and Irvine (1981), Larsen (1992) and Tsuno et *al.* (1978). In Eliosov and Argaman (1995), Mino et al. (1995) and Sollfrank and Gujer (1991), hydrolysis was function of both substrate and biomass concentrations (Model 8).

Table 10: Hydrolysis mathematical expressions (adapted from Morgenroth et *al.* (2002)

Model	Mathematical expression	Authors
1	$q_{XCB_{SB},hyd}\frac{XC_B/X_{OHO}}{K_{XCB,hyd}+XC_B/X_{OHO}}X_{OHO}$	Dold et al., (1980); Mino et al., (1995); Orhon et al., (2002); Stenstrom (1976); Tas et al., (2009)
2	$q_{XCB_{SB},hyd}\left(\frac{XC_B/X_{OHO}}{K_{XCB,hyd}+XC_B/X_{OHO}}X_{OHO}+\eta_{OHO}\frac{XC_B/X_{OHO}}{K_{XCB,hyd}+XC_B/X_{OHO}}X_{OHO}\right)$	Gujer et al., (1999, 1995); Henze et al., (1999, 1987)
3	$q'_{XCB_{SB},hyd}XC_B$	Spérandio and Paul (2000); Balmat, (1957); Gujer and Henze, (1991); Kappeler and Gujer, (1992); Mino et al., (1995); Sollfrank and Gujer, (1991)
4	$q'_{XCB_{SB},hyd}X_{OHO}$	Goel et al. (1997)
5	$k_{sbk}(XC_B)^{\frac{2}{3}}$	Hobson (1987); Sanders et al., (2000)
6	$q'_{XCB_{SB},hyd}f_{av}XC_B$	Dimock and Morgenroth (2006)
7	$q''_{XCB_{SB},hyd}$	Andrews and Tien (1977); Cliff (1980); Dennis and Irvine (1981); Larsen (1992) and Tsuno et *al.* (1978)
8	$q'_{XCB_{SB},hyd}XC_BX_{OHO}$	Eliosov and Argaman (1995); Mino et *al.* (1995) and Sollfrank and Gujer (1991)

6. EXPERIMENTAL EVALUATION OF HYDROLYSIS

In this part, we will discuss the several ways that were utilized by authors to study hydrolysis, highlighting the differences between the methods, their efficiency and their limits. Morgenroth et *al.* (2002) made an inventory of the main experimental methods that are encountered in hydrolysis literature: enzymatic activity monitoring, measurement of hydrolytic products (well defined substrates, model substrates), bulk phase mass balance and assessment of the biological activity by the means of respirometry.

6.1. ENZYMATIC ACTIVITY MONITORING

Enzymes are found to be responsible of the hydrolysis of slowly biodegradable COD in activated sludge processes. Their amount is however difficult to assess with conventional methods as mass or molecular concentration direct measurement. It is then often characterized in terms of enzymatic rates (Holme and Peck, 1993). Nevertheless, it is difficult to assess in the case of mixed bacterial cultures such as activated sludge in which numerous bacterial populations (enzymes) and substrates (with not well defined characteristics) are involved.

Several studies investigated this way to evaluate hydrolysis (Dold et al., 1991; Klapwuk et al., 1974; Teuber and Brodisch, 1977; Vaicum et al., 1965), however, they concerned activated sludge (AS) only. To our knowledge, no study investigated wastewater real influent before or after physical separation (raw WW, primary sludge, etc.). In the studies dealing with AS, extracellular enzymes activities were mainly monitored (Frolund et al., 1995; Nybroe et al., 1992; Sridhar and Pallai, 1973; Thiel and Hattingh, 1967; Boczar et al., 1992). A correlation between the hydrolysis activity and COD loading rate in AS systems was found by Richards et *al.* (1984) while (Nybroe et al., 1992b) found out a relation between the enzymatic activity and biomass concentration. In contrary, San Pedro et *al.* (1994) showed that biomass concentration did not affect the hydrolytic activity.

6.2. MEASUREMENT OF HYDROLYTIC PRODUCTS

Experiments were carried out on specific substrates with well-known hydrolysis products. The investigated model substrates were, for example, starch (Larsen and Harremoës, 1994; Mino et al., 1995; San Pedro et al., 1994), dextran (Confer and Logan, 1997b, 1997a; Haldane and Logan, 1994), BSA (Confer and Logan, 1997b, 1997a), dextrin (Confer and Logan, 1997b, 1997a; Ubukata, 1999). In contrary, Henze and Mladenovski (1991) utilized real influent (raw WW) and monitored ammonia as a hydrolysis product. Nevertheless, they hypothesized that ammonia was not uptaken by bacteria during growth as it was negligible.

This could be open to criticism because at least a small amount of ammonia is consumed by bacteria what leads certainly to biased results.

6.3. MEASUREMENT OF BIOMASS ACTIVITY WITH RESPIROMETRY

Respirometry is a powerful technique for monitoring, control and modeling of WWTP processes. It consists in the measurement of the biological oxygen consumption. During years, this technique was used to assess the biological oxygen demand (BOD) with the means of the BOD-test. But, this one was replaced progressively since the sixties with an alternative respirometric tool as it was not efficient for the study of the biokinetic behavior of wastewaters (Spanjers et al., 1996). This last one allows measuring the rate of oxygen consumption by microorganisms while permitting regular sampling for subsequent analysis.

6.3.1.Bulk-phase mass balance

As the overall respirometric profile characterizes the entire mechanisms that occur during substrate consumption by biomass (mainly growth, hydrolysis and decay), it is then difficult to accurately dissociate them one by one with this technique. The conventional IAWQ model n°1 (Henze et al., 1987) suggests however that the slowly biodegradable COD fraction could be determined with the means of COD mass balance after the determination of the rest of the COD fractions (S_B, $X_{U,INF}$, X_{OHO}, etc.).

6.3.2.Kinetic constants determination

Since the insoluble fraction of wastewater was considered as a valuable carbon source and thus as matter of interest, several studies investigated this fraction. Hydrolysis is characterized with the calculation of hydrolysis coefficients (hydrolysis rate constant, half-saturation constant for hydrolysis etc.). Currently, the majority of the studies utilized respirometry and model calibration for this purpose (Ginestet et al., 2002; Henze et al., 1987; Kappeler and Gujer, 1992; Okutman et al., 2001; Orhon et al., 1999, 1998; Sollfrank and Gujer, 1991; Spérandio and Paul, 2000; Tas et al., 2009; Wu and He, 2012). Table 11 shows some hydrolysis coefficients that were calculated under aerobic conditions.

Earlier studies considered hydrolysable matter as a unique COD fraction (XC_B) which includes all the SBCOD (Henze et al., 1987; Mino et al., 1995; Orhon et al., 1999; Sollfrank and Gujer, 1991; Spérandio and Paul, 2000; Wu and He, 2012). The values of the hydrolysis rate constants that were identified are ranged between 1.5 and 3.7 d^{-1}. They illustrate globally slowly hydrolysable COD. In contrast, recent studies splitted hydrolysable matter into rapidly

hydrolysable COD (S_H) and slowly hydrolysable COD (XC_B). The values of the identified hydrolysis coefficients are ranged between 1.6 and 3.8 d^{-1} for S_H and 1.2 and 1.9 d^{-1} for XC_B. Physical separation of WW led to the rise of the settleable COD fraction, noted "X_{SS}" in Orhon et *al.* (2002). The hydrolysis rate constants that were identified are ranged between 0.25 et 1.2 d^{-1} (Ginestet et al., 2002; Okutman et al., 2001; Orhon et al., 2002; Tas et al., 2009). They represent the weakest values compared to S_H and XC_B. It should be mentioned that Orhon et *al.* (1998) showed that considering two distinct particulate substrates (XC_B and X_{SS}) was more suitable than considering a unique single hydrolysable fraction to describe DWW degradation. The goal of SBCOD splitting into several COD fractions was to improve the characterization of the hydrolysis mechanism and thus gain more insight in the description of the global WW elimination. Overall, it could be noticed that hydrolysis coefficients vary from a model to another and from a study to another. Moreover, the kinetic characteristics of the hydrolysis process vary also depending on substrate physical properties (soluble, insoluble, settleable, etc.).

Table 11: Hydrolysis coefficients determined in studies achieved under aerobic conditions and corresponding models (see §5 for detailed information of the employed models)

Experiment	Model	Hydrolysis coefficients							Reference
		$q'_{XCB\_SB,\ hyd}$ (d^{-1})	$q_{SH\_SB,\ hyd}$ (d^{-1})	$K_{SH,\ hyd}$ (gCOD/gCOD)	$q_{XCB\_SB,\ hyd}$ (d^{-1})	$K_{XCB,\ hyd}$ (gCOD/gCOD)	$q_{XSS\_SB,\ hyd}$ (d^{-1})	$K_{XSS,\ hyd}$ (gCOD/gCOD)	
Isolated WW settled COD OUR monitoring during 20 hours	FOHM	2.5	-	-	-	-	-	-	Sollfrank and Gujer (1991)
Settled WW OUR monitoring during 6 hours	FOHM	1.5	-	-	-	-	-	-	Kappeler and Gujer (1992)
Starch degradation monitoring during 6 hours	FOHM	3.7	-	-	-	-	-	-	Mino et *al.* (1995)
Raw WW OUR monitoring during 15 hours	FOHM	3.2	-	-	-	-	-	-	Spérandio and Paul (2000)
Raw WW OUR monitoring during 5 hours	FOHM	3	-	-	-	-	-	-	Wu and He (2012)
Isolated WW Settled COD and settled WW OUR monitoring during 6.5 hours	DHM	-	3.2	0.04	1.4	0.28	1	0.10	Tas et *al.* (2009)
Isolated WW Settled COD and settled WW OUR monitoring during 10.8 hours	DHM	-	1.6	0.05	-	-	0.8	0.05	Orhon et *al.* (2002)
Isolated WW Settled COD and settled WW OUR monitoring during 6.5 hours	DHM	-	3.8	0.20	1.9	0.18	1.2	0.10	Okutman et *al.* (2001)
Raw WW OUR monitoring during 4 hours	DHM	-	3.1	0.20	1.2	0.50	-	-	Orhon et *al.* (1998)
Raw WW OUR monitoring during 24 hours	IAWQ-1	-	-	-	3	0.03	-	-	Henze et *al.* (1987)
Raw WW OUR monitoring during 5 hours	IAWQ-1	-	-	-	2.6	0.45	-	-	Orhon et *al.* (1999)
Isolated WW settled COD monitoring during 10 days	IAWQ-1	-	-	-	-	-	0.25 – 1.05	0.33 – 0.95	Ginestet et *al.* (2002)

6.4. MODEL SUBSTRATES: A TOOL FOR DISSOCIATING MECHANISMS

The characterisation of hydrolysis with real wastewaters influents is complicated as it is probably affected by the presence of other COD fractions. Thus, some authors proposed to characterise hydrolysable fractions alone by investigating well-defined artificial substrates in order to avoid interferences with the other COD fractions (e.g.: rapidly biodegradable COD, influent unbiodegradable COD, etc. see §2.1.2) (Dimock and Morgenroth, 2006; Haldane and Logan, 1994; Larsen and Harremoës, 1994). However, the disadvantage of this approach is that those substrates were not really representative of the SBCOD which is found to be a complex mixture with different chemical composition (Sophonsiri and Morgenroth, 2004). One other approach was to isolate SBCOD from real WW influent with the means of separation processes (filtration, sedimentation, etc.). Okutman et *al.* (2001) and Orhon et *al*. 2002) isolated settleable COD by settling raw WW in 150 litters settling device. They used a batch-aerobic respirometer and combined the experimental oxygen consumption profile and modeling to characterize this fraction.

A further investigation around hydrolysis evaluation is found to be necessary in order to define with more precision and thus control the SBCOD in WWTP processes. Our results as well as typical OUR profiles that are found out in literature are presented and discussed in details in the first chapter of results.

7. CONCLUSION AND THESIS OBJECTIVES

Particulate organic matter, namely primary sludge and PSS, are found to be a serious alternative to traditional external carbon sources for nitrogen removal during denitrification process.

This fraction of domestic wastewaters is degraded via the hydrolysis process which is achieved with the means of exoenzymes (mainly hydrolases). However, this step is affected by various factors such as structure, process operating conditions (pH and temperature) and the bioavailability of the substrate.

Hydrolysis was investigated either using real influent (wastewaters) or model substrates such as starch, carbohydrates (cellulose, dextran, dextrin), proteins, etc. Model substrates are interesting because of the absence of soluble COD which affects hydrolysable matter determination but do not characterise the whole wastewater.

Various tools and procedures were performed in order to handle hydrolysable matter but respirometry coupled to modeling is currently found to be the most used and efficient way to study hydrolysis on a long-term basis.

Several mathematical expressions were proposed to describe hydrolysis: zero-order reaction, first-order reaction with respect to substrate or biomass, etc. Surface-based kinetics are, however, the most used ones as hydrolysis is accepted to be a surface dependant phenomenon. Nevertheless, these mathematical expressions do not describe correctly the surface-limitation aspect as none of them takes into account in the literal sense the tight link between the bioavailable surface area and particle physical properties (size, density, shape…) which was demonstrated in various studies (Aldin et al., 2011; Balmat, 1957; Dimock and Morgenroth, 2006; Hobson, 1987; Sanders, 2001). The limits of the hydrolysis models that were presented in this chapter are summarised below:

a) About the model structures:

Studies about hydrolysis exhibit various mathematical expressions to describe the hydrolysis mechanism and hydrolysis models. Simple models (first order with respect with the XC_B concentration) were proposed at the beginning in order to describe an exponential decrease of OUR against time. However, it rapidly appeared clear that a dependence on the ratio between cell biomass and the particulate organic matter should be considered in order to better represent the experimental results and notably an increase in OUR during the first phase of degradation.

Nevertheless, it is still not clear what should be the form of the dependence between catalyst (cell biomass) concentration and the particulate organic matter concentration. Some models considered adsorption of particulate matter on biomass to take into account a notion of available surface area in dynamic evolution against time. Pursuing the same objective, other authors have proposed to consider directly the available surface area of the particulate matter. For some models like the surface-based hydrolysis models (based on Henze et al. (1987)), the term of substrate limitation is expressed in mass concentration between substrate and biomass, which is misleading as their available surface area depend on their physical properties such as particle size. For other models, a geometric form of the particles was postulated. Consequently, a simple geometric shape (corresponding to spherical particles) was chosen which does not always correspond to the diversity of forms encountered in practice. More complex models mixing the previously proposed mathematical expressions were also proposed to make the model more universal.

b) About the model validation:

From this literature review, it can be seen that the number of experiments on particulate organic matter is very low despite the importance of the hydrolysis reaction in global processes such as sludge production, denitrification and so on. Most of these experiments were performed on model substrates and the others on substrates coming from specific conditions. The knowledge on the active cell biomass added in the experiments is very poor. Hence, there is a need for further experiments on particulate organic matter of different origins with different physical and biochemical characteristics. A better knowledge on the biomass brought to the system is required.

c) About model calibration:

Our literature review showed that various methods for the characterisation of hydrolysis could be used in theory. However, in practice most of them are difficult to implement in a complex mixture and in the presence of particulate matter. Respirometry based on the acquisition of OUR against time appears to be one technics of choice in order to calibrate a model. Nevertheless, additional information should be added in order to reduce the degree of freedom of the model and increase the reliability of the calibration procedure.

Our literature review showed that the capacity of these models to describe the cases encountered is clearly questioned. As very few experiments on slowly biodegradable particulate matters

were performed in the past and as the information obtained from these experiments was partial, there is a need for additional results in order to evaluate the proposed models and in fine for getting more insights on hydrolysis mechanisms and on parameters influencing these reactions.

The purpose of this thesis is to contribute to the analysis and the representation of the hydrolysis mechanisms that occur during the biodegradation of particulate settleable solids. To satisfy this objective, experiments were performed on the wastewater settleable fraction (real influent) but also on simple (model) substrates that are commonly present in wastewater (fibers of toilet paper, cellulose, xylan…). All the experiments were held by monitoring the biodegradation of the substrates under aerobic conditions.

This thesis is composed by six chapters, including this literature review, a chapter which is dedicated to the materials and methods that were utilised and four chapters of result:

- **Chapter I: "Typical kinetics for particulate substrates under aerobic conditions"**

The aim of this chapter was to compare and analyse the results of the various studies that investigated particulate substrates under aerobic conditions.

- **Chapter II: "Experiment and WWTPs model confrontation: are existing models able to describe particulate organic matter experiments?"**

The goal of this chapter was to test existing models (conventional and unconventional models) on contrasted trends of OUR profile in order to assess their performances and thus underline their limits and weaknesses.

- **Chapter III: "Introduction of the colonization phase in a novel conceptual framework to describe hydrolysis under aerobic conditions"**

In this chapter, we will test additional features in the conventional models in link with the geometrical properties of the substrate in order to match a little more with reality and thus enhance hydrolysis description.

- **Chapter IV: "Biodegradation of wastewater particulate settleable solids (PSS): Distinguishing a specific hydrolytic microbial population in the total cellular biomass"**

In this chapter, we will be interested in the differentiation of the roles of the different bacterial populations (hydrolytic, passive…) depending on their origins in order to increase the description and the comprehension of the mechanisms of hydrolysis of real particulate settleable solids (PSS) and artificial ones (toilet paper, cellulose).

EXPERIMENTAL AND MODELING MATERIAL AND METHODS

1. INTRODUCTION

This chapter is dedicated to the detailed description of experimental and modeling materials and methods that were utilized in this thesis.

The first part of this chapter was attributed to the biological reactors description. They were described in terms of type (batch, fed-batch, etc.), components (pH regulation, stirring system, etc.) and geometry. The calculation methods that were applied to obtain the intended experimental data were presented as well.

The second part was dedicated to the description of the utilized reagents, to wit, the substrates and inocula (or biomass): their origin, their chemical composition, their physical properties and conditioning protocols were presented in details.

The third part of this chapter includes the entire measurement methods, namely the chemical and biochemical analysis, and equipment when necessary.

In the fourth part, the experiments performed in this thesis were described in terms of reactor operating conditions, substrates and inocula concentrations.

Finally, the fifth and last part deals with mathematical tools that were performed for model calibration (experimental data description and prediction).

2. EQUIPMENT USED FOR BIOLOGICAL KINETICS EVALUATION

Respirometric tools were employed since the beginning of the 20th century with the discovery of the activated sludge processes (ASP). It was found that the rate with what bacteria consume oxygen during organic matter elimination is an important factor for processes characterisation and an efficient indicator for process condition. Two distinct respirometric techniques were developed till now: the BOD-test, which consists in the measurement of the oxygen consumption. It was used since the initial period of ASP. Besides, respirometry, which raised later (in the sixties), consists in the direct measurement of the rates of oxygen consumption. These techniques and the corresponding equipment are presented in details below.

2.1.RESPIROMETRY

Even if closed respirometry is often employed as it allows determining directly the oxygen consumption rate, open respirometry was selected in this thesis. Indeed, with this configuration, we avoid structure deconstruction of particulate substrates which could occur as the bulk phase moves between the reactor and the OUR measurement cell in closed respirometry.

2.1.1.Experimental design

Contrary to the biological oxygen demand test (BOD), this technique allows sampling along the kinetic. A detailed diagram of the respirometer is presented in Figure 7. It includes an aerated reactor made of glass with a working volume of 1.5 (or 2) litters. Stirring was performed with a IKA®-WERKE RW16B motor equipped with a six-blade Rushton-type stirrer. The pH was measured (SI ANALYTICS electrode type H8481HD) and regulated. Temperature and dissolved oxygen were measured (VISIFERM™ DO, HAMILTON). The entire parameters were continuously monitored with a computer. A water jacket was used to maintain the liquid phase temperature at 20 ± 0.5°C.

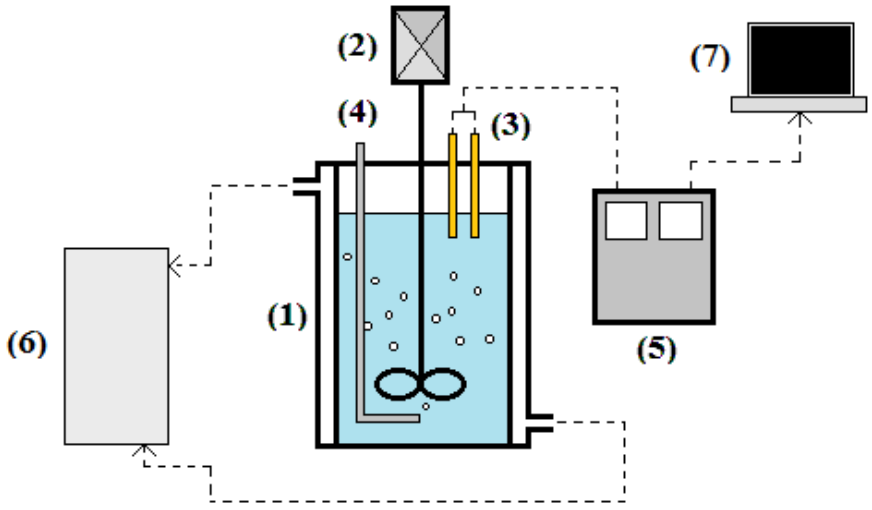

Figure 7: Diagram of the respirometer. (1) Reactor with water jacket, (2) motor, (3) pH and oxygen probes, (4) oxygen source, (5) pH and oxygen monitoring and regulation controller, (6) cryostat, (7) computer

2.1.2.Calculations for open respirometry

2.1.2.1.OUR measurement

The oxygen uptake rate (OUR) in the batch respirometer is assessed by measuring dissolved oxygen concentration decrease and the oxygen surface mass transfer that occur in the reactor (19)).

$$OUR=-\frac{d[S_{O_2}]}{dt}+K_La([S_{O_2}^*]-[S_{O_2}]) \quad (19)$$

With K_La (h^{-1}) the oxygen transfer coefficient. In this study, it was assessed for various liquid height (to take into account the sampling volume and possible evaporation) and stirring speed (which was adjusted to minimize surface transfer while maintaining proper mixing).

The K_La was estimated by measuring the oxygen concentration increase in a 0.2 µm filtered wastewater. When the oxygen concentration at saturation is known, the K_La is deducted from equation ((20)) (results in appendix 1).

$$K_La(t-t_0)=ln\left(\frac{[S_{O_2}^*]-[S_{O_2}]_0}{[S_{O_2}^*]-[S_{O_2}]_t}\right) \quad (20)$$

2.1.2.2.Biological oxygen demand

The biological oxygen demand (BOD) is calculated according to the trapezoid method numerical integration (equation (21)).

$$BOD=(t_2-t_1)\frac{OUR(t_2)+OUR(t_1)}{2} \quad (21)$$

2.1.2.3.Mass balance

Under controlled operating conditions (i.e. inhibition of nitrification) oxygen is only consumed by heterotrophic bacteria during organic carbon utilization. Oxygen mass balance was calculated in order to evaluate the correctness of the results according to equation (22).

$$COD_0=COD_t+\int_0^t OURdt \quad (22)$$

Where COD_0 (mgO_2/L) and COD_t (mgO_2/L) are respectively the chemical oxygen demand at the beginning and at the end of the experiment.

3. BACTERIA AND SUBSTRATE

3.1.INOCULUM SOURCE AND CONDITIONING

All the inocula that were used in this thesis were collected from the wastewater treatment plant (WWTP) of Ginestous which is located in the area of Toulouse (France). The considered WWTP serves a population equivalent of about 1 million residents. Biomass source was activated sludge (AS) sampled at the exit of the aerated tank. The samples were then stored between 2 and 3 days in a chamber at 4°C before each experiment.

The sludge was first concentrated by settling in a 40-L settling device then it was kept under aeration in a batch-respirometer during 4 to 8 days (depending on sludge) till it reached endogenous respiration. This last enunciated operation was applied on each sample in order to discharge the sludge from the accumulated organic matter (weak SRTs) which would affect substrate characterization. It has to be mentioned that, beside specialized (hydrolytic) bacteria, inocula may contain also nonspecialized bacterial cells near unbiodegradable matters that could come from the influent and/or generated during endogenous respiration (bacteria inert fraction).

Three different inocula were sampled during different periods of the year: autumn for AS1, winter for AS2 and spring for AS3.

The main characteristics of the collected fresh and after conditioning AS samples employed in the course of this work are presented in Table 12.

Table 12 : Main characteristics of the fresh sludge and after conditioning

Parameter	AS1		AS2		AS3	
	Fresh	Conditioned	Fresh	Conditioned	Fresh	Conditioned
SRT (days)	5	N.D.	5	N.D.	2.5	N.D.
COD_T (g/L)	3.61	6.82	4.27	7.56	3.72	3.79
COD_S (g/L)	0.10	0.16	0.04	0.33	0.05	0.14
COD_S/COD_T (g/g)	0.027	0.024	0.010	0.043	0.013	0.038
TSS (g/L)	2.69	4.74	2.75	N.D.	2.67	2.71
VSS (g/L)	2.29	3.89	2.29	N.D.	2.34	2.24
VSS/TSS (g/g)	0.85	0.82	0.84	N.D.	0.88	0.83
COD_P/VSS (g/g)	1.53	1.71	1.84	N.D.	1.57	1.63
$N\text{-}NH_4^+$ (mgN/L)	20	26	41	57	46	63
TKN (mg/L)	N.D.	N.D.	N.D.	585	308	277
Org-N/COD_P (mgN/g)	N.D.	N.D.	N.D.	73	71	59

3.2.SUBSTRATES

All the substrates that were selected in this thesis were particulate settleable solids (primary sludge) or substrates that mimic their properties (physical, chemical and/or biochemical).

Beside PSS, cellulose was investigated as it represents about 20% of primary sludge in terms of suspended solids (Honda et al., 2002). These are owing to the discharge of toilet paper which was also investigated. Near cellulose, hemicellulose is the second main biodegradable component of toilet paper (in a weaker amount). Commercial xylan was chosen to represent and study the behavior of this last one.

3.2.1.Wastewaters settleable solids or particulate settleable solids (PSS)

About 200 litters of domestic wastewater DWW were collected before the primary settling unit of the WWTP of Toulouse-Ginestous (same source as the inoculum). The pre-treated wastewater was stored in a chamber at 4°C before conditioning. The day after, 150 liters of the MWW were settled during 1 hour in a 40-L lab-scale settling device of acrylic glass material. The resulting settled fraction was once more settled in Imhoff cones during 2 hours. Three successive washing cycles have been performed in order to reduce soluble components concentrations in the final sample (settleable COD isolation). The main characteristics of the fresh and conditioned wastewater are presented in Table 13.

Table 13 : Summary of the main characteristics of the fresh pre-treated wastewater (PW-F) and after conditioning (PW-C)

Parameter	PW-F	PW-C
COD_T (g/L)	0.69	27.70
COD_S (g/L)	0.21	0.66
COD_S/COD_T (g/g)	0.30	0.02
TSS (g/L)	0.28	17.62
VSS (g/L)	0.19	15.25
VSS/TSS (g/g)	0.68	0.87
COD_P/VSS (g/g)	2.51	1.77
$N\text{-}NH_4^+$ (mgN/L)	102	80

3.2.2.Toilet paper

Commercial white toilet paper was utilized in this thesis. It was cut into about 1 cm^2 pieces to facilitate mixing.

3.2.3.Simple model substrates

Commercial reagents were used in this thesis: xylan and pure cellulose in the form of powders. These two were chosen as they represent the main biodegradable part of toilet paper components.

3.3.NUTRIENT SUPPLY

The main chemical nutrients which are required to support bacterial growth are carbon, hydrogen, oxygen, nitrogen, phosphorus and sulphates. Those mineral compounds where brought by the inorganic compounds hereinafter: potassium dihydrogen orthophosphate (KH_2PO_4), sodium phosphate dibasic (Na_2HPO_4, $12H_2O$), ammonium chloride (NH_4Cl), ferric chloride ($FeCl_3$) and magnesium sulphate ($MgSO_4$, $7H_2O$). Nutrients concentrations were calculated in order to satisfy a maximum growth yield (Y_H) of 0.44 grams of cells per gram of substrate (or 0.63 gCOD/gCOD). Nutrient limitation, especially phosphorus and nitrogen, is known to be favourable to carbon orientation into storage products and/or exopolymers (Donot et al., 2012; Goel et al., 1999). Thus, the amounts of nutrients were calculated to be provided in excess to avoid this kind of phenomena. Table 14 presents bacteria cell composition as well as nutrient needs for growth according to Metcalf and Eddy (2003).

Table 14: Bacteria cell composition and nutrient needs for a maximum growth yield of 0.63 gCOD/gCOD (Metcalf and Eddy, 2003)

Main elements	% of element/g of $C_5H_7O_2N$	% of element/gCOD of $C_5H_7O_2N$	Mg of element/gCOD of substrate (Y_{OHO}=0.63)	Element source
N	12%	8.45%	53.2	NH_4Cl
P	2%	1.41%	8.9	Na_2HPO_4, $12H_2O$; KH_2PO_4
S	1%	0.7%	4.4	$MgSO_4$, $7H_2O$
K	1%	0.7%	4.4	KH_2PO_4
Na	1%	0.7%	4.4	Na_2HPO_4, $12H_2O$
Ca	0.5%	0.35%	2.2	Tap water
Mg	0.5%	0.35%	2.2	$MgSO_4$, $7H_2O$
Cl	0.5%	0.35%	2.2	NH_4Cl
Fe	0.2%	0.14%	0.9	$FeCl_3$

4. MEDIUM CHARACTERIZATION

4.1. SAMPLING

Between 20 and 30 ml were sampled directly within the reactor under stirring with a large-opening pipette to obtain a homogeneous sample. The sampling frequency was not constant as it was adapted in function of the biological activity (OUR). A part of each sample was filtered through Whatman GF/C glass fiber filters with an effective pore size of 0.2 µm and was analysed the same day to determine the soluble parameters.

4.2. CHEMICAL AND BIOCHEMICAL ANALYSIS

A chemical and biochemical monitoring of the reactors was performed for each experiment. It includes the determination of the chemical oxygen demand (COD) with the micro-COD method using potassium dichromate (2 hours of heating at 150°C). In addition, settled COD (settleable fraction COD) was determined with the micro-COD method after 2 hours settling in Imhoff cones. Ammonia ($N\text{-}NH_4^+$) was measured on the filtered samples with respect to the *NESSLER* method. Total soluble nitrogen (TN) was measured on filtered samples with the TNM-1 unit of the SHIMADZU TOC-V_{CSN} analyzer. Total Kjeldahl nitrogen (TKN) was assessed by a BÜCHI instrument device composed by a digestion unit, a scrubber, a distillation unit and a titrator. Ionic chromatography (Dionex, DX100) was used to evaluate nitrites (NO_2^-) and nitrates (NO_3^-) in order to detect nitrification. Total and soluble sugars were measured by a High-Pressure Liquid Chromatography (Thermo Scientific, Dionex Ultimate 3000) using a sulfonated divinylbenzene-styrene copolymer column (Biorad Aminex HPX-87H) and a refractometer (ERC Refractomax S20). The determination of total sugar has been done by a prior 3 hours acid hydrolysis of the sample at 100°C. Total suspended solids (TSS) and volatile suspended solids (VSS) were assessed among Standard Methods (1989). A synthesis of the analytical methods is provided in Table 15.

Table 15: Synthesis of the chemical and biochemical analysis and the corresponding norms

Analysis	Equipment/method	Norm
Total COD	Micro-COD method using potassium dichromate (2 hours of heating at 150°C)	AFNOR NFT 90.101
Soluble COD	Micro-COD method using potassium dichromate (2 hours of heating at 150°C) after filtration through Whatman GF/C glass fiber filters (effective pore size: 0.2 µm)	AFNOR NFT 90.101
Settled COD	Settling during 2 hours in a Imhoff cone	Standard Methods
	Sonication with the BANDELIN SONOPLUS HD2200 series device with a TT13 probe (*f*=20 kHz, P=200 W) during 30 seconds	N.D.
	Micro-COD method using potassium dichromate (2 hours of heating at 150°C)	Standard Methods
$N\text{-}NH_4^+$	Micro-Nessler method	AFNOR NFT 90.015
TN	TNM-1 unit of the SHIMADZU TOC-V_{CSN} analyzer	AFNOR NFT 90.102
TKN	BÜSHI digestion unit K-435 BÜSHI scrubber B-414 BÜSHI distillation unit B-324 SCHOTT TitroLine Easy	72/23/CEE 89/336/CEE
NO_2^-	Cationic chromatography (Dionex DX-100: IC25, IonPacTM AS19)	AFNOR NFT 90.042
NO_3^-	Cationic chromatography (Dionex DX-100: IC25, IonPacTM AS19)	AFNOR NFT 90.042
TSS VSS	Centrifugation of the sample at 4,500 g during 15 minutes Drying at 105°C during 24 hours (TSS) Then drying at 500°C during 2 hours (VSS)	AFNOR NFT 90.105
Saccharides	Thermo SCIENTIFIC UltiMate 3000 (with a BioRad Aminex HPX 87H affinity column)	N.D.

4.3. MICROSCOPY: BACTERIA AND SUBSTRATE INTERACTIONS

Various microscopy tools were utilized in this study to observe the bacteria behaviours towards solid substrates.

The fluorescence-based LIFE technologies LIVE/DEAD® Backlight™ Bacterial Viability Kit L7007 was performed to distinguish between bacterial communities and the substrates. This kit

is composed by a mixture of SYTO®9 green-fluorescent nucleic stain and the red-fluorescent nucleic acid stain, propidium iodide, PI. The first component labels all bacteria in green when used alone. The second one penetrates only the damaged membranes leading in a reduction of the fluorescence of the SYTO®9 when both of them are present.

The LEICA SP2-AOBS confocal microscope which is controlled via the software LCS (Leica Confocal Software) was utilized in this study to observe bacteria and fibers interactions. It is a spectral confocal with a 405 UV laser which is able to obtain high quality images of fluorescently labelled compounds. This equipment is located at the FR-AIB in Auzeville, France. Besides this equipment, a fluorescence microscope was utilized for the same purpose.

4.3.1.1.Bacteria and fibers staining protocol

A bacterium staining was performed with the reagents enunciated above. An equivolume of SYTO®9 and PI (propidium iodide) (0.5 µl/0.5 µl) was added to 500 µl of the sample in a 6-wells plate. Then, 50 µl of calcofluor 1% was added to stain the cellulosic fibers (light blue). Then, the mixture was homogenized and kept in the dark for incubation during 5 minutes before microscopic observations.

4.3.1.2.Observation under the microscope

The following laser lines were utilized for material revelation: FITC (498-550 nm) for live bacteria, CY3 (571-630 nm) for dead bacteria and DAPI (415-450) for the cellulosic fibers. About 5 images per sample were acquired to sweep a large surface area of a microscope slide. The observations on the X, Y and Z plane allow localizing with precision the position of a bacteria toward a fiber. Figure 8 represents an image of a colonized fiber under the LEICA SP2-AOBS confocal microscope.

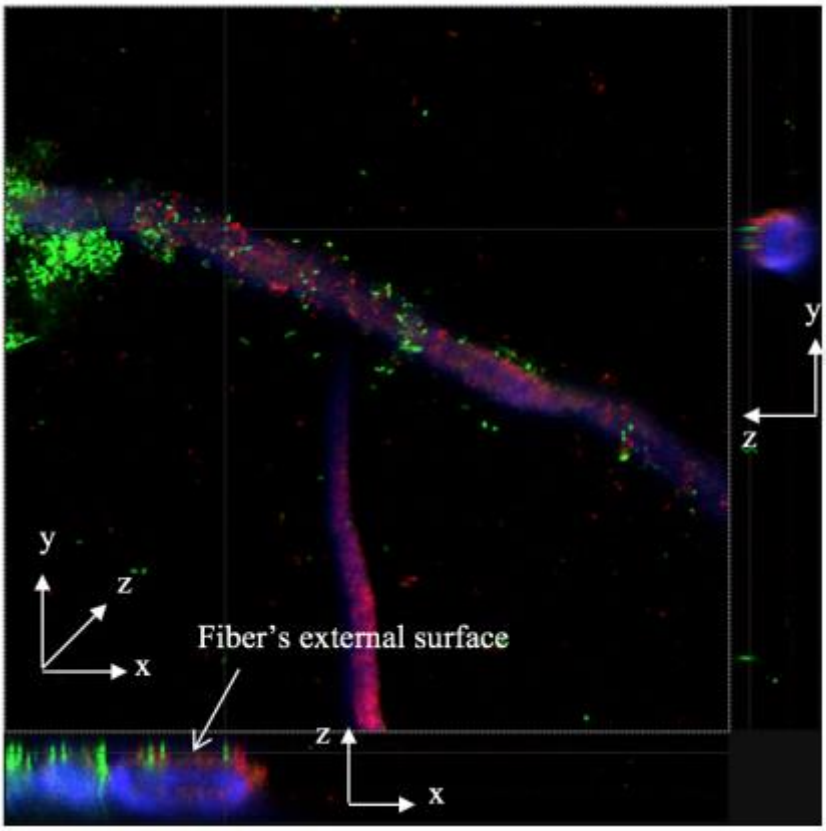

Figure 8 : Image of colonized fibers taken with the LEICA SP2-AOBS confocal microscope

5. EXPERIMENTS DESCRIPTION

All the experiments were conducted under aerobic conditions and carried out with a batch-aerobic respirometer (described in details in §2.2). They were performed at the same temperature (20°C ± 0.1°C) and the pH was maintained in the range of 6.8 and 7.2 by the means of H_2SO_4 (5%) and NaOH (20 g/L). N-Allylthiourea (20 mg/L) was added in each reactor in order to inhibit nitrification and thus avoid its contribution in the biological oxygen demand. In addition, dissolved oxygen was maintained higher than 4 $mgO_2.L^{-1}$ in each reactor in order to avoid denitrification.

Several set of experiments were performed on various substrate: particulate settleable solids (PSS), toilet paper and, simple substrates (commercial xylan and cellulose).

5.1. PARTICULATE SETTLEABLE SOLIDS (PSS) EXPERIMENTS

These experiments were performed on PSS which were conditioned in our laboratory according to the protocol presented above (§3.2.1). Two distinct batch-aerobic respirometers were used: the first one (PSS-1a) was fed PSS only and the second one (PSS-1b) with the same

amount of PSS mixed with a known amount of fresh activated sludge (AS1) which was used as an inoculum.

A high inoculum to substrate ratio (S_0/X_T) was imposed in PSS-1b in order to obtain an exploitable OUR profile (growth conditions).

5.2.TOILET PAPER EXPERIMENTS

5.2.1.Experimental set 1: batch test

A batch respirometric test was operated during 20 days. A reactor (TP-1a) was fed toilet paper that was previously in contact with an inoculum (AS2). As in PSS experiments, a high organic load of 13 gCOD/gCOD was adopted in each reactor (growth conditions) in order to obtain an exploitable OUR profile.

5.2.2.Experimental set 2: fed-batch test

A fed-batch reactor containing only toilet paper was kept under aeration (TP2-a) without OUR monitoring. Two respirometers (TP2-b and TP2-c) were fed with a mixture of toilet paper (same as TP2-a) and fresh activated sludge (AS3) that was collected in the WWTP of Ginestous-Toulouse (France). Those two reactors (TP2-b and TP2-c) were first conducted during 15 days. When the corresponding OUR profile reached a plateau (endogenous respiration phase), the reactor bulk phase of TP2-b was settled during 2h in a Imhoff cone in accordance with Standard Methods (1989). The isolated settleable fraction was kept in the reactor and was fed again the same substrate (TP-2d). Again, the final content of TP-2d (when reached endogenous respiration) was settled during 2h as after TP-2a. the isolated settleable fraction was fed the same amount of toilet paper (TP-2e).

5.3.COMMERCIAL XYLAN AND CELLULOSE EXPERIMENTS

Two batch respirometric tests were performed in the same operating conditions as PSS experiments. A Reactor (XYL) was fed a mixture of commercial xylan and fresh activated sludge (AS-3) while another reactor (CEL) was fed pure cellulose and the same AS (AS-3).

Information about the substrates and inocula as well as the operating conditions of the whole experiments presented above are reported in Table 16.

Table 16 : Experimental conditions for utilized respirometers for each experiment

Exp.	Reactor name	Substrate		Inoculum		S_0/X_T (gCOD/gCOD)	Initial pH	Dissolved oxygen (mgO_2/L) (min – max)	Thesis chapter
		Type	Initial conc. (gCOD/L)	Type	Initial conc. (gCOD/L)				
1	PSS1-a	PSS	9.23	No inoculum	-	-	6.92	3.9 – 6.3	I, II, III and IV
	PSS1-b	PSS	9.64	AS1	0.55	17.5	6.87	3.4 – 6.8	IV
	PSS1-c	PSS	9.42	AS1	2.75	3.4	6.98	3.1 – 6.2	IV
2	TP1-a	Toilet paper	8.99	AS2	0.71	13.0	6.83	4.4 – 6.6	I, II, III and IV
3	TP2-a	Toilet paper	15.2	No inoculum	-	-	-	-	IV
	TP2-b	Toilet paper	11.3	AS3	0.38 (11.68)	29.7	-	-	IV
	TP2-c	Toilet paper	10.0	AS3	1.92 (11.92)	5.2	-	-	IV
	TP2-d	Toilet paper	8.85	End of TP2-b	1.32 (10.17)	6.7	7.18	4.1 – 5.9	IV
	TP2-e	Toilet paper	9.01	End of TP2-d	1.33 (10.34)	6.8	7.14	4.0 – 5.5	IV
4	XYL	Xylan	1.00	AS3	1.02	1.0	6.92	4.7 – 8.2	I
	CEL	Cellulose	8.00	AS3	0.97	8.3	6.88	4.5 – 6.3	I, IV

6. MODEL CALIBRATION

6.1.MODELS

The mathematical models (except the developed 'colonization model') that were investigated are presented in chapter II. In all the models, the inhibition terms were suppressed. Model A1 was adapted from the IAWQ model n°1 (Henze et al., 1987). The death-regeneration model was replaced by the endogenous respiration model (they lead both to the same results) as this last one describes the increase of ammonia during bacteria decay. The rest of the models were similar to Model A1, except for the hydrolysis process: In Model A2, a first-order hydrolysis model (towards XC_B) was considered. Models B1 and B2 are Dual Hydrolysis Models adapted from Hobson (1987) as they consider two distinct solid fractions (XC_{B1} and XC_{B2}). In model B1, Contois expression was used for hydrolysis (as for Model A1) while a first-order hydrolysis model was adopted in Model B2. Models C1 and C2 are surface-based hydrolysis models (SBK model) adapted from Sanders et *al.* (2000). Model C2 considered two distinct solid fractions in addition of the surface-based hydrolysis aspect.

6.2.MODELING TOOL

Model evaluation and calibration were performed using the AQUASIM® computer program developed by Reichert (1994). It was designed for the simulation and modeling of aquatic systems in the laboratory. It allows the mathematical description of experimental sets and parameter identification.

6.3.MODELING PROCEDURE

Model calibration includes a sensitivity analysis of the state variables, kinetic parameters and stoichiometric coefficients towards the considered models followed by a parameter estimation step.

6.3.1.Sensitivity analysis

A sensitivity analysis operation was performed for each model as well as for each experiment. All the state variables, kinetic parameters and stoichiometric coefficients were considered, except those that characterize the endogenous respiration for commodity. Nevertheless, only a few ones were measured experimentally: DO, NT, $N\text{-}NH_4^+$ and COD_S in the liquid phase and the COD_P for the solid phase. The root mean square (RMS) of the absolute-relative (AR) sensitivity analysis function of the considered computer program (AQUASIM®)

was normalized by the average of the state variable. This leads to obtain the relative influence of each parameter on each state variable.

$$I=Influence(\%)=\frac{RMS}{\frac{1}{n}\sum_{1}^{n}X} \quad (23)$$

The "X" represents dissolved oxygen (S_{O2}) and/or ammonia (S_{NH4}). In this study, we chose to consider that the model is sensitive to a parameter when I>1%. Some parameters were not integrated in the sensitivity analysis operation as more the number of parameters will be important, more the parameter identification will be biased. In most of the cases, we identified only the kinetic parameters and stoichiometric coefficients that deal with the hydrolysis mechanism. The following parameters were fixed: b_{OHO}, $f_{XU\_BIO,\,Lys}$ and Y_{OHO}. It has to be noted that $\mu_{OHO,\,MAX}$ and $K_{SB,\,HYD}$ were estimated for the purpose of our PSS experiments despite their weak influence (I<1%). The reason is that their influences were found to be important during the initial short time lapse which was dedicated to S_B consumption which lasted few hours only.

6.3.2.Parameter estimation

The models were solved numerically by the mean of the "secant method" of the AQUASIM® computer program (Reichert, 1994) and the average error "*E*" was calculated with a least square method, regarding the difference between the calculated and the experimental data (equation (24)):

$$E=\frac{1}{n}\sum_{i}^{n}[X_{mod}(t_i)-X_{exp}(t_i)]^2 \quad (24)$$

The "X" represents usually the OUR in the studies that deal with WWTP processes (Cokgor et al., 2009; Dimock and Morgenroth, 2006; Ginestet et al., 2002; Orhon et al., 2002, 1998, 1997; Orhon and Sozen, 2012; Tas et al., 2009). In this work ammonia ($N\text{-}NH_4^+$) and particulate COD (COD_P) were monitored during the batch tests near the OUR. This should increase the degree of freedom on the model and, thus, constrain the mathematical model. This will help us to determine with more insight the most appropriate model and consequently enhance comprehension about what really happens during particulate organic matter (POM) elimination. As far as we know, none of the studies about long-term or short-term POM degradation utilized something else than OUR. It has to be mentioned that COD_P is the sum of the slowly biodegradable COD (XC_B), heterotrophic bacteria concentration (X_{OHO}) and the endogenous residue which is generated during endogenous respiration ($X_{U\_Bio,\,Lys}$).

7. SUMMARY

In chapter I, the experiments PSS1-a and TP1-a as well as results (experiments) picked-up from literature (Dimock and Morgenroth, 2006; Spérandio, 1998; Orhon et al., 2002; Tas et al., 2009) were investigated. The OUR was monitored besides the COD_P and ammonia evolution with time. In addition, the COD yield and BOD were also calculated. In chapter II, experiments PSS1-a, TP1-a and results picked-up from literature ((Dimock and Morgenroth, 2006; Sperandio, 1998)) will be confronted to existing conventional and non-conventional models (model calibration). In chapter III, a novel conceptual framework was proposed. The model takes into account the geometrical and physical aspects of the bacteria and substrates. The last chapter of results, (chapter IV) will be dedicated to assess the specific role of each bacterial population that are involved in the biodegradation of slowly biodegradable organic matter.

Figure 9 summaries the experiments that were performed as well as the tools that were used in each case.

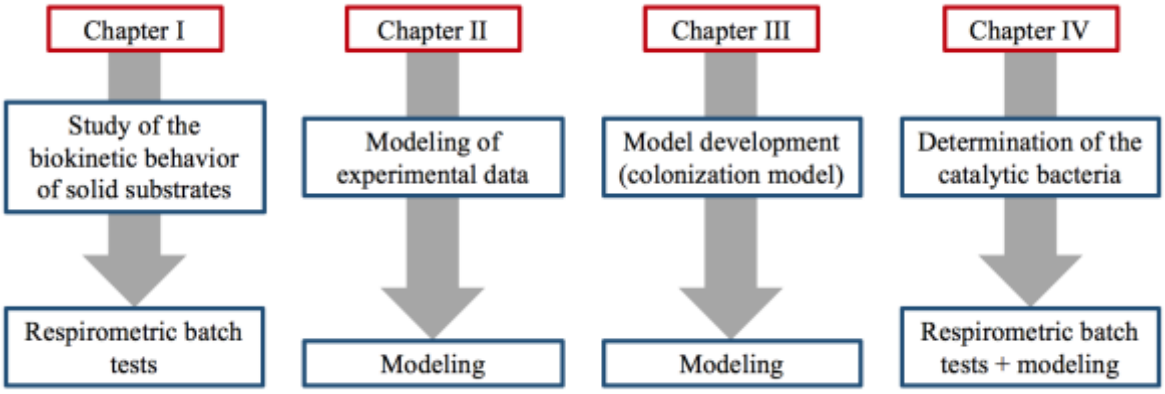

Figure 9: Summary of the experiments and the utilized tools in each case

CHAPTER I

"Typical kinetics for particulate substrates under aerobic condition"

1. INTRODUCTION

The importance of particulate organic matter (POM) elimination in design and operation of wastewater treatment plants (WWTPs) was underlined repeatedly during these last decades. The reason is that this matter is not considered anymore as a waste but as a resource as it could be a valuable carbon source for methane production under anaerobic conditions or utilized as a carbon source for the denitrification operation and phosphorus removal in the aerated tank (secondary treatment).

Many authors have studied this matter in the past, however, the majority of them investigated POM together (amalgamated) with other pollutants (soluble, colloidal, supra-colloidal…) that are contained in municipal wastewaters. Unfortunately, this way of doing leads to imprecisions in the characterisation of POM in terms of quantification and in a kinetic point of view. This certainly affects the other organic components.

Under aerobic conditions, the characterization of POM hydrolysis is generally assessed by the means of the monitoring of dissolved oxygen rate which is better known as the oxygen uptake rate (noted OUR) (Çokgör et al., 2009; Çokgör et al., 1998; Ginestet et al., 2002; Orhon and Sozen, 2012; Spérandio, 1998; Spérandio and Paul, 2000; Wu and He, 2012).

At present time, only very few authors investigated this matter alone without the presence of other components to avoid interferences. The great majority of them investigated the particulate settleable solids (PSS) which were collected from the primary sedimentation tank or isolated in the laboratory with the means of a lab-scale settling device (Eliosov and Argaman, 1995; Ginestet et al., 2002; Orhon et al., 2002; Sperandio, 1998; Tas et al., 2009). Other authors investigated model substrates that are found to be present in municipal wastewater such as starch (Mino et al., 1995; San Pedro et al., 1994), bovine serum albumin and egg-boiled whites (proteins) (Dimock and Morgenroth, 2006), xylan, cellulose and toilet paper (this work).

The objective of this chapter was to set the state of art in terms of the representation of hydrolysis of particulate matter in wastewater treatment processes by analysing in-depth the experimental responses and raise and highlight the differences and/or the similarities with the experimental data obtained in the case of various particulate substrates in order to underline key points that would enhance the characterization of the slowly biodegradable matter in order thus to learn more about the enzymatic hydrolysis process.

2. PHYSICAL DEFINITION OF PARTICUALTE MATTER

The majority of organic matter in urban wastewater (UWW) is in the particulate form (Levine et al., 1985). Levine et *al.* (1991b) have given the size distribution and chemical composition of organic matter in raw wastewater and primary effluent. Murray (1991) characterized the total solids (TS) feed of a conventional wastewater into four categories, based on the settling properties of the constituent material (Table 17).

Table 17 : Physical characterization of wastewater solids Murray (1991)

Parameter	Characteristics of particles
Floatable matter	Fat, oil and grease, which form a scum layer on surfaces, and foreign floatable matter; • visible with the naked eye, physically removable.
Coarse suspended matter	Particles readily settleable of colloidal and non-colloidal nature (particle size > 1 μm); • microscopically visible, filterable.
Colloidal dispersed matter	Fine particles not readily settleable (particle size 1 μm to 1 nm); • ultra-microscopically visible, non-filterable, chemically flocculable.
Molecular solution matter	Constituents in true solution (dissolved) (particle size < 1 nm); • not visible by any instrumental method, not removable with conventional WCW treatment processes.

As described in Rossle and Pretorius (2001), the TS material can be characterized according to a non-filterable (or SS) and a filterable solids fraction. The non-filterable fraction consists of a settleable and a non-settleable fraction, and the filterable fraction consists of a total dissolved solids (TDS) and a colloidal fraction. Each of these four fractions consists of a volatile (organic) and a mineral fraction. Typical reference data for the solids fractions, calculated as percentages of the TS, are presented in Table 18 (adapted from WRC (1984) and Tchobanoglous and Burton (1991)).

Table 18 : Classification of wastewater solids as constituent percentage (adapted from WRC (1984) and Tchobanoglous and Burton (1991)).

TS: 100%							
Non-Filterable or SS: 30%				Filterable: 70%			
Settleable: 22%		Non-Settleable: 8%		TDS: 63%		Colloidal: 7%	
Volatile: 17%	Fixed: 6%	Volatile: 6%	Fixed: 2%	Volatile: 22%	Fixed: 41%	Volatile: 6%	Fixed: 1%

Different matter fractionation methods were applied for distinguishing particulate matter. Settling, centrifugation, sieving, microfiltration, ultrafiltration, field flow fractionation, gel filtration chromatography has been used. Filtration or centrifugation are the most used methods

(Sollfrank and Gujer, 1991). Most of the authors investigating the hydrolysis processes utilized the settled fraction of urban wastewater (UWW) leading to the particulate settleable solid (PSS) fraction. In the present work, PSS obtained by settling are considered. Typically, particles larger than 100 µm are to a large extent removed in the primary sedimentation.

Model substrates were also investigated by some authors as PSS often contain rapidly biodegradable COD, which affects the characterization of the hydrolysis process of the slowly biodegradable COD: Dimock and Morgenroth (2006) studied the biodegradation of boiled-egg white particles (protein-like components) by activated sludge under aerobic conditions. Mino et *al.* (1995) and Ubukata (1999) evaluated the hydrolysis rate of degradation of particles of starch under aerobic, anoxic and anaerobic conditions.

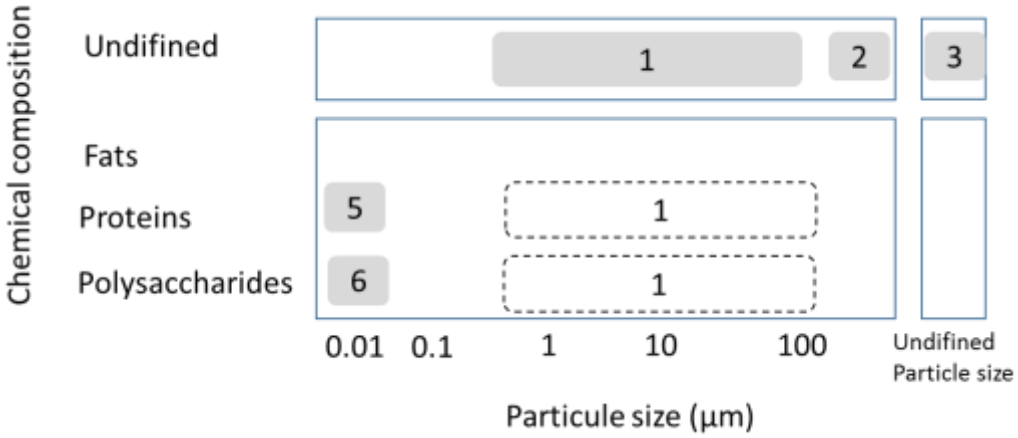

Figure 10: particle size and particle composition used for hydrolysis experiments (adapted from (Morgenroth et al., 2002). 1: filtered WW: Guellil et *al.* (2001); 2: filtered or centrifuged WW or sewer solids: Eliosov and Argaman (1995), Janning et *al.* (1998), (Vollertsen and Hvitved-Jacobsen (1999); 3: raw WW: Henze and Mladenovski (1991); 4: fats: (Sprouse and Rittmann, 1990); 5: Bovine serum albumin: Ubukata (1992);(Confer and Logan, 1997a); 6: starch and dextrin: Ubukata (1992), Larsen and Harremoës (1994), Haldane and Logan (1994), San Pedro et *al.* (1994), Goel et *al.* (1998), Confer and Logan (1997b).

In conclusion, care must be given to the nature of organic material that is considered in the tests used for characterizing the kinetic of particulate matter analysis. The origin of the particulate matter, and the separation mode to isolate the PSS from the rest of the UWW must be known.

8.LIST OF PSS BIODEGRADATION EXPERIMENTS AND COMPARISON OF PROTOCOLS

In the goal to characterize mechanisms and location of hydrolysis four experimental approaches have been implemented and described in literature: (1) specific enzyme

measurement; (2) measurement of compounds involved in the enzymatic hydrolytic reaction (either substrate or product); (3) mass balance on organic matter (for example, COD mass balance); (4) respirometric studies. The first two approaches give insights on specific mechanisms involved in hydrolysis but rely on the use of simple substrates. The latter two approaches give a more global view of hydrolysis kinetics on mixed substrates and mixed bacterial populations but are more complex to analyse.

A literature review of the studies that refer to the degradation of solid substrates in wastewater treatment and that monitored the OUR is presented Table 19.

Table 19 : Literature review of solid organic matter biodegradation monitored with respirometry (*OUR* measurement)

Author	Location	Type of wastewater	Substrate	Inoculum		Experiment duration (days)	S to X ratio (gCOD/gX)		
				Origin	Type		X in *VSS*	X in *COD*	X in COD_{XOHO}
Tas et *al.* (2009)	Istanbul, Turkey	Domestic	PSS	Istanbul, Turkey	Acclimated to sewage	0.25	0.2	N.D.	N.D.
Sperandio (1998)	Ginestous, France	Urban	PSS	Ginestous, France	Activated sludge	10	0.59	N.D.	N.D.
Dimock and Morgenroth (2006)	N.D.	N.D.	Boiled egg-whites	Urbana-Champaign Sanitary District's, USA	Activated sludge	1.5 - 2.5	N.D.	N.D.	0.29 - 0.54
Dimock and Morgenroth (2006)	N.D.	N.D.	BSA	Urbana-Champaign Sanitary District's, USA	Activated sludge	2.5	N.D.	N.D.	0.33
This thesis	N.D.	N.D.	Toilet paper	Ginestous, France	Activated sludge	13	19	13	N.D.
Ginestet et *al.* (2002)	Ginestous, France	Urban	PSS	Ginestous, France	Activated sludge	N.D.	N.D.	2.05 - 7.21	N.D.
Mino et *al.* (1995)	N.D.	N.D.	Starch	N.D.	Activated sludge	0.13	1.05 - 3.81	N.D.	N.D.
Orhon et *al.* (2002)	Ataköy, Turkey	Domestic	PSS	Ataköy, Turkey	Acclimated to sewage	0.45	0.06	N.D.	0.71
Eliosov and Argaman (1995)	Haïfa, Israel	Municipal	PSS	Haïfa, Israel	Activated sludge	N.D.	0.5 - 2	N.D.	N.D.

As it can be seen in this table, only few studies dealing with particulate organic matter biodegradation monitored using respirometry are available in literature. Moreover, the protocols used for studying the kinetic of PSS hydrolysis differ on various points: the use or not of inoculum, the substrate to biomass ratio, the duration of the experiment, etc.

Some experiments were performed by mixing the isolated PSS with activated sludge considered thus as an inoculum (Orhon et al., 2002, 1998; Tas et al., 2009); other ones utilized PSS without the addition of external bacteria considering that some microbial populations are initially adsorbed to PSS (Ginestet et al., 2002; Spérandio, 1998). This way, Orhon et *al.* (2002) estimated catalytic bacteria (by modeling) to represent about 58% of the PSS in terms of COD, accordingly, only 42% were biodegradable.

Table 19 shows that there is a huge range of S/X ratios utilized. Moreover, the "X" is supposed to represent the concentration of real active heterotrophic bacteria. However, VSS or total COD of inoculum is often used instead of a real estimation of X which may lead to a more or less strong error on active biomass quantification. The question is especially crucial when inoculum is added. In that case, concentration of catalytic cells strongly depends on the nature of activated sludge sampled especially in the case of high SRT activated sludge process (Paul et al., 2012). In addition, catalytic biomass is also present in PSS (acclimated to PSS) but its amount is difficult to assess by the conventional protocols. At the present time, modeling appeared to be the most utilized and efficient way to determine heterotrophs amounts.

Finally, the experiments duration times could be ranged into two categories: few hours or short-term experiments that lasted between 0.13 till 0.45 days (Mino et al., 1995; Orhon et al., 2002; Tas et al., 2009); and long-term experiments which lasted between 2.5 and 16 days (Dimock and Morgenroth, 2006; Sperandio, 1998; this study).

9. SYNOPSIS OF LITERATURE RESULTS ABOUT HYDROLYSIS OF PARTICULATE MATTER

9.1. REAL INFLUENT: PARTICULATE SETTLEABLE SOLIDS (PSS)

As shown in the first part of Table 19, we selected from literature the few experiments that set PSS elimination using respirometry to follow the kinetics of this degradation. In this section, the OUR profiles will be presented to illustrate the main trends obtained.

9.1.1. Calculations

In order to analyse the hydrolysis process from the OUR profiles, few calculations are necessary. OUR profiles were compared in terms of: (a) global feature or trends (simple or complex) (b) characteristic time of degradation and (c) percentage (%) of degraded substrate.

The degradation time gives information of the hydrolysis rate of the PSS. It is calculated from the beginning of the experiment up to the time where the OUR reaches the OUR value of endogenous respiration.

When readily biodegradable substrate is present, it is consumed in a first phase. The amount of readily biodegradable COD can thus be estimated: the values of OUR are integrated during this first period according to Kappeler and Gujer (1992) by calculating the difference between total respiration and respiration due to hydrolysis and endogenous respiration. We therefore assume that aerobic endogenous respiration of heterotrophs is negligible and no additional mechanism such as storage occurred during this period:

$$S_B = \frac{\int_0^t (OUR - OUR_0)dt}{1 - Y_H} \quad (25)$$

The rapidly biodegradable matter (S_B) is calculated assuming a growth yield of 0.63 gCOD/gCOD as reported in Gujer et *al.* (1995). The global biological oxygen demand (BOD) is calculated by integrating the OUR over the degradation period ((26)):

$$BOD = \int_0^t OURdt \quad (26)$$

Assuming a cell growth yield, the biodegraded COD can be calculated. Comparing the degraded COD and the added COD gives the proportion of COD degraded during the experiment. Nevertheless, this calculation is only valid in the case of negligible aerobic growth of heterotrophs (therefore at low S/X ratio, i.e. S/X <0.1).

When it is possible to assume that hydrolysis of slowly biodegradable matter (XC_B) is the rate-limiting process (Morgenroth et al., 2002; Orhon et al., 2002; Tas et al., 2009), and follows a first-order law with respect to the remaining XC_B the expression of the OUR could then be written as below:

$$OUR = (1 - Y_{OHO}) q_{XCB_{SB_{hyd}}} XC_B + b_{OHO}(1 - f_{Xu_{Bio},lys}) X_{OHO} \quad (27)$$

With:

$$XC_B = XC_{B,0} e^{-q_{XCB_{SB}hyd} t} \quad (28)$$

Decay of active biomass can be expressed as a first-order process as in the *IWA* model n°3 (Gujer et al., 1999):

$$X_{OHO}=X_{OHO_0}e^{-b_{OHO}t} \quad (29)$$

Equation (27) can be simplified by replacing XC_B and X_{OHO} with equations (28) and (29) respectively:

$$OUR=(1-Y_{OHO})q_{XCB_{SB_{hyd}}}XC_{B_0}e^{-q_{XCB_{SB}hyd}\,t}+b_{OHO}(1-f_{Xu_{Bio},lys})X_{OHO_0}e^{-b_{OHO}t} \quad (30)$$

Each response can be linearized by calculating the logarithm of the corresponding OUR profile:

$$lnOUR=ln\left\{(1-Y_{OHO})q_{XCB_{SB_{hyd}}}XC_{B_0}\right\}-q_{XCB_{SB},hyd}\,t+ln\left\{b_{OHO}\left(1-f_{Xu_{Bio},lys}\right)X_{OHO_0}\right\}-b_{OHO}t \quad (31)$$

$$lnOUR=Cste-(q_{XCB_{SB},hyd}+b_{OHO})t \quad (32)$$

9.1.2. Experiment of Tas et *al.* (2009) and Orhon et *al.* (2002)

Figure 11 illustrates the short term OUR profile obtained by Tas et *al.* (2009) in the case of the biodegradation of particulate settleable solids (PSS) under aerobic conditions.

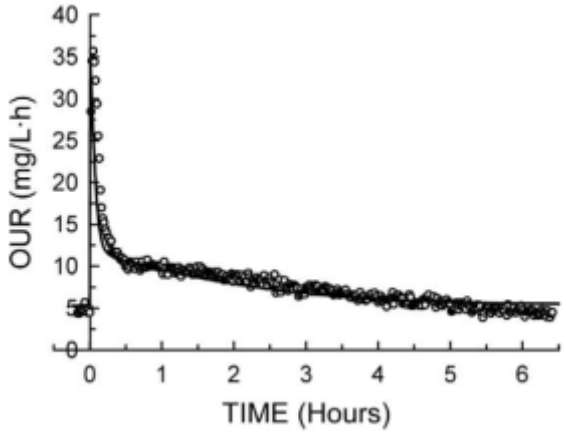

Measured parameters	
COD_{XSS}	132 mg/L
Estimated parameters (IAWQ model n°1)	
$q_{XCB\_SB,\ HYD}$	1 d^{-1}
$K_{XCB,\ HYD}$	0.12 gCOD/gCOD

Figure 11 : PSS inoculated with activated sludge (Tas et al., 2009) (S= 168 mgCOD/L; AS = 840 mgVSS)

Figure 11 shows that the OUR increased rapidly from 5 mgO_2/l/h (endogenous respiration) till 35 mgO_2/l/h immediately after PSS addition. Then, the OUR sharply decreased after around 15 min. A slower and progressive decrease of the OUR was then observed until the initial value of the OUR (5 mgO_2/l/h) was reached after 6 hours. The initial sharp peak of the OUR was attributed by the author to the consumption of the rapidly biodegradable matter (S_B) while the PSS is characterized by the following OUR decreasing phase. It may be amalgamated with the endogenous respiration phase. They estimated the hydrolysis rate constant to 1 d^{-1} while the

endogenous respiration rate constant was not estimated but fixed to 0.2 d^{-1} as reported in Ekama and Marais (1979).

Figure 12 illustrates the OUR profile obtained by Orhon et *al.* (2002) in the case of the biodegradation of PSS in aerobic condition.

(a) (b)

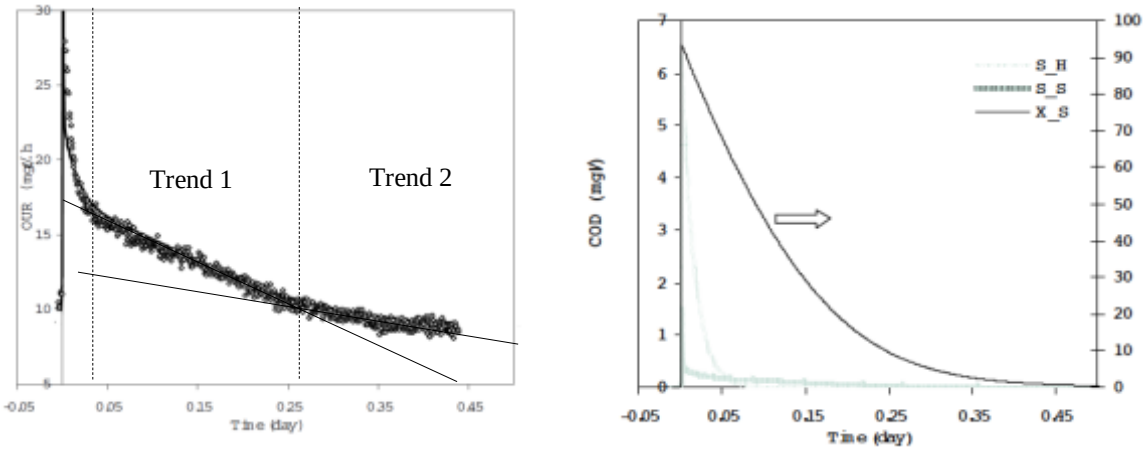

Estimated parameters (IAWQ model n°1)	
XC_B	1020 mg/L
X_{OHO}	1430 mg/L
$q_{XCB\_SB, HYD}$	0.7 d^{-1}
$K_{XCB, HYD}$	0.05 gCOD/gCOD

Figure 12 : PSS inoculated with activated sludge (Orhon et al., 2002); (a) The OUR profile and (b) the simulated main state variables (S=2 900 mgCOD/L; AS=48 000 mgCOD)

Figure 12 shows that the OUR increased from 10 to 30 $mgO_2/l/h$ immediately after PSS addition, then decreased exponentially till it reached the initial value of the OUR (10 $mgO_2/l/h$) after 6 hours. Besides S_B which is characterized by the OUR initial tight peak, two additional trends were observed (trend 1: 0.025<t<0.25 d; trend 2: 0.25<t<0.45 d). Nevertheless, according to model calibration performed by the authors (figure 16b), a unique type of substrate was identified despite the presence of those two distinct trends. The utilized model (*IAWQ* model n°1 modified for endogenous respiration) is found to be adapted for the description of the OUR profile but perhaps does not describe what really occurred during this experiment, to wit, the number of substrates, for example.

Moreover, the OUR profile is found to be similar to the profile obtained by Tas et *al.* (2009) with an initial tight peak followed by a decrease of the OUR. In this study, they estimated (by modeling) the hydrolysis rate constant to 0.7 d^{-1} and was not far from the one identified by Tas

et *al.* (2009) (1 d^{-1}). Globally, it could be concluded that wastewater characteristics in Ataköy and Istanbul are quite similar, especially for the settleable fraction (PSS).

9.1.3. Sperandio's (1998) experiment

Besides the short-term evaluation of PSS, few long-term experiments have been performed. Figure 13 illustrates the OUR profile obtained by Spérandio (1998) in the case of the biodegradation of PSS under aerobic condition.

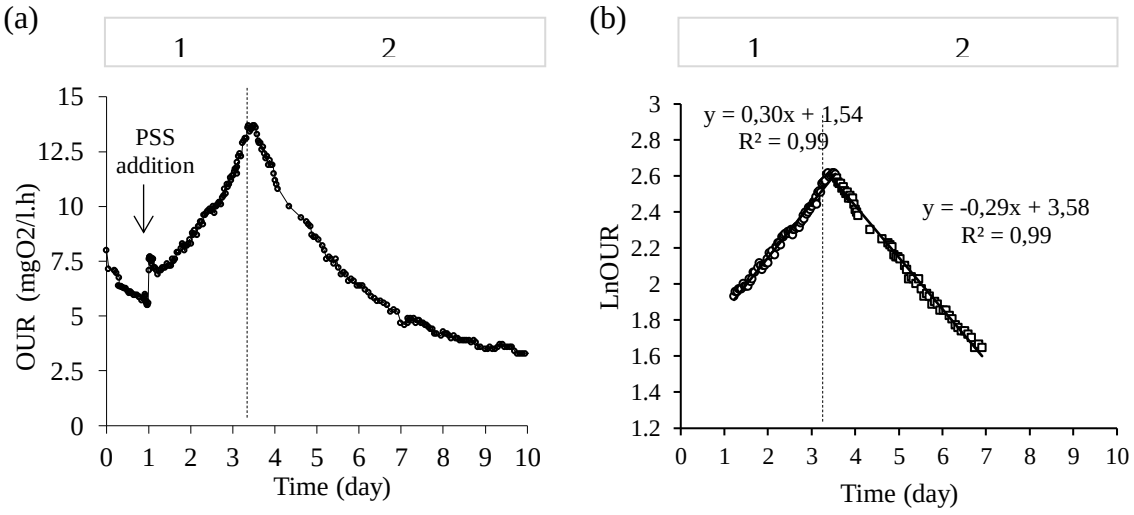

Figure 13 : (a) OUR profile obtained by Sperandio (1998) in the case of PSS biodegradation in the presence of activated sludge and (b) the logarithm of the OUR (S=830 mgCOD/L; AS=1400 mgVSS/L)

Figure 13a shows that the OUR increased exponentially from 7.5 to 13.7 $mgO_2/l/h$ after 2.5 days. Then, the activity decreased exponentially till it reached a value of 3.3 $mgO_2/l/h$ after 9 days. The author attributed the first part ($1<t<3.5$) of the kinetic to the PSS colonization by bacteria and supposed an exponential growth or a colonization phase of that bacteria. An observed maximum specific growth rate (specific colonization rate) was assessed by calculating the logarithm of the OUR during the first phase (figure 17b). A value of about 0.3 d^{-1} was calculated.

In the second part of the kinetic ($t>3,5$ days), the decrease of the OUR was attributed by the author to the decrease of the available surface area of the substrate. This hypothesis could be justified by the microscopic monitoring that was performed during the experiment (Figure 14). It appears clearly that the particulate organic matter (here mainly fibers of toilet paper) size decreases till it seems starting to disappear after 10 days.

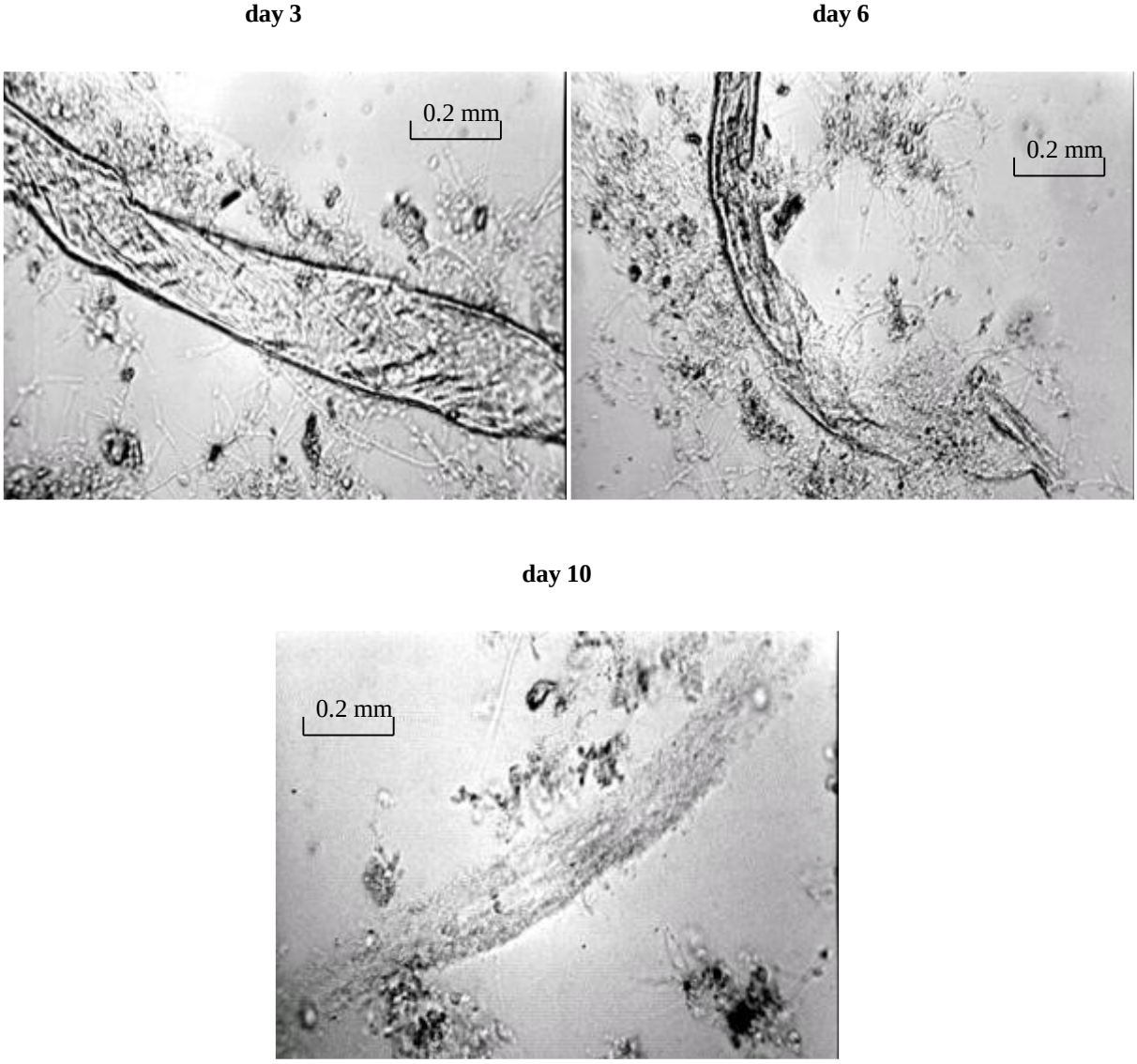

Figure 14: Microscopic monitoring of Sperandio's (1998) experiment starting from day 3 and ending at day 10

9.1.4. Experiment involving PSS (this thesis)

In our study, a 1.5L-batch aerobic respirometer was fed with a known amount of PSS (9.23 gCOD/l) without inoculum addition and was operated during 16 days. A detailed description of the experiment is reported in the Material and Methods chapter.

Figure 15 represents the evolutions of monitored parameters (OUR, COD_P and COD_S) during the batch test.

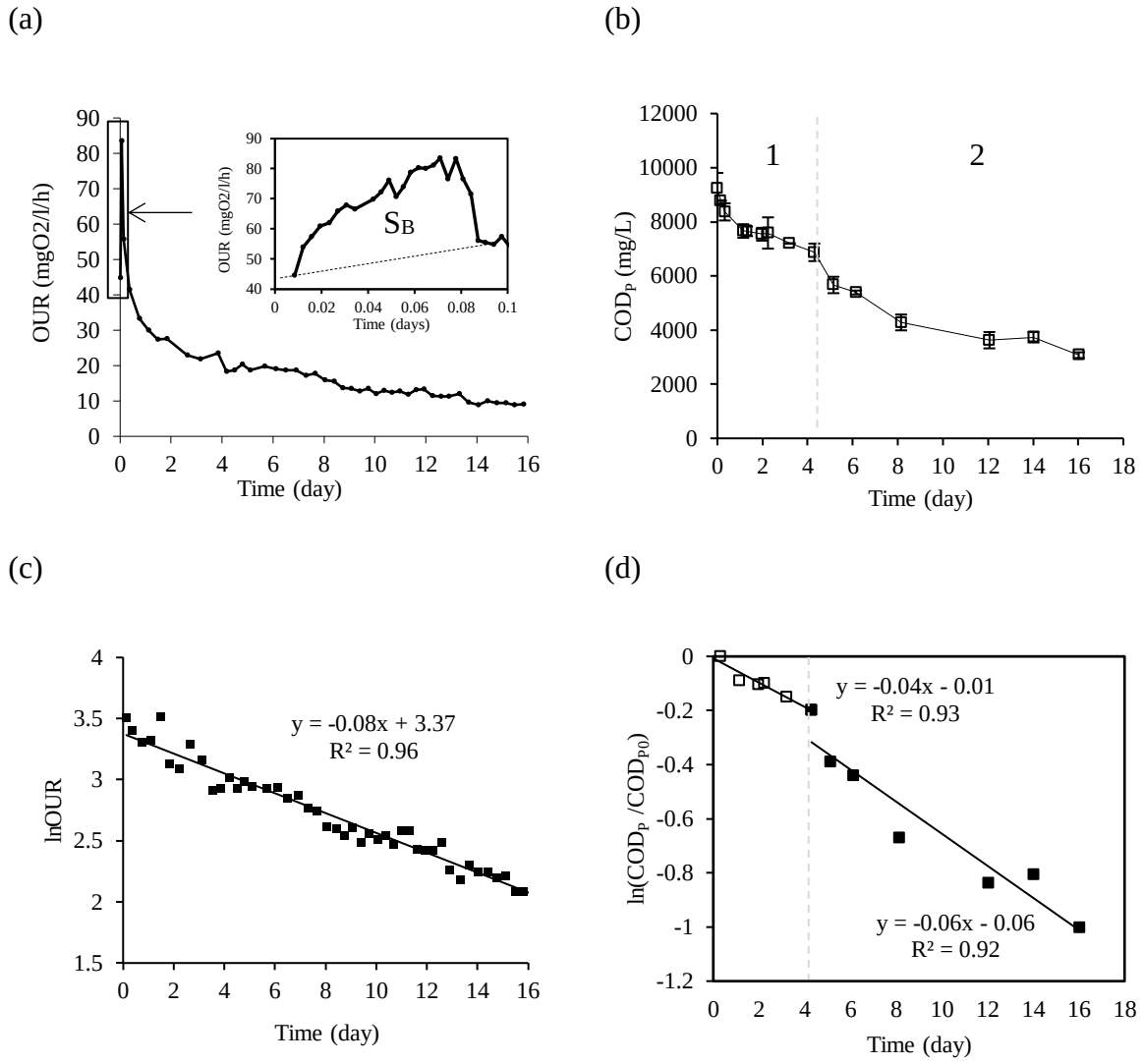

Figure 15 : (a) OUR profile, (b) evolution of particulate COD (COD_P), (c) the logarithm of the OUR and (d) the logarithm of COD_P/COD_{P0} in the case of aerobic degradation of PSS obtained by settling pre-treated municipal wastewater collected from Toulouse-Ginestous (France)

Figure 15a indicates that the OUR increased from 45 until 85 $mgO_2/l/h$ immediately after the addition of the PSS. This phase lasted less than 2 hours. At the same time, the measured soluble COD (COD_S) decreased from 395 till 243 mgCOD/L. The value of S_B calculated according to equation 1 was of 147 mgCOD/L. This value was very close to the loss of COD_S (152 mgCOD/L) during the same period (difference of less than 4%). After the initial tight peak, the OUR decreased till it reached a value of 10 $mgO_2/l/h$ after 16 days. The degradation yield in terms of total COD was 65% and the biological oxygen demand (BOD) was equal to 6915 mgO_2/L. The ratio BOD/COD was equal to 1.12.

The logarithm of the OUR during the whole experiment (Figure 15c) shows a trend line with a slope of 0.08 d^{-1} what indicates an exponential decrease of the substrate while Figure 15d, which represents the logarithm of the COD_P/COD_{P0} during the descending phase of the OUR, indicates two distinct slopes (0.04 d^{-1} when t<4 days; 0.06 d^{-1} when t>4 days).

It could be concluded that the OUR profile is not enough to understand what really happens during PSS hydrolysis as it characterizes organic matter degradation in a global way. Additional monitorings of specific parameters such as COD_P evolution would certainly strengthen the comprehension of the main mechanisms that occur, especially the hydrolysis process.

9.1.5. Summary of PSS experiments results and discussion

Table 20 regroups the whole experiments that deal with real influent substrates (PSS) which have been presented in this chapter.

Table 20 : Summary of trends and characteristic values observed during aerobic biodegradation of PSS

Experiment author	Global feature	Initial COD (g/L)	Characteristic time (day)	COD degradation yield (%)	Hydrolysis constant (d^{-1})	OUR_{ini}/ OUR_{max} ($mgO_2/l/h$)
Tas et *al.* (2009)	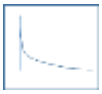	0.13	0.25	N.D.	1 first order	5 / 35
Orhon et *al.* (2002)	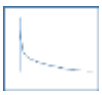	2.45	0.25	N.D.	0.7 First order	10 / 30
Sperandio (1998)		0.83	>10	N.D.	+0.3 / -0.3 Two trends	7.5 / 14
This study	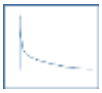	9.23	>10	65	0.08 First order	45 / 85

Figure 16 illustrates the whole OUR profiles that were presented till now about PSS.

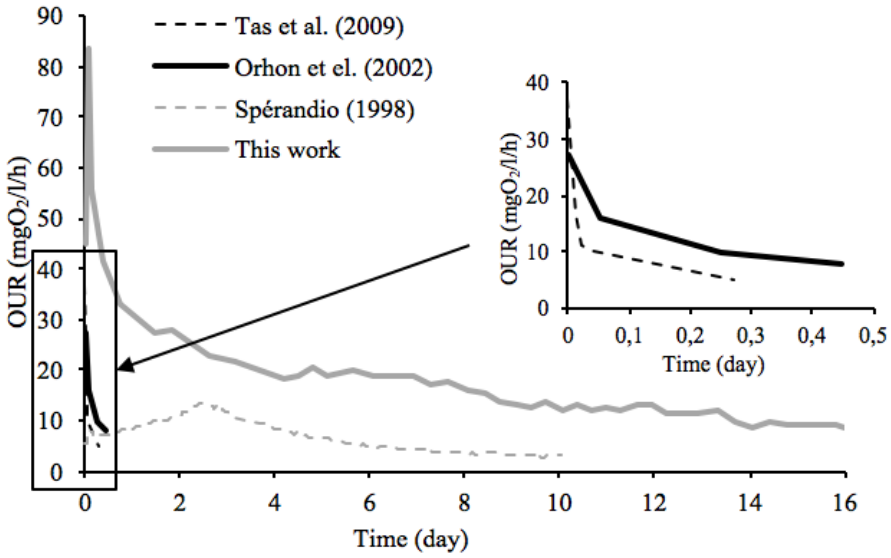

Figure 16 : Summary of the OUR profiles that deal with particulate settleable solids (literature and internal results)

Figure 16 shows clearly two types of OUR profiles according to the characteristic time: short-term experiments of few hours (Orhon et al., 1998; Tas et al., 2009) and long-term experiments of at least 10 days (Sperandio, 1998; this work).

9.1.6. Intermediate conclusion

For all case studies, whatever the presence or absence of inoculum, degradation of the added PSS occurred.

Two global features of the OUR curve were observed: an exponential decrease of OUR for the major part of the experiments (3 on 4) and an exponential increase of OUR followed by an exponential decrease. This later case will be noted in the following of this manuscript as two trends feature.

Two scales of degradation time were observed: a few hours (6) or at least 10 days. The percentage of degradation in our PSS experiment was of 65%. This information was not mentioned in the other considered studies.

The kinetic constants estimated using a first-order model (IAWQ model n°1) are 0.7 d^{-1} in Orhon et al. (2002); 1 d^{-1} in Tas et al. (2009). In our study, it was estimated to 0.08 d^{-1} by using equation (32), however, two slopes appeared when the COD_P profile was linearized (0.04 and 0.06 d^{-1}).

In Sperandio's (1998) experiment, 2 trends of the same magnitude were calculated (0.3 d^{-1}) for the OUR increasing and the decreasing phase. The first one was assimilated to the specific growth rate (μ_{OBS}) of catalytic bacteria and the second one to the PSS hydrolysis rate ($q_{OBS}=q_{XCB\_SB,\,HYD} + b_{OHO}$). In this experiment, the first phase was attributed to colonization of substrate by the bacterial cells and the second phase to the decrease of the colonisable substrate surface area based on microscopic monitoring of the batch test.

Finally, the values of initial and maximal OUR were very different from one experiment to another. The initial value characterizes the endogenous respiration of the inoculum as it was measured before substrate addition in the results collected from literature. In this study, the OUR initial value was found to be higher than in literature. This value is directly linked to the catalytic bacteria which is initially adsorbed to PSS. The maximum value of OUR was found to be higher too in our experiment compared to literature. This value could depend on the initial amount of catalytic bacteria if we suppose that involved bacterial cells (heterotrophs) in all the studies have the same maximum growth rate ($\mu_{OHO,\,max}$) and a negligible half-saturation constant ($K_{SB,\,HYD}$).

9.2. EXPERIMENTS INVOLVING MODEL SUBSTRATES

The choice of using model substrates to study mechanisms of hydrolysis can be understood as a way of better controlling the nature of substrates but also as a way of controlling the inoculation and therefore an intend to control the amount of active biomass at the beginning of the experiment.

Nevertheless, many questions arise: could the polymeric substrate be considered as a unique substrate with a unique hydrolysis (degradation) rate? Could the substrate products be degraded simultaneously? Is there a strong specificity of cells towards a given substrate?

9.2.1. Experiment of Dimock and Morgenroth (2006) with boiled-egg whites

Figure 17 represents the OUR profile in the case of large boiled-egg white particles biodegradation by activated sludge under aerobic condition.

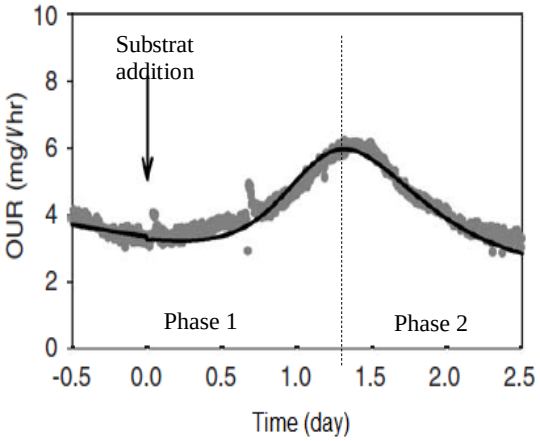

Figure 17: OUR during large boiled-egg white particles biodegradation by activated sludge (Dimock and Morgenroth, 2006)

In the case of large boiled-egg white particles (Figure 17), the OUR increased from 4 to 6 $mgO_2/l/h$ in 1.3 days. Then, it decreased and reached a value of 3 $mgO_2/l/h$ after 2.5 days. This profile is similar to Sperandio's (1998) experiment which was presented before with two distinct OUR phases. In contrast, the interpretation of the OUR profile was different. In this study, the increasing phase was attributed by the authors to the fractionation of large particles into smaller ones by the means of hydrolysis process (enzymes). This mechanism would thusly increase the substrate specific surface area that can be colonized by bacteria. In the second part of the kinetic, the decrease of the OUR was attributed to the decrease of the available specific surface area of the substrate. Figure 18 illustrates their interpretations and hypothesis.

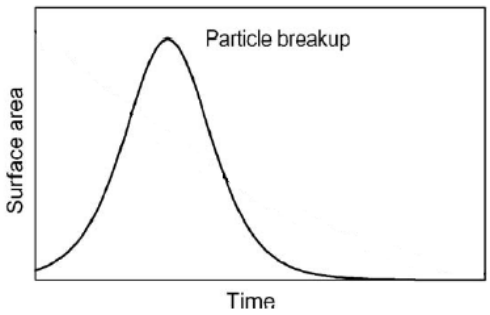

Figure 18 : (a) Substrate surface area evolution during particle breakup (Dimock and Morgenroth (2006))

9.2.2. Experiment of Mino et *al.* (1995) on starch

In this experiment, starch and fresh activated sludge were mixed and kept under aeration in a batch-reactor. Starch concentration was monitored during its biodegradation (decrease). With these data and a first-order hydrolysis model, we built the corresponding OUR profile. The values of kinetic parameters and stoichiometric coefficients were standard values (IAWQ

model n°1), except the hydrolysis rate constant. They also provided their experimental data concerning the initial concentration of starch (XC_B) and the initial concentration of activate sludge (Table 21). Figure 19 illustrates the OUR profile obtained in this experiment.

Table 21 : Batch-experiments and modeling results of Mino et *al.* (1995)

Exp.	Initial starch conc. (mg/L)	Initial starch conc. (mgCOD/L)	Initial activated sludge conc. (mgVSS/L)	Initial activated sludge conc. (mgCOD/L)	1st order rate constant (d^{-1})
1	363	387	164	233	3.83
2	350	373	332	471	3.69
3	731	780	192	273	3.79
4	785	836	400	568	3.55

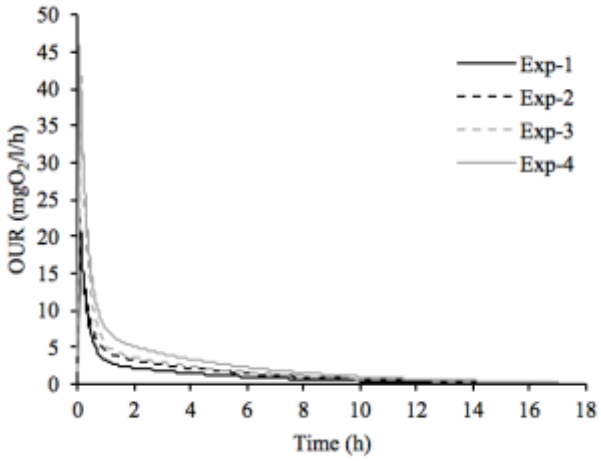

Figure 19 : OUR profile of starch degradation by activated sludge reconstructed based on experimental data of Mino et al. (1995)

Of course this experience could not be discussed in terms of the OUR profile shape as we arbitrarily utilised a first-order model to build it. But, it could be noticed that the characteristic time is 17 hours and could be included in the short-term experiments category. In addition, it could be noticed that the biomass concentration did not affect the OUR profile as the hydrolysis rate constants that were identified by the authors were of the same range (Table 21).

9.2.3. Experiment involving toilet paper (this thesis)

Toilet paper is a fully-fledged component of municipal wastewaters besides carbohydrate-like pollutants that are conventionally present in the form of glycoproteins for example. It is composed by cellulose (79%) and hemicellulose (12%) as the main biodegradable components (Figure 20). Contrarily to hemicelluloses, cellulose is found to represent a non-

negligible fraction of primary wastewaters solids (PSS and non-settleable ones). Its amount is comprised between 8 and 15% of total dry matter according to Sun and Cheng (2002).

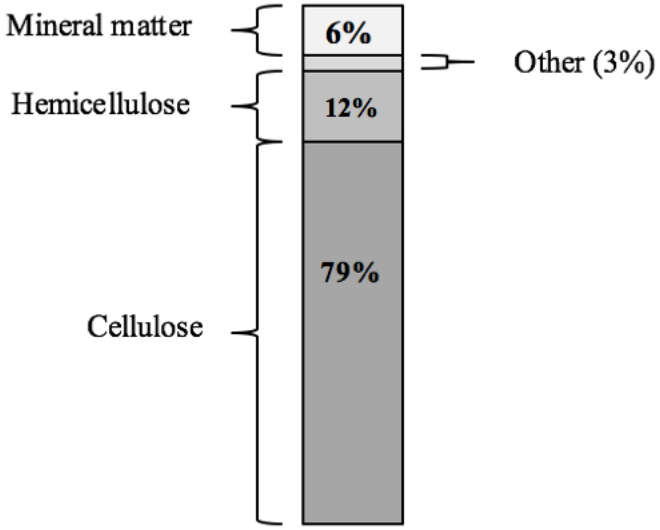

Figure 20: Composition of toilet paper (assessed in our laboratory)

In our study, a batch respirometric test was operated to observe the biodegradation of toilet paper (initial concentration: 9250 gCOD/L) during 14 days. Activated sludge (inoculum) was added in a known amount (710 mgCOD/L).

The following figure illustrates (a) the OUR profile, the evolution of (b) COD_P, (c) the logarithm of the OUR and (d) the COD yield and BOD obtained in the case of toilet paper degradation by activated sludge under aerobic condition.

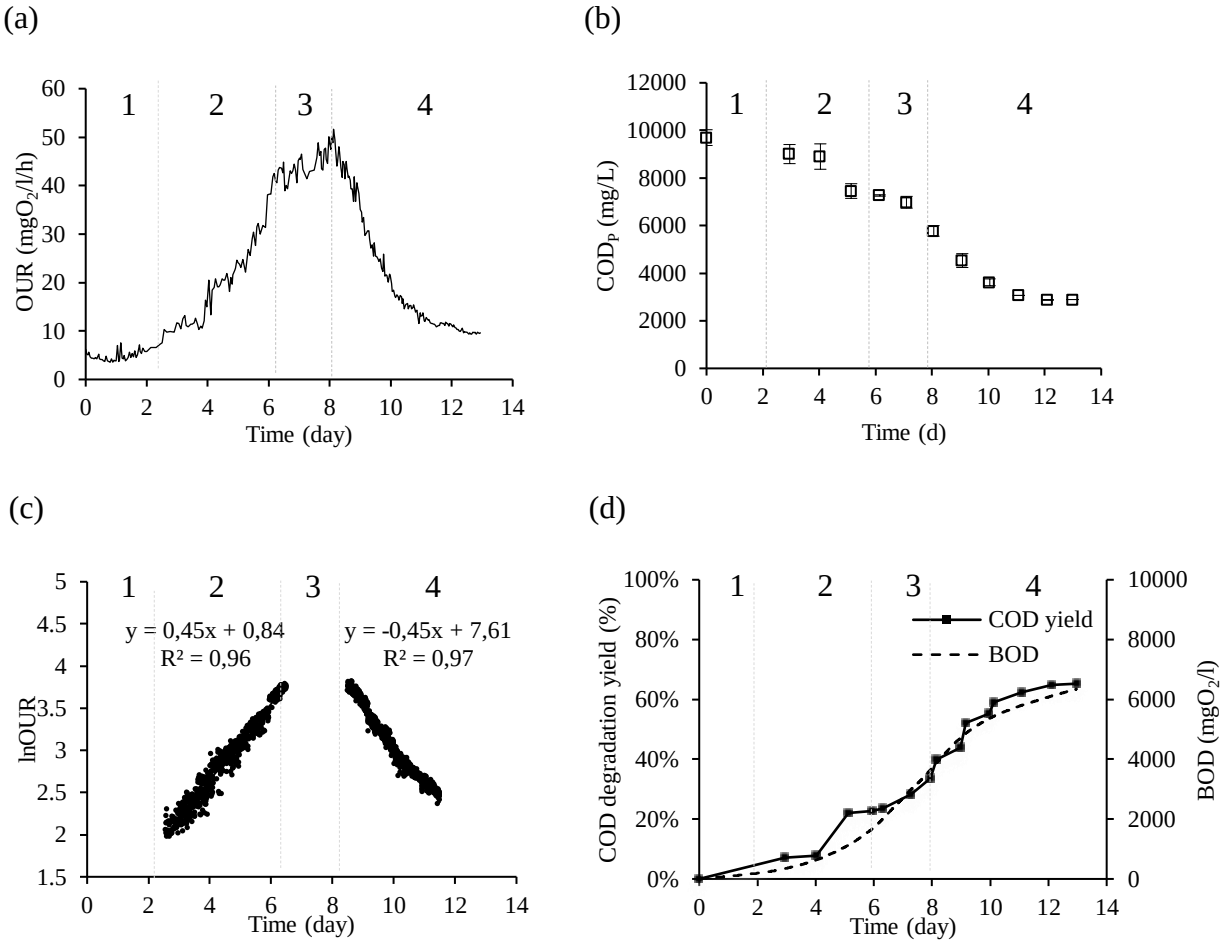

Figure 21: (a) OUR profile, (b) evolution of COD_P, (c) the logarithm of the OUR and (d) the COD yield and BOD obtained in the case of toilet paper degradation by activated sludge under aerobic condition (Substrate=8 990 $mgCOD_P/L$; inoculum=710 mgCOD/L).

Figure 25a shows that the OUR profile obtained for the degradation of toilet paper was composed by two trends: an increasing and a decreasing one as observed in Sperandio (1998). In contrast, a lag phase (1) during which the OUR kept constant during almost 2 days at around 5 $mgO_2/l/h$ was observed. This phase could be attributed to an acclimation period as the inoculum (fresh activated sludge) was not acclimated previously to the substrate. The COD_P evolution confirms this hypothesis as it was almost kept unchanged during this period (the important error bars width for the data before day 4 are due to sampling difficulties during the experiment because of toilet paper complex consistence and structure).

During phase 2, the OUR increased till about 43 $mgO_2/l/h$ and COD_P decrease from 9005 till 7266 mgCOD/L. Till there, 25% of the total COD was depleted. A transition phase (3) was observed between phases 2 and 4. During this phase, the COD_P decreased till 5788 mgCOD/L and additional 15% of total COD was degraded (40% since the beginning of the experiment).

During phase 4, the OUR decreased till 10 $mgO_2/l/h$ and reached endogenous respiration and at the same time the COD_P decreased till 2893 mgCOD/L and achieved 25% of COD degradation more. At the end of the experiment, the COD yield reached 65% (6804 gCOD/L were reduced) and the cumulated BOD was of 6245 mgO_2/L (64% of the initial COD). The ratio BOD/COD was equal to 0.92. The total duration of this degradation was 13 days.

The logarithm of the OUR during the first and the second phase presents trend lines with the same slope in absolute value of 0.45 d^{-1} (figure 25c).

9.2.4. Experiment on commercial cellulose and xylan performed in this thesis

Cellulose, or poly-β-(1→4)-D-glucose, is one of the most important component of the plant cell walls (Römling and Galperin, 2015) and the main component of toilet paper. As reported in the previous section, they represent between 8 and 15% of the total dry matter of primary wastewater solids.

Hemicelluloses are polysaccharides with β-(1→4) bonds and they are also present in the plant cell walls near cellulose (Figure 22). They include xylans, xyloglucans, mannans, glucomannans and some glucans (Scheller and Ulvskov, 2010). In toilet paper, they represent less than 10% of the total dry matter.

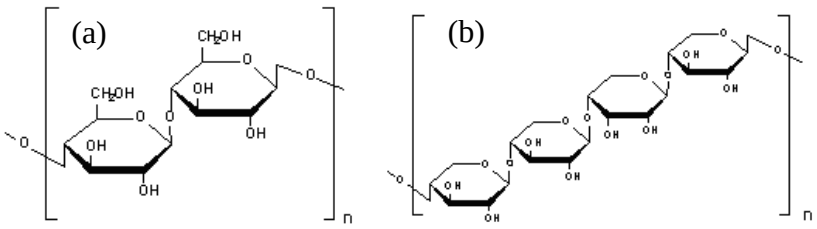

Figure 22: Structure of (a) cellulose and (b) hemicellulose

In this experiment, two batch respirometers were inoculated with about 1 g/L of activated sludge (AS of SRT equal to 2.5 days). Each reactor contained 8 gCOD/L of cellulose and 1 gCOD/L of xylan, respectively. The concentrations of the two substrates were chosen to be in the same range of the toilet paper used in the previously described experiment in order to assess their respective kinetic of degradation characteristics.

Figure 23 represents the OUR profile for the degradation of commercial cellulose in a batch respirometer inoculated with activated sludge.

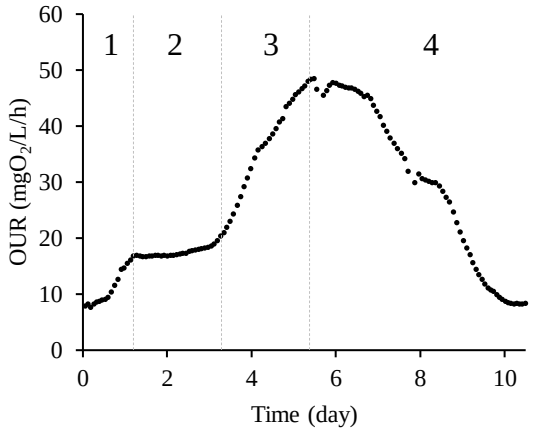

Figure 23: OUR profile obtained in the case of commercial cellulose

Figure 23 shows that the OUR increased from 8 mgO_2/l/h till 16 mgO_2/l/h during the first 24 hours (1 day). After that, a plateau was observed and lasted one more day. Since then, the biological activity increased again and reached almost 50 mgO_2/l/h at around 5.5 days. At that time, the OUR decreased and reached a plateau after 10 days and 72% of the total COD reduced.

This OUR profile is irregular and was not observed till now in our experiments as well as in literature. Thus, the mechanisms that are conventionally encountered in WWTP processes and modeling may be not sufficient to explain and characterize this kind of substrate in a kinetic aspect. Additional features may be necessary in order to characterize this experiment.

Recent studies highlighted that lignocellulosic components hydrolysis involve two types of enzymes (endo- and exoglucanases) and certainly at least that much of mechanisms (Lebaz, 2015). This leads us to think that at least two distinct substrates with distinct kinetic properties must be considered to characterize such experiments with irregular OUR profiles. This will be taken into account and investigated in the next chapter (II).

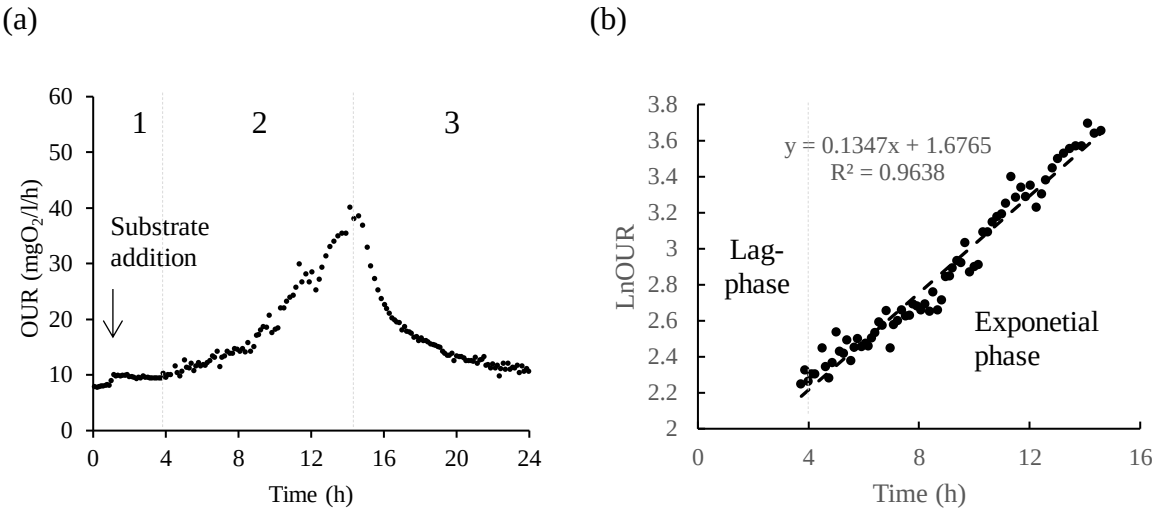

Figure 24: (a) OUR profile obtained in the case of commercial xylan and (b) logarithm of OUR during the first phase

In the case of xylan (Figure 28a), the OUR profile shows two trends as reported previously for the case of toilet paper: a lag phase (1) of 3 hours was observed after substrate addition. In phase 2, the OUR increased from 10 to 40 $mgO_2/l/h$. Since then, OUR declined exponentially till 11 $mgO_2/l/h$ and reached a plateau. A specific growth rate was calculated during the first phase according to equation 34 and was of 0.13 d^{-1}. Commercial xylan was depleted after 1 day and 88% of the total COD reduced.

9.2.5. Summary of the results on model substrates

Analysis of the OUR profile was performed in terms of time of degradation, feature of the curves, kinetic parameters obtained and percentage of degradation. Table 22 summarizes the results obtained in case of model substrates.

Table 22: Summary of trends and characteristic values observed during aerobic biodegradation of model substrates

Author/experiment	Global feature	Characteristic times (day)	COD degradation yield (%)	Hydrolysis constant (d^{-1})	OUR_{ini}/ OUR_{max} ($mgO_2/l/h$)
Large boiled-egg white; Dimock and Morgenroth, 2006)		2.5	N.D.	0.46/-0.61 Two trends	4/6
Toilet Paper; this thesis		13	65	0.45/-0.45 Two trends	5/50
Cellulose; this thesis		10	72	N.D.	8/50
Xylan; this thesis		1	88	0.13	8/40

9.2.6. Intermediate conclusion

For all cases, degradation of the added model substrate occurred. Contrarily to real influent experiments involving PSS, all the OUR profiles showed two trends: an exponential increase of OUR followed by a decreasing phase. This later case will be noted as two trends feature. Some specificities in OUR profile can be seen for cellulose (irregular OUR profile). In addition, two scales of degradation time were observed: a few days (1-2.5) or at least 10 days.

The kinetic constants estimated using a first-order model was of 0.13 d^{-1} in the case of xylan (this thesis). For the cases of toilet paper and large boiled-egg whites, the calculated specific growth rates were very close (0.45 and 0.46 d^{-1}, respectively). The hydrolysis rate constant considering a first-order hydrolysis process were estimated to 0.45 and 0.61 d^{-1} respectively. In the case of cellulose, it was not possible to linearize any of the OUR phase.

It was also noticed that degradation of the model substrates did not begin immediately after inoculation. A time for adaptation or acclimation was systematically observed though this time strongly depends on the type of substrates (a few hours for xylan or boiled-egg white and a few days for cellulose and toilet paper).

Finally, the values of initial and maximal OUR were very different from one experiment to another.

10.DISCUSSION

10.1.CHARACTERISTIC TIME AND DEGRADATION YIELD

Very different characteristic times were observed for the degradation of the different PSS and also for the degradation of model substrates. In the case of PSS, a huge difference is observed between the degradation time found in our study or in the study of Sperandio (1998), (i.e. around 13 days) and that in the study of Orhon et *al.* (2002) and Tas et *al.* (2009) (0.25 day). It is likely that either different types (mean diameter, structure) of particles or different types of molecules (types of proteins, polysaccharides, lipids…) are degraded in the two cases. This underlines the strong difference on the hydrolysis kinetic depending on the type of molecules, the possibility of their aggregation and on their geometric aspect. This is confirmed by the results obtained with model substrates: degradation of toilet paper compared to pure cellulose or degradation of xylan lasting one day compared to degradation of cellulose lasting 10 days.

The percentage of COD elimination was the highest in the xylan case study while the characteristic time was the lowest, compared to toilet paper and cellulose. Concerning the COD yield per day, it was of 0.88 gCOD/d for xylan, 0.52 gCOD/d for toilet paper and 0.57 gCOD/d for commercial cellulose. Xylan appears clearly to have the highest elimination (hydrolysis) rate compared to the other substrates. This may be attributed to its high bioavailability towards catalytic biomass. In fact, it is found that the substrate bioavailability is directly linked to the structure of the substrates (Barret et al., 2010; Perez et al., 2009). Xylan is composed by simple sugars with easily-breakable osidic bonds compared to cellulose (or toilet paper which is mainly composed by cellulose) which is known to have a more complex structure.

The percentage of degradation also varies depending on the substrate. As conventionally represented in current models, the consideration of unbiodegradable matter in the solid compartment is compulsory if we want to represent the degradation of PSS.

10.2.GLOBAL TRENDS

Two global features were observed during the different degradations performed. Either the OUR started at a high value (tight peak) at the beginning of the experiment and decreased with an exponential feature reaching at the end the OUR values corresponding to the endogenous respiration rate or the OUR started at a low value sometimes remaining a few hours or days, then increases with an exponential feature until a maximum value and then decrease with a similar feature than in the previous case. The first case can be described by a simple

model of first order with respect to the particulate substrate concentration. The second case supposes that a surface dependent process should occur. The reason why these two features could be observed (depending on substrate type) is at the present time not well understood. This aspect will be investigated in chapter II. The two trends feature was systematically observed for model substrates. On contrary, the one trend appearance was mostly found for PSS (notable exception for the experiment of Sperandio (1998)). In order to better understand the causes of these differences between the "one trend" or the "two trends" features, we must consider the complexity of the substrates that are degraded and also the mechanisms of hydrolysis that include not only the enzymatic functioning but also the substrate colonization by the catalytic biomass. In the case of a complex substrate such as PSS, the OUR curve is in majority of one trend. This might indicate that a multiple degradation processes characterizing the presence of multiple substrates with different rate constants and may be different concentrations occur simultaneously. The mean response gives the impression of the degradation of a unique substrate (Balmat, 1957). This might also indicate that even at the beginning of the respirometric test the saturation of the particulate matter surface by bacteria was already achieved. This latter assumption supposes that in case of the experiment conducted by Spérandio, (1998) the PSS were not entirely colonized by active cells contrarily to what was the case with the other experiments performed on PSS. Such a difference can be easily understood because the PSS used in Sperandio (1998) come from a part of the sewer situated at the early beginning of the network and thus very close to the release of raw materials by the inhabitants. Colonization of the particulate organic matter by the specialized bacteria had certainly just begun. Finally, each two trends OUR profile experiment, except Sperandio's (1998) experiment, showed a lag phase of few hours (xylan) or few days (toilet paper) which could be attributed to acclimation of bacterial cells (that are present in the inoculum) to the corresponding substrates. This was especially observed in the cases of model substrates that were fed none acclimated biomass. In Orhon and Sozen (2012) this phase was integrated in the modeling approach by including an additional catalytic biomass which is able to degrade a specific substrate (xenobiotics). This aspect will be further investigated with more insight in chapter IV.

10.3.KINETIC ASPECTS

10.3.1.Catalytic biomass role and extent

It is obvious that very different kinetics were observed for the different substrates that were presented in this chapter. Different levels of variation of OUR during one experiment were

observed. These variations should have for origin the increase during the test of the activity of the specialized biomass (which was able to consume the substrate). The maximum increase of the OUR (OUR_{max}/OUR_{ini}) observed in the presented experiments is of a factor of about ten that supposes a substantial increase in activity. Therefore, it is reasonable to think that colonization of the surface of the substrate occurred during this period of the test. The knowledge of the amount of active cell present at the beginning of the test is of a great importance for explaining the OUR profile. This amount should be determined with accuracy in both cases where inoculum is added or not.

In addition, a time lag phase was observed in our experiment with toilet paper while the OUR increased immediately after substrate addition (PSS) in Sperandio's (1998) experiment. This may be attributed to acclimation of bacteria towards a given substrate. In fact, in our experiment (TP), the inoculum (activated sludge) was not previously acclimated to the substrate, thus, bacterial cells needed time to get used to the substrate. In contrary, in Sperandio's (1998) experiment, we can suppose that at least a part of the bacteria was acclimated to the substrate (PSS) as they were in contact during a certain time before performing the experiment.

10.3.2.Number of particulate substrates

Literature experiments presented in this chapter mainly investigated PSS hydrolysis with the means of OUR monitoring only. The monitoring of additional features such as COD_P in our PSS experiment indicated the presence of two (very) slowly biodegradable COD fractions when the OUR showed a unique decreasing phase. This may indicate that the approach that was adopted by Tas et *al.* (2009) and Orhon et *al.* (2002) (OUR monitoring coupled to modeling) has the advantage to characterize PSS in a global way but may not give correct information concerning what really occurs in the batch reactor.

In order to conclude on the different aspects of this discussion, a model to represent hydrolysis processes in complex wastewater may have to consider various particulate substrates differing by their biodegradability and their kinetic characteristics. It should be able to consider the amount of cells really active on hydrolysis processes. In the following chapter, the models already available in literature will be assessed for their ability to represent the different features we observed for both PSS and model substrates.

11. CONCLUSION

This chapter was dedicated to observe OUR profiles either available from literature or obtained in this work to evaluate the similarities and differences and attempt to deduce the major trends on the mechanisms and the major questions to be addressed.

A first observation was that literature offered only very few experimental results on the degradation of particulate organic matter.

A second observation was that there were great differences on duration of biodegradation, appearance of the curves, initial and maximal OUR values, etc. These differences may be attributed to substrate complexity or specificities (in the case of model substrates) and/or to the cell activities and ways of attacking the particulate organic matter.

Information available from only the OUR curve is not enough for giving more insights on the mechanisms of hydrolysis. The monitoring of additional COD_P evolution in our experiments highlighted the necessity to consider not only one unique substrate but at least two distinct slowly biodegradable COD fractions in order to characterize with more accuracy PSS.

A time-lag phase was systematically observed in model substrates experiments and was attributed to acclimation. It might be necessary to integrate this process in the modeling approach in order to give more insight to experimental data description and above all for mechanisms characterisation and dissociation.

The monitoring of additional features beside the OUR such as ammonia ($N\text{-}NH_4^+$), particulate and soluble COD could be interesting to enhance the comprehension of the mechanisms that are involved (qualitatively) in the degradation and may give indications for the choice of the model (or models) to evaluate and confront to the set of experimental data.

In the following chapter, appropriately chosen models derived from wastewater conventional models (IAWQs models) and less conventional ones (taking into account physical and geometrical properties) were confronted to the experimental data performed in this thesis and picked-up from literature.

CHAPTER II

"Experiment and WWTPs model confrontation: are existing models able to describe particulate organic matter experiments?"

1. INTRODUCTION

It is now well known that modeling is a key tool for the design and operation of wastewater treatment plants. It is not only used for the simulation and prediction of wastewater processes, but also as a comprehension tool in order to decouple the main mechanisms that are involved during carbon oxidation and particularly the hydrolysis step when dealing with solid organic matter.

The characterization of the biodegradation of urban wastewater, and particularly particulate settleable solids (PSS), is usually assessed by confronting the appropriate model to real experimental data or model calibration. Models that are applied in WWTP processes (International Association on Water Quality Models) are found to describe well hydrolysis; however, in function of the case study, the identified hydrolysis rate constants (and/or other additional parameters that characterize hydrolysis) were found to be different. This indicates that model calibration is directly linked to experiment operating conditions and that hydrolysis may be affected by substrate and bacteria concentrations and/or their physical properties, the type of substrate, the presence of more than one substrate, bacteria communities, enzymatic capacities, etc.

Thusly, the objective of this chapter is to test the ability of existing models to represent the kinetics of degradation of solid organic matters and underline the advantages and weaknesses of each of them. The means that are utilized to succeed are to try different models or combination of models that are conventionally used in WWTP processes or unconventional ones in order to underline their ability or not to describe a unique case study or different ones at the same time and thus raise their limits. The models that were selected to be evaluated are presented below:

(1) the **IAWQ-1** (Henze et al., 1987) modified for endogenous respiration **(model A1)**;
(2) a first order-hydrolysis model (**FOHM**) derived from the previous one **(model A2)**;
(3) the Dual Hydrolysis model (**DHM**) of Sollfrank and Gujer (1991) **(model B1)**;
(4) a First-order Dual Hydrolysis (**FODHM**) model derived from the DHM (**model B2**);
(5) the Surface-based Kinetic model (**SBK**) developed by Hobson (1987) (**model C1**);
(6) the **DHM** coupled to the **SBK** model (**SBKDHM**) (**model C2**).

All these models will be calibrated for the cases of real influent (PSS) and model substrates (toilet paper: TP). Besides the OUR, ammonia utilization, which characterizes heterotrophic biomass growth and decay, will be also used for model calibration in order to reduce the degree of freedom of each considered model and thus evaluate their reliability.

12.BASIC AND INCREASING COMPLEXITY HYDROLYSIS MODELS

In this section, we will describe briefly the entire biological models (including the mathematical expressions of hydrolysis) which were evaluated in this work to describe both real influent (PSS) and model substrate (toilet paper) studies.

12.1.SURFACE-BASED AND FIRST-ORDER HYDROLYSIS MODELS

12.1.1.Contois mathematical expression

The extracellular hydrolysis process is commonly accepted to be a surface-based mechanism as bacteria and solid substrate need to be in contact to initiate the biochemical reaction as enunciated in the section above. It was already introduced in the earlier IAWQ model n°1, which was developed by Henze et al. (1987), as a surface-limited process. The kinetic expression of this mechanism was proposed by some IAWQ group authors (Dold et al., 1980; Ekama and Marais, 1979; Henze et al., 1987) and was maintained in further models that were developed by the same group such as the IAWQ-2, IAWQ-2d and IAWQ-3 (Gujer et al., 1999, 1995; Henze et al., 1987). That expression derived from Levenspiel's (1972) researches who studied surface limitation processes. The kinetic expression of hydrolysis in this model is written as below:

$$\frac{dXC_B}{dt} = - q_{XCB\_SB,hyd} \frac{XC_B / X_{OHO}}{K_{XCB,hyd} + XC_B / X_{OHO}} X_{OHO} \quad (1)$$

Where $q_{XCB\_SB,\,hyd}$ is the hydrolysis rate constant [d^{-1}] and $K_{XCB,\,hyd}$ is the half-saturation constant for hydrolysis [mgCOD. $mgCOD^{-1}$]. This expression could be simplified as first-order towards the substrate as reported in Balmat, (1957); Gujer and Henze, (1991); Kappeler and Gujer, (1992); Mino et al., (1995); Sollfrank and Gujer, (1991).

Indeed, when $XC_B << X_{OHO}$ and $X_{CB}/X_{OHO} << K_{XCB,\,HYD}$ then:

$$\frac{dXC_B}{dt} = - q'_{XCB\_SB,hyd} XC_B \quad (2)$$

Where $q'_{XCB\_SB,\,hyd}$ is the modified hydrolysis rate constant [mgCOD. $mgCOD^{-1}$. d^{-1}]. The previous hydrolysis expression does not depend on biomass concentration as reported in

Sollfrank and Gujer (1991) who studied wastewater settleable fraction in batch reactors. They found out that the hydrolysis rates were constant whatever biomass concentration. This was also observed by San Pedro (1994) in batch assays fed with starch. Nevertheless, Kappeler and Gujer (1992) observed an increase of the hydrolysis rate (1.5 to 10 d^{-1}) when biomass concentration was increased as well (100 to 1600 mgCOD/L). This last observation may be explained by the difference of substrate to biomass ratios that were utilized in each study.

12.1.2.Surface-based kinetic model (SBK)

The substrate to biomass ratio (XC_B/X_{OHO}) in the previously enunciated expression is supposed to represent in a mathematical point of view a surface limiting process. This is however somewhat misleading as X_{OHO} and XC_B are expressed as mass concentrations and do not consider the shape (diameter, length) and physical characteristics of those species. Underlining that hydrolysis depends on the substrate available surface area, which depend on particle size and shape, some studies underlined the weakness of the conventional *IAWQ* models to describe some case studies (Dimock and Morgenroth, 2006; Sanders et al., 2000).

Hobson (1987) introduced a model that considers hydrolysis as a surface limited reaction in a literal sense: the Surface Based Kinetic (SBK) model. This model correlates the hydrolysis rate constant to the physical or geometrical characteritics of particles. In this case, hydrolysis is limited by the solid substrate available surface area. This model assumes that active bacteria that secretes exo-enzymes cover all the substrate surface area. The hydrolysis rate constant (k_{SBK}) does not depend on particle size or diameter. The kinetic expression of hydrolysis is presented below:

$$\frac{dXC_B}{dt} = - k_{sbk} A \qquad (3)$$

In the previous expression, k_{sbk} is a surface-based hydrolysis constant [$kg.m^{-5}.d^{-1}$] and A is the available substrate (XC_B) surface area [m^2]. In this model, it is assumed that hydrolysis continuously reduces substrate particle diameter. The surface area of similar shaped particles could be replaced by $(XC_B)^{2/3}$ and equation 4 could be simplified by equation 5 when considering spherical particulate substrate.

$$\frac{dXC_B}{dt} = - k'_{sbk} (XC_B)^{2/3} \qquad (4)$$

Where k'_{sbk} is a modified surface-based hydrolysis constant [$kg^{1/3}.m^{-1}.d^{-1}$].

12.2.MULTIPLE SOLID SUBSTRATES MODELING

As reported in the first chapter of results, an OUR "one trend" curve may hide the presence of multiple solid substrates. It would be then necessary to consider more than one solid substrate (at least two distinct substrates) in the model in order to describe correctly some case studies.

Sollfrank and Gujer (1991) developed the "Dual Hydrolysis Model" (DHM), a model that takes into account two distinct particulate organic substrates. They were differentiated by their kinetic characteristics (hydrolysis rate constants and half saturation constant for hydrolysis). This model was utilized later by Orhon et *al.* (1998) to characterize industrial wastewaters (textile,…). The considered model was found to be more accurate than the conventional IAWQ model n°1.

The DHM was also used by Orhon et *al.* (2002), Orhon et *al.* (1997), and Tas et *al.* (2009) in the case of wastewater settleable solids. In these studies, the consideration of a rapidly hydrolysable fraction (XC_{B1}) near a slowly hydrolysable fraction (XC_{B2}) was necessary in order to describe correctly the OUR profiles. The system of equations is presented below.

$$\frac{dXC_{B1}}{dt} = -\,q_{XCB1\_SB,hyd}\frac{XC_{B1}/X_{OHO}}{K_{XCB1,hyd}+XC_{B1}/X_{OHO}}X_{OHO} \quad (5)$$

$$\frac{dXC_{B2}}{dt} = -\,q_{XCB2\_SB,hyd}\frac{XC_{B2}/X_{OHO}}{K_{XCB2,hyd}+XC_{B2}/X_{OHO}}X_{OHO} \quad (6)$$

Where XC_{B1} and XC_{B2} are the slowly biodegradable COD concentrations [$mgCOD.L^{-1}$], $q_{XCB1\_SB,\,hyd}$ and $q_{XCB2\_SB,\,hyd}$ are the hydrolysis rate constants for XC_{B1} and XC_{B2}, respectively [d^{-1}], $K_{XC\_B1,\,hyd}$ and $K_{XC\_B2,\,hyd}$ are the half-saturation constants for hydrolysis for XC_{B1} and XC_{B2}, respectively [mgCOD. $mgCOD^{-1}$].

Many other models were proposed in literature to describe the hydrolysis step. Table 25 regroups the previously enunciated models as well as less conventional ones which were developed for specific situations (very high or very low S/X ratio). It has to be mentioned that some of these models could give the same type of response.

All the previously enunciate models as well as combination of those models were tested to describe:

a) Experiments that were performed in this thesis on real influent (PSS) and toilet paper;
b) Sperandio's (1998) experiment on PSS.

The next section is dedicated to the presentation of the materials and methods that were achieved in this work for each case study.

13.MATERIALS AND METHODS FOR MODELING

13.1.EXPERIMENTAL DATA

All the data were collected during batch aerobic tests (respirometry). In each case, activated sludge was fed with a certain type of particulate organic matter. In this study, we utilized domestic wastewater settleable COD (or particulate settleable solids, PSS) and basic toilet paper, which is found to be representative of PSS.

PSS were obtained (in our laboratory) by settling pre-treated wastewater, which was collected before the primary sedimentation step, in the WWTP of Toulouse-Ginestous (France). This operation was described in details in the materials and methods chapter. Additional data were picked up from Sperandio (1998) who investigated PSS in the past. He collected this matter at the beginning of the sewer system.

In the last experiment, toilet paper was mixed with activated sludge. Previously, the composition of toilet paper was assessed (protocol was detailed in materials and methods chapter): it is composed by 79% of cellulose and 12% of xylose, which represents the biodegradable fraction, and 9% composed by mineral matter and other non-identified components, which are unbiodegradable. Table 23 summarises the considered experiments for model calibration.

Table 23: Summary of the experiments that were utilized for model calibration

Exp.	Substrate	Substrate concentration (gCOD/L)	Inoculum concentration (gCOD/L)	T (°C)	pH	Source
PSS-1a	PSS	9.23	0	20±0.1	7±0.2	This study
PSS-2a[1]	PSS	0.87	0.48	ND	ND	Sperandio (1998)
TP1-a	Toilet paper	8.99	0.71	20±0.1	7±0.2	This study

13.2.BIOLOGICAL MODELS

In this work, all the mathematical models are based on the IAWQ model n°1 (Henze, 1987). Beside hydrolysis, the main mechanisms that were considered were aerobic growth and decay of heterotrophs. Adsorption was not considered in any model in order to reduce the degree of freedom of the model and thus have mainly the parameters linked to hydrolysis to identifiy. Storage of substrates in the form of polymers (glycogen, PHA) was neglected as no nutrient limitation (phosphorus, nitrogen, etc.) was observed during our experiments. In addition, nitrification processes were not considered as it was inhibited by the addition of *N-Allylthiourea* (ATU). In terms of pollution, only organic carbon and ammonia were considered in these models.

Concerning carbon, it is considered that heterotrophic bacteria (X_{OHO}) secretes exo-enzymes that hydrolyses particulate substrate (XC_B) into soluble readily biodegradable substrate ($S_{B,HYD}$), which is uptaken by heterotrophic bacteria (X_{OHO}) during aerobic growth. Finally, heterotrophs (X_{OHO}) undergo endogenous respiration and release particulate unbiodegradable residue ($X_{U\_Bio\ Lys}$). It could be noticed that the death-regeneration model was replaced by the endogenous respiration model as both of them lead to the same result.

Nitrogen, in the form of ammonia (S_{NH4}), is utilized by heterotrophic bacteria during aerobic growth. It is also released by the same bacteria, in the form of biodegradable and unbiodegradable bacterial metabolites and ammonia during endogenous respiration. Table 24 regroups the models that were utilized in this work.

[1] PSS was collected at the beginning (upstream) of the sewage network in this experiment

Table 24: Models Processes stoichiometry and kinetics

Process	*Soluble species*			*Particulate species*					Process rate
	$S_{B,HYD}$	S_{O2}	S_{NH4}	XC_B	XC_{B1}	XC_{B2}	X_{OHO}	X_U	
Model A1 - IAWQ model n°1 (Henze et al., 1987)									
1	*1*			*-1*					$q_{XCB\_SB,hyd}\frac{XC_B/X_{OHO}}{K_{XCB,hyd}+XC_B/X_{OHO}}X_{OHO}$
2	*-1/Y_{OHO}*	*-(1-Y_{OHO})/Y_{OHO}*	*-i_{N_XBio}*				*1*		$\mu_{OHO,max}\frac{S_{B,hyd}}{K_{SB,hyd}+S_{B,hyd}}X_{OHO}$
3		*-(1- $f_{XU\_Bio,lys}$)*	*$f_{XU\_Bio,lys}$*$i_{N,XU}$ + i_{N_XBio}*				*-1*	*$f_{XU\_Bio,lys}$*	$b_{OHO}X_{OHO}$
Model A2 - IAWQ model n°1 with first-order hydrolysis model									
1	*1*			*-1*					$q'_{XCB\_SB,hyd}XC_B$
2	*-1/Y_{OHO}*	*-(1-Y_{OHO})/Y_{OHO}*	*-i_{N_XBio}*				*1*		$\mu_{OHO,max}\frac{S_{B,hyd}}{K_{SB,hyd}+S_{B,hyd}}X_{OHO}$
3		*-(1- $f_{XU\_Bio,lys}$)*	*$f_{XU\_Bio,lys}$*$i_{N,XU}$ + i_{N_XBio}*				*-1*	*$f_{XU\_Bio,lys}$*	$b_{OHO}X_{OHO}$
Model B1 - Dual Hydrolysis Model, DHM (U. Sollfrank and Gujer, 1991)									
1	*1*				*-1*				$q_{XCB1\_SB,hyd}\frac{XC_{B1}/X_{OHO}}{K_{XCB1,hyd}+XC_{B1}/X_{OHO}}X_{OHO}$
2	*1*					*-1*			$q_{XCB2\_SB,hyd}\frac{XC_{B2}/X_{OHO}}{K_{XCB2,hyd}+XC_{B2}/X_{OHO}}X_{OHO}$
3	*-1/Y_{OHO}*	*-(1-Y_{OHO})/Y_{OHO}*	*-i_{N_XBio}*				*1*		$\mu_{OHO,max}\frac{S_{B,hyd}}{K_{SB,hyd}+S_{B,hyd}}X_{OHO}$
4		*-(1- $f_{XU\_Bio,lys}$)*	*$f_{XU\_Bio,lys}$*$i_{N,XU}$ + i_{N_XBio}*				*-1*	*$f_{XU\_Bio,lys}$*	$b_{OHO}X_{OHO}$
Model B2 - DHM with first-order hydrolysis mechanism									
1	*1*				*-1*				$q'_{XCB1\_SB,hyd}XC_{B1}$
2	*1*					*-1*			$q'_{XCB2\_SB,hyd}XC_{B2}$

3	$-\frac{1}{Y_{OHO}}$	$-\frac{(1-Y_{OHO})}{Y_{OHO}}$	$-i_{N\_XBio}$			1		$\mu_{OHO,max}\frac{S_{B,hyd}}{K_{SB,hyd}+S_{B,hyd}}X_{OHO}$
4		$-(1-f_{XU\_Bio,lys})$	$f_{XU\_Bio,lys}*i_{N,XU}+i_{N\_XBio}$			-1	$f_{XU\_Bio,lys}$	$b_{OHO}X_{OHO}$
Model C1 - Surface-based Kinetic Model, SBK (Hobson, 1987)								
1	1			-1				$k_{SBK}XC_B^{\frac{2}{3}}$
2	$-\frac{1}{Y_{OHO}}$	$-\frac{(1-Y_{OHO})}{Y_{OHO}}$	$-i_{N\_XBio}$			1		$\mu_{OHO,max}\frac{S_{B,hyd}}{K_{SB,hyd}+S_{B,hyd}}X_{OHO}$
3		$-(1-f_{XU\_Bio,lys})$	$f_{XU\_Bio,lys}*i_{N,XU}+i_{N\_XBio}$			-1	$f_{XU\_Bio,lys}$	$b_{OHO}X_{OHO}$
Model C2 - Surface-based Kinetic Model coupled with DHM								
1	1				-1			$k_{SBK\_XCB1}XC_{B1}^{\frac{2}{3}}$
2	1					-1		$k_{SBK\_XCB2}XC_{B2}^{\frac{2}{3}}$
3	$-\frac{1}{Y_{OHO}}$	$-\frac{(1-Y_{OHO})}{Y_{OHO}}$	$-i_{N\_XBio}$			1		$\mu_{OHO,max}\frac{S_{B,hyd}}{K_{SB,hyd}+S_{B,hyd}}X_{OHO}$
4		$-(1-f_{XU\_Bio,lys})$	$f_{XU\_Bio,lys}*i_{N,XU}+i_{N\_XBio}$			-1	$f_{XU\_Bio,lys}$	$b_{OHO}X_{OHO}$

Oxygen consumption, which is measured as the oxygen uptake rate (OUR), is carried out by heterotrophs during aerobic growth and also during aerobic endogenous respiration of those bacteria. The OUR could be written as below:

$$OUR = -\frac{d[S_{O_2}]}{dt} = \left(\left(\frac{1-Y_{OHO}}{Y_{OHO}}\right)\mu_{OHO,max}\frac{S_{B,hyd}}{K_{SB,hyd}+S_{B,hyd}} + (1-f_{XU_{Bio},lys})b_{OHO}\right)X_{OHO} \quad (7)$$

13.3. DEFAULT VALUES OF KINETIC PARAMETERS AND STOICHIOMETRIC COEFFICIENTS

The initial values of parameters before model calibration were picked up from literature. The default values of kinetic and stoichiometric coefficients of the models were those identified by Henze et *al.* (1987) for the aerobic growth process. The yield for heterotrophic bacteria aerobic growth was fixed to 0.63 mgCOD/mgCOD (Gujer et *al.* (1995)). The parameters that characterize endogenous respiration were those identified by Ekama and Marais (1979). Concerning hydrolysis, the default values of parameters are those identified by the corresponding authors for each model. Table 25 regroups the kinetic and stoichiometric coefficients for each model.

Table 25: Standard values of the kinetic and stoichiometric coefficients for each model and experiment. The range of variation of each parameter is reported in Appendix 2d.

Parameter	Description	Unit	Model						Source
			A1	A2	B1	B2	C1	C2	
b_{OHO}	Endogenous respiration rate for heterotrophs	d^{-1}	0.2	0.2	0.2	0.2	0.2	0.2	Gujer et al., (1999)
$f_{XU\_Bio,\ lys}$	Inert fraction of heterotrophs	$mgCOD.mgCOD^{-1}$	0.2	0.2	0.2	0.2	0.2	0.2	Gujer et al., (1999)
$\mu_{OHO,\ max}$	Maximum X_{OHO} growth rate	d^{-1}	6	6	6	6	6	6	Henze et al., (1987)
$i_{N\_X\_BIO}$	Ammonia content of heterotrophs	$mgN.gCOD^{-1}$	0.07	0.07	0.07	0.07	0.07	0.07	Gujer et al., (1999)
i_{N_XU}	Ammonia content of particulate unbiodegradable organics	$mgN.gCOD^{-1}$	0.02	0.02	0.02	0.02	0.02	0.02	Gujer et al., (1999)
$K_{SB,\ OHO}$	Half-saturation coefficient for growth of heterotrophs	$mgCOD.L^{-1}$	20	20	20	20	20	20	Henze et al., (1987)
$K_{XCB,\ hyd}$	Half-saturation coefficient for XC_B	$mgCOD.mgCOD^{-1}$	0.03	-	-	-	-	-	Henze et al., (1987)
$K_{XCB\_1,\ hyd}$	Half-saturation coefficient for hydrolysis of XC_{B1}	$mgCOD.mgCOD^{-1}$	-	-	0.2	-	-	-	Orhon et al., (1998)
$K_{XCB\_2,\ hyd}$	Half-saturation coefficient for hydrolysis of XC_{B2}	$mgCOD.mgCOD^{-1}$	-	-	0.5	-	-	-	Orhon et al., (1998)
k_{SBK}	Surface-based hydrolysis rate constant for XC_B	$kg.m^{-5}.d^{-1}$	-	-	-	-	3	-	Sanders et al., (2000)
k_{SBK_XCB1}	Surface-based hydrolysis rate constant for XC_{B1}	$kg.m^{-5}.d^{-1}$	-	-	-	-	-	3	Sanders et al., (2000)
k_{SBK_XCB2}	Surface-based hydrolysis rate constant for XC_{B2}	$kg.m^{-5}.d^{-1}$	-	-	-	-	-	3	Sanders et al., (2000)
$q_{XCB\_SB,\ HYD}$	Hydrolysis rate constant for Hydrolysable substrate	d^{-1}	3	-	-	-	-	-	Henze et al., (1987)
$q'_{XCB\_SB,\ HYD}$	Modified hydrolysis rate constant for hydrolysable substrate	$mgCOD.mgCOD^{-1}.d^{-1}$	-	2.5	-	-	-	-	Sollfrank et al. (1991)
$q_{XCB1\_SB,\ HYD}$	Hydrolysis rate constant for XC_{B1}	d^{-1}	-	-	3.1	-	-	-	Orhon et al., (1998)
$q_{XCB2\_SB,\ HYD}$	Hydrolysis rate constant for XC_{B2}	d^{-1}	-	-	1.2	-	-	-	Orhon et al., (1998)
$q'_{XCB1\_SB,\ HYD}$	Modified hydrolysis rate constant for XC_{B1}	$mgCOD.mgCOD^{-1}.d^{-1}$	-	-	-	15,5	-	-	Orhon et al., (1998)
$q'_{XCB2\_SB,\ HYD}$	Modified hydrolysis rate constant for XC_{B2}	$mgCOD.mgCOD^{-1}.d^{-1}$	-	-	-	2,4	-	-	Orhon et al., (1998)
Y_{OHO}	Heterotrophic yield coefficient	$mgCOD.mgCOD^{-1}$	0.63	0.63	0.63	0.63	0.63	0.63	Gujer et al., (1995)

13.4.MODEL CALIBRATION

As mentioned before, all the utilized models derive from the IAWQ model n°1 (Henze, 1987) for the entire mechanisms involved except for hydrolysis. The previously detailed models and experimental data will be confronted in this section.

Each experiment will be confronted to models that are in accordance with the hypothesized occurring mechanisms. For example, toilet paper experiment (TP) will be confronted to models A1, B1 and B2 but not model A2 as it is not able to describe the colonization phase but only the OUR decreasing phase as it comes from a wide excess of X_{OHO}.

Models calibrations were performed according to conventionally utilized methods for activated sludge modelling. In this study, surface oxygen transfer (T) was not included in the modeling methodology as it was measured experimentally in each case study (the procedure is detailed in Appendix 1). Only biological processes were simulated. All the simulations were performed with the AQUASIM® computer program developed by Reichert (1994). The detailed procedure is reported in §6 of the experimental and modeling material and methods chapter.

13.4.1.Sensitivity analysis

A sensitivity analysis has been performed comparing the previously detailed models with each batch experiment (results in Appendix 2a, 2b and 2c). See §6.3.1 of the experimental and modeling material and methods chapter for more details.

13.4.2.Parameter estimation

See §6.3.2 of the experimental and modeling material and methods chapter.

14.RESULTS

14.1.PARTICULATE SETTLEABLE SOLIDS (PSS)

14.1.1.PSS-1a (This study)

All the previously enunciated models were confronted to the experimental data collected from PSS-1a with increasing model structure complexity. Oxygen mass balance was checked. More than 65% of the total COD (COD_T) was eliminated in which 99,9% was in the particulate form (COD_P).

As neither the amount of initial active bacteria (attached to the substrate) nor the initial substrate concentration were known, an additional "formula variable" which corresponds to the sum of the initial amounts of active bacteria ($X_{OHO,\ 0}$) and substrates ($X_{CB,\ 0}$) initial was created (Equation (8)). This one also integrated the unbiodegradable matter that come from the influent ($X_{U,\ Inf}$). This amount could not exceed the initial concentration of particulate COD ($COD_{P,\ 0}$).

$$COD_{P,0}=XC_{B,0}+X_{OHO,0}+X_{U,Inf} \quad (8)$$

Figure 25 shows simulated and experimental data (OUR, $N\text{-}NH_4^+$ and COD_P) during the experiment batch test. The identified kinetic parameters and stoichiometric coefficients are reported in Table 26.

The oxygen uptake rate, OUR, varied between 9 and 83 $mgO_2/L/h$. The first value defines the endogenous respiration rate and the other value the initial tight peak. The ammonia concentration decreased from 428 mgN/L down to 293 mgN/L and this decrease mainly occurred at be beginning of the experiment. The COD_P varied from 9.23 to 3.07 gCOD/L and the COD_P degradation yield is of 67%.

Model A1

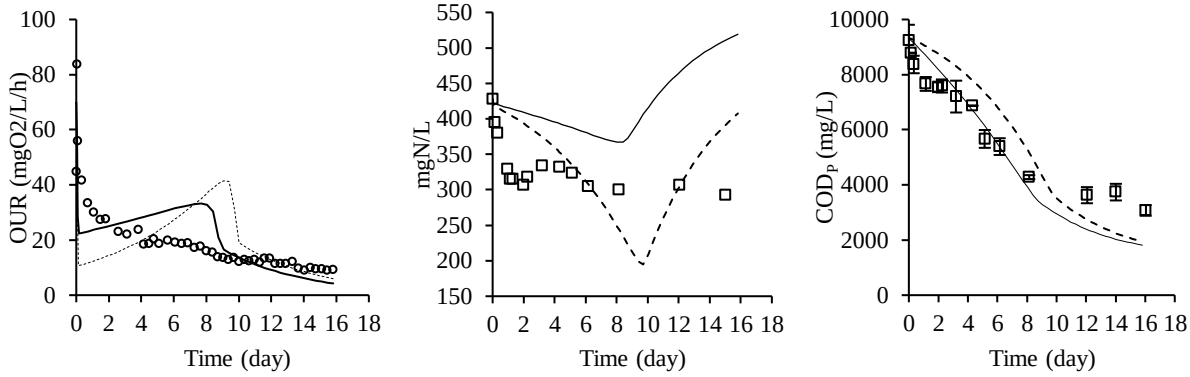

Model A2

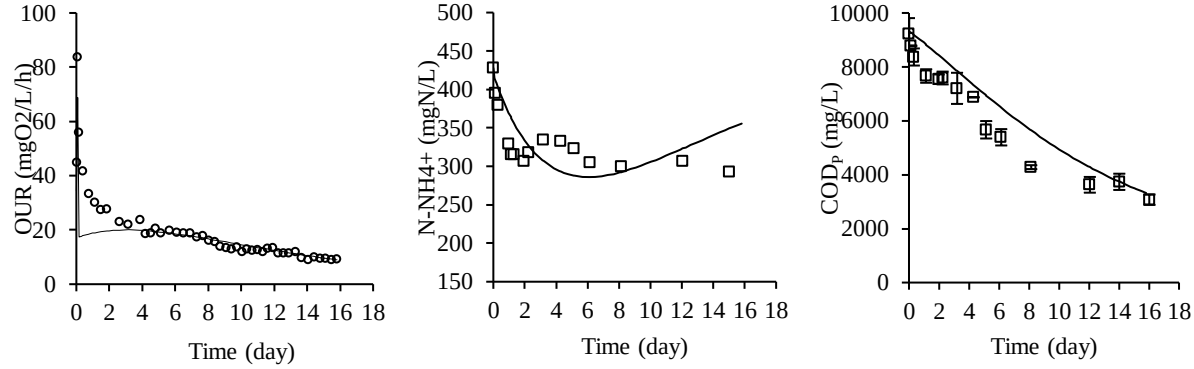

Model B1

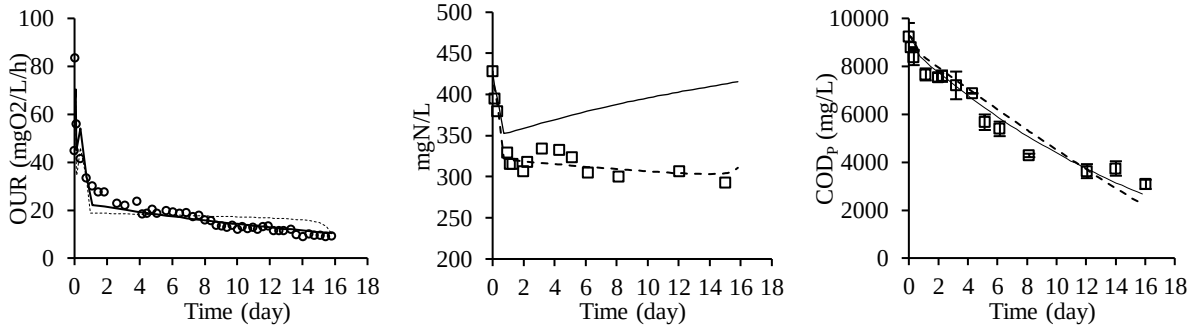

Model B2

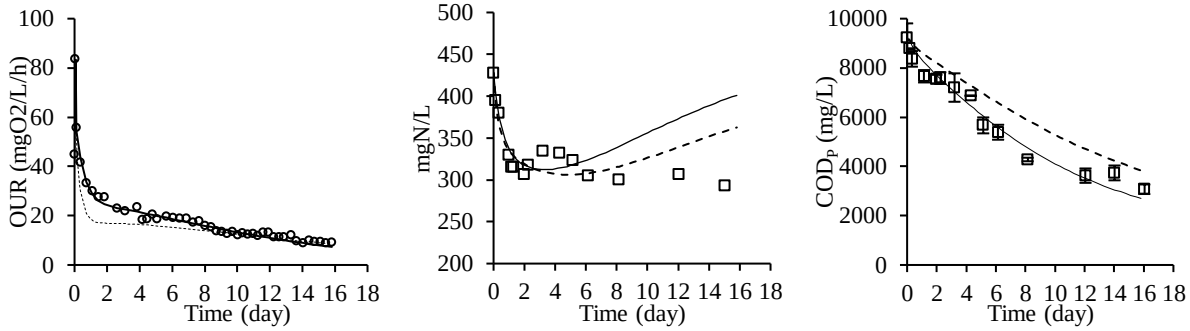

Model C1

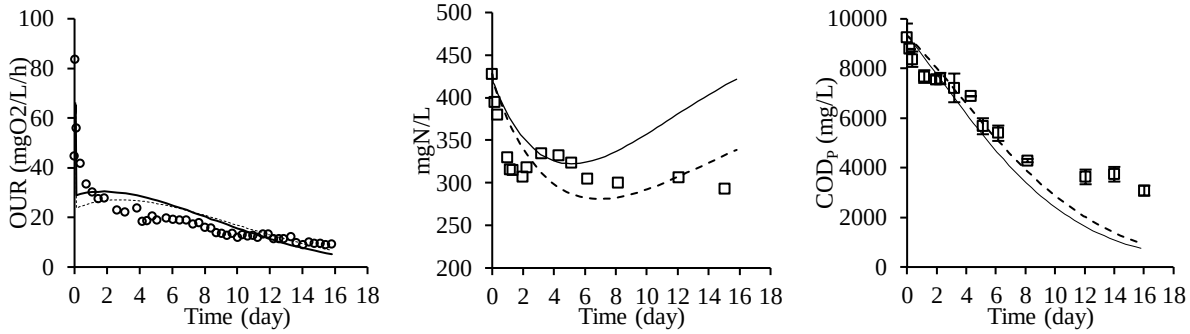

Model C2

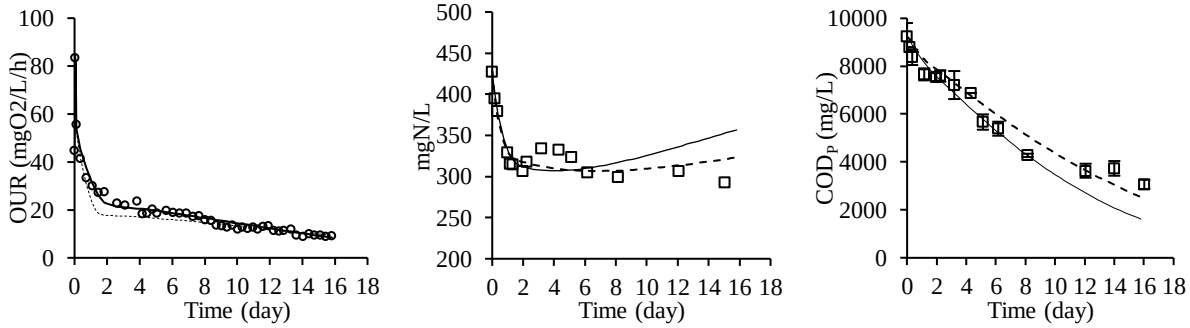

Figure 25 : Models calibration for PSS-1 experiment (continuous line (—) for OUR calibration, dashed line (---) for OUR/ N-NH_4^+ calibration).

Table 26: Models parameter estimation and initial values of state variables for model OUR calibration and OUR/N-NH_4^+ calibration. Underlined parameters were fixed.

Parameter	Unit	OUR calibration						OUR/N-NH_4^+ calibration					
		A1	A2	B1	B2	C1	C2	A1	A2	B1	B2	C1	C2
b_{OHO}	d^{-1}	0.2	0.2	0.2	0.2	0.2	0.2	0.2	0.2	0.2	0.2	0.2	0.2
$f_{XU\_Bio,\ lys}$	$mgCOD.mgCOD^{-1}$	0.2	0.2	0.2	0.2	0.2	0.2	0.2	0.2	0.2	0.2	0.2	0.2
$\mu_{OHO,\ max}$	d^{-1}	2	11	2	10	2.14	12	3.5	10	3.44	10.3	5.45	12
$i_{N\_X\_BIO}$	$mgN.gCOD^{-1}$	0.07	0.07	0.07	0.07	0.07	0.07	0.1	0.1	0.1	0.1	0.07	0.08
i_{N_XU}	$mgN.gCOD^{-1}$	0.02	0.02	0.02	0.02	0.02	0.02	0.01	0.01	0.05	0.01	0.05	0.05
$K_{SB,\ OHO}$	$mgCOD.L^{-1}$	50	1.32	0.04	0.46	0.003	23.36	43	5.10^{-4}	0.02	0.85	0.81	0.01
$K_{XCB,\ hyd}$	$mgCOD.mgCOD^{-1}$	0.03	-	-	-	-	-	0.03	-	-	-	-	-
$K_{XCB\_1,\ hyd}$	$mgCOD.mgCOD^{-1}$	-	-	0.03	-	-	-	-	-	0.03	-	-	-
$K_{XCB\_2,\ hyd}$	$mgCOD.mgCOD^{-1}$	-	-	0.03	-	-	-	-	-	0.03	-	-	-
k_{SBK}	$kg.m^{-5}.d^{-1}$	-	-	-	-	3.4	-	-	-	-	-	3.1	-
k_{SBK_XCB1}	$kg.m^{-5}.d^{-1}$	-	-	-	-	-	16.8	-	-	-	-	-	22.3
k_{SBK_XCB2}	$kg.m^{-5}.d^{-1}$	-	-	-	-	-	1.9	-	-	-	-	-	1.6
$q_{XCB\_SB,\ HYD}$	d^{-1}	0.4	-	-	-	-	-	0.6	-	-	-	-	-
$q'_{XCB\_SB,\ HYD}$	$mgCOD.mgCOD^{-1}.d^{-1}$	-	0.3	-	-	-	-	-	0.1	-	-	-	-
$q_{XCB1\_SB,\ HYD}$	d^{-1}	-	-	1.5	-	-	-	-	-	2.1	-	-	-
$q_{XCB2\_SB,\ HYD}$	d^{-1}	-	-	0.2	-	-	-	-	-	0.3	-	-	-
$q'_{XCB1\_SB,\ HYD}$	$mgCOD.mgCOD^{-1}.d^{-1}$	-	-	-	1.9	-	-	-	-	-	3.1	-	-
$q'_{XCB2\_SB,\ HYD}$	$mgCOD.mgCOD^{-1}.d^{-1}$	-	-	-	0.1	-	-	-	-	-	0.1	-	-
Y_{OHO}	$mgCOD.mgCOD^{-1}$	0.63	0.63	0.63	0.63	0.63	0.63	0.63	0.63	0.63	0.63	0.63	0.63
XC_B	$gCOD.L^{-1}$	7.62	7.92	-	-	8.26	-	8.66	9.09	-	-	8.90	-
XC_{B1}	$gCOD.L^{-1}$	-	-	1.65	1.60	-	1.94	-	-	1.56	1.00	-	1.65
XC_{B2}	$gCOD.L^{-1}$	-	-	6.46	7.46	-	7.13	-	-	7.08	8.10	-	7.46
X_{OHO}	$gCOD.L^{-1}$	1.61	0.17	1.12	0.17	0.97	0.16	0.57	0.14	0.59	0.13	0.33	0.12
$X_{U,\ inf}$	$gCOD.L^{-1}$	0	1.14	0	0	0	0	0	0	0	0	0	0
E^2	$(mgO_2/L/h)^2$	8153	1346	1010	75	2172	117	65715	18128	3077	9072	17531	3011

Model calibration considering OUR only:

Model B2 and C2 were found to be the most suitable models for the description of the OUR profile of this experiment. Accordingly, the sums of squared errors were the lowest compared to the other models (75 and 117 $(mgO_2/l/h)^2$ for B2 and C2 respectively and a minimum of 1346 $(mgO_2/l/h)^2$ for the rest of the models). In addition, ammonia consumption was best predicted by model C2 compared to model B2 (ammonia increase after 2 days was overestimated with model B2). It has to be mentioned that any of the considered models have had the ability to describe the rapid increase then decrease of ammonia after 2 days. This could be probably attributed to the hydrolysis of protein-like components which was not considered in any of the investigated models. Conversely, model B2 has slightly better described COD_P compared to model C2 which started to underestimate it after 8 days.

Concerning the identified kinetic parameters and initial values of state variables, model B2 indicates that about 18% of the total particulate organic matter (COD_P) is degraded with a rate of 1.9 d^{-1} (XC_{B1}=1.60 gCOD/L) while 82% is degraded with a rate of 0.1 d^{-1} (XC_{B1}=7.46 mgCOD/L). The initial concentration of active heterotrophs (X_{OHO}) was estimated by the model to be about 0.17 g/L, which represents 1.8% of the COD_P. In addition, model C2 indicates that about 21% of the total particulate organic matter (COD_P) is degraded with a rate of 16.8 $kg.m^{-5}.d^{-1}$ (XC_{B1}=1.94 gCOD/L) while 79% is degraded with a rate of 1.9 $kg.m^{-5}.d^{-1}$ (XC_{B2}=7.13 gCOD/L). The initial concentration of active heterotrophs (X_{OHO}) was estimated by the model to be about 0.16 g/L, which represents 1.8% of the COD_P. Despite different mathematical structures, these two hydrolysis models are in agreement as they consider that about 20% of the total COD is degraded rapidly compared to the rest 80% and that hydrolytic bacteria represented 1.8% of the COD_P.

In each study and model the estimated amounts of the influent unbiodegradable matter ($X_{U,\,inf}$) were negligible, expect in model A2 where it represented 12% of the total COD. This value is in agreement with what is found in literature. The $X_{U,\,inf}$ represented between 4 and 19% of the total COD (Ekama et al., 1986; Kappeler and Gujer, 1992; Orhon et al., 2002; Sollfrank and Gujer, 1991).

Model calibration considering simultaneously OUR and $N\text{-}NH_4^+$:

Model C2 was the closest and the best deals for the description of this experiment compared to the other models. The sum of squared errors was the lowest with only 3011 $(mgO_2/l/h)^2$. The OUR curve and ammonia were quite well described and the COD_P was accurately predicted.

Concerning the identified kinetic parameters and initial values of state variables, model C2 indicates that about 17.8% of the total organic matter (COD) is degraded with a rate of 22.3 $kg.m^{-5}.d^{-1}$ (XC_{B1}=1.65 gCOD/L) while 81.1% is degraded with a rate of 1.6 $kg.m^{-5}.d^{-1}$ (XC_{B2}=7.49 gCOD/L). The initial concentration of active heterotrophs (X_{OHO}) was estimated by the model to be about 0.12 g/L (1.1% of the COD_P).

Intermediate conclusion:

Models considering two distinct slowly biodegradable COD fractions (B2 and C2) were the most adapted for the description of PSS-1 experiment by calibrating the OUR only.

OUR was described correctly by the two models, however, period 2 to 6 days of ammonia profile was not described correctly as none of the models consider protein-like components hydrolysis and consumption what probably happened.

Models B2 and C2 were in agreement towards the percentage of each particulate substrate (20% was degraded with a higher rate than 80% of the total COD for each model). This is also available for model C2 in the case of simultaneous model calibration considering the couple OUR/N-NH_4^+.

When models were constrained with the means of simultaneously calibration considering the couple OUR/N-NH_4^+, model C2 was found to be the most efficient model. It described accurately OUR and ammonia evolution and predicted quite well the COD_P profile.

14.1.2.PSS-2a: Sperandio's (1998) experiment

Only surface-based models (A1, B1, C1 and C2) which were described in the previous section were calibrated for this experiment as all first-order models (A2 and B2) describe an initial OUR tight peak. Figure 26 represents OUR simulated and experimental data during the aerobic batch test for each utilized model (continuous line (—) for OUR calibration, points (•) for experimental data). Oxygen mass balance was checked by the author. Table 27 includes the entire kinetic parameters and stoichiometric coefficients for each model.

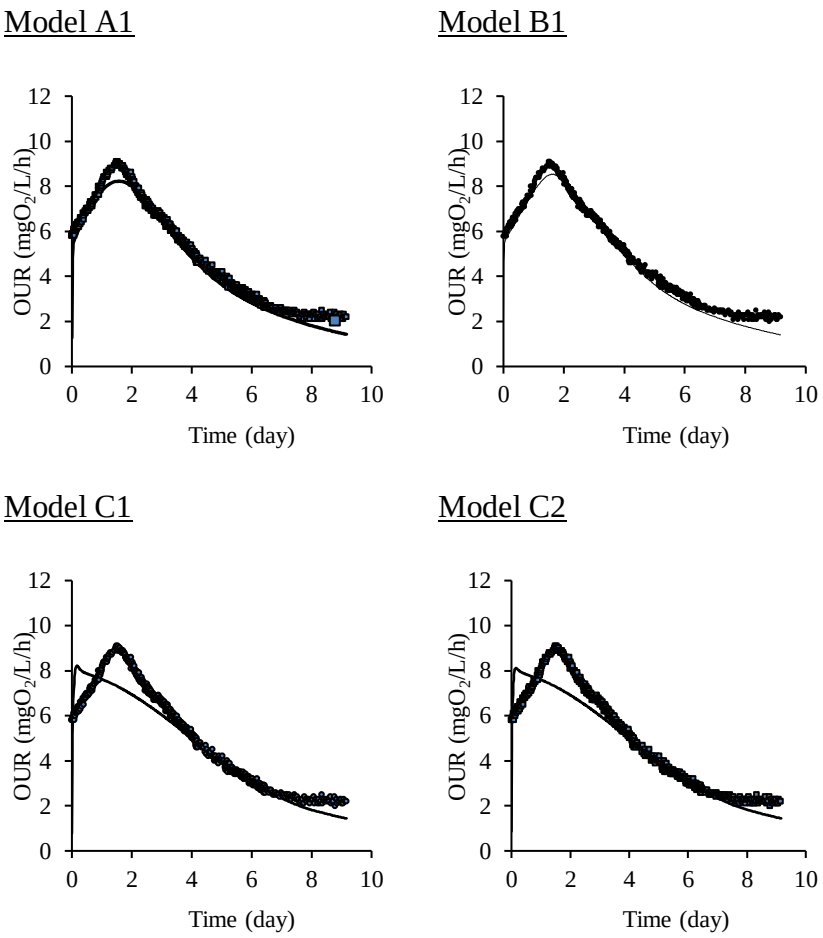

Figure 26 : Models calibration for Spérandio's (1998) PSS experiment, PSS-2 (continuous line (—) for OUR calibration, points (•) for experiment).

Table 27: Models parameter estimation for model OUR calibration – underlined parameters were fixed

Parameter	Unit	OUR calibration			
		A1	B1	C1	C2
b_{OHO}	d^{-1}	0.2	0.2	0.2	0.2
$f_{XU\_Bio,\ lys}$	$mgCOD.mgCOD^{-1}$	0.2	0.2	0.2	0.2
$\mu_{OHO,\ max}$	d^{-1}	6	6	6	6
$K_{SB,\ OHO}$	$mgCOD.L^{-1}$	20	20	20	20
$K_{XCB,\ hyd}$	$mgCOD.mgCOD^{-1}$	1.91	-	-	-
$K_{XCB\_1,\ hyd}$	$mgCOD.mgCOD^{-1}$	-	0.61	-	-
$K_{XCB\_2,\ hyd}$	$mgCOD.mgCOD^{-1}$	-	0.07	-	-
k_{SBK}	$kg.m^{-5}.d^{-1}$	-	-	3.9	-
k_{SBK_XCB1}	$kg.m^{-5}.d^{-1}$	-	-	-	2.2
k_{SBK_XCB2}	$kg.m^{-5}.d^{-1}$	-	-	-	3.7
$q_{XCB\_SB,\ HYD}$	d^{-1}	1.9	-	-	-
$q'_{XCB\_SB,\ HYD}$	$mgCOD.mgCOD^{-1}.d^{-1}$	-	-	-	-
$q_{XCB1\_SB,\ HYD}$	d^{-1}	-	0.4	-	-
$q_{XCB2\_SB,\ HYD}$	d^{-1}	-	0.8	-	-
$q'_{XCB1\_SB,\ HYD}$	$mgCOD.mgCOD^{-1}.d^{-1}$	-	-	-	-
$q'_{XCB2\_SB,\ HYD}$	$mgCOD.mgCOD^{-1}.d^{-1}$	-	-	-	-
Y_{OHO}	$mgCOD.mgCOD^{-1}$	0.63	0.63	0.63	0.63
XC_B	$gCOD.L^{-1}$	1.16	-	1.24	-
XC_{B1}	$gCOD.L^{-1}$	-	0.23	-	0.28
XC_{B2}	$gCOD.L^{-1}$	-	0.88	-	0.94
X_{OHO}	$gCOD.L^{-1}$	0.19	0.24	0.11	0.13
$X_{U,\ inf}$	$gCOD.L^{-1}$	0	0	0	0
E^2	$(mgO_2/l/h)^2$	100	89	376	379

Model B1 was the most appropriate to describe this OUR two-phases experiment, even if the tight peak at almost 2 days was not well described. The sum of squared errors between experimental data and the model was only 89 $(mgO_2/l/h)^2$ while it was comprised between 100 and 379 $(mgO_2/l/h)^2$ in models A1, C1 and C2. The two last models (C1 and C2) described a first-order reaction while model A1 described two OUR trends such as model B1.

The amount of XC_B was 1.16 gCOD/L (78% of the total COD). This result indicates that a part of the inoculum was of slowly biodegradable matter as the initial concentration of substrate (PSS) was of only 0.87 gCOD/L. However, the origin of the hydrolytic bacteria, X_{OHO}, as well as the XC_B and the distribution of these last ones between substrate and inoculum could not be achieved at this stage.

Intermediate conclusion:

- Model B1 was more adapted for this experiment compared to the rest of the models.
- At this stage, the origin of the hydrolytic bacteria and the slowly biodegradable matter and their distribution between substrate and the inoculum could not be achieved.

14.2. TOILET PAPER (TP) EXPERIMENT

All the previously detailed models were calibrated in the case of this experiment, except models A2 and B2 as they do not consider the colonization phase which is translated by an OUR increasing phase. Oxygen mass balance was checked. More than 65% of total COD (COD_T) was eliminated in which 99,8% was in the particulate form (COD_P). The oxygen uptake rate, OUR, varied between 4.5 and 51 $mgO_2/l/h$. The first one defines the endogenous respiration state and the last one the initial tight peak. The initial ammonia decreased from 523 mgN/L down to 397 mgN/L. Finally, COD_P varied from 9.70 till 2.89 mgCOD/L.

In all the models, the default value of the substrate was fixed, despite the sensitivity of the models towards this parameter, as the amount of biodegradable matter was measured experimentally. The slowly biodegradable COD fraction (XC_B) represented 91% and the inert fraction ($X_{U,\,inf}$) was of 9% of the particulate COD. In model B1, the default values of XC_{B1} and XC_{B2} were fixed as the amounts of the main components of toilet paper (hemicellulose and cellulose) were assessed before the batch test began (12% and 79% of XC_B, respectively). Table 28 includes the concentrations of substrates and inoculum for each model.

Table 28: Initial concentrations of substrate and inoculum for each model

Substrate concentration (gCOD/L)					Inoculum concentration (gCOD/L)
Particulate substrate concentration[1]	Models A1, A2 and C1 (XC_B)	Models B1, B2 and C2		Unbiodegradable fraction ($X_{U,\,inf}$)	
		Hemicellulose (XC_{B1})	Cellulose (XC_{B2})		
8.99	8.18	1.08	7.1	0.81	0.71

Figure 27 represents simulated and experimental data (OUR, $N\text{-}NH_4^+$ and COD_P) during the aerobic batch test for each utilized model (continuous line (—) for OUR calibration, dashed line (---) for OUR/ $N\text{-}NH_4^+$ calibration). Table 29 includes all the identified and fixed kinetic parameters and stoichiometric coefficients for each considered model.

[1] this is the difference between total and soluble COD

Model A1

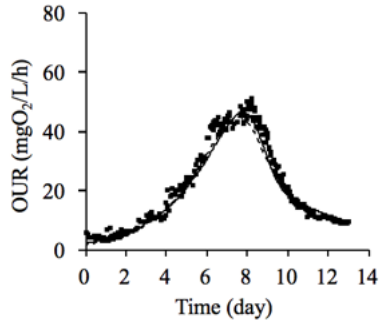

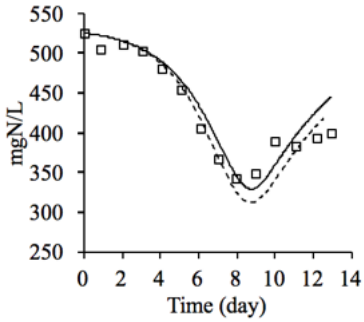

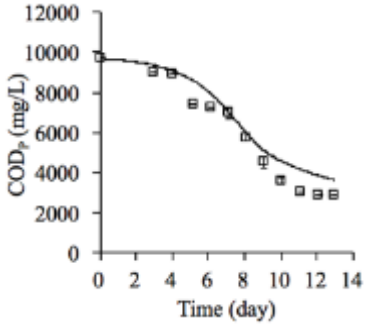

Model B1

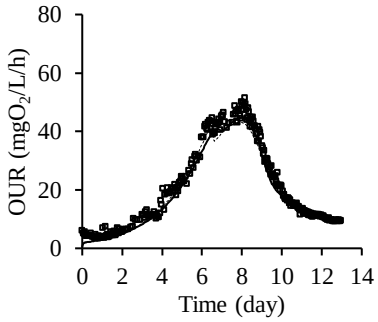

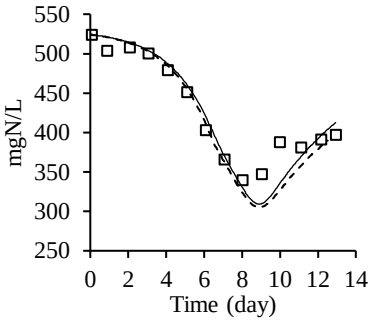

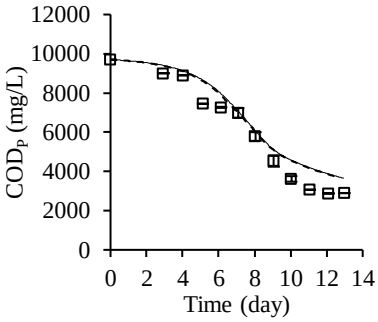

Model C1

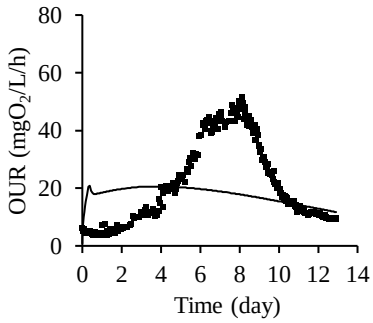

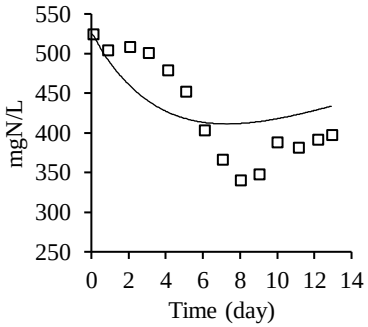

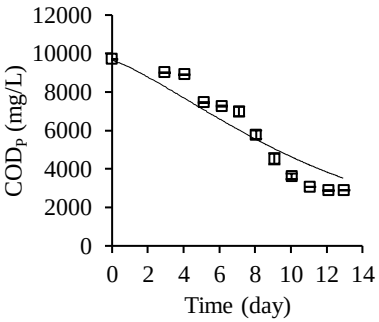

Model C2

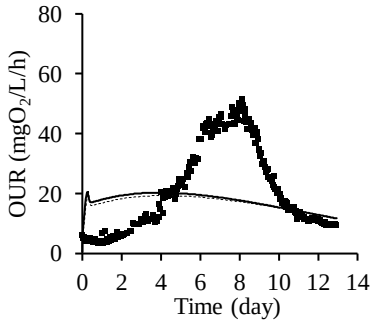

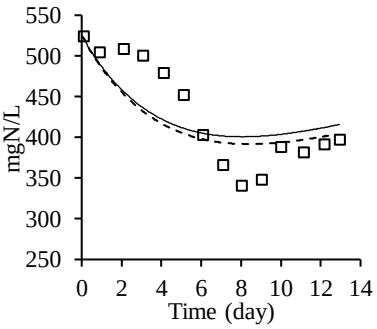

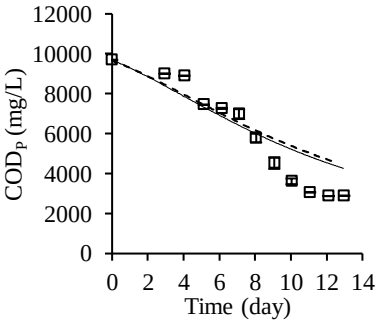

Figure 27 : Models calibration for toilet paper experiment (continuous line (—) for OUR calibration, dashed line (---) for OUR/N-NH_4^+ calibration).

Table 29: Models parameter estimation for model OUR and OUR/N-NH_4^+ calibration

Parameter	Unit	OUR calibration				OUR/N-NH_4^+ calibration			
		A1	B1	C1	C2	A1	B1	C1	C2
b_{OHO}	d^{-1}	0.2	0.2	0.2	0.2	0.2	0.2	0.2	0.2
$f_{XU\_Bio,\ lys}$	$mgCOD.mgCOD^{-1}$	0.2	0.2	0.2	0.2	0.2	0.2	0.2	0.2
$\mu_{OHO,\ max}$	d^{-1}	6	6	6	6	6	6	6	6
$i_{N\_X\_BIO}$	$mgN.gCOD^{-1}$	0.07	0.07	0.07	0.07	0.09	0.07	0.07	0.08
i_{N_XU}	$mgN.gCOD^{-1}$	0.02	0.02	0.02	0.02	0.01	0.04	0.02	0.04
$K_{SB,\ OHO}$	$mgCOD.L^{-1}$	20	20	20	20	20	20	20	20
$K_{XCB,\ hyd}$	$mgCOD.mgCOD^{-1}$	0.38	-	-	-	0.57	-	-	-
$K_{XCB\_1,\ hyd}$	$mgCOD.mgCOD^{-1}$	-	0.03	-	-	-	0.004	-	-
$K_{XCB\_2,\ hyd}$	$mgCOD.mgCOD^{-1}$	-	0.2	-	-	-	0.26	-	-
k_{SBK}	$kg.m^{-5}.d^{-1}$	-	-	2.3	-	-	-	2.3	-
k_{SBK_XCB1}	$kg.m^{-5}.d^{-1}$	-	-	-	1.2	-	-	-	1.1
k_{SBK_XCB2}	$kg.m^{-5}.d^{-1}$	-	-	-	2.3	-	-	-	2.2
$q_{XCB\_SB,\ HYD}$	d^{-1}	1.1	-	-	-	1.2	-	-	-
$q_{XCB1\_SB,\ HYD}$	d^{-1}	-	0.3	-	-	-	0.3	-	-
$q_{XCB2\_SB,\ HYD}$	d^{-1}	-	0.8	-	-	-	0.8	-	-
$q'_{XCB1\_SB,\ HYD}$	$mgCOD/mgCOD^{/}d$	-	-	-	-	-	-	-	-
$q'_{XCB2\_SB,\ HYD}$	$mgCOD/mgCOD^{/}d$	-	-	-	-	-	-	-	-
Y_{OHO}	$mgCOD.mgCOD^{-1}$	0.63	0.63	0.63	0.63	0.63	0.63	0.63	0.63
XC_B	$gCOD.L^{-1}$	8.18	-	8.18	-	8.18	-	8.18	-
XC_{B1}	$gCOD.L^{-1}$	-	1.08	-	1.08	-	1.08	-	1.08
XC_{B2}	$gCOD.L^{-1}$	-	7.10	-	7.10	-	7.10	-	7.10
X_{OHO}	$gCOD.L^{-1}$	0.10	0.08	0.13	0.09	0.08	0.08	0.13	0.07
$X_{U\_inoc,\ ini}$	$gCOD.L^{-1}$	0.61	0.63	0.58	0.62	0.63	0.63	0.58	0.64
$X_{U\_TP,\ ini}$	$gCOD.L^{-1}$	0.81	0.81	0.81	0.81	0.81	0.81	0.81	0.81
E^2	$(mgO_2/l/h)^2$	2512	1997	62100	62018	5055	5800	72830	96912

Model calibration considering OUR only:

The OUR profile of this experiment was successfully described by the means of models A1 and B1. However, the sum of squared errors was the lowest in B1 with only 1997 $(mgO_2/l/h)^2$ against a 2512 $(mgO_2/l/h)^2$ in A1. The two phases of the OUR profile were described accurately. It could be noticed that model A1 described globally the two main trends of the OUR profile but with less precision than model B2.

In addition, ammonia utilization was correctly described by models A1 and B1 and with more precision compared to the rest of the models too. In addition, COD_P profile was correctly predicted with these two models, however, it was less precise after the 8^{th} day.

Concerning the identified kinetic parameters and initial values of state variables, model A1 indicates that the substrate (cellulose + hemicellulose) was degraded with a rate of 1.1 d^{-1} and the half-saturation hydrolysis constant was of 0.38 $gCOD.gCOD^{-1}$. The initial concentration of active heterotrophs (X_{OHO}) was estimated by the model to about 0.1 gCOD/L, which represents 14% of the total COD of the inoculum (86% are unbiodegradable particulate matter, $X_{U\_inoc,\ ini}$)

Model B1 indicates that hemicellulose was degraded with a rate of 0.3 d^{-1} (XC_{B1}=1.08 gCOD/L) while cellulose was degraded with a higher rate which is equal to 0.8 d^{-1} (XC_{B2}=7.10 mgCOD/L). The half-saturation hydrolysis constants were of 0.03 and 0.2 $gCOD.gCOD^{-1}$ respectively. The initial concentration of active heterotrophs (X_{OHO}) was estimated by the model to about 0.08 gCOD/L, which represents 11% of the total COD of the inoculum (89% are unbiodegradable particulate matter, $X_{U\_inoc,\ ini}$).

Model calibration considering simultaneously OUR and N-NH_4^+:

In this case, models A1 and B1 were also the most efficient and described correctly the entire experimental data (OUR, N-NH_4^+, COD_P). The identified kinetic parameters and initial values of state variables were of the same range as to those identified with OUR calibration only. Thus, even if the model was constrained with the addition of ammonia, this did not affect model calibration.

Intermediate conclusion:

Models A1 and B1 were the most suitable models to describe toilet paper biodegradation. It described correctly what we considered as an acclimation phase (t<2 days) besides the OUR increasing and decreasing phases. The model calibration ways (OUR and OUR/N-NH_4^+) led to the same results.

In model A1, the identified hydrolysis rate constant was of 1.1 d^{-1} and the half-saturation hydrolysis constant was of 0.38 $gCOD.gCOD^{-1}$. In model B1, the identified hydrolysis rate constants for hemicellulose and cellulose were of 0.3 and 0.8 d^{-1}, respectively, while the half-saturation hydrolysis constants were of 0.03 and 0.2 $gCOD.gCOD^{-1}$, respectively.

The initial concentration of active heterotrophs was estimated to 0.1 mgCOD/L in A1 and 0.08 gCOD/L in B1. These values are very weak compared to the initial concentration of the inoculum (0.71 gCOD/L). They represent between 11 and 14% of the total COD of the inoculum. The rest of cellular biomass was considered as unbiodegradable particulate matter

(X_{U_inoc}). But, in reality, this matter could contain other additional components besides unbiodegradable matter (X_{U_inoc}) as bacteria that could only consume the hydrolytic products (X_{OHO}) without the ability to hydrolyze and bacteria that only undergo endogenous respiration (X_{OHO_ER}). The distribution of these components in the total cellular biomass will be investigated in chapter IV.

15. DISCUSSION

15.1. MODELS EFFICIENCY

Model and experimental data confrontation underlined the fact that first-order models are more suitable for the description the "one-trend" OUR profile experiment (PSS1-a) while surface-based models were more suitable for the experiments with "two-trends" OUR profiles (PSS1-a and TP1-a). However, the SBK models (C1 and C2) did not match to these last enunciated experiments.

Regardless of the model's structures, the consideration of two distinct types of solid substrates (XC_{B1} and XC_{B2}) was found to be necessary in order to describe with accuracy the whole experiments presented in this chapter (except for TP1-a were model A1 gave also quite good results). This indicates that at least two slowly biodegradable COD fractions or type of substrates with distinct kinetic characteristics are present in the batch reactor and in the wastewater settleable fraction in general. Orhon et *al.* (1998) then Tas et *al.* (2009) have already reported this kind of results in the past when they studied domestic sewage elimination. In addition, Balmat (1957) earlier identified many substrate COD fractions (in which solid and colloid fractions are found) and classified them in function of their elimination rate.

Model calibration of the whole experiments that have been achieved in this work showed that models B2 and C2 were the most adapted for the one-trend OUR experiment, namely PSS1-a, for the description of the OUR profiles while the two-trends OUR experiments, PSS2-a and TP1-a, were better described with the Contois-based model (B1), which is able to describe the colonization phase (OUR increase) where the rest of the models failed. However, the simulated COD_P evolution in TP1-a experiment was overestimated after 9 days.

In this chapter, the whole models were constrained with the addition of ammonia besides OUR in order to increase the degree of freedom in the models and thus improve their prediction performances while, in the previous works that concerned this subject, only the OUR was considered. In TP1-a experiment, this did not affect model calibration as the results were the same for both OUR and OUR with ammonia calibration. In contrary, it described with more insight ammonia evolution with models B2 and C2 but not the OUR, in PSS1-a experiment, which was better described with OUR calibration only. Moreover, model C2 was more accurate in the description of COD_P evolution compared to model B2.

It could be concluded that at least one of the tested models was able to describe the OUR profile of each experiment. Nevertheless, the identified set of parameters for each experiment were quite different. This may indicate that models' structures and/or modelling procedures that were used till now are not sufficiently robust. Thus, we thought that it would be suitable to make efforts to gain more insight by improving the performances of existing models with additional features (see chapter III).

15.2. COMPARISON OF ESTIMATED KINETIC PARAMETERS AND INITIAL STATE VARIABLES

As discussed in the previous section, the dual hydrolysis based models were able to describe all the experiments (model A1, the single-hydrolysis model, was also efficient in the case of TP experiment). The identified hydrolysis rate constants that were identified in each experiment according to the most representative model are presented in Table 30.

Table 30: Summary of the identified hydrolysis rate constants (with modeling) under aerobic conditions in this work and Sperandio (1998).

Exp.	Reference	$q_{XCB1\_SB,\ HYD}$	$q_{XCB2\_SB,\ HYD}$	$q'_{XCB1\_SB,\ HYD}$	$q'_{XCB2\_SB,\ HYD}$
PSS-1a	This work			1.9	0.1
PSS-2a	Sperandio (1998)	0.4	0.8		
TP1-a	This work	0.3	0.8		

The magnitude of the identified hydrolysis rate constants in PSS-1 experiment were of 1.9 and 0.1 d^{-1} for model B2. The first value (1.9 d^{-1}) is of the same order of the hydrolysis rate constant that was identified by Kappeler and Gujer (1992) in the case of settled domestic wastewater (SWW). The second one (0.1 d^{-1}) was comparable to the value identified by Gujer and Henze (1991) for the case of raw wastewater (Both of them were identified according to a first-order hydrolysis model (IAWQ model n°1)). Nevertheless, in these studies XC_B represented the entire particulate organic matter, not only settleable COD. Moreover, the characterized wastewaters contained non-negligible amounts of S_B which could certainly affect hydrolysis constants identification and thus the hydrolysis process characterization. Even in our studies, the presence of RBCOD was observed but was negligible (less than 2% of the total COD).

The identified values in PSS2-a and TP1-a were of the same magnitude: about 20% of the substrate (XC_{B2}) was degraded at a rate of 0.4 d^{-1} in PSS-2 while 13% (XC_{B1}) was degraded at

a rate of 0.3 d^{-1} in TP1-a. About 80% of the substrate (XC_{B1}) was degraded at a rate of 0.8 d^{-1} in PSS-2a while about 87% of the substrate (XC_{B2}) was degraded at the same rate in TP1-a. The values identified by Orhon et *al.* (1998) were higher and were comprised between 0.8 and 1.8 d^{-1} for the XC_{B1} (slowly hydrolysable COD) and between 2.1 and 4.5 d^{-1} for XC_{B2} (rapidly hydrolysable COD).

There is unfortunately no matter to compare surface-based kinetic constants which were identified in the case of model C2 as, to our knowledge, only Sanders et *al.* (2000) utilized this hydrolysis model and their study was achieved under anaerobic conditions what involves different bacteria with different kinetic characteristics compared to aerobic (anaerobic mechanisms are found to be slower). But still, this model could be a serious alternative to the conventional DHM (B2).

The initial amounts of slowly biodegradable substrates (XC_{B1} and XC_{B2}) and active bacteria (X_{OHO}) were also assessed with the means of model calibration for PSS experiments, as settleable COD contains not only slowly biodegradable matter but also active bacteria (and other components), which is difficult to assess accurately with the conventional Standard Methods (1989) such as TSS and VSS measurements. As biodegradable substrates amounts were assessed in the case of TP1-a experiment (79% of cellulose and 9% of hemicellulose), only initial active bacteria were integrated in model calibration. It was observed in our experiments (PSS1-a and TP1-a) that the estimated amounts of active bacteria that initiate hydrolysis are in reality very weak. They were of about 0.17 gCOD/L for PSS1-a and only 0.08 gCOD/L in TP1-a experiment. In this last one, the initial amount of active bacteria represents only 10% of the inoculum total COD (COD_{inoc}=0.71 gCOD/L). In PSS2-a experiment, initial active bacteria represented 18% of the total COD and 50% of the inoculum (X_T), however, the origin of active (hydrolytic) bacteria is not known as both the inoculum and the PSS may contain it.

Table 31 regroups the experimental and estimated (model) initial values of substrates and inocula for each experiment.

Table 31: Comparison between experimental and model estimation of the initial amounts of bacteria. The results are those of the most efficient model of each experiment.

Exp.	Total COD (mgCOD/L) [2]	$XC_{B,\,ini}$ (mgCOD/L)	Inoculum (gCOD/L)		X_{OHO}/X_T (%)	X_{OHO}/COD_T (%)
			Experimental (X_T)	Model estimation ($X_{OHO,\,ini}$)		
PSS1-a	9.23	9.06	-	0.17	-	1.8
PSS2-a	1.36	1.11	0.48	0.24	50	18
TP1-a	9.96	8.18	0.71	0.08	10	0.8

[2] this includes the sum of the particulate (COD_P) and soluble (COD_S) fractions of the reactor content

15.3.MODEL OUTPUTS FOR THE MAIN STATE VARIABLES

Figure 28 illustrates the evolution of the main particulate state variables (X_{OHO}, XC_{B1} and XC_{B2}) for the best models in the cases of PSS1-a, PSS2-a and TP1-a (models B2 for PSS1-a and model B1 for TP1-a and PSS2-a).

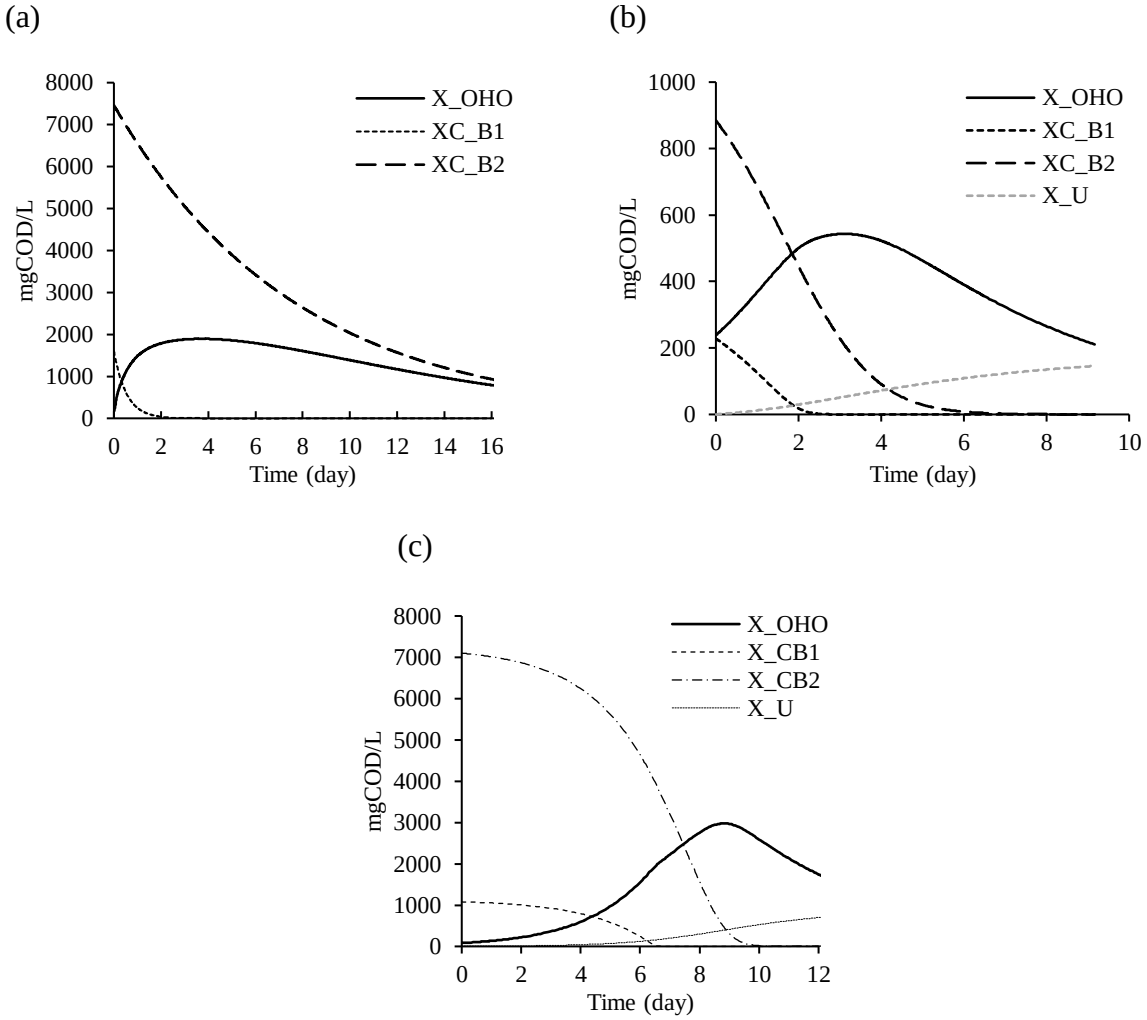

Figure 28 : Evolution of the main state variables after model calibration: (a) PSS1-a experiment (model B2), (b) PSS2-a experiment (model B1) and (c) TP1-a experiment (model B1).

15.3.1.PSS1-a experiment

Figure 28a indicates that XC_{B1} is degraded after about 2 days. The rest of the bioreaction was then controlled by XC_{B2}. Nevertheless, this one was not depleted completely after 20 days and thus the endogenous respiration phase was not attained according to this model. This result

could be open criticism as the COD_P was almost unchanged during the last days of the batch test (COD_P (t>12 days) = 3.35±0.28 gCOD/L), which is a sign of total substrate depletion. It is then necessary to search for an alternative or new modeling approach to describe this experiment.

15.3.2.PSS2-a experiment

Figure 28b indicates that XC_{B1} is depleted after about 2.2 days where XC_{B2} is degraded simultaneously but was completely depleted after 6.5 days. After that, the endogenous respiration phase controlled the reaction.

15.3.3.TP1-a experiment

Figure 28c indicates that both hemicellulose (XC_{B1}) and cellulose (XC_{B2}) were completely depleted after 6.5 days and 10 days respectively. The slight OUR decrease that was observed after about 6 days was attributed to hemicellulose elimination. After that, cellulose depletion controlled the rest of the OUR decreasing phase.

Contrarily to PSS-1 experiment, the substrates degradation rates were lower during the first days of the bioreactions. This may be translated by an acclimation phase in which bacteria that are not able to degrade these types of substrates acquire the ability to eliminate them. It has to be mentioned that this mechanism was not integrated in the modeling approaches that have been considered till now.

It could be noticed that despite the same magnitude of the identified hydrolysis rate constants, the substrates in TP1-a were degraded slower than in PSS2-a. This may be attributed to the fact that bacteria had to acclimate first to toilet paper in TP1-a experiment and this was translated in the model by a weaker affinity of active bacteria to the substrates (especially cellulose which controlled the reaction) than in PSS2-a.

This aspect of acclimation and colonization are not well defined and integrated in conventional and current models. In addition, the hydrolysis characteristics (set of kinetic parameters and coefficients) that were identified by modeling change according to the experiment (type of substrate, operating conditions…) and thus certainly affect process prediction. This way, the development of more realistic model is found to be necessary to reach a unique modeling approach that describes any experiment. Thus, the next chapter is dedicated to the development of a novel conceptual framework that presumes to describe any experiment that deal with (or

includes) slowly biodegradable COD. This model will be based on well-grounded hypothesis such as based on microscopic observations and will take into account physical properties and geometrical aspects of involved matter (substrate and biomass) in a literal sense, as mentioned in chapter I.

16. CONCLUSION

In this chapter, conventional (models of the IAWQ group) and unconventional models, that were developed for the purpose of hydrolysis description, were evaluated for a set of experiments that were achieved during this work and some experiment picked-up from literature.

It was found that single-hydrolysis models (A1, A2 and C1) were not able to describe the PSS-1 and PSS-2 experiments. The consideration of at least two types of slowly biodegradable COD fractions (XC_{B1} and XC_{B2}) in the models (B1, B2 and C2) was primordial in order to describe correctly experimental data. This way, the DHM models (original and modified versions, B1 and B2) were suitable for all the experiments. The surface-based kinetic models (C1 and C2) was also a great alternative in the case PSS1-a (not TP1-a and PSS2-a).

In TP1-a experiment, appropriate models described accurately the initial time-lag phase, which was attributed to "acclimation" of bacterial communities to the substrate (toilet paper), even if this aspect was not integrated in any of the models. The increasing and the decreasing OUR phases as well as ammonia utilization were also described with precision. It has also predicted correctly the evolution of particulate COD during the time of the experiment.

In PSS2-a experiment, the shape of the two-trend OUR profile was quite described by the appropriate model.

In PSS1-a experiment, appropriate models described with a good agreement the OUR decreasing phase as well as ammonia utilization and predicted quite well COD_P evolution. Nevertheless, the modeling of PSS1-a experiment could be open to criticism as the COD_P was almost unchanged during the last days of the batch test (COD_P ($t>12$ days) $=3.35\pm0.28$ gCOD/L) while XC_{B2} was not completely depleted according to the model.

Concerning the amount of the hydrolytic bacteria, it was estimated to only 1.8% of the COD_P in experiment PSS1-a while it was of 18% of the COD_P in PSS2-a and 50% of the COD_P of the inoculum. In PSS1-a experiment, as no inoculum was added, the origin of the hydrolytic bacteria was attributed to the initially attached bacteria to PSS. However, in PSS2-a experiment, the origin of the hydrolytic bacteria is not clear whether it comes from the in inoculum or it is attached to the PSS. Moreover, the estimated XC_B was higher than the initial concentration of substrate what indicates that the inoculum provided some slowly biodegradable matter. In TP1-

a, the amount of hydrolytic bacteria was very weak. It represented 10% of the amount of the inoculum in COD unit. The rest of the cellular biomass in the experiments that involve inocula were attributed to unbiodegradable particulate) matter (X_{U_inoc}) but it could also contain other components as bacterial communities that consume the hydrolytic products but without a hydrolytic potential (X_{OHO}) and/or bacteria that only undergo endogenous respiration (X_{OHO_ER}). With these contrasted results, it is difficult at this stage to define the real origin of the hydrolytic bacteria, whether it comes from the substrate (initially attached) or from the inoculum (a further investigated of this question is achieved in chapter IV).

All the considered models were calibrated considering OUR only but also OUR and ammonia simultaneously. This last one, would give more insight on experimental description by constraining the models by increasing the degree of freedom in the model. This did not have effect on TP1-a experiment as both of them led to the same result. In contrary, it described with more insight ammonia evolution with models B2 and C2 but not the OUR, in PSS1-a experiment, which was better described with OUR calibration only.

It was observed also that model calibration identified different sets of parameters in each case study which means that the model was not universal. That way, in the following chapter (III), a novel and more realistic conceptual framework derived from the conventional WWTP models will be developed. According to solid hypothesis especially around bacterial cells and substrates interactions, this model will take into account additional features such as the physical properties and geometrical aspects of substrates and biomass.

CHAPTER III

"Introduction of the colonization phase in a new conceptual framework to describe the hydrolysis of slowly biodegradable matter under aerobic conditions"

1. INTRODUCTION

To model the degradation of carbonaceous matter and the removal of nitrogen and phosphorus, the influent COD is commonly divided into fractions in the well-known IAWQ models (Gujer et al., 1999, 1995; Henze et al., 1999). In order to simplify these models, a single hydrolysable fraction was considered and the degradation of very slowly biodegradable substances was not included. Consequently, for modelling purposes, slowly biodegradable substances were partially included in the heterotrophic biomass of the sewage or in the inert particulate matter. The goal of this work is to specifically study the degradation of slowly biodegradable substances which are present in the form of large particles.

Bibliography evidenced the important role of the hydrolysis process in the elimination of slowly biodegradable COD in WWTP. That way, in order to predict the performances of wastewater treatment processes, the hydrolysis rate should be characterized with more precision.

Hydrolysis is commonly considered as a surface-based mechanism (Aldin et al., 2011; Morgenroth et al., 2002; Yu et al., 2008). This was explained by the fact that the hydrolysis exo-enzymes were secreted by bacterial cells and stay attached to their surface. Thus, those bacterial cells need to get in contact with slowly biodegradable COD in the form of solid particles in order to perform hydrolysis. Those bacteria grow-up and colonize gradually the available surface area of the solid substrate, resulting in the increase of the surface occupied by bacteria and thus the decrease of the substrate available surface area. The colonization rate should then depend on particles geometrical and physical properties such as shape (cylinder, sphere…), size (diameter, length…) and density.

Conventionally, the term "surface-based" is represented by mass concentration ratios between substrate and biomass in the *IAWQ* models (Henze et al., 1987; Gujer et al., 1995, 1999) but this is misleading as the available surface area of substrate depend on particle size and shape (Dimock and Morgenroth, 2006; Sanders et al., 2000). In the SBK model (Hobson, 1987), the dynamic evolution of particle size is integrated in the hydrolysis process and the rate of hydrolysis is proportional to the available substrate surface area. It assumes that the substrate is completely covered with bacteria and thus does not either consider the colonization mechanism. This may explain the difficulty of those models to describe the OUR profiles of a wide variety of substrates that were presented in chapter I and II.

Colonization is the third step after "adsorption" and "attachment" in the process of adhesion of bacteria onto solid substrate (Fletcher, 1980). It involves the growth and proliferation of bacterial cells all over the available surface area of the solid substrate. The adsorption process was integrated in the conventional WWTP models by Ekama and Marais in 1979, then Dold in 1980. Those authors found out that contact between bacteria and the solid substrate is required in order to perform hydrolysis. They hypothesized that the quality of adsorbable substrate is limited by the quantity of active bacteria and a maximum adsorbable fraction "f_{ma}". The value of this constant is however different from an author to another (Dold et *al.* (1980) (f_{ma}=1); Spérandio and Paul (2000) (f_{ma}=1.06); Lagarde et *al.* (2005) (f_{ma}=4)). Nevertheless, this model describes only the preliminary contact between substrate and bacteria and does not take into account the physical properties of the substrate and bacteria which is primordial when dealing with surface phenomena. In addition, it considers that it is the solid substrate which adsorbs to the bacteria in activated sludge systems. In contrary, Sperandio (1998) showed that it was the bacteria that colonizes the substrate surface area before degrading it. Actually, till now, any author has introduced the colonization phase in the WWTP modeling approaches. Consequently, a more realistic framework including this phase should be developed.

The purpose of the current chapter is to set a conceptual surface-based model that takes into account substrate colonization by microbial communities and thus, at the same time, the dynamic evolution of substrate particle size. The model is based on experimental observations that were obtained in our laboratory and some literature hypothesis (Sperandio, 1998). After a brief presentation of the experimental tools, the construction of the model structure is presented. In the second part, the model is confronted to real experimental data either collected from the literature or in our laboratory and compared to models from literature. Finally, it is theoretically evaluated in regard with geometrical parameters (shape and size) and active biomass considerations (in terms of concentration and pre-contamination level of the substrate) to provide some paths for the discussion (a summary of the theoretical evaluation of the new model is reported in Appendix 3).

2. MATERIALS AND METHODS

2.1. RESPIROMETRY EXPERIMENTS

A detailed diagram of the respirometer is illustrated by Figure 7 (see the experimental material and methods chapter, §2.1.1).

All the experiments were inoculated with activated sludge (AS) collected from the aerated tank of the 1 million population equivalent WWTP of Ginestous (Toulouse, France). The estimated SRT being low (lower than 5 days), AS was kept under aeration during few days till it reached endogenous respiration in order to discharge the sludge from the accumulated slowly biodegradable organic matter.

Then the reactor was fed a nutriment medium together with the particulate substrate. A model substrate (basic toilet paper, TP) and a real one (particulate settleable solids, PSS) were investigated in this study. The commercial white toilet paper (TP) was cut into 1 cm^2 pieces to favour homogenization and biomass-TP contact. The experimental chemical oxygen demand of this TP was of 1.27 gCOD/g. Two PSS experiments were considered. The first one was obtained (in this study) by settling pre-treated wastewater, which was collected before the primary sedimentation step. It was settled during 1 hour in a 40-L lab-scale settling device of acrylic glass material. The resulting settled fraction was once more settled in Imhoff cones during 2 hours (Standard Methods, 1989). Three successive washing cycles have been performed in order to reduce soluble components concentrations in the final sample of PSS. For the second one, additional data were picked up from Sperandio (1998) who investigated PSS collected at the beginning of the sewer system. The Table 32 summarizes the considered experiments.

Table 32: Summary of the experiments

Exp.	Substrate	Substrate concentration (gCOD/L)	Inoculum concentration (gCOD/L)	Source
PSS1-a	PSS	9.23	0	This study
PSS2-a	PSS	0.88	0.48	Sperandio (1998)
TP1-a	Toilet paper	8.99	0.71	This study
EP (small)	Egg white particles	0.25	ND	Dimock and Morgenroth (2006)
EP (large)	Egg white particles	0.25	ND	Dimock and Morgenroth (2006)

Oxygen Uptake Rate (OUR) was measured until it decreased down to the endogenous respiration level. Open respirometry was performed in this study to avoid structure deconstruction of particulate substrate. The OUR was assessed by measuring dissolved oxygen concentration decrease when aeration is stopped, from 3 to 1.5 mgO_2/L, and the oxygen surface mass transfer that occur in the reactor. In addition, 20 mg/L of ATU (N-Allylthiourea) were added to inhibit nitrification and mass-balances performed on nitrogen compounds evidenced that anoxic mechanisms were negligible.

2.2. ANALYTICAL METHOD

See Experimental and modeling material and methods chapter, §4.2.

2.3. MODELING

All simulations and parameters identifications were performed using AQUASIM® (Reichert, 1994). The basic model used in this work is the *IAWQ* model n°1 (Henze et al., 1987), which is generally used in the cases studies that deal with hydrolysis of slowly biodegradable COD and especially particulate settleable solids (Morgenroth et al., 2002; Orhon et al., 2002, 1998; Orhon and Sozen, 2012). However, the death-regeneration model was replaced by endogenous respiration.

Concerning the mathematical expression of hydrolysis mechanism, various choices were done in this study:

(i) the conventional hydrolysis mathematical expression used in the *IAWQ* model n°1 (Henze et al., 1987) (model A1);
(ii) the Dual Hydrolysis model of Sollfrank and Gujer (1991), noted DHM (model B1);
(iii) the Surface-Based-Model modified in this study in order to take into account the substrate surface area and not the mass of the particulate substrate (Modified SBK Model, noted M_SBK).

All these models, whose stoichiometric and rates matrix is presented in Table 33, will be calibrated based on OUR signals for the cases of model substrates (toilet paper, TP1-a, and egg-white particles, EP)) and real substrates (Particulate settleable solids PSS1-a and PSS2-a).

Table 33: processes stoichiometry and kinetics of models from literature

Process	*Soluble species*			*Particulate species*					Process rate
	$S_{B,HYD}$	S_{O2}	S_{NH4}	XC_B	XC_{B1}	XC_{B2}	X_{OHO}	X_U	
Model A1 - IAWQ model n°1 (Henze et al., 1987)									
1	*1*			*-1*					$q_{XCB_{SB},hyd}\frac{XC_B/X_{OHO}}{K_{XCB,hyd}+XC_B/X_{OHO}}X_{OHO}$
Model B1 - Dual Hydrolysis Model, DHM (Sollfrank and Gujer, 1991)									
1	*1*				*-1*				$q_{XCB1_{SB},hyd}\frac{XC_{B1}/X_{OHO}}{K_{XCB1,hyd}+XC_{B1}/X_{OHO}}X_{OHO}$
1'	*1*					*-1*			$q_{XCB2_{SB},hyd}\frac{XC_{B2}/X_{OHO}}{K_{XCB2,hyd}+XC_{B2}/X_{OHO}}X_{OHO}$
Common processes for all the models									
2	$-1/Y_{OHO}$	$-(1-Y_{OHO})/Y_{OHO}$	$-i_{N\_XBio}$				*1*		$\mu_{OHO,max}\frac{S_{B,hyd}}{K_{SB,hyd}+S_{B,hyd}}X_{OHO}$
3		$-(1-f_{XU\_Bio,lys})$	$f_{XU\_Bio,lys}*i_{N,XU}+i_{N\_XBio}$				*-1*	$f_{XU\_Bio,lys}$	$b_{OHO}X_{OHO}$

3. MODEL DEVELOPMENT

3.1. MODEL HYPOTHESIS: WHAT IS MISSING TO DEVELOP A CONCEPTUAL MODEL?

The purpose of this section is to assess what is missing to develop a more realistic model that will be able to describe the biodegradation and the fate of slowly biodegradable COD in aerobic conditions. To that purpose, an overview of the biochemical and physical aspects and properties of the components that are involved in such biological reactions will be discussed in details in order to set the basis of the model.

Firstly, this section focuses on the shapes, particle size distribution and chemical composition of wastewater particulate settleable solids (PSS) which represents a part of the slowly biodegradable COD which is contained in municipal wastewaters. Secondly, the following section deals with the interactions between solid substrates and microbial communities in order to highlight the important role of colonization in such biological processes.

3.1.1. Substrate amount and characteristics

3.1.1.1. Physical properties

3.1.1.1.1. Particles shape

Only very few models take into account particle size. Moreover, they all consider that substrate is spherical (Aldin et al., 2011 ; Mino et al., 1995 ; Sanders et al., 2000 ; Sanders, 2001). This can be open to criticism when dealing with real influents (wastewater). In fact, the solid fraction of wastewater, especially the settleable fraction (PSS), is found to be mainly composed by "fibers" in the form of cylinders of different lengths and diameters (Figure 29). Their biochemical nature and composition are difficult to determine as it is hard to isolate them. Spérandio (1998) hypothesized that they were of cellulosic composition, as they result from toilet paper breakdown (hydrolysis).

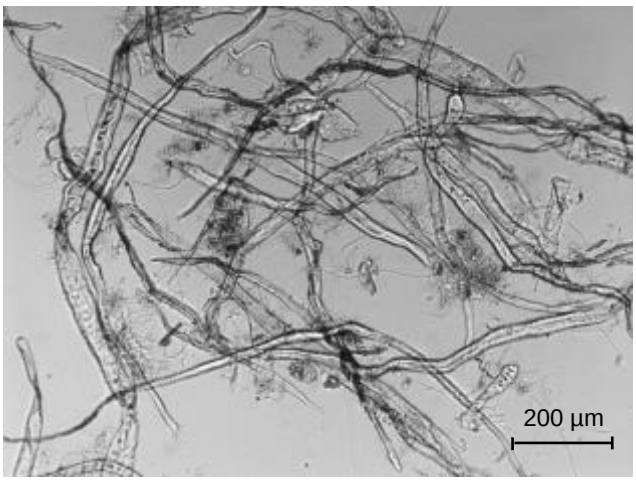

Figure 29 : Picture of a sample of urban wastewater PSS which was taken with an optical microscope

3.1.1.1.2. Particle size distribution

A literature review underlined that particle size distribution of such solid substrates depend on the separation process used (settling, filtration, coagulation…) (Lawrence et al.,

1995). Table 34 illustrates an overview of particle size distribution of municipal wastewaters. There is no consensus between authors on the definition of frontiers of particle size fractions. Regarding the settleable fraction, Balmat (1957) defined PSS as particles which have a size over 100 µm while Sophonsiri and Morgenroth (2004) and Levine et *al.* (1985) considered lower thresholds for those particles (63 and 12 µm, respectively). Instead of particle size, the VSS measured after a given time of settling was used in this study to characterize and define PSS. This choice leads to a potential high variability in the particle size of the PSS because they include various materials.

Table 34 : Particle size distribution (in µm) in municipal wastewater

Sample	Soluble	Colloidal	Supra-colloidal	Settleable	Reference
Raw wastewater	<0.22	>0.22	>0.22	2h of settling	Guellil et *al.* (2001)
Raw wastewater	<0.01	0.01 - 1	>2	N.D.	Hu et *al.* (2002)
Primary effluent	<0.1	0.1 - 1.2	1.2 - 63	>63	Sophonsiri and Morgenroth (2004)
Raw wastewater	0.08<	0.08 - 1	1 - 100	>100	Balmat (1957)
Raw wastewater	<0.1	0.1 - 1	1 - 12.0	>12	Levine et *al.* (1985)
Pretreated WW	ND	ND	ND	2h of settling	In this study

3.1.1.2. Biochemical properties and composition

The biochemical composition of primary and secondary effluents of municipal wastewater is presented in Table 35. Municipal wastewater is classically composed by simple components either of organic nature or mineral nature (nitrogen and phosphorus) and by more complex ones such as proteins, carbohydrates (polysaccharides) and lipids as it can be seen in Table 35. Besides, other components are present but in weak proportions, such as nucleic acids, volatile fatty acids (VFA), urea, creatinine and micropollutants (Perez et al., 2009). The Table 35 also underlines the huge variability in the composition of wastewater and also the presence of a non-negligible undefined fraction which ranged from 22 to 78% of the total COD. This may be explained by two distinct hypotheses: (i) there are other components that could not be defined with the current analytical methods or (ii) some components that are in weak proportion create interferences in the analytical methods and it can provoke an underestimation of the amounts of the main components which are proteins, carbohydrates and lipids.

Currently, the studies where the chemical composition of particulate settleable solids (PSS) was assessed are scarced compared to that reporting data on raw wastewater. At micro-scale, PSS is found to be composed by the same components as raw wastewater and primary effluent (Kole

et al., 2012), i.e. proteins, sugars, grease, etc. However, when regarding to macro-scale, Huang et *al.* (2010) showed that it was mainly composed by fibers of cellulose (without précising their nature) then proteins and, finally, carbohydrates. Moreover, Ramasamy et *al.* (1981) determined the amount of fibers that are contained in PSS. They quantified this material as of cellulosic nature which accounted for 50% (w/w) of PSS. Honda et *al.* (2002) indicated that this cellulosic material represents only 20% of the primary sludge. Those fibers were attributed to the discharge of toilet paper by these authors.

Heukelekian (1959) showed that the wastewater settleable fraction was composed by 23.6% of carbohydrate. The main fractions were attributed (in order) to cellulose, lignin and hemicellulose. The settleable fraction had a higher content of cellulose (in % of dry matter) compared to supracolloidal or colloidal components. Besides, hemicellulose and lignin proportions were also higher in the case of settleable matter (Table 36).

Table 35: Biochemical composition of municipal wastewater primary and secondary effluent expressed in terms of the percentage of the total COD

Sample	Location	COD (mg/L)	Carbohydrates (%)	Proteins (%)	Lipids (%)	Other [13] (%)	Unidentified (%)	Source
Primary effluent	Tokyo, Japan	259	6	12	19	14	49	Tanaka et *al.* (1991)
Primary effluent	Urbana, USA	309	6	12	82	0	0	Sophonsiri and Morgenroth (2004)
Primary effluent	ND	203	16	31	45	0	8	Heukelekian (1959)
Secondary effluent	Urbana, USA	35	11	38	44	0	7	Sophonsiri and Morgenroth (2004)
Primary effluent	ND	ND	18	28	31	1	22	Raunkjær et *al.* (1994)

Table 36: Comparison of carbohydrate components in different fractions of municipal wastewater (Heukelekian (1959))

Carbohydrate	% of total dry matter		
	Colloidal	Supracolloidal	Settleable
Cellulose	1.9	2.2	14.2
Hemicellulose	2.1	2.4	3.1
Lignin	2.4	5.6	6.1

[13] The term « other » englobes wastewater small percentage components such as tannin, volatile fatty acids, humic acids, nucleic acids…

3.1.2. Bacteria and substrate interaction

3.1.2.1. Biofilm formation

Growth and survival of some microbial communities requires colonization of a surface and in some cases this leads to the development of a biofilm, which depend on many factors, such as the initial attachment of bacteria to a solid support, growth, species involved and bacterial density (Lawrence et al., 1995). Biofilm formation is carried out after several distinct phases that are presented in the following scheme (Figure 30).

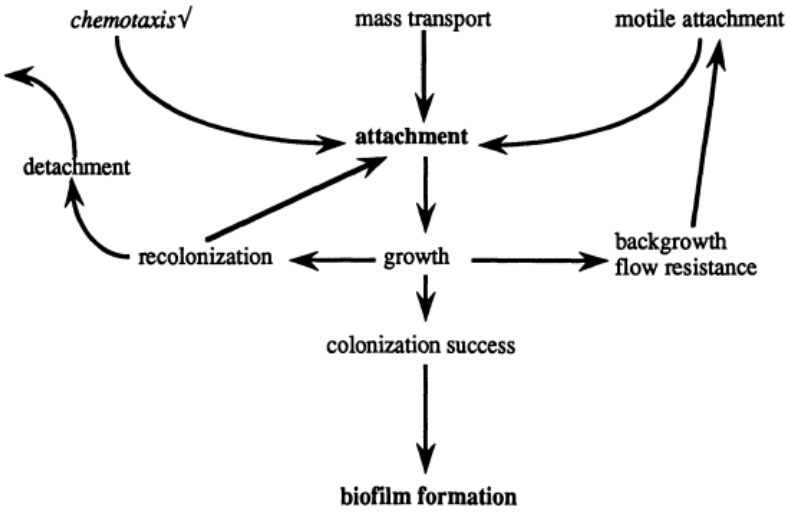

Figure 30 : Scheme representing surface colonization behavior steps for a part of microbial communities (Lawrence et al., 1995)

3.1.2.2. Bacterial adhesion to particulate substrate

Initial attachment of cells to the solid substrate strongly depends on hydrodynamics but also on the substrate roughness and composition and on bacteria surface properties (Fletcher, 1977).

The Figure 31a and Figure 31b represent pictures of a sample of PSS-1a taken at the beginning of the experiment (t_0) with an optical microscope (x20) and with a fluorescence microscope (x63). Fluorescence-based LIFE technologies LIVE/DEAD® Backlight™ Bacterial Viability Kit L7007 was performed to distinguish active bacteria from the fibers and enhance their visualization.

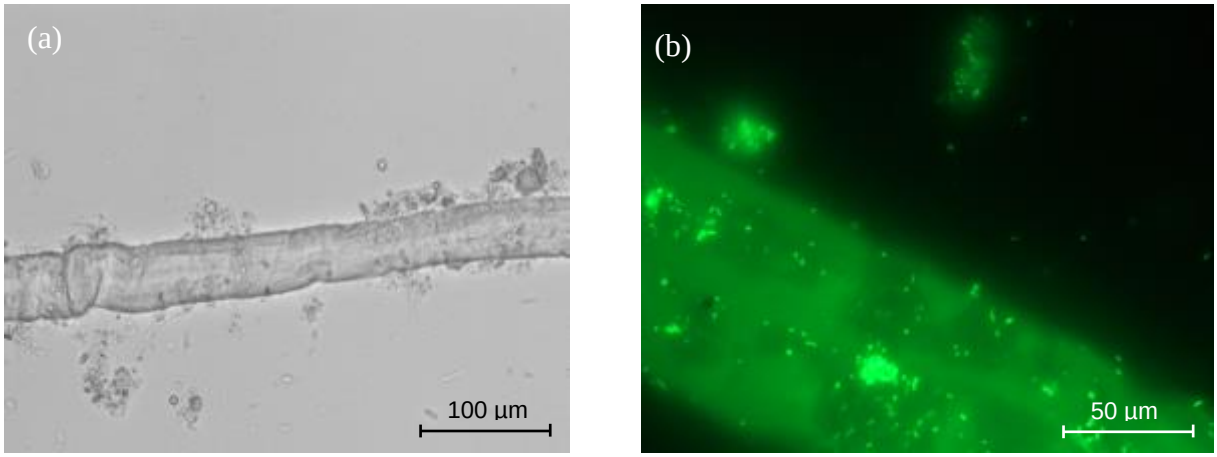

Figure 31: Picture of a fiber in PSS1-a at t_0 taken with (a) an optical microscope (x20) and (b) a fluorescence microscope (x63) in the presence of the fluorescence-based LIFE technologies LIVE/DEAD® Backlight™ Bacterial Viability Kit

The pictures show that microbial communities are 'initially' present at the surface of the fiber (substrate). Some cells are present in the form of aggregates (colonies) while other ones appear solitary. This precolonization of the substrate was certainly involved in the sewerage system before wastewater attained the WWTP and may play a determinant role in the initiation of colonization phase.

3.1.2.3. Bacterial cells location

One of the main solid components present in PSS is fibers owing to the discharge of toilet paper and to residues from food.

Figure 32 represents pictures of fibers of toilet paper that were mixed with activated sludge and taken with a LEICA SP2-AOBS confocal microscope in the presence of the fluorescence-based LIFE technologies LIVE/DEAD® Backlight™ Bacterial Viability Kit and calcofluor 1% to mark cellulosic material (fibers).

Bacterial cells were found to attach to the surface of the fibers (Figure 32a) while in some cases cells break into pores (Figure 32b). The origin of those pores is currently not clear as they could have been generated mechanically with the effect of stirring in the reactor or involved by hydrolytic enzymes.

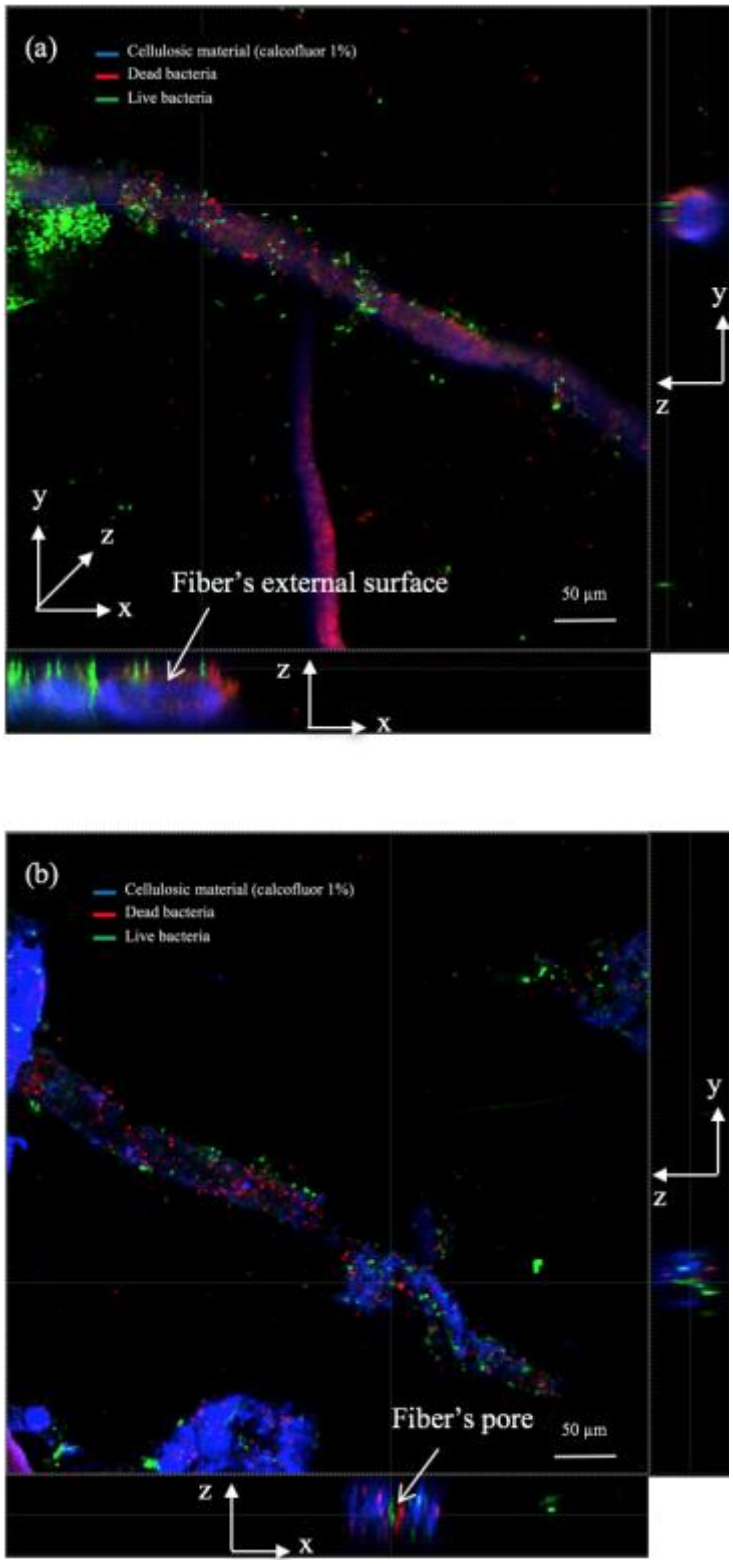

Figure 32: Pictures of fibers taken with a LEICA SP2-AOBS confocal microscope in the presence of the fluorescence-based LIFE technologies LIVE/DEAD® Backlight™ Bacterial Viability Kit and calcofluor 1%

3.1.2.4. Evidence of the colonization phase

The colonization of fibers of toilet paper (TP1-a) was experimentally demonstrated by the means of microscopic monitoring in our laboratory. A batch-aerobic reactor was fed by toilet paper mixed with an inoculum from activated sludge (see Table 32). The Figure 33 represents the microscopic monitoring of toilet paper degradation by bacteria under aerobic conditions during 6 days.

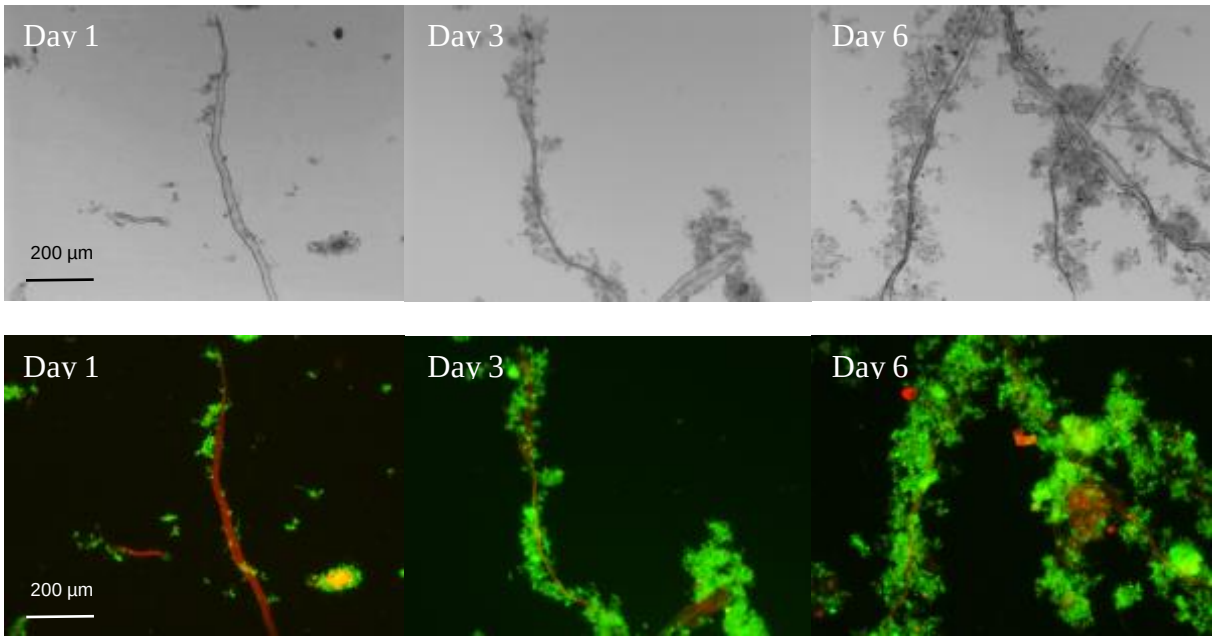

Figure 33 : Microscopic monitoring of the biodegradation of toilet paper under aerobic conditions (6 first days of experiment TP1-a)

In Figure 33, the fibers were gradually colonized by bacteria forming cell aggregates that are attached to the solid substrate. Some bacterial aggregates are however detached or present in the liquid phase. Two explanations for that feature can be given: (i) detachment is caused by shear stress generated by stirring in the reactor (ii) not all the bacteria that are contained in activated sludge were able to adsorb to the PSS. According to Dias and Bhat (1964), only some of the bacteria can be active in degradation of wastewater constituents. Regarding colonization, bacteria appear not uniformly spread on the whole surface of fibers in comparison with conventional biofilms. Parts of the fibers are likely not attacked by bacterial cells. This observation may rise the question of an eventual effect of the biochemical or physical heterogeneity of the substrate at the level of the enzyme function. The question of biochemical

heterogeneity and its influence on fiber colonization by bacteria will unfortunately not be addressed in this study.

3.1.2.5. Relation between cell growth limitation and substrate surface area

Conventionally, limitation of cell growth on particulate substrate is attributed to the substrate available surface area. During degradation, this surface area decreases. In our studies, the surface area decrease was checked during experiments on Toilet Paper (TP1-a).

Figure 34 illustrates pictures of toilet paper that were taken with an optical microscope right after the colonization phase that was evidenced above.

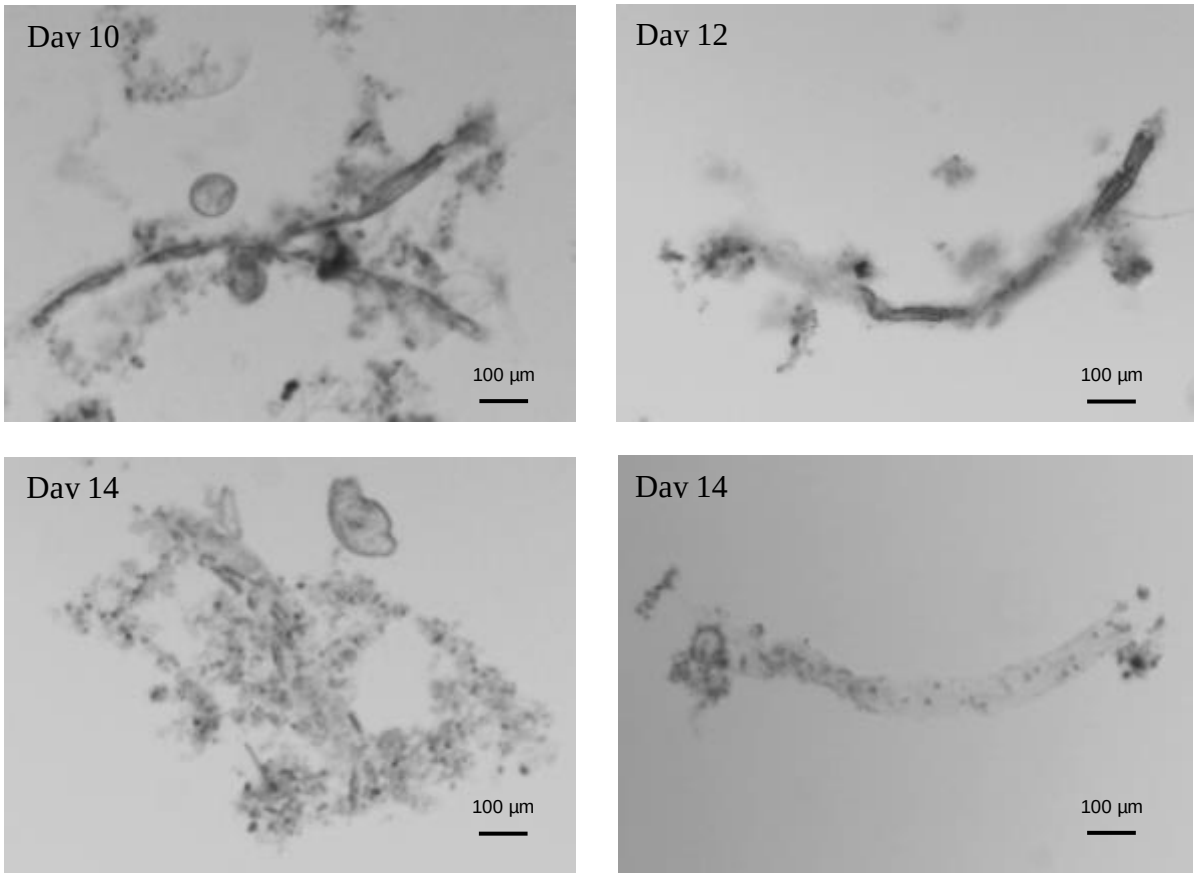

Figure 34 : Microscopic monitoring of the biodegradation of PSS-1a under aerobic conditions

In Figure 34, it seems that the fibers size is gradually decreasing with time. If we refer to the respirometric monitoring that was presented in chapter I, these microscopic observations may help to understand the two phases trend observed on the OUR profile against time. The first phase (OUR increasing phase) of the OUR profile would correspond to an exponential growth phase due to an increase in substrate availability making possible by fiber colonization. The

second one (OUR decreasing phase) is a phase where growth is limited by the available surface area.

3.1.2.6. Conclusion of the experimental observations and hypothesis

Experimental results obtained in our laboratory and literature highlighted several important phenomena and properties:

- PSS are found to be mainly fibers composed by 23.6% of carbohydrates that are mainly owing to the discharge of toilet paper. They are globally of cylindrical shape; other particulate substrates may be entrapped in aggregates and not easily visible.
- In PSS, fibers are found to be initially colonized by microbial communities that have grew-up inside the sewerage system before they attained the WWTP;
- The colonization of fibers of toilet paper by microbial communities is not uniform. It forms cell aggregates beside some solitary bacterial cells. Those aggregates show similarities with biofilm systems but they are less organized and maybe less dense and less strong. It is not clear whether these aggregates results from entrapment of bulk bacteria or from bacteria growth on the particulate substrate. Hence, the fraction of bacteria really active on hydrolysis is questioned;
- In the case of toilet paper, it may be supposed, according to microscopic monitoring, that the increasing phase of the OUR profile is an exponential colonization/growth phase and that the decreasing one is a phase where growth is limited by the available surface area, which decreases with time.

These conclusions underlined some interesting issues that could be a basis for thinking about improvement in the mathematical expression of hydrolysis mechanisms including colonization and detachment. The final objective target a more accurate and robust description of the biodegradation of large particles considered as slowly biodegradable COD.

The following aspects will be considered:

- Colonization; a rate of colonization will be considered dependent on the initial concentration of active cells. Active cells mean that some cells are not active for hydrolysis or not able to colonize the particulate substrate.
- A maximum surface area for cell colonization is also considered.

- The geometry of the particles will be considered in order to study its influence on the degradation kinetics.

The following section of the current chapter is dedicated to the description of the conceptual approach that was adopted for the development of this model.

3.2. CONCEPTUAL MODEL DEVELOPMENT APPROACH

3.2.1. Description of the conceptual model

Four COD fractions were taken into account in the developed model: the hydrolysable COD was subdivided into soluble readily hydrolysable ($S_{B,\,hyd}$) and a slowly hydrolysable COD (XC_B). The modified hydrolysis surface-based mechanism including the colonization phase describes the hydrolysis of XC_B into $S_{B,\,hyd}$ which is directly uptaken by heterotrophs (X_{OHO}) during growth. Here, hydrolysis depends on the substrate colonized surface area (A_{XCB}). Thus, it is controlled by the colonizing biomass ($A_{XOHO,\,ads}$) till the entire A_{XCB} is covered by the microorganisms. Since then, it is controlled by the remaining A_{XCB} that is not degraded yet. The endogenous respiration of heterotrophs generates particulate unbiodegradable organics ($X_{U\_Bio,\,Lys}$). A schematic representation of the colonization model (M_SBK) is presented in Figure 35. The stoichiometric and process rates are of the M_SBK are presented in Peterson's matrix (Table 39).

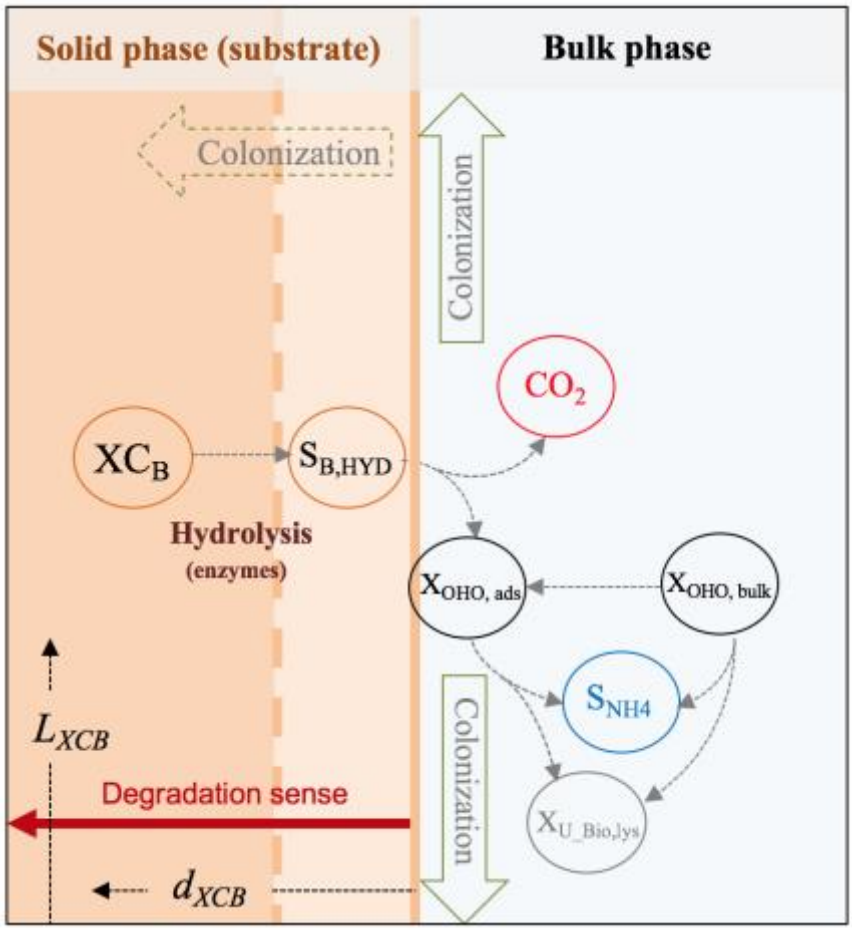

Figure 35 : Conceptual surface-based colonization model schematic representation

3.2.2. Basis of the biological model

Alternative hydrolysis description taking into account a surface-based colonization has been implemented and is thoroughly described in the next section. Hydrolysis parameters were estimated based on OUR profile while other parameters come from typical values proposed in ASM1.

3.2.2.1. Processes

A two-step process is considered: adsorption of biomass to the particulate substrate (equation (33)) and the hydrolysis of XC_B by the previously adsorbed (and/or grown on the surface) biomass ($X_{OHO, ads}$) as described in equation (34). In the conventional IAWQ model n°1, the notion of surface is described with a mass concentration ratio between substrate and bacteria (XC_B/X_{OHO}). In this thesis, through the conceptual model M_SBK, this mass

concentration ratio was replaced by a "surface ratio" which is function of concentration but also the physical and geometrical properties (cf. §Table 37):

$$-\frac{dX_{OHO,bulk}}{dt}=\frac{dX_{OHO,ads}}{dt}=k_{ADS}.X_{OHO,bulk}XC_B(f_{ma}-\frac{X_{OHO,ads}}{XC_B}) \quad (33)$$

Where k_{ADS} is the adsorption rate [L. mgCOD^{-1}. d^{-1}] and $f_{ma}=\frac{X_{OHO,\ ads,\ max}}{XC_B}$

$X_{OHO,\ ads}$ and $X_{OHO,\ bulk}$ are the concentration of bacterial cells adsorbed to the substrate and in suspension respectively. $X_{OHO,\ ads,\ max}$ is the maximum concentration of bacterial cells that can be adsorbed related to the total surface area of substrate [gCOD/L].

A surface-based kinetics was used in which the rate of hydrolysis was proportional to the adsorbed surface area of $X_{OHO,\ ads}$ to take into account the enzyme production capacity:

$$-\frac{dXC_B}{dt}=\frac{dS_{B,hyd}}{dt}=q''_{XCB_{SB},hyd}\frac{A_{XCB}/A_{XOHO,ads}}{K''_{XCB,hyd}+A_{XCB}/A_{XOHO,ads}}A_{XOHO,ads} \quad (34)$$

Where:

$q''_{XCB\_SB,\ hyd}$ is a modified hydrolysis rate constant [mgCOD.L^{-1}.d^{-1}.m^{-2}],

$K''_{XCB,\ hyd}$ is a modified half-saturation constant for hydrolysis [m^2.m^{-2}].

When $A_{XCB} >> A_{XOHO,\ ads}$, the hydrolysis rate becomes of first-order with respect to the surface occupied by the microorganisms. When $A_{XOHO,\ ads} >> A_{XCB}$, the hydrolysis rate becomes of first-order with respect to the available surface area of substrate.

Growth of heterotrophic bacteria under aerobic conditions is described with a first-order term with respect to X_{OHO} (Dold et al., 1980). The mechanism is limited by the bioavailability of $S_{B,\ HYD}$ as described below:

$$\frac{dX_{OHO}}{dt}=\mu_{OHO,max}\frac{S_{B,hyd}}{K_{SB,hyd}+S_{B,hyd}}X_{OHO} \quad (35)$$

Where:

X_{OHO} is heterotrophic bacteria concentration [mgCOD.L^{-1}], adsorbed and/or in the bulk depending on the hypothesis considered,

$\mu_{OHO,\ max}$ is the maximum growth rate [d^{-1}],

$K_{SB,\,hyd}$ is the half-saturation constant for growth [mgCOD.L^{-1}].

The endogenous respiration model was chosen to describe bacteria degradation and lysis. The rate of endogenous respiration is expressed with a first-order reaction with respect to X_{OHO} (Ekama and Marais, 1979):

$$\frac{dX_{OHO}}{dt} = -b_{OHO}X_{OHO} \tag{36}$$

Where:

b_{OHO} is the endogenous respiration rate constant [d^{-1}].

A part of the lysed heterotrophic bacteria is oxidized to generate energy for maintenance while the other part, which is in the particulate form, accumulates as unbiodegradable matter or endogenous residue ($X_{U\_Bio,\,Lys}$):

$$\frac{dX_{U_{Bio,\,Lys}}}{dt} = -f_{XU_{Bio,\,lys}}b_{OHO}X_{OHO} \tag{37}$$

Where:

$f_{XU\_Bio,\,Lys}$ is the inert fraction of heterotrophs [mgCOD. mgCOD^{-1}]

Oxygen utilization is carried out during the previously enunciated mechanisms. The corresponding oxygen uptake rate (OUR) could be expressed as below:

$$OUR = -\frac{d[S_{O_2}]}{dt} = \left(-\left(\frac{1-Y_{OHO}}{Y_{OHO}}\right)\mu_{OHO,max}\frac{S_{B,hyd}}{K_{SB,hyd}+S_{B,hyd}} - (1-f_{XU_{Bio,\,lys}})b_{OHO}X_{OHO}\right. \tag{38}$$

Where:

Y_{OHO} is the aerobic growth yield [mgCOD. mgCOD^{-1}].

3.2.2.2. Geometrical properties of particulate variables

To be able to evaluate the consequences of shape and size of the particulate substrate on the hydrolysis process, additional geometrical and physical properties of the particulate compounds (substrate and hydrolytic biomass) were introduced.

(a) Cylindrical solid substrate: particle diameter (d_{XCB_cyl}), length (L_{XCB_cyl}), density (ρ_{XCB_cyl}) and number of particles (n_{XCB_cyl});

(b) Spherical solid substrate: particle diameter (d_{XCB_sph}), density (ρ_{XCB_sph}) and number of particles (n_{XCB_sph});

(c) Spherical bacteria: cell diameter (d_{XOHO}), density (ρ_{XOHO}) and number of bacterial cells (n_{XOHO}).

In order to compare spherical particles with cylindrical ones, three hypotheses will be theoretically evaluated: the solid substrate has (i) the same colonizable surface, (ii) the same number of particles and (iii) the same surface for one particle than the reference cylindrical substrate.

The values of each new constant, and the link between d_{XCB_sph} and d_{XCB_cyl} are presented in Table 37.

Table 37: Geometrical and physical properties of solid substrate and bacterial cells

Component	Geometrical or physical property	Value	Unit	Source
Cylindrical Solid substrate	Diameter (d_{XCB_cyl})	100	µm	our results
	Length (L_{XCB_cyl})	2000	µm	our results
	Density (ρ_{XCB_cyl})	1.1	g/cm^3	INRS (2011)
Spherical Solid substrate	Diameter (d_{XCB_sph})	$\frac{3}{2} d_{XCB,cyl}$	µm	Same colonizable surface
		$\left(\frac{3}{2} L_{XCB} d_{XCB,cyl}^2\right)^{1/3}$	µm	Same number of particles
		$\left(L_{XCB} d_{XCB,cyl}\right)^{1/2}$	µm	Same surface for one particle
	Density (ρ_{XCB_sph})	1.1	g/cm^3	INRS (2011)
Bacterial cell	Diameter (d_{XOHO})	1	µm	Garrett and Grisham (2000)
	Density (ρ_{XOHO})	1.002	g/cm^3	Loferer-Krößbacher et *al.* (1998)

3.2.2.3. Relation between substrate particle properties and concentration of particulate variables

Cylindrical and/or spherical particulates substrates were considered. In both cases the number of particles (n_{XCB}) was kept constant and the developed model considers that particle diameter continuously decreases during the substrate utilization by biomass as in the work of Sanders et *al.* (2000). Furthermore, for cylindrical particles, the substrate particle length (L_{XCB}) was also kept constant.

Bacterial cells are supposed of spherical shape with 1µm diameter.

Table 38 summarizes the dependence of physical parameters to state variables (i.e. XC_B and $X_{OHO,\,bulk}$ and $X_{OHO,\,ads}$). It has to be noticed that the surface area of substrate particles decreases proportionally to $XC_B^{1/2}$ and to $XC_B^{2/3}$ for cylindrical and spherical particles respectively.

Table 38 : Main geometrical-based definition of parameters

	Cylindrical particles	Spherical particles
n_{XCB} (-)	$\frac{4XC_{B,0}V_R}{\pi\cdot\rho_{XCB}L_{XCB}d_{XCB,0}^{\ 2}}$	$\frac{4XC_{B,0}V_R}{\pi\cdot\rho_{XCB}d_{XCB,0}^{\ 3}}$
d_{XCB} (m)	$\frac{d_{XCB,0}}{XC_{B,0}^{\ 1/2}}XC_B^{\ 1/2}$	$\frac{d_{XCB,0}}{XC_{B,0}^{\ 1/3}}XC_B^{\ 1/3}$
A_{XCB} (m^2)	$n_{XCB}\pi d_{XCB}L_{XCB}$ $=\frac{4V_RXC_{B,0}^{\ 1/2}}{\rho_{XCB}d_{XCB,0}}XC_B^{\ 1/2}$	$n_{XCB}\pi d_{XCB}^2$ $=\frac{6V_RXC_{B,0}^{\ 1/3}}{\rho_{XCB}d_{XCB,0}}XC_B^{\ 2/3}$
A_{XOHO} (m^2)	$\frac{3V_R}{2d_{XOHO}\rho_{XOHO}}X_{OHO,ads}$	
$f_{ma}=\frac{X_{OHOads,max}}{XC_B}$	$\frac{8}{3}\frac{d_{XOHO}\rho_{XOHO}}{d_{XCB,0}\rho_{XCB}}XC_{B,0}^{\ 1/2}XC_{B,t}^{\ -1/2}$	$4\frac{d_{XOHO}\rho_{XOHO}}{d_{XCB,0}\rho_{XCB}}XC_{B,0}^{\ 1/3}XC_{B,t}^{\ -1/3}$

Table 39 : Peterson's matrix of model M_SBK

Process	*Soluble species*			*Particulate species*				Process rate
	$S_{B,\,HYD}$	S_{O2}	S_{NH4}	XC_B	$X_{OHO,\,bulk}$	$X_{OHO,\,ads}$	$X_{U\_bio,\,lys}$	
Adsorption					*-1*	*1*		$k_{ADS} \cdot X_{OHO,bulk} XC_B (f_{ma} - \frac{X_{OHO,ads}}{XC_B})$
Detachment *					*1*	*-1*		$k_{det} \left({}^{A_{XOHO,ads}} \big/ _{A_{XCB}} \right)^{500}$
Surface based colonization-hydrolysis	*1*			*-1*				$q''_{XCB_{SB},hyd} \frac{{}^{A_{XCB}} \big/ _{A_{XOHO,ads}}}{K''_{XCB,hyd} + {}^{A_{XCB}} \big/ _{A_{XOHO,ads}}} A_{XOHO}$
Aerobic growth of the colonizing heterotrophs	$-1/Y_{OHO}$	$-(1-Y_{OHO})/Y_{OHO}$	$-i_{N\_XBio}$			*1*		$\mu_{OHO,max} \frac{S_{B,hyd}}{K_{SB,hyd} + S_{B,hyd}} X_{OHO}$
Aerobic endogenous respiration of the colonizing heterotrophs		$-(1-f_{XU\_Bio,\,lys})$	$f_{XU\_Bio,\,lys} * i_{N,\,XU} + i_{N\_XBio}$			*-1*	$f_{XU\_Bio,\,lys}$	$b_{OHO} X_{OHO,\,ads}$
Aerobic endogenous respiration of the non-adsorbed heterotrophs		$-(1-f_{XU\_Bio,\,lys})$	$f_{XU\_Bio,\,lys} * i_{N,\,XU} + i_{N\_XBio}$		*-1*		$f_{XU\_Bio,\,lys}$	$b_{OHO} X_{OHO,\,bulk}$

* process active only when investigating the fate of daughter cells (see §5.3).

4. EXPERIMENTAL RESULTS AND CONFRONTATION TO MODEL SIMULATION

In this section, particulate substrates degradation was followed in batch-respirometers by measuring the OUR against time. The results of simulations obtained using the three models, which could be distinguished by the mathematical expression of the utilized hydrolysis mechanism, are presented together with the experimental data. After model calibration, parameters obtained for each model are listed. Firstly, the case of model substrates, i.e. TP of cylindrical shape and EP (egg white particles) of spherical shape, is presented. Secondly, real substrates, PSS-1a and PSS-2a, that are constituted by mixtures of large particles of different shapes and sizes are considered.

4.1. OUR PROFILES FROM BATCH RESPIROMETRY

4.1.1. Model substrates

Results from respirometric experiments on a substrate composed of commercial TP are presented in Figure 36.

Contrary to what can be observed on substrate containing readily biodegradable compounds (see chapter II), OUR did not increase immediately after TP addition (Figure 36a). A two days lag phase was observed followed by an exponential increase of OUR with OUR_{max} reaching 50 $mgO_2/L/h$ at 8 days of culture. Then, the OUR decreased, first sharply during two days and slower and slower until a degradation time estimated at 12 days. The net increase of OUR is high as OUR_{max}/OUR_{min} was equal to 10.

Figure 36b shows the OUR measured during the consumption of egg white particles by Dimock and Morgenroth (Dimock and Morgenroth, 2006). The shape of the OUR obtained is similar to the one observed with toilet paper. The following phases were also observed: stable OUR, OUR exponential increase, OUR sharp decrease then followed by a slow decrease. However, the characteristics time for each phase and the amplitude of OUR increase were highly different. One key difference observed between TP degradation and EP degradation was the trend of the decrease of the OUR after reaching OUR_{max}. A sharp decrease was observed in the case of TP whereas this decrease is much slower in the case of EP. In addition, when considering results obtained with EP, smaller particles (60µm) were more rapidly hydrolyzed than larger particles (390 µm) and the OUR reached a higher maximum rate.

a)

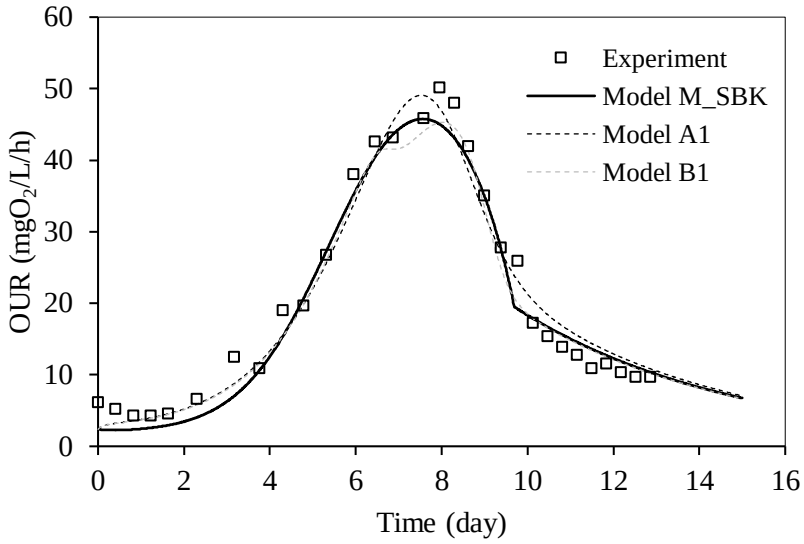

b)

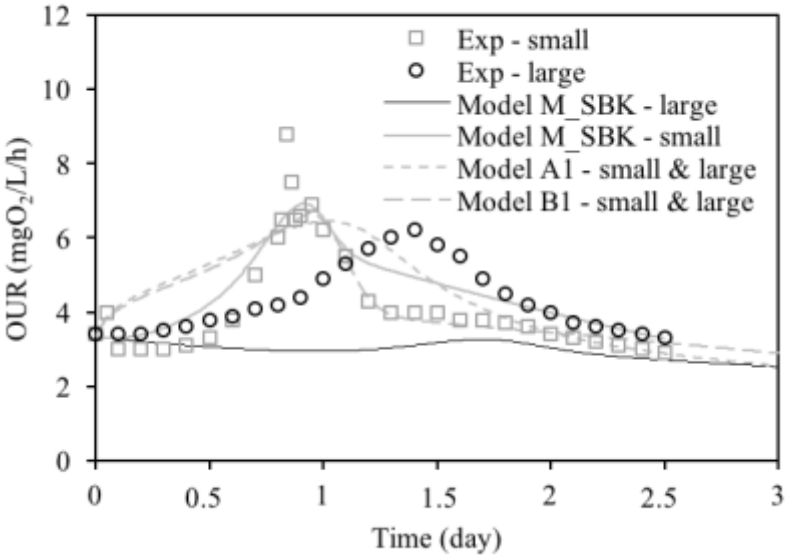

Figure 36: Comparison between models simulations (models A1, B1 and M-SBK) and experimental data for a) toilet paper (cylinder: d_{XCB}=100 µm) and b) egg white particles (spherical EP: small=60 µm ; large=390 µm) (Dimock and Morgenroth, 2006).

4.1.2. Real substrate (PSS)

Results of respiration experiments on particulate settleable solids (PSS) from wastewater are presented in Figure 37.

4.1.2.1. PSS from the inlet of the WWTP (PSS1-a)

Figure 37a shows the time course of the OUR for a batch experiment performed with aged PSS (PSS1-a) coming from the inlet of the settling tank of the WWTP of Toulouse-Ginestous (France). No exogenous inoculum was added. The OUR starting from a high value of 45 $mgO_2/l/h$ increased very quickly until 85 $mgO_2/l/h$ immediately after the addition of the PSS. This phase lasted less than 2 hours. After this initial tight peak, the OUR decreased till it reached a value of 10 $mgO_2/l/h$ after 16 days.

4.1.2.2. PSS from the beginning of the sewer (PSS2-a)

On contrary, when PSS were obtained from wastewater sampled in the network closed to production location (PSS2-a), the OUR showed a completely different feature. It started to increase exponentially from 7.5 $mgO_2/l/h$ to 13.7 $mgO_2/l/h$ after 2.5 days. Then, the activity decreased exponentially till it reached a value of 3.3 $mgO_2/l/h$ after 9 days (Figure 37b).

a)

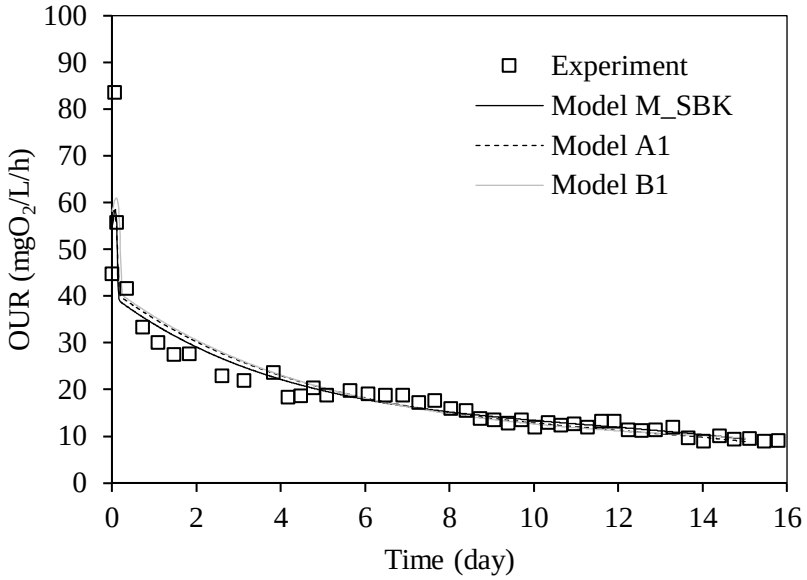

b)

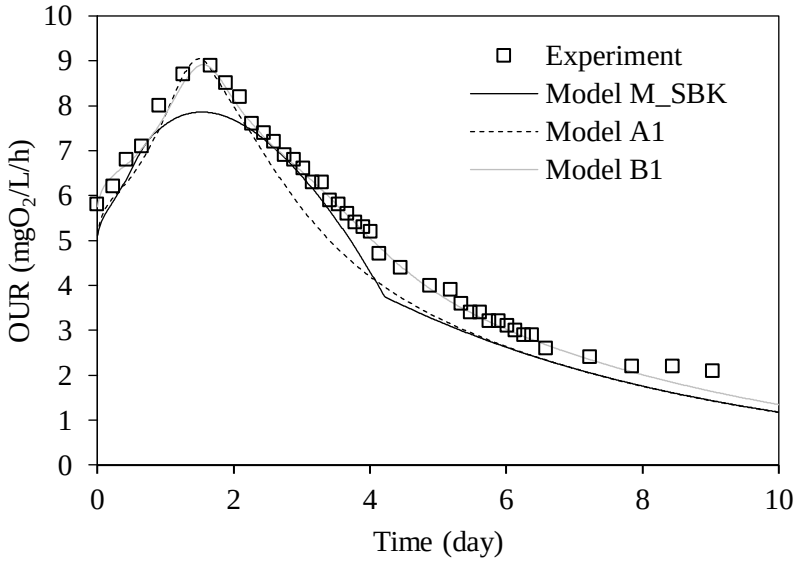

Figure 37: Comparison between model simulations (models A1, B1 and M-SBK) and experimental data for a) PSS1-a ("aged" PSS) and b) PSS2-a ("fresh" PSS).

4.2. CONFRONTATION OF MODELS TO EXPERIMENTAL DATA

Parameters relative to active biomass and hydrolysis processes were estimated based on measured OUR for three different models: mono- (A1) or bi- (B1) substrate conventional model and the geometrically surface-based model developed in this study (M_SBK). Table 40 summarizes which parameters were taken from experimental data and the ones estimated with the Aquasim® computer program.

Table 40: Models parameters estimated from calibrations for the model substrates and PSSs

Experiment		Experimental values	Fixed	Estimated
TP1-a	Substrate	XC_B		q_{XCB} (q''_{XCB}), K_{XCB} (K''_{XCB})
	Inoculum		$X_{U\_inoc,\ ini}$	X_{OHO}, X_{ER}
EP	Substrate	XC_B		q_{XCB} (q''_{XCB}), K_{XCB} (K''_{XCB})
	Inoculum	$X_{OHO}+X_{ER}$		X_{OHO}
PSS1-a	Substrate	$XC_B+X_{OHO}+X_{ER}$		q_{XCB} (q''_{XCB}), K_{XCB} (K''_{XCB})
	Inoculum			
PSS2-a	Substrate	$XC_B+X_{OHO}+X_{ER}$		q_{XCB} (q''_{XCB}), K_{XCB} (K''_{XCB})
	Inoculum	$XC_B+X_{OHO}+X_{ER}$		X_{OHO}, X_{ER}, X_{U_inoc}

4.2.1. Model substrates

In Figure 36, the results of OUR profiles predictions given by the models are shown for both *TP* and small egg white particles (*EP*) biodegradation. To evaluate the ability of the models to capture the trends of OUR, biomass fractions estimated with model A1 was taken as fixed values for models B1 and M_SBK. The identified parameters are presented in Table 41.

Table 41: Parameter identification for the different models on model substrate. Underlined parameters are fixed based on experimental data.

Parameter	Unit	Toilet Paper			Small egg white particles		
		TP1-a *A1*	TP1-a *B1*	TP1-a *M_SBK*	EP *A1*	EP *B1*	EP *M_SBK*
$K_{XCB,\ hyd}$	$mgCOD.mgCOD^{-1}$	0.71	-	-	1	-	-
$K''_{XCB,\ hyd}$	$m^2.m^{-2}$	-	-	0.04	-	-	1.42
$K_{XCB\_1,\ hyd}$	$mgCOD.mgCOD^{-1}$	-	0.2	-	-	0.17	-
$K_{XCB\_2,\ hyd}$	$mgCOD.mgCOD^{-1}$	-	0.08	-	-	0.13	-
$q_{XCB\_SB,\ HYD}$	d^{-1}	1.3	-	-	3.1	-	-
$q''_{XCB\_SB,\ HYD}$	$mgCOD.d^{-1}.m^2$	-	-	596	-	-	10000
$q_{XCB1\_SB,\ HYD}$	d^{-1}	-	0.82	-	-	1.9	-
$q_{XCB2\_SB,\ HYD}$	d^{-1}	-	0.46	-	-	0.39	-
XC_B	$mgCOD.L^{-1}$	8180	-	8180	250	-	250
XC_{B1}	$mgCOD.L^{-1}$	-	6713	-	-	129	-
XC_{B2}	$mgCOD.L^{-1}$	-	1467	-	-	121	-
Inoc_COD	$mgCOD.L^{-1}$	710	710	710	ND	ND	ND
X_{U_inoc}	$mgCOD.L^{-1}$	355	355	355	ND	ND	ND
X_{ER}	$mgCOD.L^{-1}$	305	305	305	448	448	448
$X_{OHO,\ ads}$	$mgCOD.L^{-1}$	50	50	0	52	52	0
$X_{OHO,\ bulk}$	$mgCOD.L^{-1}$	-	-	50	-	-	52
E^2	$(mgO_2/l/h)^2$	1902	1417	1722	36	24	16

The M_SBK model considers that the inoculum contains the active biomass that needs first to adsorb to fulfil its hydrolytic potential. On the TP experiment, as the XC_B is initially high, all the $X_{OHO,\ bulk}$ can adsorb and hydrolyze the particulate substrate. The estimated initial $X_{OHO,\ bulk}$ concentration is then of 50 mgCOD/L for 710 mgCOD/L of inoculum. The endogenous respiration has a big effect on the OUR. The maximum active biomass concentration is 3 150 mgCOD/L (not shown).

Concerning egg white particles (EP), the initial XC_B value is low. Thus, the increase of the OUR is obtained by the way of a hydrolysis constant relatively high. Models A1 and B1 does not allow to describe the exponential increase. Considering two particulate substrates (model B1) allows to properly describe the OUR decrease. M_SBK captures the trends of the OUR for both sizes of particles. However, considering a same inoculum and a same set of kinetic parameters does not allow to describe the profiles obtained for the two sizes and the differences between simulated and experimental values are high for one of the curves (Figure 36). Considering the diameter as an adjustable parameter is not enough to address the problem. This is illustrated on

Figure 38 which includes the modelling results with a spherical XC_B diameter of 94 µm that allowed minimizing the E^2.

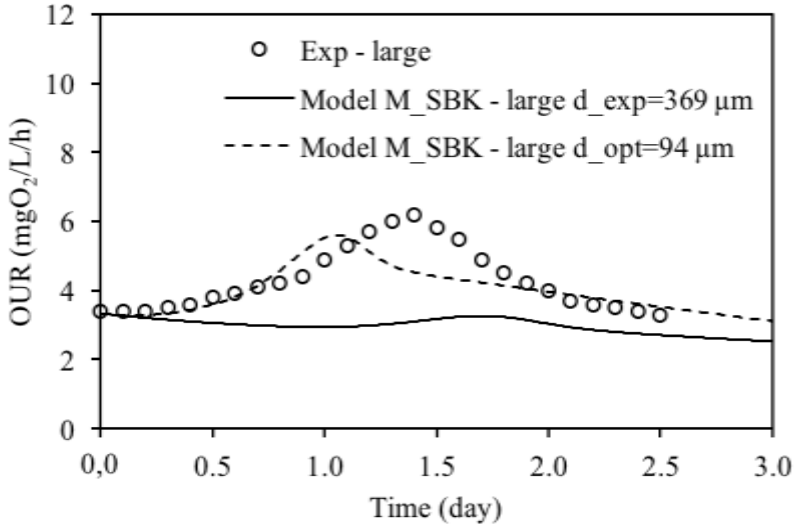

Figure 38: Effect of particulate substrate size optimization to describe large eggs white particles OUR profile with the M_SBK model (all the other parameters are identical).

4.2.2. Real substrates, PSSs

The trend of the OUR profile obtained during the degradation of PSS2-a sampled upstream of the sewer is quite well simulated by the three considered models as it results in a two-trends profile: a first step of OUR increase followed by a decreasing step. In contrast the models have more difficulties to represent the OUR profile obtained with PSS1-a as there is no first increasing step. Indeed, to simulate a direct decrease of OUR, all the models enforce a really high concentration in $X_{OHO,\,ads}$, close to the total COD of the sample which results in considering that the XC_B concentration is negligible (result not shown). This is not consistent with the experimental observations and it appears necessary to consider a biomass that only performs endogenous respiration that accounts for 90% of the total biomass (see Table 42).

Table 42: Parameter identification for the different models on real substrate

Parameter	Unit	PSS1-a			PSS2-a		
		PSS1-a A1	PSS1-a B1	PSS1-a M_SBK	PSS2-a A1	PSS2-a B1	PSS2-a M_SBK
$K_{XCB,\ hyd}$	$mgCOD.mgCOD^{-1}$	0.21	-	-	2.4	-	-
$K'_{XCB,\ hyd}$	$m^2.m^{-2}$	-	-	0.05	-	-	0.2
$K_{XCB\_1,\ hyd}$	$mgCOD.mgCOD^{-1}$	-	0.01	-	-	0.4	-
$K_{XCB\_2,\ hyd}$	$mgCOD.mgCOD^{-1}$	-	0.02	-	-	0.6	-
$q_{XCB\_SB,\ HYD}$	d^{-1}	0.37	-	-	3.2	-	-
$q'_{XCB\_SB,\ HYD}$	$mgCOD.d^{-1}.m^2$	-	-	287	-	-	2185
$q_{XCB1\_SB,\ HYD}$	d^{-1}	-	3.75	-	-	0.8	-
$q_{XCB2\_SB,\ HYD}$	d^{-1}	-	0.33	-	-	1.7	-
XC_B	$mgCOD.L^{-1}$	3607	-	3607	575	-	575
XC_{B1}	$mgCOD.L^{-1}$	-	102	-	-	505	-
XC_{B2}	$mgCOD.L^{-1}$	-	3505	-	-	70	-
$Inoc\_COD$	$mgCOD.L^{-1}$	0	0	0	477	477	477
X_{U_inoc}	$mgCOD.L^{-1}$	0	0	0	9	9	9
X_{ER}	$mgCOD.L^{-1}$	5149	5149	5149	727	727	727
$X_{OHO,\ ads}$	$mgCOD.L^{-1}$	474	474	129	41	41	17
$X_{OHO,\ bulk}$	$mgCOD.L^{-1}$	-	-	345	-	-	24
E^2	$(mgO_2/l/h)^2$	1055	931	899	309	20	99

5. DISCUSSION

Evolution of OUR with time were found really different on contrasted substrates distinguished by their geometry, biochemical nature and initial colonization level. Some substrates, qualified as "model", whose main biochemical characteristics are known were used to represent a simplified hydrolysis process. Then reals substrates, thus with various biochemical composition and geometrical structure and characterized by different inoculation level were used. This set of various conditions should help in evaluating how a given mathematical model is able to represent the entire set of conditions and thus its capacity to simulate the numerous kinetic profiles of OUR versus time.

Processes governing OUR profiles due to hydrolysis of an organic particulate material are numerous and diverse in terms of characteristics and origin. These particulate materials mainly differ in terms of size and characteristic time necessary for their degradation. Hydrolysis is first due to enzymes produced by microorganisms. A synergy between several enzymes often occurs to favour an efficient and entire hydrolysis of substrates despite the heterogeneity in structure and biochemistry of those substrates. In our experimental conditions, a diversity of hydrolytic micro-organisms exists and a progressive adaptability to the substrate may occur with time. All the heterotrophic microorganisms are not necessary involved in the hydrolysis process making the hydrolytic biomass estimation difficult. For real substrates, a diversity in the biochemical nature (grease, polysaccharides, proteins, etc.) of the particles may be expected. As aforementioned the substrate evolves during its degradation and its geometrical structure is impacted. Progressive consumption and/or particle breakage lead to a size distribution that is time dependent. This description certainly non-exhaustive of processes that govern OUR evolution due to hydrolysis underlines that a mathematical description of complex hydrolytic processes will necessarily result from a compromise between a high complexity to properly fit experimental profiles and a simplicity allowing a robust use.

In this work, a compromise is searched. We compared the conventional surface based IAWQ model with one (model A1) or two (model B1) substrates with more complex models that aim to consider the dynamic evolution of the specific surface area of the substrates and of the active hydrolytic cells (M_SBK). The interest of better taking into account the reaction surface will be first evaluated.

5.1. MODEL CAPACITY TO SIMULATE DEGRADATION OF VARIOUS PARTICULATE SUBSTRATES

Model A1 well captures the trend of OUR profile obtained with TP1-a and PSS2-a. On contrary, simulated OUR for egg white particles of small and large size does not fit the experimental data and the shape itself is different. Similar observations could be done when using the model B1 even if taking into account two particulate substrates allows to better describe the decrease in OUR observed with small egg proteins.

M_SBK model allows describing contrasted OUR profiles. By taking into account the size of the particles and its dynamic evolution it qualitatively captures the effect of the size experimentally observed in Dimock and Morgenroth (2006) with egg white particles: the OUR increased more rapidly for smaller particles and also reached a larger maximum rate. However, it failed in predicting the values based on the experimental data provided, possibly due to substrate specific surface considerations.

5.2. FATE OF THE EVOLUTION OF THE SUBSTRATE SPECIFIC SURFACE

Intuitively, hydrolysis is a process whose rate depends on the available specific surface area of the particulate substrate for the hydrolytic microorganisms. Our analysis of the literature showed that models taking into account this specific area in the hydrolysis rate calculation, such as the SBK model, do not take into account microbial colonization of the substrate. That is why this model is not able to report a step of increase of observed hydrolysis rate. The colonization rate should then depend on particles geometrical and physical properties such as shape (cylinder, sphere), size (diameter, length) and density.

For model substrates evaluated in this work, cellulose fibers coming from toilet paper and eggs proteins (experiment from Dimock and Morgenroth (2006)) were chosen as representative of cylindrical and spherical shape respectively. The trends of the OUR profile present two or three steps that possibly correspond to the simultaneous occurrence of mechanisms involved in the whole process, i.e. adsorption, colonization, and hydrolysis itself. The most obvious difference between the OUR profiles obtained for cellulose fibers and egg proteins correspond to the decreasing phase (see Figure 36a and b). One can also observe that the increase of OUR follows an exponential trend but that the acceleration is lower in the case of big eggs proteins compared to the small ones. Our study then moved on to examine if those differences could be explained only based on the differences in geometrical properties. To achieve this, we used the modified SBK model (M_SBK) to evaluate the effect of both geometry and size of particles.

Results obtained for substrate of cylindrical or spherical shape of different sizes are presented in Figure 39. In order to study the effect of the size of particles on the OUR profile, three diameters for spherical particles were considered within the following hypothesis: a same total particle surface, a same number of particles and a same surface for one particle. Hence, the resulting diameters of the spherical particles were d_{XCB}=150 µm, 311 µm and 447 µm, respectively and were compared to a 100µm in diameter cylinder (see Table 37). Three main points regarding the obtained OUR are up for discussion: the lag phase, the acceleration step and the decrease phase.

From Figure 39a, it can be observed that the shape of the particulate substrate itself does not affect significantly the obtained trend when comparing a cylinder substrate with a spherical one developing the same total surface of contact. However, the size of the particles may significantly affect both OUR and the characteristic time of biodegradation. Indeed, for diameters from 150 µm to 447 µm, the OURmax decreases from 45 down to 22 $mgO_2/l/h$. The corresponding time necessary to degrade 90% of XC_B concomitantly increases from 8.5 to 20.6 days.

The size of particles has an effect on both the adsorption and growth phenomena (cf. Figure 39 b and d) which are of interest to investigate the lag phase as well as the acceleration step. Cell adsorption rate and cell quantity is reduced when the specific surface area decrease (larger particles). Consequently, the growth rate becomes predominant after 1.5 days for the small particles, while adsorption is still the main mechanism for covering the surface up to 2.2 days in the case of 447 µm particles, as illustrated by the ratio between the rates of those two mechanisms (cf. Figure 39c). This has direct consequences on hydrolysis potential due to higher active biomass. This is emphasized, when the entire substrate surface is covered, when looking at the hydrolysis rate which becomes first-order with respect to the available surface area of substrate leading to a maximum OUR almost three times higher for 150 µm compared to 447 µm in diameter for the same initial quantity of substrate. Concerning the decreasing phase, its shape directly results from the previous information: when the majority of substrate is consumed, decay mechanism becomes preponderant on OUR profile. Its rate is higher in the case of initial small particles as it is a kinetic with a first order with respect to the active biomass. Thus, high substrate particle diameter cause the OUR drag on longer.

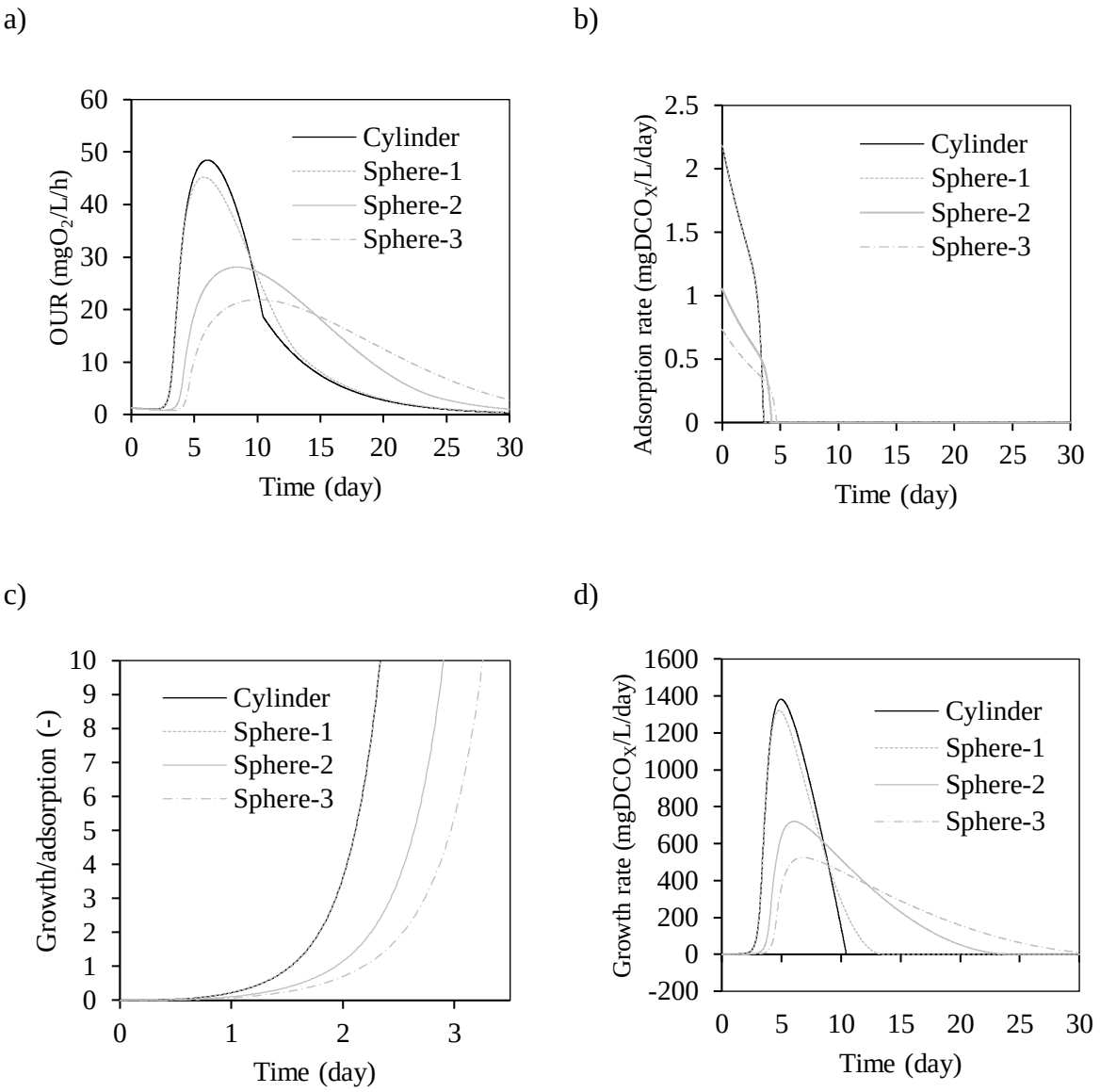

Figure 39: Comparison for different geometry of particles of a) the oxygen uptake rate b) adsorption rate c) ratio growth rate to adsorption rate d) growth rate. Cylinder diameter = 100 µm. Sphere-1 has the same total surface of particle (d_{XCB}=150 µm), Sphere-2 has the same number of particles (d_{XCB}=311 µm), Sphere-3 has the same surface for one particle (d_{XCB}=447 µm). $XC_{B,0}$=10 000 gCOD/m^3; $X_{OHO,\,bulk,0}$=200 gCOD/m^3 (all the other parameters are identical).

In order to represent the case of complex substrates like PSS that contain various substrates of various shapes, the M_SBK model was used considering mixtures of cylindrical substrates of different sizes.

Figure 40 presents the evolution of OUR with time obtained for a mono-size substrate compared to multiple-size substrate. 3 classes of particles have been considered (from 100µm to ten times

higher or lower) and distributed arbitrarily as a third of the total substrate concentration (in g_{COD}/m^3). The kinetic and stoichiometric parameters were the same for all the substrates.

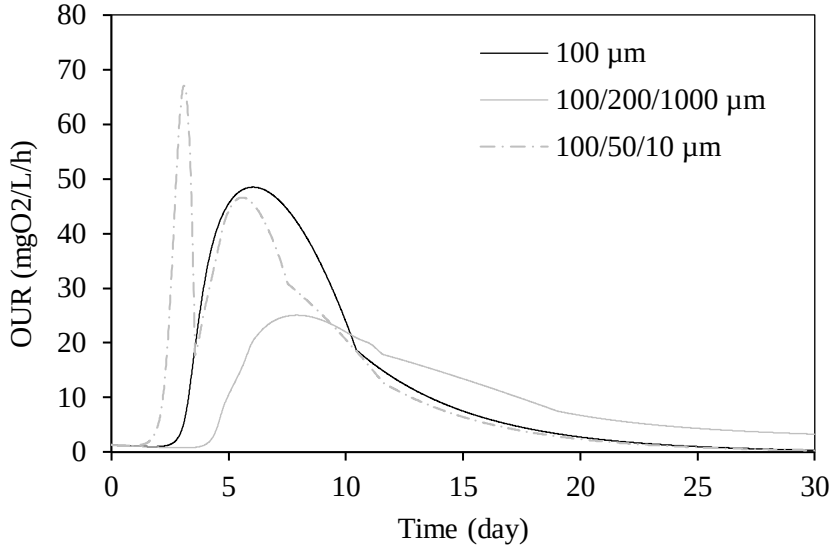

Figure 40 : Evolution of OUR for different particle size distribution. Cylinder L_{XCB}=2 000 µm; $XC_{B,0}$=10 000 gCOD/m^3; $X_{OHO,\ bulk,0}$=200 gCOD/m^3 (all the other parameters are identical).

For a same quantity (in gCOD) of substrate, considering a size distribution instead of a single size modifies both the shape and the typical values of the signal. More precisely the presence of small particles reveals two visible picks in the OUR signal, with a maximum OUR of 68 $mgO_2/L/h$ corresponding to the hydrolysis of the particles of 10µm in diameter and sub product consumption. Due to a longer colonization phase, associated to a reduced specific area, the degradation of particles of 50 and 100 µm is delayed. This phenomenon is emphasized when taking into account big particles (from 100 to 1000 µm in diameter): the maximum OUR is 25 $mgO_2/l/h$ and the time to degrade 90% of the substrate is significantly increased.

In the M_SBK model, size represents the distribution in terms of mass, which when considering a constant density of particulate substrate corresponds to a volume distribution. In contrary, in the work of Dimock and Morgenroth (2006) the data is a squared-weight length, i.e. a surface average value. Furthermore, the initial particle size distribution obtained by Dimock and Morgenroth (2006) on large proteins spread over a wide range from 1 to 1,000 µm. The resulting distribution in substrate specific surface area could explain why the OUR profile last more than with small egg white particles and also why the maximum OUR is higher than the one predicted by M_SBK model with an average size of 360 µm.

5.3. ROLE OF COLONIZATION BY MICROORGANISMS

Among the considered experiments, living the lag phase in one side, the two trends OUR profile, that shows an exponential increase of OUR after the effective contact between cells and particulate substrate, is mainly observed. That implies a progressive increase of the observed hydrolysis rate. When considering that the specific hydrolysis rate is constant, it meant an increase of concentration in active cells that can come from a progressive colonization of the interfacial area of the particle and/or from a breakup of particles into smaller ones. This last hypothesis results in a transitory increase of the surface of contact between cells and particulate substrate.

16.1.1.Are detached cells still able to perform hydrolysis?

Models of colonization may have different forms. Indeed, the growth of the cells does not give rise to daughter cells which are necessarily bound to the surface of the particulate substrate and the question of the fate of the daughter cells arises. To answer that question, various scenarios for daughter cell behaviours were simulated to evaluate their influence on hydrolysis kinetics. Once all the surface area of the particulate substrate is covered, daughter cells may be either active for both hydrolysis and growth on soluble substrate or active only for growth on soluble substrate or completely inactive. For the two last cases, the mechanism "detachment" (see Table 39) is activated. In the last case, produced cells only contribute to the OUR signal through the endogenous respiration only.

Figure 41 presents the evolution of OUR against time for those three hypothesis of daughter cell behaviours.

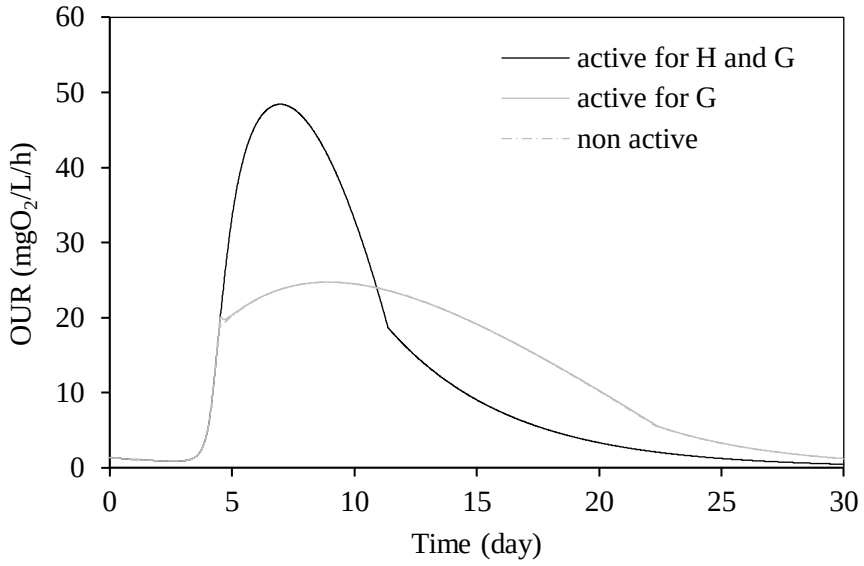

Figure 41 : Evolution of OUR for different activation hypothesis. Cylinder d_{XCB}=100 µm; L_{XCB}=2,000 µm. $XC_{B,0}$=10 000 gCOD/m^3; $X_{OHO,\ ads,0}$+$X_{OHO,\ bulk,0}$=200 gCOD/m^3

When daughter cells do not perform hydrolysis, similar OUR profiles are obtained whether they grow or not. Hydrolysis being the limiting process, the hydrolysis rate determines the available soluble substrate flux and hence the electron acceptor consumption rate. This result leads to compare only the cases when daughter cells are able to perform hydrolysis or not. For both these cases, similar OUR increase is observed at the beginning of degradation until 4.6 days. This can be easily understood because this period corresponds to the progressive coverage of the particulate substrate by daughter cells which, by definition, remain attached to the substrate. After 4.6 days, the OUR of the two hypothesis strongly differ. When daughter cells can perform hydrolysis though they are not in direct contact with the substrate surface, the OUR still increase. This increase lasts until XC_B becomes limiting. On contrary, when daughter cells which moves away from the particulate substrate cannot hydrolyze anymore, the OUR stabilizes very quickly. The maximum OUR is around 25 mgO_2/L/h and the time necessary to degrade 90% of the XC_B exceeds 24 days.

Considering that the cells cannot perform hydrolysis may represent either a case where diffusion limitation occur, preventing the produced enzyme from reaching the substrate to degrade, or a process in which hydrodynamic constraints lead to detachment.

16.1.2.Impact of the initial colonization by hydrolytic microorganisms

A contamination, and more precisely a distribution in the contamination level, may impact the experimental characterization of the degradation. This may appear for example when considering the residence time in the sewers.

A lag phase is often observed at the beginning of the degradation experiments. This may be attributed to the amount of cells able to perform the hydrolytic reaction (limitation due to contact with the substrate and to enzymatic induction)

Figure 42 presents the evolution of OUR with time obtained for an uncontaminated substrate compared to a substrate diversely colonized. 3 classes of particles have been considered depending on the quantity of hydrolytic biomass already attached to their surface (from 0 to 5% of active biomass attached) and distributed arbitrarily as a third of the total substrate concentration. The kinetic and stoichiometric parameters as well as their geometrical properties were the same for all the substrates.

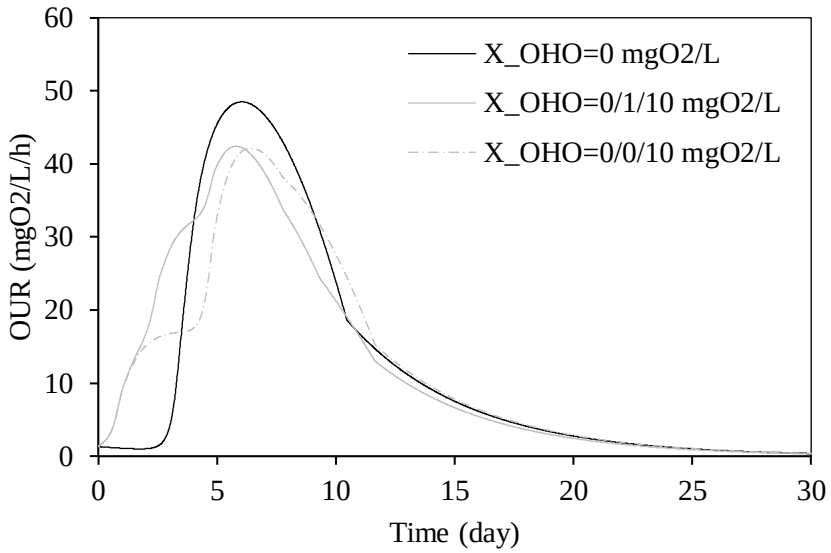

Figure 42 : Evolution of OUR for different contamination. Cylinder d_{XCB}=100 µm; L_{XCB}=2 000 µm. $XC_{B,0}$=10 000 gCOD/m^3; $X_{OHO,0}$+$X_{OHO,\,det,0}$=200 gCOD/m^3

The main consequence of a pre-colonization is to decrease the lag before the OUR increase. The adsorption of only 5% of the hydrolytic biomass (10 over 200 mgCOD/L) leads to an immediate increase of the OUR which then reach a maximum value of 42 mgO_2/l/h.

16.1.3.Effect of solid substrate to active heterotrophic bacteria ratio ($XC_B/X_{OHO,bulk}$)

The rate-limiting mechanism being the modified hydrolysis process including colonization, the shape of the OUR profile will be dictated by this mechanism which is itself dependent upon the ratio of solid substrate to hydrolytic cells.

Figure 43 represents model simulations for several solid substrates to active heterotrophic bacteria ratios. All of the simulations were performed for an initial concentration of XC_B of 10 gCOD/L.

a)

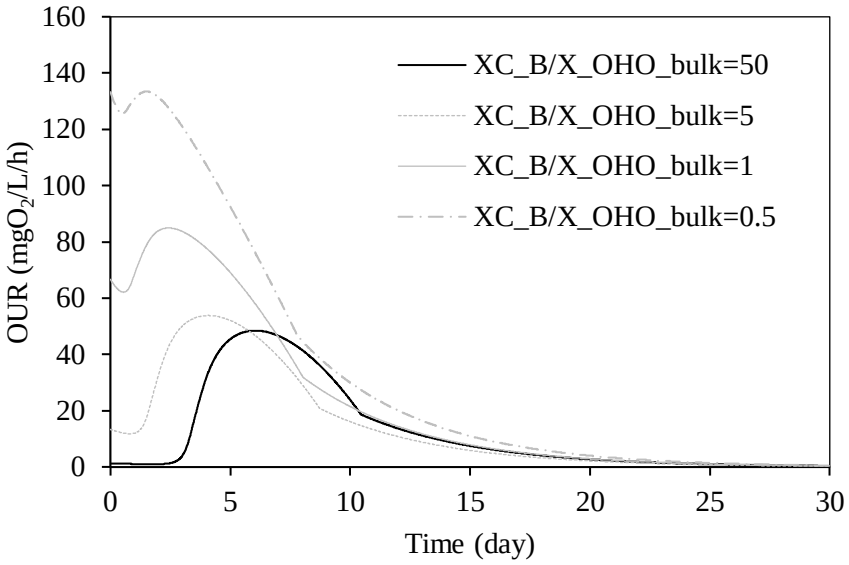

b)

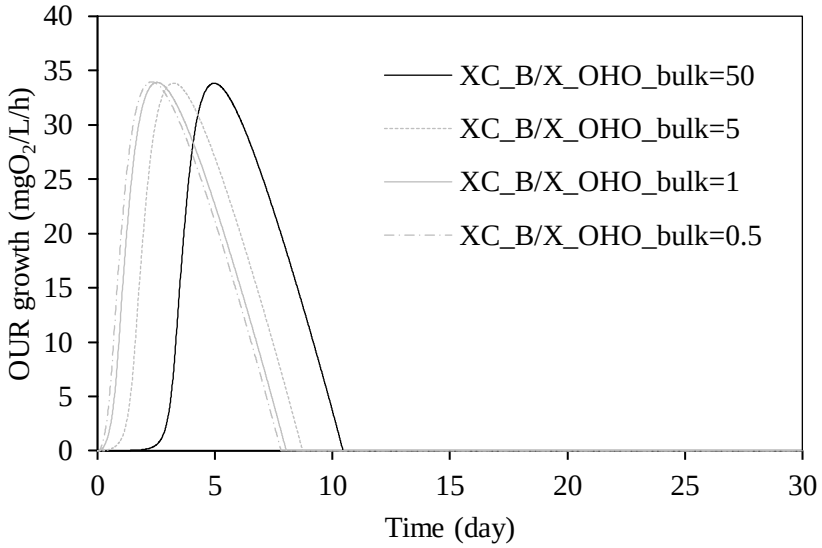

Figure 43 : Evolution of OUR for different initial $XC_B/X_{OHO,\ det}$ ratios. a) total OUR b) OUR of growth mechanism. Cylinder L_{XCB}=2 000 µm. $XC_{B,0}$=10 000 gCOD/m^3; $X_{OHO,\ bulk,0}$ from 200 gCOD/m^3 to 20 000 gCOD/m^3.

The COD associated to the cells concentration significantly affects the OUR, in particular through the decay mechanism. Indeed, the biological oxygen demand significantly increases

when $XC_B/X_{OHO,\ bulk}$ decreases for a same initial particulate substrate concentration (cf. Figure 43a).

Consequently, when considering only the OUR due to the growth – and thus to the hydrolysis-mechanism, as in Figure 43b, the OUR curve is logically the same, except for the lag length prior to the OUR increase. This lag phase is related to the adsorption mechanisms that is slower for high $XC_B/X_{OHO,\ bulk}$.

6. CONCLUSIONS

The aim of this chapter was to develop and to assess a conceptual model which is able to describe realistically and with more precision the fate and degradation of slowly biodegradable COD. The model was designed in order to integrate the substrate colonization by microbial communities. In addition, geometrical and physical properties of both the large particles and the bacteria were also included in the developed model to take into account the dynamic evolution of substrate particle size.

A literature review about the colonization phase was performed from where the main hypotheses of the model were defined: (i) particle shape (bacteria were supposed spherical and solid substrate cylindrical); (ii) the relation between particle size and substrate concentration and (iii) the introduction of a maximum colonizable fraction (f_{ma}).

This model was confronted to experimental data that were collected from our laboratory and from literature and compared to two existing models used to represent hydrolysis prior to substrate consumption by microorganisms.

The choice of particulate substrates used in this study was based on their difference in shape (TP against EP), on size (EP with large and small particles), in biochemistry (TP against EP), in diversity of biochemical and physical characteristics (PSS) and on the degree in initial colonization (very light initial colonization for model substrates, different degree for PSS depending on their origin in the sewer).

The following main conclusions could be drawn:

- As underlined by a theoretical evaluation of the model, considering a size distribution of the particulate substrate may allow to improve experimental fitting;
- The description of contrasted kinetics was not significantly improved using our developed model compared to the use of the existing models. However, our model allowed to qualitatively describe the trends of a modification of initial size of the substrate. This underlines that taking into account the real surface of the particulate substrate is useful for a true representation of the degradation kinetic.
- Finally, the contamination level, linked to the active biomass concentration, was also shown to be a crucial parameter.

As expected, a model taking into account the shape and size of particles requires that the fractionation of the particles in terms of shape and size would be given. Whether it is realistic or not should be assessed for each case.

The use of the model to simulate different cases of hydrolysis depending on the size and shape of particles allowed to underline some global features:

- Influence of size: the size of particles has an effect on both the adsorption and growth phenomena. The larger the size is, the lower the OURmax and the longer the duration of biodegradation. The adsorption rate is significantly enhanced in case of small particles compared to large particles. This is in favour of grinding the pretreatment of substrates to increase kinetic rate of biodegradation.
- The shape itself does not affect significantly the obtained trend and characteristic times of biodegradation when comparing a cylinder substrate with a spherical one developing the same total surface of contact.
- For a same quantity (in gCOD) of substrate, considering a size distribution instead of a single size modifies both the shape and the typical values of the OUR profile and thus of the activity along time.
- The presence or absence of detachment of daughter cells is also a crucial hypothesis for the capacity of a model to correctly represent the colonization and biodegradation steps of a large particle. Moreover, the initial degree of colonization of the particles determines the initial rate of biodegradation and the colonization rate.

From these conclusions, the initial biomass contamination of the substrate seems to greatly influence the degradation kinetics. Hence, the purpose of the next and last chapter is to study and assess the specific role of bacterial populations involved in the biodegradation of slowly biodegradable substrates. These bacteria may come from an inoculum or may be already present adsorbed on the large particles prior to the degradation experiment. There may be a difference in the hydrolytic capacity and activity of these cells depending on their origins.

CHAPTER IV

"Biodegradation of wastewater particulate settleable solids (PSS): distinguishing a specific hydrolytic microbial population in the total cellular biomass"

1. INTRODUCTION

A significant part of the organic matter entering wastewater treatment plants (WWTPs) is in a particulate form (Roeleveld and van Loosdrecht, 2002). Measurements of the size distribution of the organic matter for various wastewaters showed a content of particulate settleable solids (PSS) from 15 till 49% of the total organic content of the urban wastewater (WW) (Sophonsiri and Morgenroth, 2004). In the WW treatment line, PSS can be degraded by bacteria under aerobic, anoxic and anaerobic conditions but can also be enmeshed in the activated sludge or removed in the primary sedimentation step and transferred into the sludge treatment line for further anaerobic digestion. The fraction degraded in the WW treatment line or removed by primary or secondary sedimentation depends on treatment plant design and operation and on characteristics of the wastewater (Morgenroth et al., 2002; Orhon et al., 1997). Depending on their extent and rate of biodegradation PSS should be preferentially used as a carbon source for biological nutrient removal or should be removed by primary settling in order to decrease the sludge production and increase the net energy recovery when degraded in anaerobic digester (Morgenroth et al., 2002). For both engineering and environmental points of view it is therefore important to characterize the kinetic of PSS degradation. In a more general framework, and particularly in the field of waste treatment and valorisation, the mechanism of biodegradation of particulate matter should be also better understood (Vavilin et al., 2008).

The PSS fraction is mostly composed by grease, proteins, cellulose and lignin (Heukelekian, 1959; Huang et al., 2010) with minimum size, fixed by the settling conditions, commonly considered up to 50 µm (Levine et al., 1985; Munch et al., 1980). Chemical composition and size distribution of PSS however can greatly vary in time and depending on the origin of the wastewater (Balmat, 1957; Heukelekian, 1959; Levine et al., 1985; Sophonsiri and Morgenroth, 2004). PSS also contents a great amount of adsorbed microorganisms but the contamination degree is not documented in the literature. Before being metabolized by microorganisms, PSS must be first broken down into monomers. This transformation is mainly ensured in biological treatment by enzymatic extracellular hydrolysis processes (Dold et al., 1991; Mino et al., 1995; Morgenroth et al., 2002; Wood et al., 2012). As the process of PSS degradation is composed of a sequence of reactions, according to Hill et *al.* (1977), the overall rate is determined by the slowest reaction, namely the rate-limiting step. Because degradation of the produced soluble substrate is by nature a very rapid process (soluble COD does not accumulate in the supernatant), the degradation of PSS is considered as controlled by the hydrolysis process.

Mechanisms of hydrolysis and associated models have been described in details in (Morgenroth et al., 2002). Hydrolysis can be generally considered as a first order reaction, limited by the concentration of solid substrate (Eastman and Ferguson, 1981; Eliosov and Argaman, 1995; Gujer, 1980; Henze and Mladenovski, 1991) or as a surface-limited process as it has been chosen in the ASM models (Gujer et al., 1995, 1999; Henze et al., 1987). In order to reduce complexity, a unique hydrolysable fraction (noted XC_B) has been considered in these models, and the degradation of more slowly biodegradable substances (typically the large particles) was not included. Consequently, the corresponding COD fraction of these substances is partially included into the heterotrophic biomass of sewage or the inert particulate matter. This assumption can be supported by the fact that the rate of hydrolysis of very slowly biodegradable substances (first order hydrolysis constant typically ranging from 0.05 to 0.2 d^{-1}) is of the same range than the decay rate (b_{OHO}) of the heterotrophic biomass. However, this simplification leads to kinetic parameters for heterotrophic growth and COD conversion which are hybrid values. Then, the same set of model parameters is valid only for a small range of SRT, or a defined oxic reactor fraction. This could become a problem for predicting the excess sludge production and leads to the underestimation of the denitrification potential of activated sludge plant with no primary settling (Nowak et al., 1998).

In the wastewater treatment field, the term hydrolysis may recover various complex mechanisms and not only the enzymatic reaction. Takahashi et *al.* (1969) showed, for example, that the rate of hydrolysis of PSS depends on the particle size, the type of pollutant and the extra-cellular enzyme activities. Consequently, more complex models were therefore proposed in order to better fit the experimental data. Introduction of hydrolysis-associated processes such as adsorption of particulate substrate to biomass prior hydrolysis (Dold et al., 1980; Spérandio and Paul, 2000), or considering more than one fraction of particulate matter (Lagarde et al., 2005; Orhon et al., 1998; Sollfrank and Gujer, 1991; Tas et al., 2009; Vollertsen and Hvitved-Jacobsen, 1999) have sometimes helped to better represent experimental responses. The specific case of large particles degradation was considered by (Dimock and Morgenroth, 2006) who performed experiments on boiled-eggs whites cut in particles of different sizes. Hydrolysis could thus be described as the breakup of large particles, resulting in both an increase of the specific surface area and the production of soluble substrate allowing for increasing hydrolysis rates over the first period of degradation.

Considering the reaction rate expressions proposed in the literature (see review of Morgenroth et al., 2002), except the simplest kinetics of first-order reaction with respect to the substrate,

the rate of hydrolysis has been written as a function of the biomass concentration. However, in general, only one biomass has been considered for the consumption of both the slowly and readily biodegradable organic substrates. This has led to consider that all the active biomass participates in the hydrolysis of the whole particulate substrates. Moreover, this biomass would be immediately active in the entire particle surface. This is certainly a strong simplification of reality. Vavilin et al., (2008) have suggested to take into account side-processes in addition to hydrolysis by enzymatic actions: bacterial colonization of the particulate substrate and growth of daughter cells that can remain attached to the particles or fall into the liquid. Hence, the introduction of some degree of dependence of hydrolysis to the real hydrolytic biomass concentration or even to the real hydrolytic activity seems necessary (Eliosov and Argaman, 1995).

The term biomass must be carefully and clearly defined because its meaning and thus the corresponding concentration and activity may greatly vary depending on the method which is used for its determination (Vollertsen et al., 2001). In the framework of the hydrolytic biomass characterisation, this is not an easy task. A direct quantification of the enzyme activities or the hydrolytic products could allow studying the specific mechanisms involved in hydrolysis but unfortunately has limited applicability in the case of the complex matrix of PSS enmeshed into activated sludge. Measurement of bulk parameters and/or of microbial population respiration rate allowing quantifying the overall processes seems more realistic (Insel et al., 2003). However, very few experimental studies have been performed on the degradation of slowly biodegradable matter (Ginestet et al., 2002; Okutman et al., 2001; Orhon et al., 2002; Tas et al., 2009) and even less on degradation of large particles (Dimock and Morgenroth, 2006) such as those present in PSS.

The objective of the present work was to bring more insight on the role of biomasses on the degradation rate of large particles such as those contained in PSS or in model substrates (Toilet paper (TP) and pure cellulose), and *in fine* to bring a contribution in the better understanding of the hydrolysis of particulate settleable solids (PSS) under aerobic condition. Addition to the selected substrates of external biomass more or less acclimated and at different concentrations was performed. Distinction was thus made between the degradation activity of endogenous biomass already present with the substrate and of the added biomass. Degradation dynamics were followed by respirometry as well as COD measurements in the bulk-liquid phase allowing to characterize growth/colonisation and hydrolysis kinetic parameters. Modelling of the degradation kinetics was performed using the "surface-based" kinetic model as presented in the

ASM1 model (Henze et al., 1987). The model was used to estimate the active biomass for hydrolysis distinguished from the biomass performing only endogenous respiration.

2. MATERIALS AND METHODS

2.1. INOCULA CONDITIONING

All the experiments were inoculated with activated sludge (AS) collected from the aerated tank of the 1 million population equivalent WWTP of Ginestous, which is located in the area of Toulouse (France). The estimated SRT being low (lower than 5 days), AS was kept under aeration in batch-respirometers during few days till it reached endogenous respiration in order to discharge the sludge from the accumulated slowly biodegradable organic matter. The volatile fraction of the resulting inoculum was around 0.82±0.01 gVSS/L. For each experiment that were performed in this study, the AS samples were collected the same day than the raw wastewater from which PSS were recovered.

2.2. SUBSTRATES PREPARATION

2.2.1.Particulate settleable solids (PSS)

Wastewater was collected either just before the primary settling unit of the WWTP of Toulouse-Ginestous (PSS1-a to PSS1-c) and in the upstream part of the sewage network (PSS2-a to PSS2-d). In the first case, PSS were qualified as "aged" PSS because of their long residence time in the sewage network. On contrary, PSS2s were considered as "young" PSS. The PSS was settled during 1 hour in a 40-L lab-scale settling device of acrylic glass material. The resulting settled fraction was once more settled in Imhoff cones during 2 hours (Standard Methods, 1989). Three successive washing cycles have been performed in order to reduce soluble COD in the final sample of PSS.

2.2.2.Toilet paper

Commercial white toilet paper (*TP*) was cut into 1 cm^2 pieces to favour homogenization and biomass-TP contact. The experimental chemical oxygen demand of this TP was of 1.27 gCOD/g.

2.2.3.Pure cellulose

Commercial pure cellulose was used in this thesis in the form of powders. This reagent was chosen as it represents the main biodegradable part of toilet paper.

2.3. CULTURE MEDIUM

See the experimental and modeling material and methods chapter, §3.3.

2.4. THE RESPIROMETER

All the experiments were achieved with the means of open respirometry in order to avoid substrate structure deconstruction which could occur during liquid phase transfer between the reactor and the OUR measurement cell in closed respirometry.

2.4.1.Experimental design

A detailed diagram of the respirometer is illustrated by Figure 7 (see the experimental material and methods chapter, §2.1.1).

2.4.2.Calculations for open respirometry

See the experimental material and methods chapter, §2.1.1.

2.5. EXPERIMENTS

Batch experiments were performed under various initial conditions that are summarized in Table 43. The experiments on PSS were performed to evaluate the substrate biodegradation when an activated sludge inoculum was added. In the experiments TP2, following a first batch inoculated with activated sludge, two successive batches were further performed using the TP-previously acclimated cells as inoculum. Neither glycogen nor PHA accumulation was observed during these experiments.

Table 43: Overview of the experiments performed to assess the degradation capacity of indigenous biomass present enmeshed with the settled particulate matter and of an external biomass sampled from an activated sludge and added as inoculum.

Experiment	Reactor name	Substrate		Inoculum	
		Type	Initial conc. (mgCOD/L)	Type	Initial conc. (mgCOD/L)
PSS from **downstream** part of sewer	PSS1-a	PSS	9 230	No inoculum	0
	PSS1-b	PSS	9 641	AS	550
	PSS1-c	PSS	9 420	AS	2 750
PSS from **upstream** part of sewer	PSS2-a	PSS	875	AS	477
	PSS2-b	PSS	417	AS	2 826
	PSS2-c	PSS	553	AS	426
	PSS2-d	PSS	833	AS	1 775
Toilet paper (TP)	TP1-a	TP	8 890	AS	710
	TP2-a	TP	15 220	No inoculum	0
	TP2-b	TP	11 300	AS	384
	TP2-c	TP	10 001	AS	1 920
	TP2-d	TP	8 850	End of TP2-b	1 320
	TP2-e	TP	9 010	End of TP2-d	1 333
Cellulose	Cellulose	Cellulose	8 000	AS	970

2.6. ANALYTICAL METHODS

See the experimental and modeling material and methods chapter, §4.2.

2.7. MODELING

2.7.1.Model description

A modified version of the *IAWQ* model n°1 (Henze et al., 1987) was utilized in this study: the death-regeneration model was replaced by endogenous respiration. This model also differentiates between hydrolytic (active) bacteria (X_{OHO_hyd}) and passive ones (X_{OHO_ER}), which undergo endogenous respiration only. Slowly biodegradable COD (XC_B) was considered coming both from PSSs (XC_{B_PSS}) and inoculum (XC_{B_inoc}). Only aerobic processes were considered in this model as no oxygen limitation was observed in our experiments. The structure of the model adopted in this study is presented in Table 44.

2.7.2.Parameter estimation

See the experimental and modeling material and methods chapter, §6.3.2.

Table 44: Matrix representing adopted model structure including two biomass fractions

Process	*Soluble species*			*Particulate species*				Process rate
	$S_{B,\,HYD}$	S_{O2}	S_{NH4}	XC_B	X_{OHO_hyd}	X_{OHO_ER}	$X_{U\_Bio,\,lys}$	
Hydrolysis of XC_B	*1*			*-1*				$q_{XCBS_{SB},hyd}\frac{\frac{XC_B}{X_{OHO_{hyd}}}}{K_{XCB,hyd}+\frac{XC_B}{X_{OHO_{hyd}}}}X_{OHO_{hyd}}$
Aerobic growth of X_{OHO_hyd}	$-1/Y_{OHO}$	$-(1-Y_{OHO})/Y_{OHO}$	$-i_{N\_XBio}$		*1*			$\mu_{OHO,max}\frac{S_{B,hyd}}{K_{SB,hyd}+S_{B,hyd}}X_{OHO_{hyd}}$
Aerobic endogenous respiration of X_{OHO_hyd}		$-(1-f_{XU\_Bio,\,lys})$	$f_{XU\_Bio,\,lys}*i_{N,\,XU}+i_{N\_XBio}$		*-1*		$f_{XU\_Bio,\,lys}$	$b_{OHO}X_{OHO_{hyd}}$
Aerobic endogenous respiration of X_{OHO_ER}		$-(1-f_{XU\_Bio,\,lys})$	$f_{XU\_Bio,\,lys}*i_{N,\,XU}+i_{N\_XBio}$			*-1*	$f_{XU\_Bio,\,lys}$	$b_{OHO}X_{OHO_{ER}}$

3. RESULTS

3.1. EXPERIMENTAL DESIGN

Experiments in aerobic batch reactors were performed to study the degradation of large particles by heterotrophic bacteria and more specifically the role of different active biomass fractions on hydrolysis. Hence, addition of different concentrations of inoculum from activated sludge samples collected at a full-scale plant, to the particulate substrates was carried out. The idea was to evaluate the efficiency of this added biomass in terms of hydrolysis kinetic in comparison with indigenous biomass which would have already colonized the substrate. Therefore, a distinction was made between, in one hand, the indigenous biomass present in the wastewater and recovered with the particulate matter after settling (or indigenous biomass present on the toilet paper) and, in the other hand, an external biomass brought by addition of a given amount of activated sludge and added as a potential inoculum.

OUR was continuously recorded and various parameters in the bulk liquid such as the particulate COD (COD_P) and the soluble COD (COD_S), were sequentially measured in order to determine kinetic parameters and the COD fractionation. Various particulate matters, i.e. various PSS (real substrate) but also toilet paper (model substrate), were considered in order to evaluate the influence of the origin and nature of the particulate substrate on the role of the biomasses.

3.2. EFFECT OF ACTIVATED SLUDGE ADDITION ON PSS DEGRADATION

3.2.1. PSS sampled at the downstream part of the sewage network

The degradation of aged-PSS obtained from raw wastewater sampled at the entrance of the WWTP of Toulouse was studied for three concentrations of activated sludge inoculum (Table 44). Three batches, PSS1-a, PSS1-b and PSS1-c, run in parallel, were fed with a similar initial concentration of PSS (on a COD basis) but with different amounts of inoculum (Table 43). The percentages of the total COD coming from the AS inoculum were hence 0, 5.6% and 23% for PSS1-a, PSS1-b and PSS1-c, respectively. Figure 44 represents the evolution of both experimental and simulated values of the OUR and of the remaining COD_P concentration in the supernatant, for PSS1-a (Figure 44a), PSS1-b (Figure 44b) and PSS1-c (Figure 44c) (note that OUR of PSS1-c was not recorded due to a technical problem).

a)

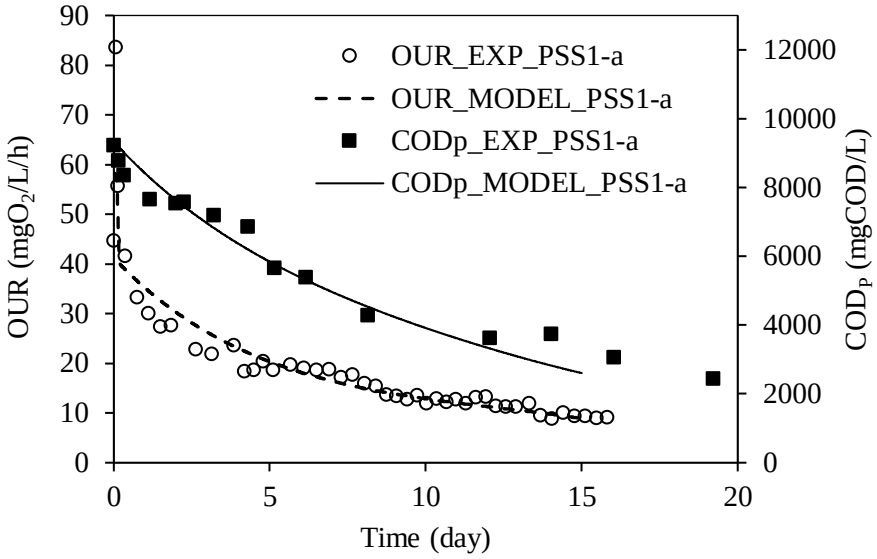
OUR_EXP_PSS1-a
OUR_MODEL_PSS1-a
CODp_EXP_PSS1-a
CODp_MODEL_PSS1-a
OUR (mgO2/L/h)
CODP (mgCOD/L)
Time (day)

b)

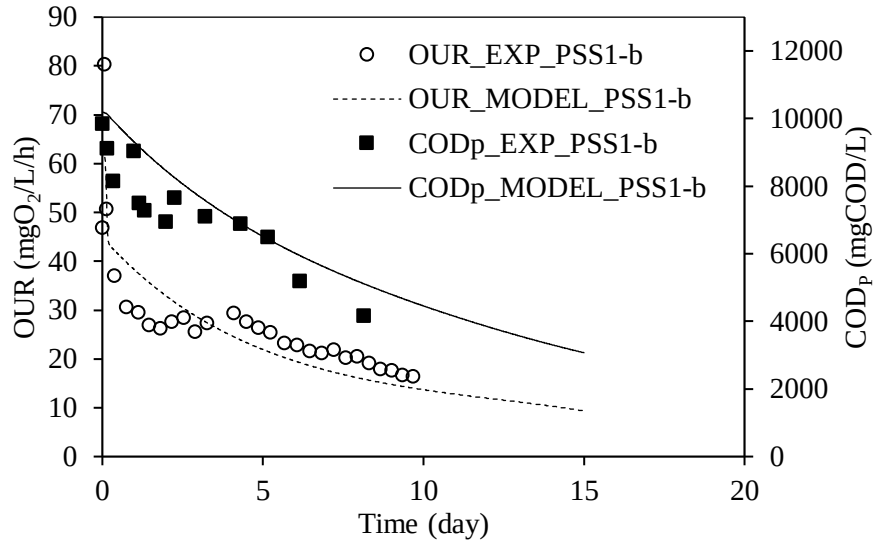
OUR_EXP_PSS1-b
OUR_MODEL_PSS1-b
CODp_EXP_PSS1-b
CODp_MODEL_PSS1-b
OUR (mgO2/L/h)
CODP (mgCOD/L)
Time (day)

c)

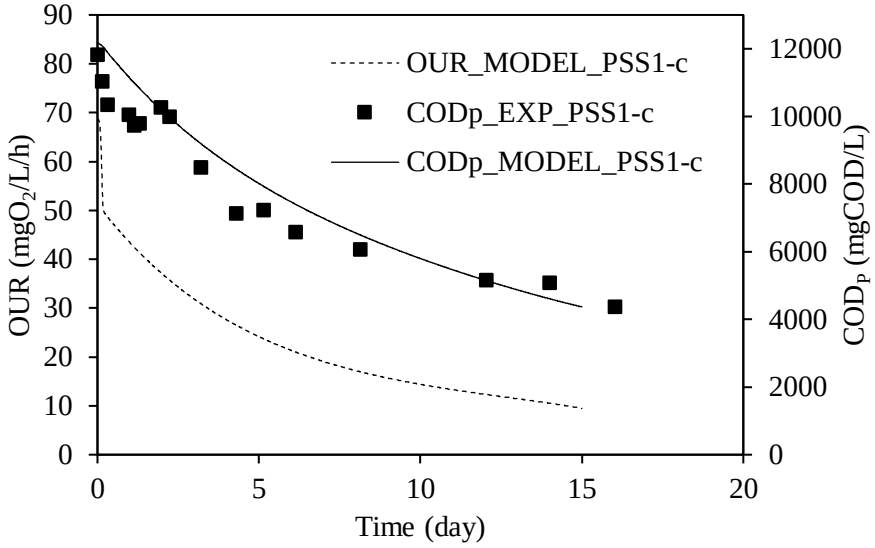

Figure 44: Time evolution of the OUR and CODp during the degradation of the PSS1 inoculated with different concentrations of AS. The inoculum COD added were 0, 550 and 2750 mgCOD/L for a) PSS1-a , b) PSS1-b and c) PSS1-c, respectively. The PSS were sampled at the downstream of the sewer network.

Table 45: Parameters estimated for OUR calibration (PSS1 experiments)

Parameter	Unit	Fractions	Experiment		
			PSS1-a	PSS1-b	PSS1-c
$K_{XCB,\ hyd}$	$mgCOD.mgCOD^{-1}$		0.21	0.21	0.21
$q_{XCB\_SB,\ HYD}$	d^{-1}		0.37	0.37	0.37
PSS_COD	$mgCOD.L^{-1}$		9230	9641	9420
$XC_{B\_PSS,\ ini}$	$mgCOD.L^{-1}$	0.39	3607	3767	3681
$X_{OHO\_hyd\_PSS,\ ini}$	$mgCOD.L^{-1}$	0.05	474	495	484
$X_{OHO\_ER\_PSS,\ ini}$	$mgCOD.L^{-1}$	0.56	5149	5378	5255
Inoc_COD	$mgCOD.L^{-1}$		0	550	2750
$XC_{B\_inoc,\ ini}$	$mgCOD.L^{-1}$	0	0	0	0
$X_{U\_inoc,\ ini}$	$mgCOD.L^{-1}$	0.5	0	275	1375
$X_{OHO\_ER\_inoc,\ ini}$	$mgCOD.L^{-1}$	0.5	0	275	1375
$X_{OHO\_hyd\_inoc,\ ini}$	$mgCOD.L^{-1}$	0	0	0	0
E^2	$(mgO_2/l/h)^2$		1055	3655	N.D.

The profile of the OUR showed a maximum almost immediately after mixing the PSS with the activated sludge. Then, it decreased over time, relatively sharply during the first days of

degradation and more and more slowly afterwards. The evolution of the COD_P against time in Figure 44b showed a coherent feature with the OUR profile, i.e. a rapid degradation at the beginning that slowed down progressively. The amounts of degraded COD_P in the three batches were found between 63 and 73% after 17 days (Figure 44). These slight differences could be attributed to the initial heterogeneity of the PSS. Moreover, these percentages included the biodegradation of the COD from the added inocula (present only in PSS1-b and PSS1-c). Calibration of the model performed on the three batches together led to the conclusion that the biomass active for hydrolysis of these PSS1s might be exclusively brought by the PSS themselves or at least that the fraction brought by the AS inoculum was very low (Table 45). Indeed, comparing the various profiles obtained in the three batch experiments, it is obvious that the evolution of the measured and simulated parameters was quite similar whatever the concentration of inoculum added, though this later varied to a very large extent (from 0 to 2750 mgCOD/L for an initial concentration of PSS1 of around 9600 mgCOD/L).

3.2.2.PSS sampled in the upstream part of the sewage network

Experiments of spiking increasing concentrations of activated sludge to PSS in order to assess the capacity of this inoculum to increase the degradation rate of the PSS were repeated two other times. In that case, the PSS were sampled in the upstream part of the sewage network of Toulouse (France) at the outlet of residential buildings. Two sets of experiments were performed at different times of the year, winter and spring. Each of the two batches run in each set of experiments, PSS2-a and PSS2-b and then PSS2-c and PSS2-d could not be run in parallel but samples of both PSS and AS came from the same collection sites and were collected at the same period of the year. For each set of experiments, the initial concentration of PSS was similar while different initial inoculum concentrations of AS were added (see Table 43, PSS2s). The percentages of the total COD coming from the AS inoculum on the total initial COD were 35% and 80% for PSS2-a and PSS2-b and 40% for PSS2-c, and 70% PSS2-d, respectively. Figure 45 represents the evolution of both experimental and simulated values of the OUR and of the remaining CODp concentration in the supernatant, for PSS2-a and PSS2-b (Figure 45a) and for PSS2-c and PSS2-d (Figure 45b). COD mass balances were also performed between the beginning and the end of the experiments to check the reliability of the data.

a)

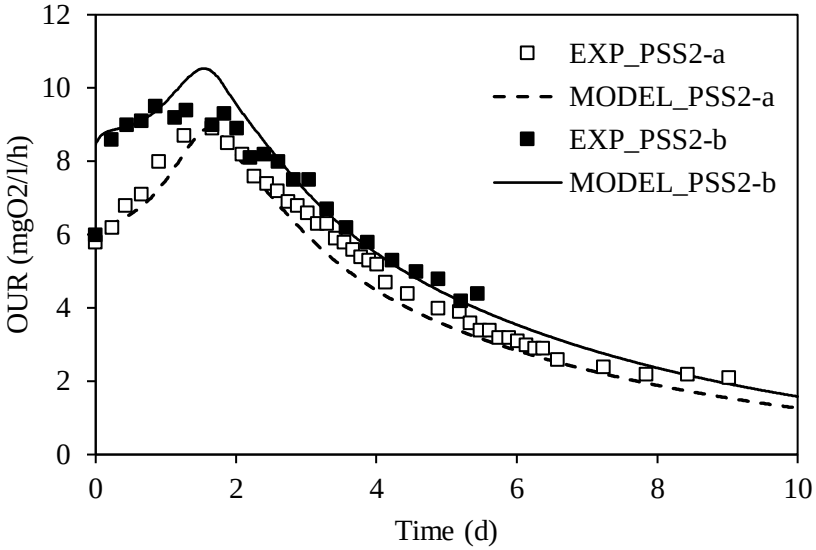

b)

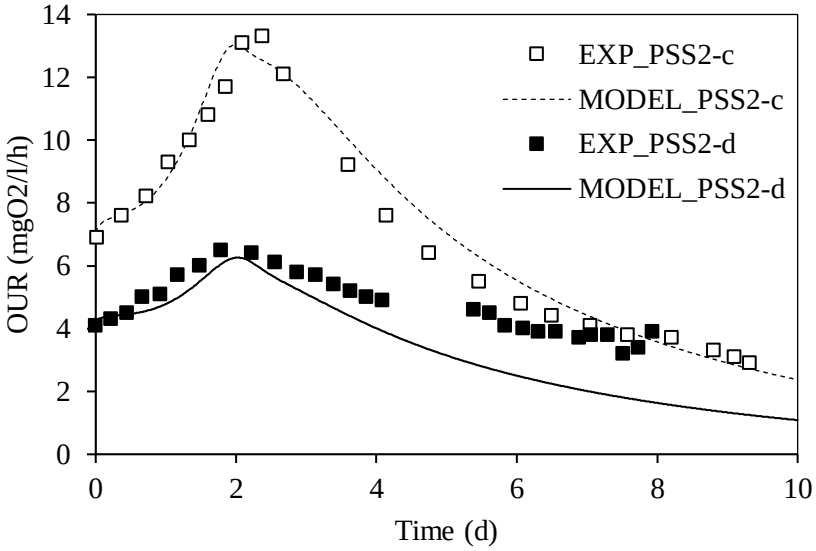

Figure 45: Time evolution of the OUR during the degradation of the PSS2 inoculated by different concentrations of AS: in a) the inoculum COD concentration added were 477 and 2826 mgCOD/L for PSS2-a and PSS2-b respectively. b), the inoculum COD added were 426 and 1775 mgCOD/L for PSS2-c and PSS2-d respectively. The PSS were sampled at the upstream of the sewer network.

In these experiments, the OUR firstly increased steadily for around 3 days after the addition of the PSS and subsequently decreased over approximately 4 to 6 days. This feature was strongly

different than the one observed in the previous experiments on PSS1s (Figure 44) which originated from raw wastewater sampled at the entrance of the WWTP, i.e. at the downstream part of the sewage network. Some processes involved in the degradation should be therefore different. Moreover, for each of the two set of experiments, the proportion of AS inoculum COD added was high. This addition did not change the degradation duration. Hence, addition of AS did not accelerate PSS2 degradation and a first phase where the OUR first increase before decreasing was observed.

Table 46: Parameters estimated for OUR calibration (PSS2 experiments) – underlined parameters were fixed.

Parameter	Unit	Experiments					
		Fraction	PSS2-a	PSS2-b	Fraction	PSS2-c	PSS2-d
$K_{XCB,\ hyd}$	$mgCOD.mgCOD^{-1}$		2.4	2.4		3.76	3.76
$q_{XCB\_SB,\ HYD}$	d^{-1}		3.2	3.2		3.3	3.3
PSS_COD	$mgCOD.L^{-1}$		875	417		553	833
$XC_{B\_PSS,\ ini}$	$mgCOD.L^{-1}$	0.55/0.72	478	299	0.52/0.62	285	513
$X_{OHO\_hyd\_PSS,\ ini}$	$mgCOD.L^{-1}$	0.034	30	14	0.034	19	28
$X_{OHO\_ER\_PSS,\ ini}$	$mgCOD.L^{-1}$	0.42/0.25	368	104	0.45/0.35	249	292
INOC_COD	$mgCOD.L^{-1}$		477	2828		426	1775
$XC_{B\_inoc,\ ini}$	$mgCOD.L^{-1}$	0.057	27	161	0.39	165	689
$X_{U\_inoc,\ ini}$	$mgCOD.L^{-1}$	0.17/0.59	79	1658	0.01/0.26	4	462
$X_{OHO\_ER\_inoc,\ ini}$	$mgCOD.L^{-1}$	0.77/0.35	367	990	0.60/0.35	256	621
$X_{OHO\_hyd\_inoc,\ ini}$	$mgCOD.L^{-1}$	0.0067	3.2	19	0.0017	0.7	3
E^2	$(mgO_2/l/h)^2$		151	183		92	432
			334			524	

The experiments performed on PSSs suggested that an addition of external cell biomass from AS did not significantly change the rate of degradation of the CODp coming from the PSSs. Moreover, the OUR profiles that are linked to the substrate degradation rate showed two very different trends depending on the collection location of PSSs along the sewage network.

3.3. EFFECT OF ACTIVATED SLUDGE ADDITION ON TP DEGRADATION

As PSS is a complex substrate whose biodegradation properties can vary depending on the sampling time and location and in order to study more in details the effect of added bacteria on the degradation kinetic of a particulate substrate, cellulosic materials were chosen as model substrates. Experiences on toilet paper (TP2-a, TP1-a, TP2-b, TP2-c) but also on pure cellulose were performed. The percentages of the total COD coming from the AS inoculum were 0, 3.2%, 4.5% and 16% of the total COD_P for TP2-a, TP1-a, TP2-b and TP2-c, respectively. Figure 46 represents the evolution of the OUR (except for TP2-a) and the COD_P during aerobic digestion of TPs in the case of the addition of different amounts of AS (inoculum). A similar initial concentration of COD from TP was added for all the experiments (Table 43).

Contrarily to what was observed for PSS, the increase of OUR started with apparently a delay estimated of around 3 to 4 days whatever the amount of AS added (this will be discussed later). Then, the OUR showed a similar trend than that observed for PSS2s sampled in the upstream part of the sewage network. It first increased steadily for around 4 days after the lag phase and subsequently decreased over approximately 6 to 8 days. However, due to the high amount of the TP substrate, the increase in OUR was much stronger than in the case of PSS2s. The maximum values of OUR were reached after 8 days whatever the amount of AS added. At day 13, a short peak of OUR was observed for TP2-b but not for the other two experiments. The COD concentration at first remained constant then decreased slowly but then more and more rapidly until 8 days. At the end of the experiments, more than 90% of the total COD was degraded in the case of toilet paper but only 45% (around 5000 mgCOD/L) was degraded at day 9. The model was calibrated simultaneously on the OUR and CODp data of the four TPs (Table 47). Comparison between results of simulations and experimental data will be done in the discussion section.

One additional experiment was performed with pure cellulose as substrate (Figure 47) with an initial concentration of AS of 972 mgCOD/L that is rather high. A similar profile of OUR and of CODp concentration than those obtained for toilet paper was observed though some waves on the profile could be identified. A lag phase was first observed where the initial OUR was

imposed in majority by endogenous respiration. This lag phase was followed by an increase of OUR until day 6 and then by a decrease of OUR up to reach an endogenous respiration level. The complete degradation time of the cellulose including the time to return to the endogenous respiration is around 10 days.

a)

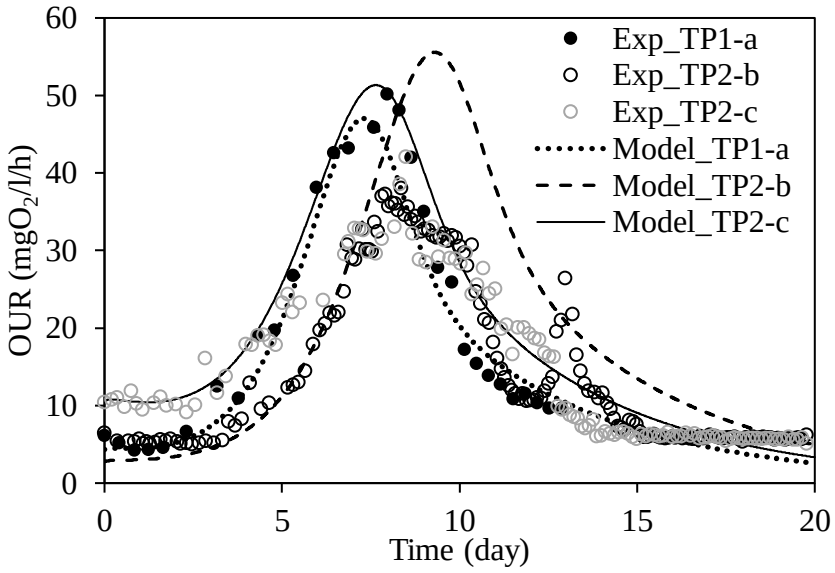

b)

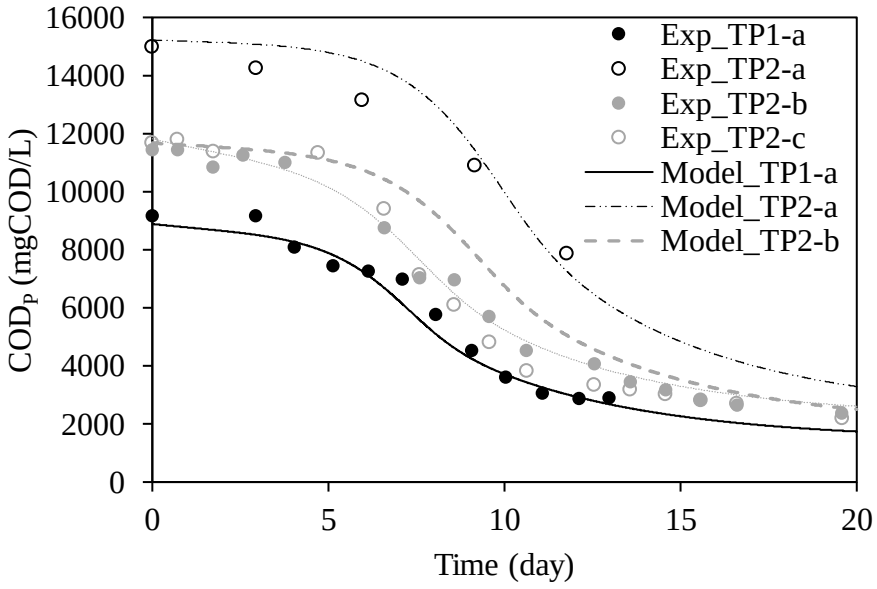

Figure 46: Time evolution of (a) the OUR and the (b) COD_P during the degradation of the TP inoculated by different concentrations of AS: the inoculum COD added were 0, 384, 1820 and

710 mgCOD/L for TP2-a and TP2-b, TP2-c and TP1-a, respectively. Model calibration was performed simultaneously on experiments TP2-a and TP2-b, TP2-c and TP1-a.

Table 47: Kinetic and stoichiometric coefficients estimated for OUR calibration (TP1 and TP2 experiments) – underlined parameters were fixed

Parameter	Unit	Fraction	Results from calibration of OUR			
			TP2-a	TP1-a	TP2-b	TP2-c
$K_{XCB,\ hyd}$	mgCOD.mgCOD^{-1}		0.9	0.9	0.9	0.9
$q_{XCB\_SB.\ HYD}$	d^{-1}		1.3	1.3	1.3	1.3
PSS_COD	mgCOD.L^{-1}		15 220	8 180	11 300	10 001
$XC_{B\_PSS,\ ini}$	mgCOD.L^{-1}	0.89	13 569	7 292	10 074	8 916
$X_{U\_PSS,\ ini}$	mgCOD.L^{-1}	0.1	1 522	818	1 130	1 000
$X_{OHO\_ER\_PSS,\ ini}$	mgCOD.L^{-1}	0.007	107	57	79	70
$X_{OHO\_Hyd\_PSS,\ ini}$	mgCOD.L^{-1}	0.0015	23	12	17	15
Inoc_COD	mgCOD.L^{-1}		0	710	384	1 820
$XC_{B\_inoc,\ ini}$		0	0	107	0	*0*
$X_{U\_inoc,\ ini}$	mgCOD.L^{-1}	0.13/0.28	0	92	108	510
$X_{OHO\_ER\_inoc,\ ini}$	mgCOD.L^{-1}	0.7	0	497	269	1 274
$X_{OHO\_Hyd\_inoc,\ ini}$	mgCOD.L^{-1}	0.02	0	14	8	36

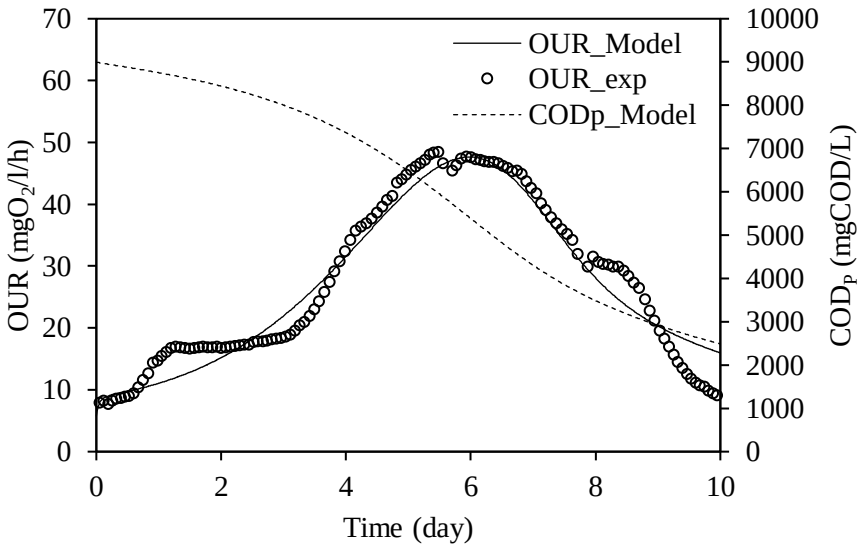

Figure 47: Time evolution of the OUR during the degradation of pure cellulose at a given concentrations of AS: the inoculum COD added was of 970 mgCOD/L.

Table 48: Kinetic and stoichiometric coefficients estimated for OUR calibration (cellulose experiment) – underlined values were fixed

Parameter	Unit	Fraction	Value
$K_{XCB,\ hyd}$	$mgCOD.mgCOD^{-1}$		0,68
$q_{XCB\_SB,\ HYD}$	d^{-1}		1.16
Cellulose_COD	$mgCOD.L^{-1}$		8000
$XC_{\_PSS,\ ini}$	$mgCOD.L^{-1}$	0.98	7840
$X_{OHO\_hyd\_PSS,\ ini}$	$mgCOD.L^{-1}$	0.02	160
$X_{OHO\_ER\_PSS,\ ini}$	$mgCOD.L^{-1}$	0	0
Inoc_COD	$mgCOD.L^{-1}$		970
$XC_{B\_inoc,\ ini}$	$mgCOD.L^{-1}$	0.395	383
$X_{U\_inoc,\ ini}$	$mgCOD.L^{-1}$	0.074	72
$X_{OHO\_ER\_inoc,\ ini}$	$mgCOD.L^{-1}$	0.5	485
$X_{OHO\_hyd\_inoc,\ ini}$	$mgCOD.L^{-1}$	0.031	30
E^2	$(mgO_2/L/h)^2$		1138

3.4. EFFECT OF ADAPTATION OF THE BIOMASS ON TP DEGRADATION

In order to assess the adaptation capacity of the cells to the substrate, three successive batches were performed on clean TP. The first batch corresponded to TP2-b and was inoculated with AS (380 mgCOD/L). TP2-d was inoculated by a certain amount (1320 mgCOD/L) of the residual COD_P of TP2-b and TP2-e was inoculated with a certain amount (1330 mgCOD/L) of the residual COD_P of TP2-d. Figure 48 represents the evolution of the (a) OUR and (b) the residual COD_P concentration in the supernatant during aerobic digestion of TP.

In the first experiment on TP (TP2-b), the conventional two trends profile of OUR was observed. In the second experiment (TP2-d), the addition of the microbial biomass recovered from the first experiment had a drastic effect on the OUR dynamic. The delay before the OUR augmentation disappeared and the degradation time was shortened from 15 days to around 11 days. In the third experiment (TP2-e), again the inoculation to new TP substrate of the microbial biomass recovered from the second experiment led to a decrease in the degradation time to 9 days.

a)

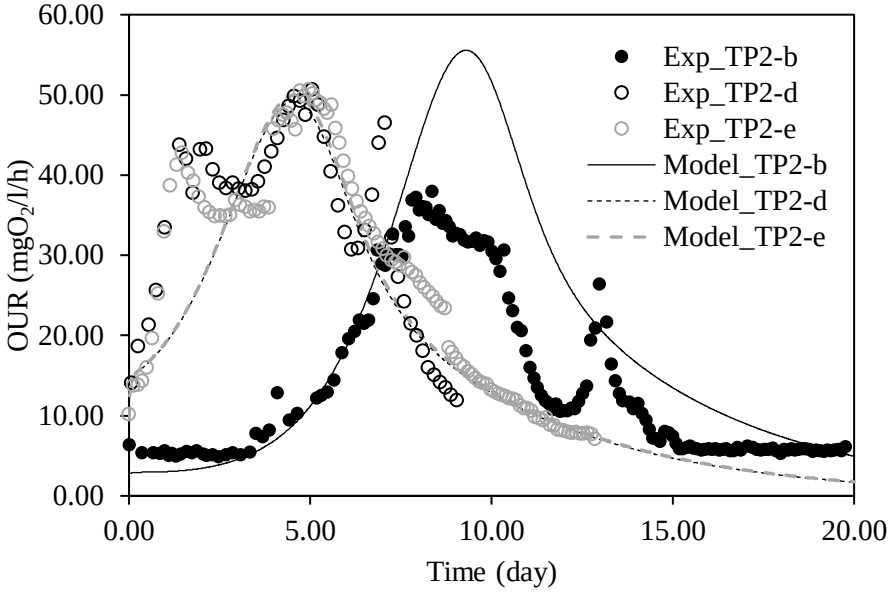

b)

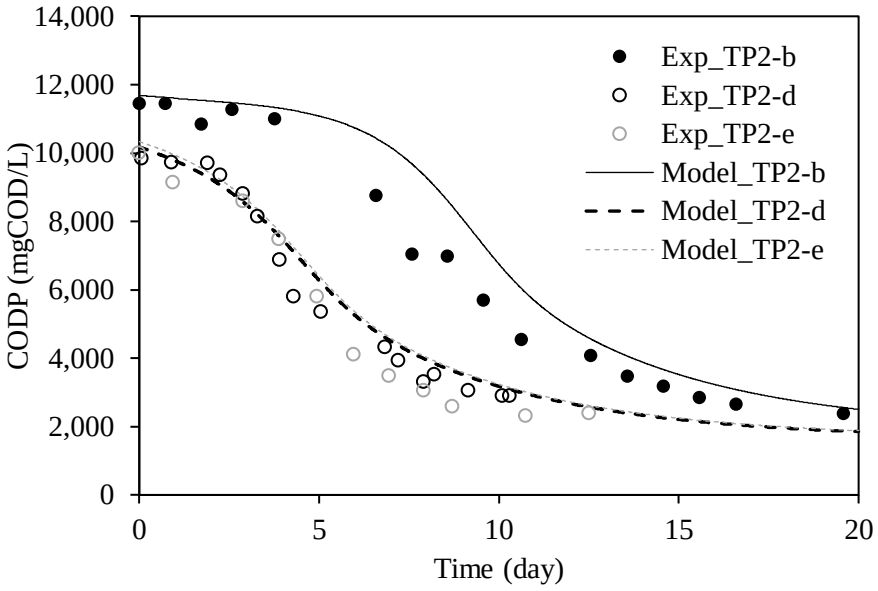

Figure 48: Experimental and modeling data of (a) the OUR and (b) the COD_P evolution during TP degradation: TP2-b was inoculated with activated sludge (384 mgCOD/L), TP2-d was inoculated with the residual COD_P of TP2-b (1320 mgCOD/L) and TP2-e was inoculated with the residual COD_P of TP2-d (1330 mgCOD/L)

The resulting COD_P evolutions were found to be coherent with the OUR profiles with the disappearance of the time-lag phase in TP2-d and TP2-e. These successive enrichments with

acclimated cells to TP did not affect considerably the COD degradation yields as they were quite similar for TP2-b, TP2-d and TP2-e and between 71 and 79%. Thus, bacteria acclimation to TP allowed to reduce the characteristic time of degradation (from 15 down to 9 days).

4. DISCUSSION

4.1. EFFECT OF AS INOCULUM ADDITION ON THE DEGRADATION KINETIC OF LARGE PARTICLES

Various substrates containing large particles with different chemical compositions, surface properties and geometrical characteristics were used in this study. These particles came from the settled fraction of raw urban wastewaters but also from toilet paper and even from pure commercial cellulose. They were put in contact with very different amounts of AS samples from zero (no AS added) to a high concentration representing up to 80 % of the total initial COD_P concentration. Note that the ASs were sampled the same day than the raw wastewater used for producing PSSs. If we suppose that all the bacteria present in the AS samples were significantly active for the hydrolysis processes, the addition of increasing concentrations of AS should have led to a proportional increase in hydrolysis rates and consequently to biodegradation times much shorter. Results obtained in this study obviously demonstrate that this is not the case whatever the substrate used. In the case of PSS1 (Figure 44), the OUR and CODp profiles were found identical independently of the added concentrations of AS. This result was observed even for batches run in parallel and fed with a same PSS sample and a same AS but this latter added at different concentrations. The duration of biodegradation was not significantly different for these experiments. For PSS2, the proportions of COD from AS used in the experiments were high in comparison with the COD from PSS. Therefore, the addition of AS led to a significant increase in the respiration rate. However, neither the acceleration rate in the first phase (colonization phase) nor the OURmax value increased proportionally to the amount of AS added (Figure 45). It seems that a large majority of the COD from AS was involved in endogenous processes rather than in hydrolysis of the PSS. Again, the same duration of biodegradation is observed despite a 5 times greater amount of inoculum. Similar conclusions can be drawn from experiments on TP, a model substrate containing a high fraction of purified cellulose and xylan and theoretically a very low microbial contamination degree. In that case, the amount of the substrate COD was very high decreasing the importance of the endogenous respiration on the global OUR. For TP2 experiments, significant differences were

observed neither in the acceleration rate of the first phase, nor in the OURmax value nor in the global biodegradation duration despite the increasing proportions of AS added (Figure 46). However, the slight increase in the biodegradation time observed for TP2-a where no AS was added showed that a small fraction of AS was able to perform hydrolysis of the TP.

The effect of cell acclimation to hydrolysis of large particles of substrate was clearly demonstrated in experiments TP2-b, TP2-d and TP2-e where the biomass recovered at the end of a batch is reinjected in another batch to degrade a fresh TP. A reduction of the lag phase duration and an increase in the degradation rate were observed. Similar adaptation was observed on starch when degraded in a sequential batch reactor (Mino et al. 1995). In this study, the hydrolysis rate has increased by a factor of two to three over a period of 70 days of operation.

As a first conclusion, taking into account that the heterotrophic activity of the AS was systematically checked by respirometry on a reference substrate (glucose or acetic acid) before its addition, our results clearly demonstrated that the very large majority of the cells brought with the ASs did not significantly participate to the hydrolysis of the large particles whether they come from PSS or TP or cellulose. The degree of initial contamination of the "aged" PSS (PSS1) by hydrolytic bacteria was obviously high and on contrary, no active cells from the AS inocula was able to participate to the hydrolysis of the large particulate matter. In a different way, for "fresh" PSS (PSS2), less initial contamination of the particles allowed a small fraction of the bacteria of AS to be efficient for PSS hydrolysis. This result is similar for TP, though the fraction of efficient bacteria of the inoculum was much higher, certainly due to a nearly virgin surface of the particles.

4.2. ESTIMATION OF THE HYDROLYTIC BIOMASS CONCENTRATION

A rough estimation of the fractions of X_{OHO_Hyd} present either in the AS inoculum or already attached to the substrates was done using the model presented in the Material and Method section. The estimation of X_{OHO_Hyd}, X_{OHO_ER} and X_{CB} present both on the substrates (PSSs or TP) and inside the AS inocula was performed together with the estimation of the kinetic parameters $K_{XCB,\ hyd}$ and $q_{XCB\_SB,\ hyd}$. For a given set of experiments, the parameter estimation was done on the basis of all the OUR curves and if available all the CODp curves. Values of X_U and X_{OHO_ER} in substrates and inocula were considered as experience-specific and used to match with the total biological oxygen demand and with the initial OUR. Indeed, this degree of freedom was found necessary because for example, an increase in X_U and X_{OHO_ER} proportion in the inoculum was observed when increasing its concentration. A process of

flocculation of the organic matter when the concentration of AS increased might explain this result. Our estimation of the hydrolytic activity both in the AS inoculum and in the substrates should be rather robust because for a given set of experiments (except for PSS2), the OUR tests were done in parallel with very different ratios inoculum COD on substrate COD. Moreover, two other aspects strengthened the reliability of the conclusions: firstly, both real and model substrates with different behavior and contamination degree were selected, and, secondly, a model substrate (TP) on which the initial cell concentration and inert material proportion should be really low was used.

The Figure 49 summarizes the estimated fractions of hydrolytic heterotrophic bacteria and their origins, either from the AS inoculum or from the particulate substrates.

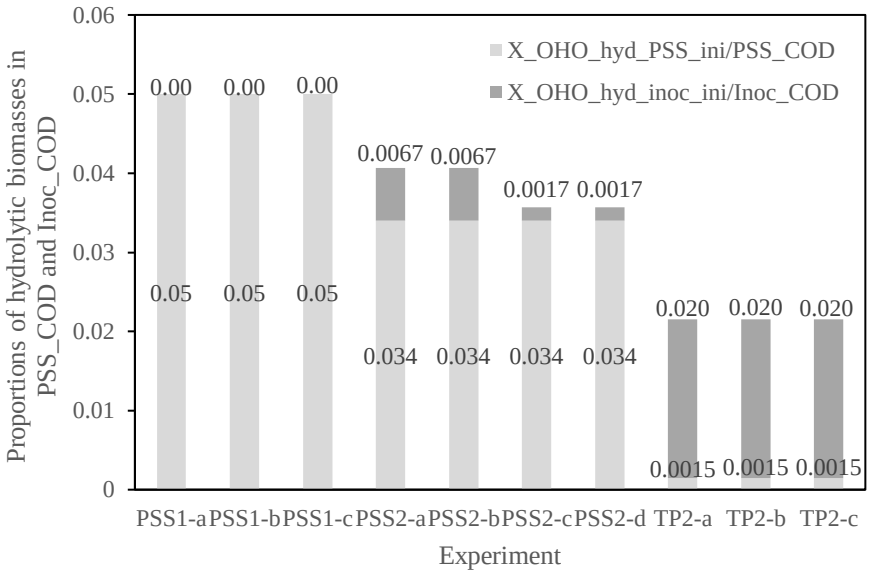

Figure 49: Estimated fractions of hydrolytic heterotrophic bacteria and their origins, either from the AS inoculum (dark grey) or from the particulate substrates (light grey)

It can be seen that PSS1 contained the largest proportion of the already attached and acclimated hydrolytic bacteria followed by PSS2s. TP, as expected contains only a very small fraction of bacteria able to perform the hydrolysis of the cellulose and Xylan, However, this fraction is significant. Of course, considering the amount of cell mass found, it can also come from an external contamination rather than from TP. Moreover, when considering the fraction of hydrolytic bacteria present in the AS inoculum, this fraction tends to zero for PSS1s, is very low for PSS2s but represent the major source of hydrolytic bacteria for TP. Compared to PSS1s, the PSS2s classified as "fresh" are certainly less contaminated and a larger fraction of bacteria from the AS inoculum can be effective in carrying out the hydrolysis or in colonizing the surface

area of the particles. Finally, TP is made in majority of purified cellulose exempt of biofilm that can be relatively easily attacked by various microbial species present in the AS inoculum.

As shown in Figure 50, the model calibration also indicates that a large amount of the PSSs COD is composed of bacteria performing endogenous respiration. This proportion reaches up to 56% for PSS1s leading to a fraction of X_{CB} representing less than 40% of the PSS1. On contrary, in the case of PSS2 sampled from the upstream part of the sewage network, the majority of the COD_P should be particulate substrate (X_{CB}). It means that for long sewer network, the state of degradation of matter is already well advanced and / or cell adsorption to the particulate matter is subsequent, both cases leading to a great proportion of cells in the PSS1. More predictably, the inoculum X_{OHO_ER} fraction of the AS was found also high and relatively similar whatever the experiment. Higher fractions of X_{OHO_ER} in the inoculum was found when the amount of inoculum was low. It may be due to lack of accuracy of the estimation of this fraction in that case.

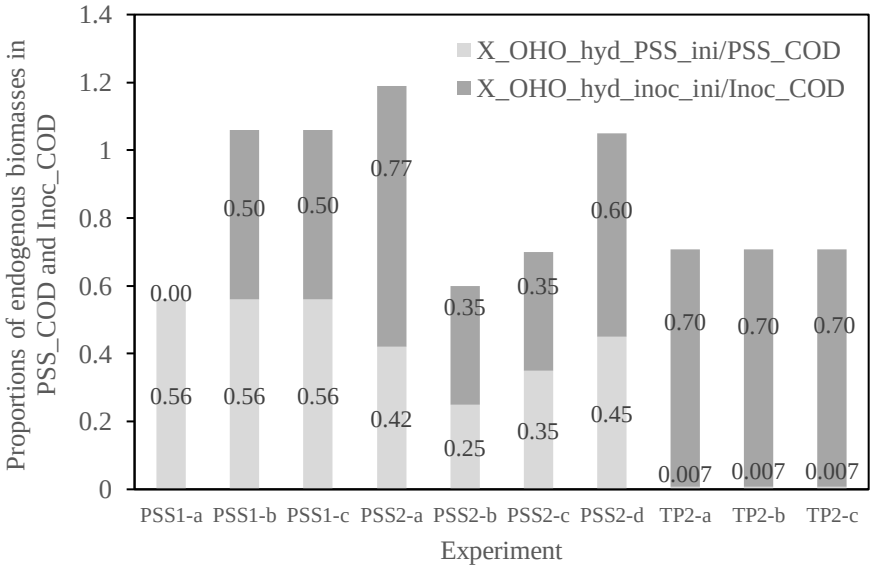

Figure 50: Estimated fractions of bacteria performing only endogenous respiration and their origins, either from the AS inoculum (dark grey) or from the particulate substrates (light grey).

4.3. BIODEGRADATION TRENDS

Particle size and surface properties are key factors that determine the degradation rate of particles (Balmat, 1957). The sizes of the particles used in this study are high and much greater than the bacteria size. Consequently, instead of assuming an adsorption of substrate on

bacteria in the case of colloidal matter (Stenstrom 1975; Dold et al., 1980, Spérandio and Paul, 2000), it is more realistic to assume that bacteria have to colonize the whole surface of the large particles of substrate. Therefore, the ratio between the initial hydrolytic bacteria concentration and the surface to be colonized should be an important parameter to consider in order to understand the degradation dynamics of large particles. Two trends in the OUR dynamics were observed in our experiments on PSS. The first one was characterized by a sharp initial peak in OUR when the degradation started to be recorded, followed by a slow decline up to endogenous respiration levels as the biodegradable substrate became depleted. This trend is similar to the one found by Okutman et al., (2001) or by Orhon et al., (2002) although the degradation time was much shorter in these cases. The second one was characterized by a first increase in OUR during a few days until a maximal value and then a slow decline to endogenous respiration levels similarly to what was observed in the first trend. OUR dynamics observed for TP and pure cellulose were identical to that second trend but a delay in the initial OUR increase was systematically observed. A similar trend has been observed by Ginestet et al., (2002b) on PSS and by Dimock and Morgenroth (2002) on egg-white particles.

The mathematical expression to describe hydrolysis included in the ASM1 model is able to represent both a one trend OUR profile and a two trends OUR profile. Thus, the simulations using the model help to better understand the OUR profiles. It confirms that the one trend OUR profile can be explained by a high degree of colonization of the PSS at the beginning of the batch experiment. All the particulate material surface area is already colonized by active hydrolytic bacteria. The degradation rate thus decreases against time due to a decrease in the available surface of the particles. The bacteria from the inoculum cannot access to the particle organic materials and hence are not involved in hydrolysis of the large particles. On contrary, in the two trends OUR profile, the particles are only partially colonized by a small initial cell concentration. As a consequence, these bacteria are able to further colonize the particles and to grow. Some bacteria from the inoculum which have the capacity to hydrolyze the specific substrate can also colonize the particles and participate to its degradation. This is the case for PSS2s. A same description can be made for TP of cellulose but in that case the degree of initial contamination of the substrate is very low or nil. Therefore, the inoculum from AS becomes performant though the bacteria must first adapt to the substrate and colonize the particles. The consideration of these later processes explains the 2 to 3 days delay in observing the OUR acceleration phase. The complex OUR profiles observed for TP inoculated with acclimated cells might be due to the superposition of several factors involved in hydrolysis.

To understand all these results, it is necessary to consider the whole hydrolysis mechanisms. Indeed, in waste and wastewater treatment fields the term hydrolysis refers to all mechanisms that make slowly biodegradable organic matter available for the bacterial growth (Gujer et al., 1999). Therefore, as underlined by Morgenroth et al. (2002), hydrolysis processes do not refer only to the breakdown of a polymer into smaller units by the addition of water but rather integrates all processes involved from the colonization of the substrate surface area by bacteria until the consumption of the produced monomers. This clearly includes biological processes (microbial selection, colonization, attachment and detachment, enzymatic potential, metabolic adaptation and regulations, etc.) but also chemical dissolution and mass transport processes. Hence, even if an inoculum contains bacteria with a real hydrolytic potential, these bacteria may not be involved in hydrolysis if the particulate substrate is already highly colonised or if transport limitation avoid adsorption. Our results also suggest that bacteria previously adsorbed on a particulate substrate are very efficient in degrading it.

5. CONCLUSION

The purpose of this chapter was to characterize the role of cell biomasses, differentiated according to their origins, on the hydrolysis of particulate substrates such as PSS or cellulose fibers. To achieve this objective, some experiments were carried out using various organic substrates seeded with different levels of inoculum collected from an activated sludge at the purification plant in Toulouse, France. The various substrates included PSSs of different origins. Indeed, these PSSs were taken either at the head of the network or at the bottom of the network. The degree of advancement of the biodegradation reactions was thus potentially different. The substrates also included TP and cellulose fibers. This choice was based on the fact that these substrates should not contain inoculum and were not (or very slightly) contaminated by microorganisms. It also made possible to study the same substrate over time since they can be perfectly conserved. The choice of an activated sludge to inoculate the substrates rested on the fact that the cells should be acclimated to the particulate substrates not only of the PSS but also of the TP.

Experiments and simulations based on the ASM1 model for COD degradation were used better understanding the role of bacteria from either the substrate sample or from the AS-inoculum on hydrolysis. A calibration procedure has been set up. It aimed to calibrate simultaneously the experiments carried out in parallel. The following points emerge:

- The degradation time for large particles is around at least 10 days. The duration of experiments should be appropriate.
- Even the addition of a large amount of inoculum sampled from AS to various PSS or to TP does not significantly increase the hydrolysis kinetics of the organic particulate matter. The particulate substrates chosen in this study showed contrasted OUR profiles indicating that their degree of pre-colonization by hydrolytic bacteria was different. “Aged” PSS1s were highly contaminated by hydrolytic bacteria whereas “fresh” PSS2 were much less pre-colonized and TP and cellulose only very slightly pre-colonized.
- On the basis of total COD, only a small fraction of the inoculum AS was found to correspond to active cells able to perform the hydrolysis of PSSs, TP and cellulose. However, this fraction increases when the particle surface is less contaminated by microorganisms. As a consequence, the inoculum added in the experiences brought bacteria performing endogenous respiration, XC_B and X_U. It is interesting to note that

X_U increases when the concentration of inoculum is augmented may be due to a decrease of the organic material accessibility.

- PSS arriving at the sewage treatment plant after a long stay in the sewage network contain a large proportion (approximately 50%) of cellular biomass involved in endogenous respiration. The content in X_{CB} does not represent more than 40% of the mass of initial PSS. It is the opposite for the PSS taken at the head of the network.
- Very different OUR profiles over time were observed which were grouped into two groups: directly decreasing profiles and successively increasing and decreasing profiles. From this analysis, hypotheses about the mechanisms of hydrolysis have been postulated. In particular, and in continuity with the results of chapter III, the hydrolytic cells must colonize the particulate substrate in order to degrade it. The kinetics is therefore dependent on the relative proportion between X_{CB} and X_{OHO_Hyd}. This led us to use the Comtois model to represent the hydrolysis of our substrates. Moreover, it became evident that a significant part of the respiration signals was due to the endogenous respiration of bacteria unable of effecting the hydrolysis of the material and even to use the hydrolysis by-products, certainly because these last ones were captured more rapidly by hydrolytic bacteria.

These results lead us to a surprising conclusion: hydrolysis of PSS in activated sludge appears to be more influenced by the initial adsorbed bacteria in the sewage than the activated sludge concentration.

The role of specialized biomass in the hydrolysis of particulate organic matter should be further investigated. For this, it would be necessary to show, for example, the colonization of the cellulosic fibers specifically by certain bacteria. Confocal microscopy could be a tool of choice for studying this point if hydrolytic cells could be specifically labeled. It would also be possible to label the substrate molecules by the carbon 13 and isolate the DNA from the cells that consumed this carbon. It would then be possible to unequivocally determine the fraction of the bacteria capable of effecting the hydrolysis of this particular substrate as well as their identity. These experiments require a solid know-how in the methods that should be developed within the Symbiosis team.

FINAL CONCLUSION AND PERSPECTIVES

The goal of this thesis was to contribute in the analysis and the comprehension of the fate and biodegradation of particulate matter, which is classified as slowly biodegradable matter and commonly called “PSS”. These PSS were found to represent a high percentage of the organic matter contained in municipal wastewaters (more than half of the total COD). The literature review underlined the potential and feasibility of utilizing it as a cheap alternative carbon source to the conventional expensive carbon sources (e.g. methanol) that are now utilized in nutrient removal processes, if and only if their fate in the treatment chain can be correctly assessed. This requires to better understand mechanisms that are involved in their biodegradation. Hydrolysis is a very widespread reaction in the framework of waste and wastewater treatment. It is then important to describe this process with accuracy.

Modeling is a useful tool both to help understanding processes and to predict results for designing. The typical modeling approaches that are commonly used in WWTP processes (IAWQ models) were found to be not all the time efficient to describe and predict the kinetic behaviour of this matter. Especially a lack concerning a mechanistic analysis of hydrolysis processes remains. The characterization of the hydrolysis process is difficult to perform as its own definition is not clear. In the waste water treatment domain, this mechanism may involve a chain of processes of physical (transport and the adsorption of the bacterial cells onto the substrate), biological (colonization of the substrate, enzymes secretion…) or even chemical nature (behaviour depends on the composition of the substrate). In this context, this thesis focussed on the characterization of the hydrolysis of slowly biodegradable matter.

A literature review highlighting that **particulate matter biodegradation is not extensively studied**. It showed also that the knowledge around the interactions between substrate and bacteria is not clearly taken into account. Especially the importance of the substrate to biomass ratio, which is implemented in the models in terms of mass concentration, which is misleading as the available surface area of substrate and bacteria depend on their physical properties such as their size which varies depending on the substrate but also dynamically. There is also a lack of information concerning the mode of action of the bacterial communities in the hydrolysis process. In conventional WWTP modeling, all the cellular biomass is most of the time assimilated as the hydrolytic active bacteria. This postulate was questionable when considering the high diversity of the communities present in WWTP and several questions have to be addressed: does the total cellular biomass have the capacity to hydrolyse? Do the same bacterial communities perform hydrolysis and at the same time consumes the hydrolytic products? The initial amounts of hydrolytic bacteria are found to be somewhat crucial in the characterization of the hydrolysis process.

In order to answer these questions around the hydrolysis process, our methodology consisted in performing (or taking from literature) respirometric batch tests of substrates of different origins (PSS collected upstream vs downstream the WWTP), shapes (toilet paper "TP" fibers and spherical hard-boiled egg white particles "EP") and sizes (small and large EP) and confronting the resulting experimental data to modeling. Additional analytical parameters were monitored in parallel of these batch tests (particulate COD and ammonia) in order to constrain the models. Some major results obtained in this thesis work are summarized below:

Chapter I: **Observation** of kinetics of biodegradation of large particles of organic matter.

Chapter I focused on observations the OUR profiles of various experiments, the few found in the literature and some carried out during this study. These profiles were compared based on different criteria in order to try to define the main mechanisms that are involved in hydrolysis of large particles. Only very few OUR profiles could be found in the literature. It demonstrates that only a very small number of studies has focused on the degradation of PSSs.

Concerning PSS experiments, a first very striking observation concerns the duration of the biodegradation experiment of a material which is supposed to be on average relatively similar. Biodegradation times are divided into two classes: a few hours or around 10 days. This result raises the question of the origin of PSSs, their size, biochemical composition, etc.

A second observation was that two types of OUR profile could be observed. From PSSs sampled on the downstream parts of the network, a one trend decreasing profile was observed while for PSSs sampled at the upstream of the sewer network and for model substrates, a two trend OUR profile was systematically observed. In addition, a lag phase was seen on the OUR profile for model substrates. Our first conclusion was that the degree of colonization of the matter by hydrolytic bacteria was certainly a key factor to explain these differences.

The difficulty to interpret the response obtained for PSSs underlined the necessity to consider other simpler substrates with different physical, chemical and/or biochemical properties. We have chosen to work on model substrates in this thesis (toilet paper and cellulose) because they are large particles composed of fibers of different sizes, involved complex enzymatic processes, are not contaminated by bacteria. Indeed, those substrates were inoculated with AS which was possibly not generated in the presence of these substrates.

The results of this chapter also underlined the necessity to monitor not only the OUR but also other parameters such as COD_P and ammonia in order to dissociate the mechanism of hydrolysis and growth from endogenous processes.

Chapter II: **Modeling** of kinetics of biodegradation of large particles with **existing models for comparison**

In this chapter, models available in the literature were used to simulate the experiments presented in chapter I. The differences in the chosen models are: (i) the type of mathematical expression of hydrolysis: a first order equation or a Contois equation; (ii) the number of variables to represent the particulate substrate; (iii) the consideration of the available surface of the particulate substrate; (iv) combination of these models.

The first conclusion was that the whole experiments required to consider at least two distinct categories of substrates (XC_{B1} and XC_{B2}), except in TP1-a where a single-hydrolysis model (IAWQ-1) was also adapted. The SBK model was also an interesting alternative to the DHM for this experiment, either for experimental data fitting (OUR and ammonia) as well as for particulate COD prediction.

Besides hydrolytic bacteria, model calibration showed that the inocula (cellular biomass) may contain other fractions such as unbiodegradable particulate matter (X_{U_inoc}), other bacterial communities without hydrolysis potential (X_{OHO}) or undergoing endogenous respiration (X_{OHO_ER}) as well as slowly biodegradable matter (XC_B). Moreover, at this stage, the origin of the hydrolytic bacteria is in reality not clear whether it comes from the inoculum or the PSS. In PSS1-a experiment, however, the hydrolytic bacteria were clearly those attached to the PSS as no inoculum was added. This aspect will be specifically investigated in chapter IV.

The first-order models were more suitable for the PSS1-a experiment: the initial tight peak (OUR_{max}) as well as the OUR decreasing phase were accurately described. Time evolution of ammonia was also described with precision and the COD_P evolution was quite well predicted. In contrary, the surface-based models were more adapted for TP1-a and PSS2-a. In TP1-a, the time-lag phase that was attributed to "acclimation" of unspecialized bacteria to the substrate was adequately described by the appropriate model, even if this process was not taken into account in the model. In addition, the two-trend OUR shape (increasing and decreasing phase) were described correctly. Concerning ammonia, it was quite well described. The appropriate model was also efficient to predict the behaviour of the COD_P. In PSS2-a, modeling allowed to describe the global OUR shape correctly, even if any model fitted with precision the tight peak corresponding to the OUR_{max}. Nevertheless, even if each experiment was independently described with an appropriate model, a specific set of kinetic parameters was identified for each experiment. This may be explained by the fact that current modeling approaches do not consider with enough insight the interactions between bacteria and substrate which would involve to

take into account their physical properties. That way, the following chapter was dedicated to the development of a new conceptual model.

Chapter III: **Adaptation of the SBK model: colonization and hydrolysis** of large particles are **surface dependent**

In chapter III, a novel conceptual framework (M_SBK) was developed in order to describe with more insight and more realistically the hydrolysis of slowly biodegradable matter. This model includes the colonization of solid substrates by microbial communities. Based on the IAWQ model n°1, this new model took into account the physical properties (density) and geometrical aspects (size, shape…) of the involved bacterial cells and particulate substrate. The model was compared to the single (A1) and dual (B1) hydrolysis models and confronted to different shaped (TP1-a, EP, PSS1-a) and sized substrates (small and large EP). The aspects included in the model were: (i) the particle shape (bacteria were supposed spherical and solid substrate cylindrical for cellulose or spherical for proteins); (ii) the relation between particle size and substrate concentration based on surface areas and (iii) the introduction of a maximum colonizable fraction (f_{ma}).

The M_SBK model did not significantly improve the description of the experiments compared to the other evaluated models. This can be due to the fact that the shape and size of particles are not known in our experiments. However, the M_SBK model had the advantage to be able to simulate the dynamic evolution of particle size during the hydrolysis step and it is thus more realistic in a mechanistic point of view. It allowed to qualitatively describe the trends of a modification of initial size of the substrate in the case of experiments performed on EP by Dimock and Morgenroth 2006). This underlines that taking into account the real surface of the particulate substrate is useful for a true representation of the degradation kinetic.

The M_SBK is therefore an excellent tool for learning about the hydrolysis processes.

In addition, the evaluation of the M_SBK model showed some interesting aspects: particle size was proportional to the time of degradation and that:

- Adsorption was enhanced in the case of small particles compared to large particles as the specific surface area of the first one was higher.
- For a same colonizable surface area, the shape of particles was found not to affect the global trends and the bioreaction characteristic time.
- The detachment process and the degree of colonization of the substrate were found to be crucial considerably affecting the ability of model to describe the experimental data.

The initial biomass contamination may greatly affect the biodegradation kinetics. This aspect was finally investigated in the fourth and last chapter.

Chapter IV: **Who is active** for hydrolysis of large particles of PSSs, TP and cellulose?

The purpose of the last chapter (IV) was to assess the role of the different bacterial communities depending on their origin: the substrate or an inoculum of AS. One goal was also to quantify the hydrolytic population which is responsible for the initiation of the hydrolysis process.

To reach this objective, substrates with different initial degree of bacterial contamination and origins were investigated: (i) PSS collected downstream (PSS1) and (ii) upstream (PSS2) the sewage network which are initially highly and partially colonized by microorganisms, respectively; (iii) Toilet paper and pure cellulose which are not (or only very slightly) contaminated by bacteria. The PSS1 and PSS2 experiments were inoculated with activated sludge (AS) in order to evaluate the competition between the initially attached (adsorbed) bacteria and bacterial populations from the AS-inoculum. The calibration procedure that was adopted involves the simultaneous calibration of each set of experiments performed in parallel (PSS1s, PSS2s and TPs).

It was concluded that regardless of the amount of AS, the hydrolytic kinetics of the PSSs did not increase significantly. Based on the total COD, only a very small fraction of the AS-inoculum contributed to the hydrolysis of the COD of the large particles in those experiments. However, this fraction was found to be higher in the model substrates (toilet paper, cellulose) compared to the contaminated ones (PSSs).

Consequently, the AS inoculum was found to bring bacteria that undergo only endogenous respiration, unbiodegradable matter ($X_{U\_inoc,\ ini}$) and slowly biodegradable matter ($XC_{B\_inoc,\ ini}$) for PSS1s already highly colonized by bacteria due to their prolonged time spent in the sewer. A fraction slightly higher of the AS inoculum COD was found to have the capacity t hydrolyse the PSS2s. This may be due either to the less degree of colonization of the particles or to the highest biodegradability of the "fresher" matter. Logically, even more bacteria of the AS inoculum were able to hydrolyse TPs and cellulose as these substrates are more easily biodegradable and not colonised.

The conclusion of this part was that the hydrolysis of PSS in activated sludge processes appears more influenced by the initially adsorbed bacteria onto the sewage than by the added AS-inoculum concentration.

As the majority of the models developed takes into account only one biomass that performed both the hydrolysis of the particles and the biodegradation of the by-products, the parameters

used to describe hydrolytic capacity of a global biomass are composite parameters. This aspect represents a strong limitation for the analysis of hydrolysis mechanisms.

Perspectives in modelling of hydrolysis of large particles:

In order to go further in the analysis of both mechanisms and consequences of hydrolysis, the following points could be proposed:

Using the M_SBK model should require to take into account the size distribution of the particles as the specific area of the particle was found to be a key point. Rapid tools for assessing the particle size distribution and shape could hence be used.

A validation of the dynamic evolution of the size would highly strengthen the approach. This point is far to be trivial for different reasons: on the one hand, it is difficult to distinguish the substrate itself from the bacteria attached. Clearly laser granulometry cannot provide such an information. We thus need to focus on visualisation techniques, what we started in this work but we still have to improve the differentiation between the two matrix and work on image analysis to be able to statistically characterize enmeshed objects. On the other hand, some of our observations indicates that the internal porosity of solid substrates may change depending on the compositions of the wall. Once again, microscopic observation may bring some information, specifically through confocal microscopy.

Experiments should be performed with different types of particulate matters of different biochemical composition, shapes and sizes to strengthen our conclusions. Other model substrates should be used. In that case, the controlled parameters of these substrates (biochemical and physical characteristics) are key points to allow better understanding the relevant parameters controlling hydrolysis.

The role of specialized biomass in the hydrolysis of slowly biodegradable matter that has been highlighted in this work should clearly be further investigated. Analysis of the diversity evolution when an inoculum from activated sludge is used for a non-contaminated substrate (such as clean toilet paper) would give interesting information about the acclimation and subsequent mechanisms. Substrate molecules labelling with carbon 13 and DNA isolation from the cells that are able to consume this carbon could also confirm some of our hypothesis and give quantitative data about hydrolytic biomass.

In a modelling point of view, the knowledge of the fraction of the hydrolytic bacteria in an inoculum sample is crucial to correctly study the degradation of particulate matter. The same conclusion could be drawn for activated processes.

Our results obtained in aerobic conditions should be supplemented by other results in anaerobic conditions on waste substrates. Indeed, it will help to better describe the waste biodegradation.

BIBLIOGRAPHY

`

Æsøy, A., Ødegaard, H., 1994. Nitrogen removal efficiency and capacity in biofilms with biologically hydrolysed sludge as a carbon source. Water Sci. Technol. 30, 63–71.

Aldin, S., Nakhla, G., Ray, M.B., 2011. Modeling the Influence of Particulate Protein Size on Hydrolysis in Anaerobic Digestion. Ind. Eng. Chem. Res. 50, 10843–10849.

Andrews, G.F., Tien, C., 1977. New Approach to Bacterial Kinetics in Wastewater. J. Environ. Eng. Div. 103, 1057–1074.

Aravinthan, V., Mino, T., Takizawa, S., Satoh, H., Matsuo, T., 2001. Sludge hydrolysate as a carbon source for denitrification. Water Sci. Technol. 43, 191–199.

Aslan, S., Türkman, A., 2003. Biological denitrification of drinking water using various natural organic solid substrates. Water Sci. Technol. J. Int. Assoc. Water Pollut. Res. 48, 489–495.

Balmat, J.L., 1957. Biochemical Oxidation of Various Particulate Fractions of Sewage. Sew. Ind. Wastes 29, 757–761.

Bansal, P., Vowell, B.J., Hall, M., Realff, M.J., Lee, J.H., Bommarius, A.S., 2012. Elucidation of cellulose accessibility, hydrolysability and reactivity as the major limitations in the enzymatic hydrolysis of cellulose. Bioresour. Technol. 107, 243–250.

Barlindhaug, J., Ødegaard, H., 1996. Thermal hydrolysis for the production of carbon source for denitrification. Water Sci. Technol., Water Quality International '96 Part 1: Nutrient Removal 34, 371–378.

Barret, M., Carrère, H., Delgadillo, L., Patureau, D., 2010. PAH fate during the anaerobic digestion of contaminated sludge: Do bioavailability and/or cometabolism limit their biodegradation? Water Res. 44, 3797–3806.

Blackwell, L.G., 1971. A theoretical and experimental investigation of the transient response of the activated sludge process. Clemson University, South Carolina, USA.

Boczar, B.A., Begley, W.M., Larson, R.J., 1992. Characterization of enzyme activity in activated sludge using rapid analyses for specific hydrolases. Water Environ. Res. 64, 792–797.

Boley, A., Müller, W.-R., Haider, G., 2000. Biodegradable polymers as solid substrate and biofilm carrier for denitrification in recirculated aquaculture systems. Aquac. Eng. 22, 75–85.

Bolzonella, D., Innocenti, L., Pavan, P., Cecchi, F., 2001. Denitrification potential enhancement by addition of anaerobic fermentation products from the organic fraction of municipal solid waste. Water Sci. Technol. 44, 187–194.

Burgess, J.E., Pletschke, B.I., 2008. Hydrolytic enzymes in sewage sludge treatment: A mini-review. Water SA 34, 343–350.

Cadoret, A., Conrad, A., Block, J.-C., 2002. Availability of low and high molecular weight substrates to extracellular enzymes in whole and dispersed activated sludges. Enzyme Microb. Technol. 31, 179–186.

Cameron, S.G., Schipper, L.A., 2010. Nitrate removal and hydraulic performance of organic carbon for use in denitrification beds. Ecol. Eng., Managing Denitrification in Human Dominated Landscapes 36, 1588–1595.

Canziani, R., Pollice, A., Ragazzi, M., 1995. Feasibility of using primary-sludge mesophilic hydrolysis for biological removal of nitrogen and phosphorus from wastewater. Bioresour. Technol. 54, 255–260.

Carley, B.N., Mavinic, D.S., 1991. The Effects of External Carbon Loading on Nitrification and Denitrification of a High-Ammonia Landfill Leachate. Res. J. Water Pollut. Control Fed. 63, 51–59.

Caudan, C., Filali, A., Lefebvre, D., Sperandio, M., Girbal-Neuhauser, E., 2012. Extracellular Polymeric Substances (EPS) from Aerobic Granular Sludges: Extraction, Fractionation, and Anionic Properties. Appl. Biochem. Biotechnol. 166, 1685–1702.

Christensson, M., Lie, E., Welander, T., 1994. A comparison between ethanol and methanol as carbon sources for denitrification. Water Sci. Technol. 30, 83–90.

Clark, P.B., Nujjoo, I., 2000. Ultrasonic Sludge Pretreatment for Enhanced Sludge Digestion. Water Environ. J. 14, 66–71.

Cliff, R.C., 1980. A dynamic model for predicting oxygen utilization in activated sludge processes (Thesis). University of Huston, USA.

Cokgor, E.U., Insel, G., Aydin, E., Orhon, D., 2009. Respirometric evaluation of a mixture of organic chemicals with different biodegradation kinetics. J. Hazard. Mater. 161, 35–41.

Çokgör, E.U., Sözen, S., Orhon, D., Henze, M., 1998. Respirometric analysis of activated sludge behaviour—I. Assessment of the readily biodegradable substrate. Water Res. 32, 461–475.

Confer, D.R., Logan, B.E., 1997b. Molecular weight distribution of hydrolysis products during the biodegradation of model macromolecules in suspended and biofilm cultures. II. Dextran and dextrin. Water Res. 31, 2137–2145.

Confer, D.R., Logan, B.E., 1997a. Molecular weight distribution of hydrolysis products during biodegradation of model macromolecules in suspended and biofilm cultures I. Bovine serum albumin. Water Res. 31, 2127–2136.

Corominas, L., Rieger, L., Takacs, I., Ekama, G., Hauduc, H., Vanrolleghem, P.A., Oehmen, A., Gernaey, K.V., van Loosdrecht, M.C.M., Comeau, Y., 2010. New framework for standardized notation in wastewater treatment modelling. Water Sci. Technol. 61, 841–857.

Costerton, J.W., Cheng, K.J., Geesey, G.G., Ladd, T.I., Nickel, J.C., Dasgupta, M., Marrie, T.J., 1987. Bacterial biofilms in nature and disease. Annu. Rev. Microbiol. 41, 435–464.

Dawes, E.A., Ribbons, D.W., 1964. Some aspects of the endogenous metabolism of bacteria. Bacteriol. Rev. 28, 126–149.

Dennis, R.W., Irvine, R.L., 1981. A stoichiometric model of bacterial growth. Water Res. 15, 1363–1373.

Dias, F.F., Bhat, J.V., 1964. Microbial Ecology of Activated Sludge I. Dominant Bacteria. Appl. Microbiol. 12, 412–417.

Dignac, M.-F., Ginestet, P., Rybacki, D., Bruchet, A., Urbain, V., Scribe, P., 2000. Fate of wastewater organic pollution during activated sludge treatment: nature of residual organic matter. Water Res. 34, 4185–4194.

Dimock, R., Morgenroth, E., 2006. The influence of particle size on microbial hydrolysis of protein particles in activated sludge. Water Res. 40, 2064–2074.

Ding, W., Li, D., Zeng, X., Long, T., 2006. Enhancing excess sludge aerobic digestion with low intensity ultrasound. J. Cent. South Univ. Technol. 13, 408–411.

Dold, P., Ekama, G., Marais, G., 1980. The Activated Sludge Process 1. a General Model for the Activated Sludge Process. Prog. Water Technol. 12, 47–77.

Dold, P.L., Pleit, E., Han, J., 1991. Hydrolysis of α (1–4) glucan bonds in activated sludge mixed bacterial communities. Environ. Technol. 12, 871–879.

Donot, F., Fontana, A., Baccou, J.C., Schorr-Galindo, S., 2012. Microbial exopolysaccharides: Main examples of synthesis, excretion, genetics and extraction. Carbohydr. Polym. 87,

951–962.

Eastman, J.A., Ferguson, J.F., 1981. Solubilization of Particulate Organic Carbon during the Acid Phase of Anaerobic Digestion. J. Water Pollut. Control Fed. 53, 352–366.

Ekama, G.A., Dold, P.L., Marais, G. v R., 1986. Procedures for Determining Influent COD Fractions and the Maximum Specific Growth Rate of Heterotrophs in Activated Sludge Systems. Wat. Sci. Technol. 18 (6), 91–104

Ekama, G.A., Marais, G. v. R., 1979. Dynamic Behavior of the Activated Sludge Process. J. Water Pollut. Control Fed. 51, 534–556.

Elefsiniotis, P., 1993. The effect of operational and environmental parameters on the acid-phase anaerobic digestion of primary sludge (Thesis). University of British Columbia.

Elefsiniotis, P., Li, D., 2006. The effect of temperature and carbon source on denitrification using volatile fatty acids. Biochem. Eng. J. 28, 148–155.

Eliosov, B., Argaman, Y., 1995. Hydrolysis of particulate organics in activated sludge systems. Water Res. 29, 155–163.

Fletcher, M., 1980. Microbial adhesion to surfaces. Ellis Horwood, Chichester.

Fletcher, M., 1977. The effects of culture concentration and age, time, and temperature on bacterial attachment to polystyrene. Can. J. Microbiol. 23, 1–6.

Fonseca, A.D., Crespo, J.G., Almeida, J.S., Reis, M.A., 2000. Drinking Water Denitrification Using A Novel Ion-exchange Membrane Bioreactor. Environ. Sci. Technol. 34.

Frolund, B., Griebe, T., Nielsen, P., 1995. Enzymatic-Activity in the Activated-Sludge Floc Matrix. Appl. Microbiol. Biotechnol. 43, 755–761.

Galí, A., Dosta, J., Mata-Álvarez, J., 2006. Use of Hydrolyzed Primary Sludge as Internal Carbon Source for Denitrification in a SBR Treating Reject Water via Nitrite. Ind. Eng. Chem. Res. 45, 7661–7666.

Garrett, R.H., Grisham, C.M., 2000. Biochimie. De Boeck Supérieur.

Garrett, T.R., Bhakoo, M., Zhang, Z., 2008. Bacterial adhesion and biofilms on surfaces. Prog. Nat. Sci. 18, 1049–1056.

Gibert, O., Pomierny, S., Rowe, I., Kalin, R.M., 2008. Selection of organic substrates as potential reactive materials for use in a denitrification permeable reactive barrier (PRB). Bioresour. Technol. 99, 7587–7596.

Ginestet, P., Maisonnier, A., Spérandio, M., 2002. Wastewater COD characterization: biodegradability of physico-chemical fractions. Water Sci. Technol. 45, 89–97.

Goel, R., Mino, T., Satoh, H., Matsuo, T., 1999. Modeling hydrolysis processes considering intracellular storage. Water Sci. Technol. 39, 97–105.

Goel, R., Mino, T., Satoh, H., Matsuo, T., 1998. Comparison of hydrolytic enzyme systems in pure culture and activated sludge under different electron acceptor conditions. Water Sci. Technol. 37, 335–343.

Goel, R., Mino, T., Satoh, H., Matsuo, T., 1997. Effect of electron acceptor conditions on hydrolytic enzyme synthesis in bacterial cultures. Water Res. 31, 2597–2603.

Gómez, M.A., González-López, J., Hontoria-García, E., 2000. Influence of carbon source on nitrate removal of contaminated groundwater in a denitrifying submerged filter. J. Hazard. Mater. 80, 69–80.

Grady, L.C.P., Daigger, G.T., Lim, H.C., 1999. Biological Wastewater Treatment, 2nd Edition. M. Dekker, New York.

Greenan, C.M., Moorman, T.B., Kaspar, T.C., Parkin, T.B., Jaynes, D.B., 2006. Comparing Carbon Substrates for Denitrification of Subsurface Drainage Water. J. Environ. Qual. 35, 824–829.

Guellil, A., Thomas, F., Block, J.-C., Bersillon, J.-L., Ginestet, P., 2001. Transfer of organic matter between wastewater and activated sludge flocs. Water Res. 35, 143–150.

Gujer, W., 1980. The effect of particulate organic material on activated sludge yield and oxygen requirement. Prog. Wat. Tech. 12, 79–95.

Gujer, W., Henze, M., 1991. Activated-Sludge Modeling and Simulation. Water Sci. Technol. 23, 1011–1023.

Gujer, W., Henze, M., Mino, T., Matsuo, T., Wentzel, M., Vonmarais, G., 1995. The Activated-Sludge Model No-2 - Biological Phosphorus Removal. Water Sci. Technol. 31, 1–11.

Gujer, W., Henze, M., Mino, T., van Loosdrecht, M., 1999. Activated Sludge Model No. 3. Water Sci. Technol. 39, 183–193.

Heukelekian, J.L.B., 1959. Chemical Composition of Particulate Fractions of Domestic Sewage. Sew. Ind. Wastes 31, 413–423.

Haldane, G.M., Logan, B.E., 1994. Molecular size distributions of a macromolecular polysaccharide (dextran) during its biodegradation in batch and continuous cultures.

Water Res. 28, 1873–1878.

Hallin, S., Lindberg, C.-F., Pell, M., Plaza, E., Carlsson, B., 1996. Microbial adaptation, process performance and a suggested control strategy in a pre-denitrifying system with ethanol dosage. Water Sci. Technol., 34, 91–99.

Hallin, S., Pell, M., 1998. Metabolic properties of denitrifying bacteria adapting to methanol and ethanol in activated sludge. Water Res. 32, 13–18.

Henze, M., 2008. Biological Wastewater Treatment: Principles, Modelling and Design. IWA Publishing.

Henze, M., Grady, C., Gujer, W., Marais, G., Matsuo, T., 1987. A General-Model for Single-Sludge Waste-Water Treatment Systems. Water Res. 21, 505–515.

Henze, M., Gujer, W., Mino, T., Matsuo, T., Wentzel, M.C., Marais, G. v. R., Van Loosdrecht, M.C.M., 1999. Activated sludge model No.2D, ASM2D. Water Sci. Technol., Modelling and microbiology of activated sludge processes 39, 165–182.

Henze, M., Kristensen, G.H., Strube, R., 1994. Rate-Capacity Characterization of Wastewater for Nutrient Removal Processes. Water Sci. Technol. 29, 101–107.

Henze, M., Mladenovski, C., 1991. Hydrolysis of particulate substrate by activated sludge under aerobic, anoxic and anaerobic conditions. Water Res. 25, 61–64.

Her, J.-J., Huang, J.-S., 1995. Influences of carbon source and C/N ratio on nitrate/nitrite denitrification and carbon breakthrough. Bioresour. Technol. 54, 45–51.

Hill, D.W., Reynolds, J.H., Filip, D.S., Middlebrooks, E.J., 1977. Series Intermittent sand filtration of wastewater lagoon effluents. Utah Water Research Laboratory, Utah State University, Logan, Utah.

Hobson, P.N., 1987. A model of some aspects of microbial degradation of particulate substrates. J. Ferment. Technol. 65, 431–439.

Holme, D.J., Peck, H., 1993. Analytical biochemistry, 2nd ed. Longman Scientific & Technical.

Honda, S. 'ichi, Miyata, N., Iwahori, K., 2002. Recovery of biomass cellulose from waste sewage sludge. J. Mater. Cycles Waste Manag. 4, 46–50.

Hu, Z., Chandran, K., Smets, B.F., Grasso, D., 2002. Evaluation of a rapid physical–chemical method for the determination of extant soluble COD. Water Res. 36, 617–624.

Huang, M., Li, Y., Gu, G., 2010. Chemical composition of organic matters in domestic wastewater. Desalination 262, 36–42.

INRS, 2011. Fiche toxicologique FT 282.

Insel, G., Orhon, D., Vanrolleghem, P.A., 2003. Identification and modelling of aerobic hydrolysis – application of optimal experimental design. J. Chem. Technol. Biotechnol. 78, 437–445.

Isaacs, S.H., Henze, M., 1995. Controlled carbon source addition to an alternating nitrification-denitrification wastewater treatment process including biological P removal. Water Res. 29, 77–89.

Isaacs, S.H., Henze, M., Søeberg, H., Kümmel, M., 1994. External carbon source addition as a means to control an activated sludge nutrient removal process. Water Res. 28, 511–520.

Israel, S., Engelbrecht, P., Tredoux, G., Fey, M.V., 2009. In Situ Batch Denitrification of Nitrate-Rich Groundwater Using Sawdust as a Carbon Source—Marydale, South Africa. Water. Air. Soil Pollut. 204, 177–194.

Janning, K., Letallec, X., Harremoes, P., 1998. Hydrolysis of organic wastewater particles in laboratory scale and pilot scale biofilm reactors under anoxic and aerobic conditions. Water Sci. Technol. 38, 179–188.

Jenkins, S.H., 2013. Advances in Water Pollution Research: Proceedings of the Fourth International Conference held in Prague 1969. Elsevier.

Kappeler, J., Gujer, W., 1992. Estimation of Kinetic Parameters of Heterotrophic Biomass under Aerobic Conditions and Characterization of Wastewater for Activated Sludge Modelling. Water Sci. Technol. 25, 125–139

Kaprelyants, A.S., Kell, D.B., 1996. Do bacteria need to communicate with each other for growth? Trends Microbiol. 4, 237–242.

Klapwuk, A., Drent, J., Steenvoorden, J.H.A.M., 1974. A modified procedure for the TTC-dehydrogenase test in activated-sludge. Water Res. 8, 121–125.

Klopp, R., Koppe, P., 1990. Die quantitative Charakterisierung von Abwässern hinsichtlich ihrer Dispersität und Abbaubarkeit. Vom Wasser 75, 307–329.

Kole, C., Joshi, C.P., Shonnard, D.R., 2012. Handbook of Bioenergy Crop Plants. CRC Press.

Kountz, R.R., Forney, C., 1959. Metabolic Energy Balances in a Total Oxidation Activated Sludge System. Sew. Ind. Wastes 31, 819–826.

Lagarde, F., Tusseau-Vuillemin, M.-H., Lessard, P., Héduit, A., Dutrop, F., Mouchel, J.-M., 2005. Variability estimation of urban wastewater biodegradable fractions by

respirometry. Water Res. 39, 4768–4778.

Larsen, T.A., 1992. Degradation of colloidal organic matter in biofilm reactors (Thesis). Technical University of Denmark, Denmark.

Larsen, T.A., Harremoës, P., 1994. Degradation mechanisms of colloidal organic matter in biofilm reactors. Water Res. 28, 1443–1452.

Laspidou, C.S., Rittmann, B.E., 2002. A unified theory for extracellular polymeric substances, soluble microbial products, and active and inert biomass. Water Res. 36, 2711–2720.

Lawrence, J.R., Korber, D.R., Wolfaardt, G.M., Caldwell, D.E., 1995. Behavioral Strategies of Surface-Colonizing Bacteria, in: Jones, J.G. (Ed.), Advances in Microbial Ecology, Advances in Microbial Ecology. Springer US, pp. 1–75.

Lebaz, N., 2015. Modélisation de l'hydrolyse enzymatique de substrats lignocellulosiques par bilan de population (Thesis). University of Toulouse.

Levine, A.D., Tchobanoglous, G., Asano, T., 1985. Characterization of the Size Distribution of Contaminants in Wastewater: Treatment and Reuse Implications. J. Water Pollut. Control Fed. 57, 805–816.

Levine, A.D., Tchobanoglous, G., Asano, T., 1991b. Particulate contaminants in wastewater: a comparison of measurement techniques and reported particle size distributions. Fluid Particle Separation Journal. Fluid Particle Separation Journal 4, 89–106.

Liu, G.Y., Zhang, H.Z., Li, W., Zhang, X., 2012. Advances of External Carbon Source in Denitrification. Adv. Mater. Res. 518–523, 2319–2323.

Loferer-Krößbacher, M., Klima, J., Psenner, R., 1998. Determination of Bacterial Cell Dry Mass by Transmission Electron Microscopy and Densitometric Image Analysis. Appl. Environ. Microbiol. 64, 688–694.

Marais, G.R., Ekama, G.A., 1976. The activated sludge process part I-steady state behaviour. Water SA 2, 164–200.

Márquez, M.C., Vázquez, M.A., 1999. Modeling of enzymatic protein hydrolysis. Process Biochem. 35, 111–117.

Metcalf, Eddy, 2003. Wastewater engineering: treatment, disposal, reuse, 4th Edition. Tata McGraw-Hill, New Delhi.

Mino, T., San Pedro, D.C., Matsuo, T., 1995. Estimation of the rate of slowly biodegradable COD (SBCOD) hydrolysis under anaerobic, anoxic and aerobic conditions by

experiments using starch as model substrate. Water Sci. Technol. 31, 95–103.

Morgenroth, E., Kommedal, R., Harremoes, P., 2002. Processes and modeling of hydrolysis of particulate organic matter in aerobic wastewater treatment - a review. Water Sci. Technol. 45, 25–40.

Munch, R., Hwang, C.P., Lackie, T., 1980. Wastewater fractions add to total treatment picture. Wat. Swge. Wks 127, 49–54.

Murray, K., 1991. Wastewater Treatment and Pollution Control (2nd edition.). Water Research Commission.

Nielsen, P.H., Frølund, B., Keiding, K., 1996. Changes in the composition of extracellular polymeric substances in activated sludge during anaerobic storage. Appl. Microbiol. Biotechnol. 44, 823–830.

Nowak, O., Svardal, K., Franz, A., Kühn, V., 1998. Degradation of particulate organic matter. A comparison of different model concepts. Fourth Kollekolle Seminar on Activated Sludge Modelling, Denmark, 16-18 mars.

Nybroe, O., Jorgensen, P.E., Henze, M., 1992. Enzyme activities in waste water and activated sludge. Water Res. 26, 579–584.

Okutman, D., Övez, S., Orhon, D., 2001. Hydrolysis of settleable substrate in domestic sewage. Biotechnol. Lett. 23, 1907–1914.

Orhon, D., Ateş, E., Sözen, S., Cokgör, E.U., 1997. Characterization and COD fractionation of domestic wastewaters. Environ. Pollut. Barking Essex 1987 95, 191–204.

Orhon, D., Cokgor, E.U., Sozen, S., 1998. Dual hydrolysis model of the slowly biodegradable substrate in activated sludge systems. Biotechnol. Tech. 12, 737–741.

Orhon, D., Okutman, D., Insel, G., 2002. Characterisation and biodegradation of settleable organic matter for domestic wastewater. Water Sa 28, 299–305.

Orhon, D., Sozen, S., 2012. Fate and effect of xenobiotics on biodegradation processes: basis for respirometric appraisal. Environ. Technol. 33, 1517–1522.

Orhon, D., Ubay Çokgör, E., Sözen, S., 1999. Experimental basis for the hydrolysis of slowly biodegradable substrate in different wastewaters. Water Sci. Technol., Modelling and microbiology of activated sludge processes 39, 87–95.

Park, C., Abu-Orf, M.M., Novak, J.T., 2006. The digestibility of waste activated sludges. Water Environ. Res. 78, 59–68.

Park, C., Novak, J.T., 2007. Characterization of activated sludge exocellular polymers using several cation-associated extraction methods. Water Res. 41, 1679–1688.

Park, J.Y., Yoo, Y.J., 2009. Biological nitrate removal in industrial wastewater treatment: which electron donor we can choose. Appl. Microbiol. Biotechnol. 82, 415–429.

Paul, E., Sperandio, M., Bessière, Y., 2012. Sludge production: Quantification and prediction for urban treatment plants and assessment of strategies for sludge reduction, in: Biological Sludge Minimization and Biomaterials/Bioenergy Recovery Technologies. Wiley.

Pellicer-Nacher, C., Domingo-Felez, C., Mutlu, A.G., Smets, B.F., 2013. Critical assessment of extracellular polymeric substances extraction methods from mixed culture biomass. Water Res. 47.

Perez, S., Paul, E., Lefebvre, D., Lefebvre, X., 2009. Effect of moderate heat pre-treatment before anaerobic activated sludge digestion: a biochemical and biophysical characterisation. Water Res.

Pirt, S.J., 1965. The Maintenance Energy of Bacteria in Growing Cultures. Proc. R. Soc. Lond. B Biol. Sci. 163, 224–231.

Porges, N., Jasewicz, L., Hoover, S.R., 1953. Aerobic Treatment of Dairy Wastes. Appl. Microbiol. 1, 262–270.

Ramasamy, K., Meyers, M., Bevers, J., Verachtert, H., 1981. Isolation and Characterization of Cellulolytic Bacteria from Activated Sludge. J. Appl. Bacteriol. 51, 475–481.

Ramdani, A., Dold, P., Gadbois, A., Deleris, S., Houweling, D., Comeau, Y., 2012. Biodegradation of the endogenous residue of activated sludge in a membrane bioreactor with continuous or on-off aeration. Water Res. 46, 2837–2850.

Ras, M., Elisabeth, G.-N., Etienne, P., Dominique, L., 2008. A high yield multi-method extraction protocol for protein quantification in activated sludge. Bioresour. Technol. 99, 7464–7471.

Raszka, A., Chorvatova, M., Wanner, J., 2006. The role and significance of extracellular polymers in activated sludge. Part I: Literature review. Acta Hydrochim. Hydrobiol. 34, 411–424.

Raunkjær, K., Hvitved-Jacobsen, T., Nielsen, P.H., 1994. Measurement of pools of protein, carbohydrate and lipid in domestic wastewater. Water Res. 28, 251–262.

Reichert, P., 1994. Aquasim a tool for simulation and data analysis of aquatic systems. Water Sci. Technol. 30, 21–30.

Richards, S.R., Hastwell, C., Davies, M., 1984. The comparative examination of 14-activated-sludge plants using enzymatic techniques. Water Pollut. Control 83, 300–313.

Rickert, D.A., Hunter, J.V., 1971. General nature of soluble and particulate organics in sewage and secondary effluent. Water Res. 5, 421–436.

Robertson, W. d., Blowes, D. w., Ptacek, C. j., Cherry, J. a., 2000. Long-Term Performance of In Situ Reactive Barriers for Nitrate Remediation. Ground Water 38, 689–695.

Robertson, W.D., 2010. Nitrate removal rates in woodchip media of varying age. Ecol. Eng., Managing Denitrification in Human Dominated Landscapes 36, 1581–1587.

Robertson, W.D., Cherry, J.A., 1995. In Situ Denitrification of Septic-System Nitrate Using Reactive Porous Media Barriers: Field Trials. Ground Water 33, 99–111.

Roeleveld, P.J., van Loosdrecht, M.C.M., 2002. Experience with guidelines for wastewater characterisation in The Netherlands. Water Sci. Technol. J. Int. Assoc. Water Pollut. Res. 45, 77–87.

Römling, U., Galperin, M.Y., 2015. Bacterial cellulose biosynthesis: diversity of operons, subunits, products, and functions. Trends Microbiol. 23, 545–557.

Rossle, W., Pretorius, W., 2001. A review of characterisation requirements for in-line prefermenters: Paper 1 : Wastewater characterisation. Water SA 27.

San Pedro, D.C., Mino, T., Matsuo, T., 1994. Evaluation of the rate of hydrolysis of slowly biodegradable COD (SBCOD) using starch as substrate under anaerobic, anoxic and aerobic conditions. Water Sci. Technol. 30, 191–199.

Sanders, W., M, G., G, Z., G, L., 2000. Anaerobic hydrolysis kinetics of particulate substrates.

Sanders, W.T.M., 2001. Anaerobic Hydrolysis During Digestion of Complex Substrates (Thesis). Wageningen University, The Netherlands.

Scheller, H.V., Ulvskov, P., 2010. Hemicelluloses. Annu. Rev. Plant Biol. 61, 263–289.

Schipper, L.A., Vojvodić-Vuković, M., 2000. Nitrate removal from groundwater and denitrification rates in a porous treatment wall amended with sawdust. Ecol. Eng. 14, 269–278.

Schläfer, O., Sievers, M., Klotzbücher, H., Onyeche, T.I., 2000. Improvement of biological activity by low energy ultrasound assisted bioreactors. Ultrasonics 38, 711–716.

Schomburg, Di., 1997. Handbook of Enzymes, Springer.

Shao, L., Wang, T., Li, T., Lu, F., He, P., 2013. Comparison of sludge digestion under aerobic and anaerobic conditions with a focus on the degradation of proteins at mesophilic temperature. Bioresour. Technol. 140, 131–137.

Shao, L., Xu, Z.-X., Jin, W., Yin, H.-L., Zhu, B.-R., 2009. [Nitrate removal from wastewater using rice straw as carbon source and biofilm carrier]. Huan Jing Ke Xue Huanjing Kexue 30, 1414–1419.

Sheng, G.-P., Yu, H.-Q., Li, X.-Y., 2010. Extracellular polymeric substances (EPS) of microbial aggregates in biological wastewater treatment systems: A review. Biotechnol. Adv. 28, 882–894.

Sheng, G.-P., Yu, H.-Q., Yue, Z.-B., 2005. Production of extracellular polymeric substances from Rhodopseudomonas acidophila in the presence of toxic substances. Appl. Microbiol. Biotechnol. 69, 216–222.

Soares, M.I.M., Abeliovich, A., 1998. Wheat straw as substrate for water denitrification. Water Res. 32, 3790–3794.

Soares, M.I.M., Brenner, A., Yevzori, A., Messalem, R., Leroux, Y., Abeliovich, A., 2000. Denitrification of groundwater: Pilot-plant testing of cotton-packed bioreactor and post-microfiltration. Water Sci. Technol. 42, 353–359.

Sollfrank, U., Gujer, W., 1991. Characterisation of Domestic Wastewater for Mathematical Modelling of the Activated Sludge Process. Water Sci. Technol.

Sollfrank, U., Gujer, W., 1991. Characterisation of Domestic Wastewater for Mathematical Modelling of the Activated Sludge Process. Water Sci. Technol. 23, 1057–1066.

Sophonsiri, C., Morgenroth, E., 2004. Chemical composition associated with different particle size fractions in municipal, industrial, and agricultural wastewaters. Chemosphere 55, 691–703.

Spanjers, H., Vanrolleghem, P., Olsson, G., Doldt, P., 1996. Respirometry in control of the activated sludge process. Water Sci. Technol., Water Quality International ’96 Part 2 34, 117–126.

Sperandio, M., 1998. Développement d’une procédure de compartimentation d’une eau résiduaire urbaine et application à la modélisation dynamique de procédés à boues activées (Thesis). INSA, Toulouse, France.

Spérandio, M., Paul, E., 2000. Estimation of wastewater biodegradable COD fractions by combining respirometric experiments in various So/Xo ratios. Water Res. 34, 1233–1246.

Sprouse, G., Rittmann, B.E., 1990. Colloid removal in fluidized-bed biofilm reactor. J. Environ. Eng.- ASCE 116, 314–329.

Standard Methods, L.., 1989. Standard methods for the examination of water and wastewater. American Public Health Association, Washington.

Stenstrom, M.K., 1976. A Dynamic Model and Computer Compatible Control Strategies for Wastewater Treatment Plants (Thesis). Clemson University.

Subramanian, S.B., Yan, S., Tyagi, R.D., Surampalli, R.Y., 2010. Extracellular polymeric substances (EPS) producing bacterial strains of municipal wastewater sludge: Isolation, molecular identification, EPS characterization and performance for sludge settling and dewatering. Water Res. 44, 2253–2266.

Sun, Y., Cheng, J., 2002. Hydrolysis of lignocellulosic materials for ethanol production: a review. Bioresour. Technol., Reviews Issue 83, 1–11.

Takahashi, S., Fujita, T., Kato, M., Saiki, T., Maeda, M., 1969. Metabolism of suspended matter in activated sludge treatment. Adv. Wat. Poll. Res, Pergamon Press 341–352.

Tam, N.F.Y., Wong, Y.S., Leung, G., 1992. Significance of External Carbon Sources on Simultaneous Removal of Nutrients from Wastewater. Water Sci. Technol. 26, 1047–1055.

Tanaka, S., Ichikawa, T., Matsuo, T., 1991. Removal of Organic Constituents in Municipal Sewage Using Anaerobic Fluidized Sludge Blanket and Anaerobic Filter. Water Sci. Technol. 23, 1301–1310.

Tas, D.O., Karahan, O., Insel, G., Ovez, S., Orhon, D., Spanjers, H., 2009. Biodegradability and Denitrification Potential of Settleable Chemical Oxygen Demand in Domestic Wastewater. Water Environ. Res. 81, 715–727.

Tauber, H., Stern, K.G., 1949. “The chemistry and technology of enzymes.” Henry Tauber, Wiley, New York, 1949, 558 pp., $7.50. J. Polym. Sci. 4, 773–774.

Tchobanoglous, G., Burton, F.L., 1991. Wastewater engineering: treatment, disposal, and reuse. McGraw-Hill.

Tchobanoglous, G., Burton, F.L., Stensel, H.D., 2003. Wastewater Engineering: Treatment and

Reuse. McGraw-Hill Professional.

Teuber, M., Brodisch, K.E.U., 1977. Enzymatic activities of activated sludge. Eur. J. Appl. Microbiol. Biotechnol. 4, 185–194.

Tiehm, A., Nickel, K., Neis, U., 1997. The use of ultrasound to accelerate the anaerobic digestion of sewage sludge. Water Sci. Technol. 36, 121–128.

Tiehm, A., Nickel, K., Zellhorn, M., Neis, U., 2001. Ultrasonic waste activated sludge disintegration for improving anaerobic stabilization. Water Res. 35, 2003–2009.

Torrijos, M., Cerro, R.-M., Capdeville, B., Zeghal, S., Payraudeau, M., Lesouef, A., 1994. Sequencing Batch Reactor: A Tool for Wastewater Characterization for the IAWPRC Model. Water Sci. Technol. 29, 81–90.

Tsuno, H., Goda, T., Somiya, I., 1978. Kinetic model of activated sludge metabolism and its application to the response of qualitative shock load. Water Res. 12, 513–522.

Ubukata, Y., 1999. Kinetics and fundamental mechanisms of starch removal by activated sludge: Hydrolysis of starch to maltose and maltotriose is the rate-determining step. Water Sci. Technol. 40, 61–68.

Ubukata, Y., 1992. Kinetics of polymeric substrate removal by activated sludge: Hydrolysis of polymers is the rate-determining step. Water Sci. Technol. 29, 2457–2460.

Vaicum, L., Gruia, E., Godeanu, S., 1965. The determination of some enzymatic activities as a research method in activated sludge. Rev. Roum. Biochim. 2, 87.

Van Loosdrecht, M.C.M., Henze, M., 1999. Maintenance, endogenous respiration, lysis, decay and predation. Water Sci. Technol., Modelling and microbiology of activated sludge processes 39, 107–117.

Vavilin, V.A., Fernandez, B., Palatsi, J., Flotats, X., 2008. Hydrolysis kinetics in anaerobic degradation of particulate organic material: An overview. Waste Management 28, 939–951.

Vavilin, V.A., Rytov, S.V., Lokshina, L.Y., 1996. A description of hydrolysis kinetics in anaerobic degradation of particulate organic matter. Bioresour. Technol. 56, 229–237.

Vollertsen, J., Hvitved-Jacobsen, T., 1999. Stoichiometric and kinetic model parameters for microbial transformations of suspended solids in combined sewer systems. Water Res. 33, 3127–3141.

Vollertsen, J., Jahn, A., Nielsen, J.L., Hvitved-Jacobsen, T., Nielsen, P.H., 2001. Comparison

of methods for determination of microbial biomass in wastewater. Water Res. 35, 1649–1658.

Volokita, M., Abehovich, A., Soares, M.I.M., 1996a. Denitrification of groundwater using cotton as energy source. Water Sci. Technol., Water Quality International '96 Part 1: Nutrient Removal 34, 379–385.

Volokita, M., Belkin, S., Abeliovich, A., Soares, M.I.M., 1996b. Biological denitrification of drinking water using newspaper. Water Res. 30, 965–971.

Wang, Z.-W., Liu, Y., Tay, J.-H., 2007. Biodegradability of extracellular polymeric substances produced by aerobic granules. Appl. Microbiol. Biotechnol. 74, 462–466.

Watson, S.D., Akhurst, T., Whiteley, C.G., Rose, P.D., Pletschke, B.I., 2004. Primary sludge floc degradation is accelerated under biosulphidogenic conditions: Enzymological aspects. Enzyme Microb. Technol. 34, 595–602.

Whiteley, C., Pletschke, B., Rose, P., Ngesi, N., 2002. Specific sulphur metabolites stimulate β-glucosidase activity in an anaerobic sulphidogenic bioreactor. Biotechnol. Lett. 24, 1509–1513.

Whiteley, C.G., Enongene, G., Pletschke, B.I., Rose, P., Whittington-Jones, K., 2003. Co-digestion of primary sewage sludge and industrial wastewater under anaerobic sulphate reducing conditions: enzymatic profiles in a recycling sludge bed reactor. Water Sci. Technol. J. Int. Assoc. Water Pollut. Res. 48, 129–138.

Wood, I.P., Elliston, A., Ryden, P., Bancroft, I., Roberts, I.N., Waldron, K.W., 2012. Rapid quantification of reducing sugars in biomass hydrolysates: Improving the speed and precision of the dinitrosalicylic acid assay. Biomass Bioenergy 44, 117–121.

WRC, 1984. Theory, design and operation of nutrient removal activated sludge processes. Water Research Commission.

Wu, J., He, C., 2012. The effect of settlement on wastewater carbon source availability based on respirometric and granulometric analysis. Chem. Eng. J. 189–190, 250–255.

Xu, S., Shi, W., 2001. Nitrate removal and denitrification bacteria cultivation using rice chaff as a medium. Journal of Dalian Railway Institute 22, 98.

Xu, Z., Shao, L., Yin, H., Chu, H., Yao, Y., 2009. Biological Denitrification Using Corncobs as a Carbon Source and Biofilm Carrier. Water Environ. Res. 81, 242–247.

Yu, G.-H., He, P.-J., Shao, L.-M., Zhu, Y.-S., 2008. Extracellular proteins, polysaccharides and

enzymes impact on sludge aerobic digestion after ultrasonic pretreatment. Water Res. 42, 1925–1934.

Zhang, L., Feng, X., Zhu, N., Chen, J., 2007. Role of extracellular protein in the formation and stability of aerobic granules. Enzyme Microb. Technol. 41, 551–557.

Zhang, Y.-X., Ji, M., Li, C., Wang, X.-D., Wang, S.-H., 2008. Biodegradability of extracellular polymeric substances (EPS) produced by aerobic granules. Huan Jing Ke Xue. 29, 3124–3127

Zhang, Z., Dai, X., Wang, C., Qi, W., Li, X., Zhang, J., Xia, S., 2013. Ultrasound-promoted extraction of cheap microbial flocculant from waste activated sludge. Environ. Technol. 34, 1219–1224.

Appendix

APPENDIX 1:

CORRELATION BETWEEN K_LA AND THE COUPLE (V, Ω)

Correlations between oxygen transfer coefficient (K_La) and reactor liquid height and between the K_La and bulk stirring speed were experimentally assessed in this study. The hydrodynamic stress differs from a reactor to another as they have different geometrical properties. A 1.5L- and a 2L-working volume reactors (R-α and R-ß, respectively) were used in this study in each experiment. Municipal wastewater (MWW) collected from the Toulouse-Ginestous WWTP (France) was used to achieve K_La calculation. The MWW was first centrifuged (4,500 rpm, 15 minutes) then the supernatant was filtered with a Whatman GF/C glass fiber filters with an effective pore size of 0.2 µm in order to eliminate bacteria which would affect dissolved oxygen variations. The use of filtered wastewater was carried out in order to imitate the hydrodynamic and transfer behavior that occurred in our experiments (more or less the same viscosity and oxygen diffusion coefficient). The temperature was maintained at 20°C during K_La assessment to be in the same conditions as experiments. Figure 51 represents the oxygen transfer coefficient (K_La) correlations with reactor liquid height (V) and bulk stirring speed (Ω) for reactors R-α and R-ß.

(a)

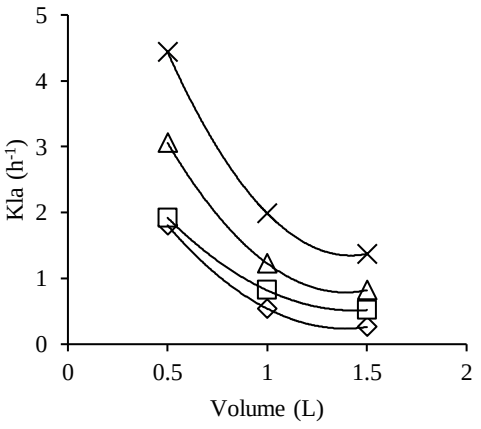

◇80 rpm	y = 1.97x² - 5.49x + 4.06
□120 rpm	y = 2.85x² - 7.94x + 6.31
△160 rpm	y = 1.61x² - 4.61x + 3.82
×270 rpm	y = 3.66x² - 10.39x + 8.72

(b)

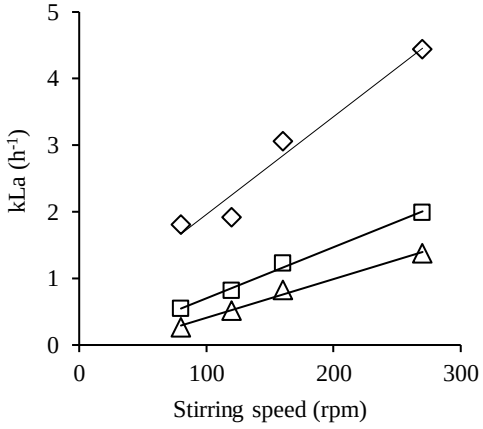

◇0,5 L	y = 0.0147x + 0.4918 R² = 0.9606
□1 L	y = 0.0077x - 0.0668 R² = 0.9951
△1,5 L	y = 0.0058x - 0.1727 R² = 0.9918

(c)

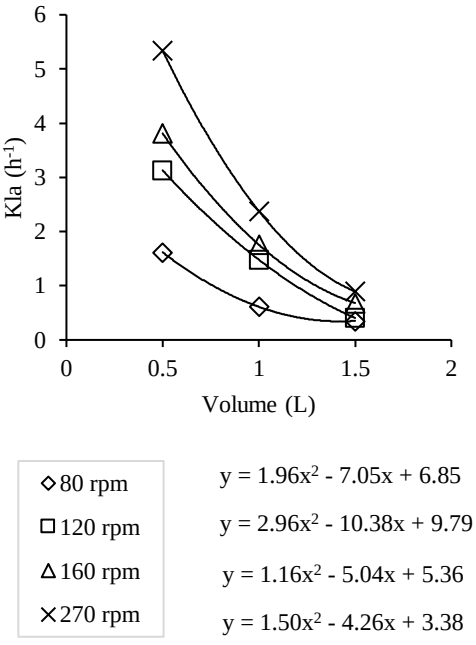

(d)

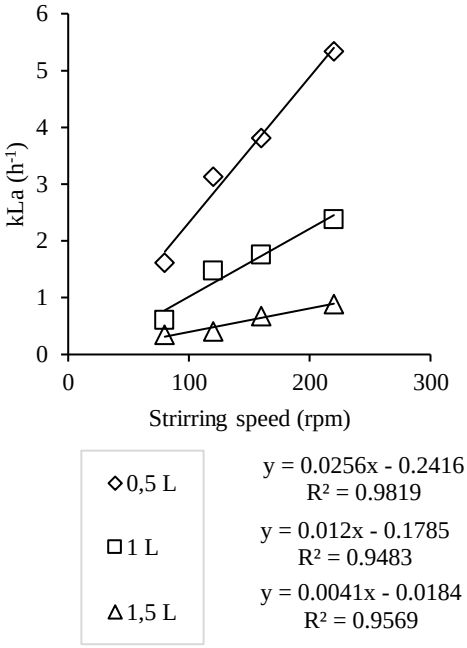

Figure 51: Relation between K_La and (a) V for various Ω for R-α. (b) Ω for various V for R-α. (c) V for various Ω for R-ß. (d) Ω for various V for R- ß.

APPENDIX 2 :

A) SENSITIVITY ANALYSIS OF TOILET PAPER EXPERIMENT

The sensitivity analysis of models towards the OUR and ammonia for PSS1-a experiment) is presented in Table 49

Table 49: Sensitivity analysis of OUR and ammonia (S_{NH4}) for PSS-1 experiment. Underlined parameters were fixed despite I>1%.

State variable	Influence (%)	Models					
		A1	A2	B1	B2	C1	C2
OUR	>0.01	X_{CB_ini} $\underline{f_{XU\_BIO\_LYS}}$ $\underline{b_{OHO}}$ $q_{XCB\_SB\_HYD}$ $X_{OHO,\ ini}$	XC_{B_ini} $\underline{f_{XU\_BIO\_LYS}}$ $\underline{b_{OHO}}$ X_{OHO_ini} $q_{XSS\_SB\_HYD}$ μ_{OHO_MAX}	XC_{B2_ini} XC_{B1_ini} $\underline{b_{OHO}}$ X_{OHO_ini} $\underline{f_{XU\_BIO\_LYS}}$ $q_{XCB1\_SB\_HYD}$ $q_{XCB2\_SB\_HYD}$ μ_{OHO_MAX}	X_{SS2_ini} X_{SS1_ini} $\underline{f_{XU\_BIO\_LYS}}$ $\underline{b_{OHO}}$ X_{OHO_ini} μ_{OHO_MAX} $q'_{XCB1\_SB\_HYD}$ $q'_{XCB2\_SB\_HYD}$	X_{CB_ini} k_{SBK} $\underline{b_{OHO}}$ $\underline{f_{XU\_BIO\_LYS}}$ X_{OHO_INI}	XC_{B2_ini} XC_{B1_ini} k_{SBK_XCB1} k_{SBK_XCB2} $\underline{b_{OHO}}$ $\underline{f_{XU\_BIO\_LYS}}$ X_{OHO_INI}
	<0.01	K_{XCB} μ_{OHO_MAX} K_{SB_HYD} i_{N_XU} i_{N_XBio}	K_{SB_HYD} $i_{N\_X\_BIO}$ i_{N_XU}	K_{XCB2_HYD} K_{XCB1_HYD} K_{SB_HYD} $i_{N\_X\_BIO}$	K_{SB_HYD} $i_{N\_X\_BIO}$ i_{N_XU}	μ_{OHO_MAX} K_{SB_OHO} $i_{N\_X\_BIO}$ i_{N_XU}	μ_{OHO_MAX} K_{SB_OHO} $i_{N\_X\_BIO}$ i_{N_XU}
S_{NH4}	>0.01	X_{CB_ini} i_{N_XBio} $\underline{b_{OHO}}$ $q_{XCB\_SB\_HYD}$ X_{OHO_ini} $\underline{f_{XU\_BIO\_LYS}}$ i_{N_XU}	X_{CB_ini} $i_{N\_X\_BIO}$ $\underline{b_{OHO}}$ X_{OHO_ini} $q_{XSS\_SB\_HYD}$ μ_{OHO_MAX} i_{N_XU} $\underline{f_{XU\_BIO\_LYS}}$	$i_{N\_X\_BIO}$ XC_{B1_ini} XC_{B2_ini} $\underline{b_{OHO}}$ X_{OHO_ini} $q_{XCB1\_SB\_HYD}$ $q_{XCB2\_SB\_HYD}$ $\underline{f_{XU\_BIO\_LYS}}$ i_{N_XU}	$i_{N\_X\_BIO}$ XC_{B2_ini} XC_{B1_ini} $\underline{b_{OHO}}$ X_{OHO_ini} μ_{OHO_MAX} i_{N_XU} $\underline{f_{XU\_BIO\_LYS}}$ $q'_{XCB1\_SB\_HYD}$ $q'_{XCB2\_SB\_HYD}$	$\underline{b_{OHO}}$ X_{CB_ini} $i_{N\_X\_BIO}$ k_{SBK} X_{OHO_INI} i_{N_XU} $\underline{f_{XU\_BIO\_LYS}}$	$\underline{b_{OHO}}$ XC_{B2_ini} XC_{B1_ini} $i_{N\_X\_BIO}$ k_{SBK_XCB1} k_{SBK_XCB2} X_{OHO_INI} i_{N_XU} $\underline{f_{XU\_BIO\_LYS}}$
	<0.01	K_{XCB} μ_{OHO_MAX} K_{SB_HYD}	K_{SB_HYD}	μ_{OHO_MAX} K_{XCB2_HYD} K_{XCB1_HYD} K_{SB_HYD}	K_{SB_HYD}	μ_{OHO_MAX} K_{SB_OHO}	μ_{OHO_MAX} K_{SB_OHO}

B) SENSITIVITY ANALYSIS OF TP1-A EXPERIMENT

The sensitivity analysis of models towards the OUR and ammonia for toilet paper experiment (TP1-a) is presented in Table 50.

Table 50: Sensitivity analysis of OUR and ammonia (S_{NH4}) for TP1-a experiment. Underlined parameters were fixed.

	Influence (%)	Models					
		A1	A2	B1	B2	C1	C2
OUR	>0.01	$\underline{X_{CB\_ini}}$ $\underline{Y_{OHO}}$ $\underline{f_{XU\_BIO\_LYS}}$ $\underline{b_{OHO}}$ $q_{XCB\_SB\_HYD}$ X_{OHO_ini}	$\underline{X_{CB\_ini}}$ $\underline{f_{XU\_BIO\_LYS}}$ $\underline{b_{OHO}}$ X_{OHO_ini} $q'_{XCB\_SB\_HYD}$ μ_{OHO_MAX}	XC_{B1_ini} $\underline{Y_{OHO}}$ $\underline{b_{OHO}}$ $\underline{f_{XU\_BIO\_LYS}}$ XC_{B2_ini} $q_{XCB2\_SB\_HYD}$ X_{OHO_ini} $q_{XCB1\_SB\_HYD}$	XC_{B1_ini} $\underline{f_{XU\_BIO\_LYS}}$ $\underline{b_{OHO}}$ XC_{B1_ini} X_{OHO_ini} μ_{OHO_MAX} $q_{XCB1\_SB\_HYD}$	$\underline{X_{CB\_ini}}$ k_{SBK} $\underline{b_{OHO}}$ $\underline{f_{XU\_BIO\_LYS}}$ X_{OHO_ini}	XC_{B2_ini} XC_{B1_ini} k_{SBK_XCB1} k_{SBK_XCB2} $\underline{b_{OHO}}$ $\underline{f_{XU\_BIO\_LYS}}$ X_{OHO_INI}
	<0.01	$K_{XCB,\ HYD}$ μ_{OHO_MAX} K_{SB_HYD} i_{N_XBio} i_{N_XU}	K_{SB_HYD} i_{N_XBio} i_{N_XU}	μ_{OHO_MAX} $K_{XCB\_2,\ HYD}$ K_{SB_HYD} $K_{XCB\_1,\ HYD}$ i_{N_XBio} i_{N_XU}	$q_{XCB2\_SB\_HYD}$ K_{SB_HYD} i_{N_XBio} i_{N_XU}	μ_{OHO_MAX} K_{SB_HYD} i_{N_XBio} i_{N_XU}	μ_{OHO_MAX} K_{SB_OHO} $i_{N\_X\_BIO}$ i_{N_XU}
S_{NH4}	>0.01	$\underline{Y_{OHO}}$ $\underline{X_{CB\_ini}}$ i_{N_XBio} $\underline{b_{OHO}}$ $q_{XCB\_SB\_HYD}$ X_{OHO_ini} $\underline{f_{XU\_BIO\_LYS}}$ i_{N_XU}	$\underline{X_{CB\_ini}}$ i_{N_XBio} $\underline{b_{OHO}}$ X_{OHO_ini} μ_{OHO_MAX} $q'_{XCB\_SB\_HYD}$ i_{N_XU} $\underline{f_{XU\_BIO\_LYS}}$	$\underline{Y_{OHO}}$ XC_{B1_ini} i_{N_XBio} $\underline{b_{OHO}}$ $q_{XCB2\_SB\_HYD}$ X_{OHO_ini} $\underline{f_{XU\_BIO\_LYS}}$ i_{N_XU} XC_{B1_ini} $q_{XCB1\_SB\_HYD}$	i_{N_XBio} XC_{B1_ini} $\underline{b_{OHO}}$ XC_{B1_ini} X_{OHO_ini} μ_{OHO_MAX} $q_{XCB1\_SB\_HYD}$ $\underline{f_{XU\_BIO\_LYS}}$ i_{N_XU}	$\underline{b_{OHO}}$ $\underline{X_{CB\_ini}}$ i_{N_XBio} k_{SBK} X_{OHO_ini} $\underline{f_{XU\_BIO\_LYS}}$ i_{N_XU}	$\underline{b_{OHO}}$ XC_{B2_ini} XC_{B1_ini} $i_{N\_X\_BIO}$ k_{SBK_XCB1} k_{SBK_XCB2} X_{OHO_INI} i_{N_XU} $\underline{f_{XU\_BIO\_LYS}}$
	<0.01	$K_{XCB,\ HYD}$ μ_{OHO_MAX} K_{SB_HYD}	K_{SB_HYD}	μ_{OHO_MAX} $K_{XCB\_2,\ HYD}$ K_{SB_HYD} $K_{XCB\_1,\ HYD}$	$q_{XCB2\_SB\_HYD}$ K_{SB_HYD}	μ_{OHO_MAX} K_{SB_HYD}	μ_{OHO_MAX} K_{SB_OHO}

C) SENSITIVITY ANALYSIS OF SPERANDIO'S (1998) EXPERIMENT (PSS1-A)

The sensitivity analysis of models towards the OUR in Sperandio's (1998) experiment on PSS (PSS2-a) is presented in Table 51.

Table 51: Sensitivity analysis for Sperandio's (1998) on PSS. Underlined parameters were fixed.

Influence (%)	Models			
	A1	B1	C1	C2
>0.01	X_{CB_ini} X_{OHO_ini} $q_{XCB\_SB\_HYD}$ X_{OHO_ini} $K_{XCB,\ HYD}$ $\underline{b_{OHO}}$ $\underline{f_{XU\_BIO\_LYS}}$	XC_{B1_ini} XC_{B2_ini} X_{OHO_ini} $q_{XCB1\_SB\_HYD}$ $q_{XCB2\_SB\_HYD}$ $\underline{b_{OHO}}$ $\underline{f_{XU\_BIO\_LYS}}$ $K_{XCB\_1,\ HYD}$ $K_{XCB\_2,\ HYD}$	X_{CB_ini} X_{OHO_ini} k_{SBK} $\underline{b_{OHO}}$ $\underline{f_{XU\_BIO\_LYS}}$	XC_{B2_ini} XC_{B1_ini} X_{OHO_INI} k_{SBK_XCB1} k_{SBK_XCB2} $\underline{b_{OHO}}$ $\underline{f_{XU\_BIO\_LYS}}$
<0.01	μ_{OHO_MAX} K_{SB_HYD}	μ_{OHO_MAX} K_{SB_HYD}	μ_{OHO_MAX} K_{SB_HYD}	μ_{OHO_MAX} K_{SB_OHO}

D) VARIATION RANGES OF MODEL PARAMETERS

The ranges of variation of the parameters of the whole models that were tested in this thesis are reported in Table 52.

Table 52: Variation ranges of model parameters

Parameter	Unit	Min	Max
Maximum X_{OHO} growth rate μ_{OHO_MAX}	gCOD/gCOD/d	2	12
Half-saturation coefficient for growth of X_{OHO} K_{SB_HYD}	gCOD/gCOD	N.D.	50
Hydrolysis rate constants $q_{XCB1\_SB\_HYD}$ $q_{XCB2\_SB\_HYD}$ $q_{XCB\_SB\_HYD}$ $q'_{XCB\_SB\_HYD}$	gCOD/gCOD/d	N.D.	12
Half-saturation constant for hydrolysis $K_{XCB,\ HYD}$ $K_{XCB\_1,\ HYD}$ $K_{XCB\_2,\ HYD}$	gCOD/gCOD	N.D.	1
Surface-based hydrolysis rate constants k_{SBK} k_{SBK_XCB1} k_{SBK_XCB2}	$Kg/m^5/d$	N.D.	25
Ammonia content of X_{OHO} $i_{N\_X\_BIO}$	mgN/gCOD	0.01	0.1
Ammonia content of particulate unbiodegradable organics i_{N_XU}	mgN/gCOD	0.01	0.05

APPENDIX 3 :

SUMMARY OF THEORETICAL MODEL EVALUATION

Analysis of model's prediction was performed in terms of feature of the curves, time of degradation and OUR max. Table 53 summarizes the results obtained for the different characteristics evaluated: geometric properties (shape and size) or hydrolytic biomass considerations (contamination, concentration, activation).

Table 53 : Summary of trends and characteristic values observed during model evaluation

Condition	Condition	Global feature	Time to degrade 90% of XC_B (days)	OUR_{ini}/ OUR_{max} (mg_{O2}/l/h)
Cylinder	Standard case (d=100µm; L=2000µm)		8.48	1.33/48.49
Size / spherical shape	150µm		9.22	1.33/45.23
	311µm		15.46	1.33/25.10
	447 µm		20.57	1.33/21.93
Size distribution	100/200/1000		>30	1.33/25.06
	100/50/10		8.09	1.33/67.08
Contamination	0/1/10		8.32	1.33/42.42
	0/0/10		9.20	1.33/42.17
S/X	5		6.75	13.33/53.86
	1		6.05	66.67/84.97
	0.5		5.83	133.3/133.5
Activation model	No H, G		16.54	1.33/24.74
	No H, no G			

Generally, a two-trend feature of the OUR is predicted by the model: after a lag phase, an exponential increase of the OUR is observed, followed by an exponential decrease. However, two exceptions can be observed: (i) in the presence of a distribution (either in size or in contamination level) several peaks of OUR are observed; (ii) when the initial active hydrolytic biomass concentration is high the OUR is early on at its maximum value. The lower is the substrate to biomass ratio, the higher is the factor between initial OUR and maximal OUR.

The initial value of OUR is directly linked to the total amount of bacteria performing endogenous respiration. The maximum OUR value, when considering as in our model evaluation that the maximum growth rate is the same and the half-saturation constant is low,

can be, as expected, attributed to the initial amount of hydrolytic bacteria, either initially adsorbed or in the bulk, as underlined by the S/X consequences.

In addition, considering geometrical properties make appears a clear dependence of this maximum value to the size of the particles for identical mass concentrations of both substrate and hydrolytic biomass.

Thus, the specific area appears as a key parameter determining OUR dynamics, as well in terms of amplitude as in terms of characteristic times which double when the size is increased by a factor of less than three, for the same quantity of substrate.